Function and Regulation of Equilibrative Nucleobase Transporter 1 in Acute Lymphoblastic Leukemia

by

Nicholas Matthew Ruel

A thesis submitted in partial fulfillment of the requirements for the degree of

Doctor of Philosophy

Department of Pharmacology
University of Alberta

Abstract

Background: 6-Mercaptopurine (6-MP) is a purine nucleobase analog used for the treatment of acute lymphoblastic leukemia (ALL), inflammatory bowel disease, and other disorders. 6-MP is primarily used in ALL, the most common childhood cancer. Enzymes involved in 6-MP metabolism have been shown to cause variability in 6-MP efficacy and toxicity in ALL patients. However, they only partially explain some of the variability seen. A major understudied factor was that the transport pathway for 6-MP into cells remained unknown, a requirement for 6-MPs mechanism of action. In 2015, it was discovered that the *SLC43A3* gene encoded for the Equilibrative Nucleobase Transporter 1 (ENBT1). ENBT1 exists as two separate isoforms, differing by 13 amino acids in the first extracellular loop. Notably, it was determined to be potentially responsible for the uptake of nucleobase analogs, like 6-MP, into cells. If ENBT1 is responsible for the uptake of 6-MP into leukemic cells, then it could potentially modify its toxicity and overall efficacy, providing a biomarker for the success of 6-MP therapy in patients.

Hypothesis: It is hypothesized that ENBT1 is responsible for the transport of 6-MP into leukemia cells and that the variability of the cellular toxicity of 6-MP is due to variation in the expression of ENBT1 in leukemia cells.

Methods: ENBT1 will be characterized in HEK293 cells, which are innately deficient in ENBT1, with recombinantly expressed ENBT1. Endogenously expressed ENBT1 will also be investigated, specifically in leukemia cells. Furthermore, the induction of oxidative stress and activation of protein kinase C (PKC) will be assessed in leukemia cells, and the impact of this on the ENBT1-mediated 6-MP uptake.

Results: HEK293 cells were stably transfected with both isoforms of recombinant *SLC43A3* and characterized. *SLC43A3*-encoded ENBT1 was confirmed to be a purine-selective nucleobase transporter that mediated the bidirectional transport of 6-MP. Notably, *SLC43A3*-transfected HEK293 cells exhibited 10-fold greater sensitivity to 6-MP than empty-vector transfected cells, showing that ENBT1 is critical for 6-MP activity. In a panel of leukemia cells, endogenous *SLC43A3* expression varies and is correlated to the overall uptake of 6-MP into the cells. However, *SLC43A3* expression did not correlate to the efficacy of 6-MP across the panel of cells. However, knockdown of *SLC43A3* in RS4;11 leukemia cells showed a reduction in the uptake of 6-MP and a decreased sensitivity to 6-MP, showing that the endogenous regulation and plasma membrane expression of ENBT1 is important to 6-MP activity. When looking at the regulation of ENBT1, ENBT1-mediated uptake of 6-MP is decreased following induction of oxidative stress by menadione, which can be reversed by the antioxidant TEMPOL. Finally, activation of PKC by the phorbol ester, phorbol 12-myristate 13-acetate, decreases ENBT1-mediated 6-MP uptake via the phosphorylation of threonine 231 on the largest predicted intracellular loop of ENBT1.

Conclusion: *SLC43A3*-encoded ENBT1 is integral to the cellular transport of 6-MP and significant changes in expression can significantly impact the efficacy of 6-MP in leukemia cells. Induction of oxidative stress and activation of PKC decreases ENBT1 functional uptake of 6-MP, providing a potential therapeutic target for 6-MP in ALL patients. Taken together, *SLC43A3*/ENBT1 is a significant determinant in 6-MP efficacy and sensitivity in leukemia cells and should be investigated further in patients to serve as a potential biomarker for 6-MP therapy.

Words: 532

Preface

This thesis is an original work by Nicholas Matthew Ruel.

Chapter 4 of this thesis has been published as **Ruel, N. M**., K. H. Nguyen, G. Vilas and J. R. Hammond (2019). "Characterization of 6-Mercaptopurine Transport by the SLC43A3-Encoded Nucleobase Transporter." Mol Pharmacol 95(6): 584-596. I was responsible for the data collection and analysis and the manuscript composition. K. H Nguyen assisted with the data collection. G. Vilas assisted with developing the models used. J. R. Hammond was the supervisory author involved with concept formation and manuscript composition.

Chapter 5 of this thesis has been published as **Ruel, N. M**., K. H. Nguyen, C. S. Kim, L. P. S. Andrade and J. R. Hammond (2022). "Impact of SLC43A3/ENBT1 Expression and Function on 6-Mercaptopurine Transport and Cytotoxicity in Human Acute Lymphoblastic Leukemia Cells." J Pharmacol Exp Ther 382(3): 335-345. I was responsible for the data collection and analysis and the manuscript composition. K. H. Nguyen, C. S. Kim, and L. P. S. Andrade assisted with data collection. J. R. Hammond was the supervisory author involved with concept formation and manuscript composition.

Chapter 6 of this thesis was done in collaboration with several undergraduate students under my supervision. I was responsible for data collection and analysis and the composition of the thesis chapter. Undergraduate students David Lee, Kerrylei Jabilona, and Nicholas Yamamoto contributed to data collection and analysis.

The research project, specifically the **Appendix**, which this thesis is a part, received research ethics approval from the Health Research Ethics Board of Alberta (Cancer Committee), “Effect of the expression/activity of the nucleobase transporter (ENBT1), encoded by *SLC43A3*, on the therapeutic efficacy of 6-mercaptopurine and development of drug resistance in acute lymphoblastic leukemia”, HREBA.CC-18-0503, November 21, 2018.

Dedication

To my wife, Evangeline

Acknowledgments

Members of my supervisory committee, Dr. Elaine Leslie and Dr. David Eisenstat
Your breadth of knowledge was integral to enhancing the scientific importance of my work throughout the years. This thesis is a testament to your expertise and guidance throughout the years.

Dr. Frances Plane
I have known you since my undergraduate degree, and you have always been supportive and willing to listen to and guide me on my journey when needed. I appreciate your support on every endeavour I embarked on.

Past and present members of the Hammond Lab.
Working with all the fantastic and friendly people over the years has been a pleasure. Thank you for your assistance and support over the years. This thesis would not have been half as coherent without you all.

My supervisor, Dr. James Hammond
Thank you for taking a chance on me eight years ago when I asked to join your lab at the last minute for one of my best summers. You introduced me to research, I fell in love with it, and you made me feel like I could make a difference with my work. Your continuous guidance and support have moulded me into who I am today, and I am forever grateful.

To my "brown cow" and furry fellow, Willow
Your snuggles and love when I come home have constantly reminded me that you will always be there no matter what day I have.

My family
Thank you for constantly reminding me that I was a "forever student" and was married to school. Your jokes and support always reminded me that I needed to leave at some point and grow further. Thank you for always listening to what I worked on, even if you had no idea what I was talking about.

And finally, to my rock Evangeline Ruel
You have supported me through my undergraduate and graduate degrees, whether I had good or bad days. You bring immense joy to my life and have always grounded me when I needed it most. I could not have achieved this without you. At this point, you could have almost written this thesis for me after listening to me talk endlessly about it every day.

Table of Contents

List of Tables

Chapter 3

Chapter 5

List of Figures

Chapter 1

Chapter 4

Chapter 5

Chapter 6

Chapter 7

Appendix

Abbreviations

ABC	ATP-binding cassette
ABL	Abelson
ALL	acute lymphoblastic leukemia
BCR	breakpoint cluster region
cAMP	cyclic adenosine monophosphate
cDNA	complementary DNA
CDDO	2-cyano-3,12-dioxooleana-1,9(11)-dien-28-oic acid
CK2	casein kinase 2
2-ClAdo	2-chloroadenosine
CML	chronic myelogenous leukemia
CNT	concentrative nucleoside transporter
CYP	cytochrome P450
D22	decynium-22
DAG	diacylglycerol
DMSO	dimethyl sulfoxide
DNA	deoxyribonucleic acid
Dox	doxycycline
D-PBS	Dulbecco's phosphate-buffered saline
DY	dipyridamole
EC_{50}	half maximal effective concentration
EDTA	ethylenediaminetetraacetic acid
ENBT1	equilibrative nucleobase transporter 1

ENT	equilibrative nucleoside transporter
FBS	fetal bovine serum
G418	geneticin
GAPDH	glyceraldehyde-3-phosphate dehydrogenase
GFP	green fluorescent protein
GMPS	guanosine monophosphate synthetase
GSH	glutathione
HEK293	human embryonic kidney 293
HEPES	4-(2-hydroxyethyl)-1-piperazineethanesulfonic acid
HPRT	hypoxanthine-guanine phosphoribosyl transferase
HRP	horseradish peroxidase
IgG	immunoglobulin G
IMPDH	inosine monophosphate dehydrogenase
KEAP1	Kelch-like ECH-associated protein 1
K_i	inhibitory constant
K_m	Michaelis constant
LLC-PK1	Lilly Laboratories culture-porcine kidney 1
MDCK	Madin-Darby canine kidney
6-MeMP	6-methylmercaptopurine
6-MetIMP	6-methylthioinosine monophosphate
MFS	major facilitator superfamily
mM	millimolar
6-MP	6-mercaptopurine

mRNA	messenger RNA
MRP	multidrug resistance protein
MTT	3-(4,5-dimethylthiazol-2-yl)-2,5-diphenyltetrazolium bromide
MTX	methotrexate
MVEC	microvascular endothelial cells
MYC	myelocytomatosis oncogene
NAC	N-acetyl-L-cysteine
NADPH	nicotinamide adenine dinucleotide phosphate hydrogen
NaOH	sodium hydroxide
NaPyr	sodium pyruvate
NBMPR	nitrobenzylthioinosine
nm	nanometer
nM	nanomolar
NMG	N-methyl-D-glucamine
Nrf2	nuclear factor erythroid 2–related factor 2
NUDT15	nudix hydrolase 15
OAT	organic anion transporter
PAGE	polyacrylamide gel electrophoresis
PBS	phosphate-buffered saline
PCR	polymerase chain reaction
Ph	Philadelphia
PKA	protein kinase A
PKC	protein kinase C

PMA	phorbol 12-myristate 13-acetate
RNA	ribonucleic acid
RNS	reactive nitrogen species
ROS	reactive oxygen species
RT-PCR	reverse transcriptase polymerase chain reaction
RT-qPCR	reverse transcriptase quantitative polymerase chain reaction
SD	standard deviation
SDS	sodium dodecyl sulphate
shRNAi	short hairpin ribonucleic acid interference
siRNA	short interfering RNA
SLC	solute carrier
SOD	superoxide dismutase
TBHP	tert-butyl hydroperoxide
TBS	tris-buffered saline
TBS-T	tris-buffered saline-0.2% v/v Tween-20
TBS-TM	tris-buffered saline-0.2% v/v Tween-20 and 5% w/v skim milk powder
6-TG	6-thioguanine
6-TGN	6-thioguanine nucleotides
6-tIMP	6-thioinsoine monophosphate
TKI	tyrosine kinase inhibitor
TM	transmembrane
TPMT	thiopurine methyl transferase
µM	micromolar

V_{max}	maximum rate of velocity
XDH/XO	xanthine oxidase

Glossary of Genes

ABCB1	P-glycoprotein
ABCC4	multidrug resistance protein 4
ABCC5	multidrug resistance protein 5
ABL1	Abelson 1
ACTB	β-actin
BCR	breakpoint cluster region
CDKN1B	cyclin-dependent kinase inhibitor 1B
CDKN2A	cyclin-dependent kinase inhibitor 2A
ETV6	translocation-Ets-leukemia virus
GAPDH	glyceraldehyde 3-phosphate dehydrogenase
GMPS	guanosine monophosphate synthetase
HPRT1	hypoxanthine-guanine phosphoribosyltransferase 1
IMPDH1	inosine-5′-monophosphate dehydrogenase 1
KEAP1	Kelch-like ECH-associated protein 1
MAFF	bZip Maf transcription factor F
MAFG	bZip Maf transcription factor G
MAFK	bZip Maf transcription factor K

MSH6	mutS homolog 6
mTORC1	mechanistic target of rapamycin kinase
NT5C2	5'-nucleotidase, cytosolic II
NT5E	5'-nucleotidase ecto
NUDT15	nudix hydrolase 15
NQO1	NADPH quinone oxidoreductase 1
PRPS1	phosphoribosyl pyrophosphate synthetase 1
RB1	retinoblastoma protein
RNA18SN5	18S ribosomal N5
RUNX1	runt-related transcription factor 1
SLC5A2	sodium-glucose cotransporter-2
SLC22A6	organic anion transporter 1
SLC22A8	organic anion transporter 3
SLC23A4P	sodium-dependent nucleobase transporter 1 pseudogene
SLC29A1	equilibrative nucleoside transporter 1
SLC29A2	equilibrative nucleoside transporter 2
SLC29A4	equilibrative nucleoside transporter 4

SLC43A1	L-type amino acid transporter 3
SLC43A2	L-type amino acid transporter 4
SLC43A3_1	equilibrative nucleobase transporter 1 isoform 1
SLC43A3_2	equilibrative nucleobase transporter 1 isoform 2
TPMT	thiopurine methyltransferase
TXNRD1	thioredoxin reductase 1
XDH/XO	xanthine dehydrogenase/oxidase

Chapter 1: Introduction

1.1) Acute lymphoblastic leukemia

1.1.1) Demographics and subtype classification

Acute lymphoblastic leukemia (ALL) is a disease arising from the bone marrow, with a peak incidence of 0 - 4 years of age (Katz et al. 2015). In Canada, leukemia is the most common cancer in children aged 0 – 14, representing 35% of all cancers in that age group. More specifically, ALL accounts for ~80% of all leukemias in children ('Release notice - Canadian Cancer Statistics 2023' 2024; Snodgrass et al. 2018). In adults, leukemia is rare and represents ~2% of all cancers in adults ('Release notice - Canadian Cancer Statistics 2023' 2024). ALL is characterized by the overproduction of immature lymphoblast cells. **Figure 1** shows the development of blood cells from their stem cell origin, with ALL development occurring in the lymphoblast cell prior to becoming a fully matured lymphocyte (Sawyers, Denny, and Witte 1991). ALL is classified under specific immunophenotypes based on the cellular surface expression of specific biomarkers (DiGiuseppe and Cardinali 2019). The most common are B and T-cell, with ~80-85% of cases having B-cell surface markers, ~15% having T-cell surface markers, and a small proportion of <5% displaying an ambiguous/mixed surface markers (Hrusak et al. 2018).

Figure 1: Development of blood cells

Blood cell development from stem cells leads to the formation of various blood cells in humans, including red blood cells, platelets, granulocytes, monocytes, and lymphocytes. In the development of ALL, the immature blast cell (highlighted in the red box), rapidly divides, leading to leukemia. Image taken from the Canadian Cancer Society website: https://cancer.ca/en/cancer-information/cancer-types/leukemia/what-is-leukemia

Figure 1

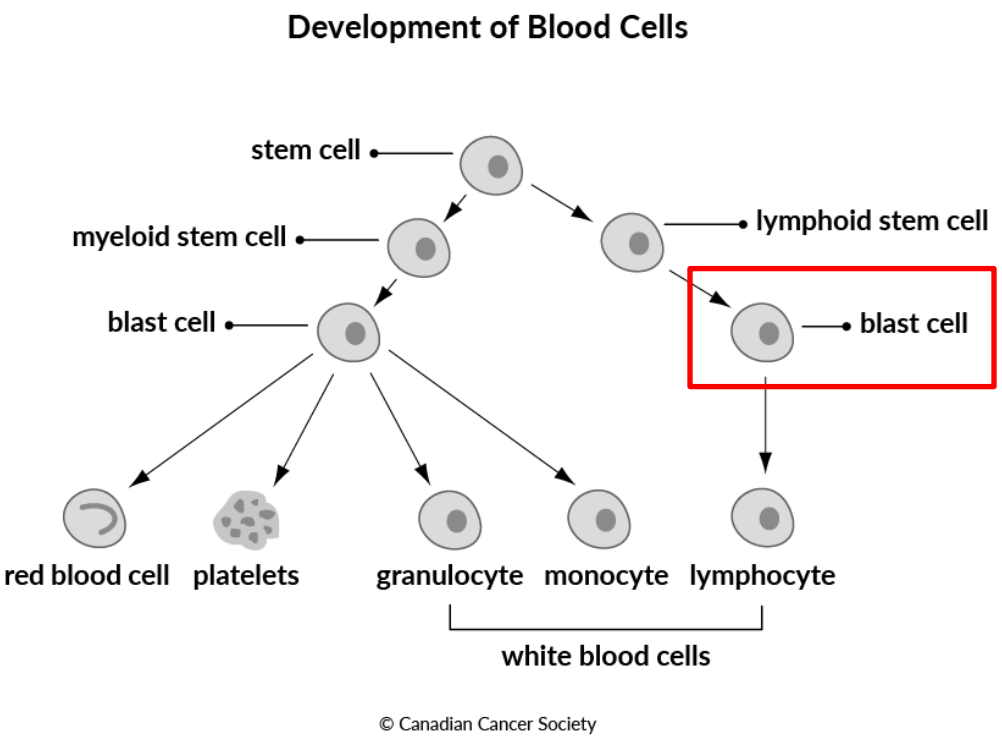
Development of Blood Cells
stem cell
myeloid stem cell
lymphoid stem cell
blast cell
blast cell
red blood cell
platelets
granulocyte
monocyte
lymphocyte
white blood cells
© Canadian Cancer Society

1.1.2) Genetics

ALL is further characterized by notable genetic mutations in patients that lead to the abnormal development of these lymphoblast cells. Extensive research has elucidated various genetic mutations strongly associated with ALL pathogenesis, shedding light on the molecular mechanisms underlying the disease and providing potential targets for therapy.

One of the most common genetic alterations observed in ALL is the presence of chromosomal translocations involving genes crucial for lymphoid development. For instance, the translocation event t(12;21)(p13;q22) leading to the formation of the *ETV6-RUNX1* fusion gene occurs in approximately 25% of pediatric ALL cases, leading to the formation of the *ETV6-RUNX1* fusion protein (Sun, Chang, and Zhu 2017; Kuiper et al. 2007). This fusion protein disrupts normal hematopoiesis by interfering with crucial regulatory pathways, contributing to leukemogenesis. Another significant genetic aberration in ALL involves the translocation of t(9;22)(q34;q11), called the Philadelphia (Ph) chromosome, leading to the breakpoint cluster region-Abelson 1 (BCR-ABL1) fusion gene. This translocation leads to the formation of the BCR-ABL1 that encodes a constitutively active tyrosine kinase that drives aberrant proliferation and survival of leukemic cells. The presence of the Ph chromosome is associated with a poorer prognosis and occurs in approximately 5% of pediatric ALL cases (Foa and Chiaretti 2022).

Additionally, alterations in genes involved in the regulation of cell cycle progression and cell proliferation/survival are frequently observed in ALL. For instance, mutations in the *CDKN2A*, *CDKN1B* and *RB1* that regulate cell cycle progression through the G1/S phase have been observed in ALL and lead to aberrant lymphocyte development (Kuiper et al. 2007). Furthermore, dysregulation of cytokine signalling pathways, such as the Janus kinase/signal transducers and activators of transcription pathway, is due to mutations in genes encoding Janus

kinase family kinases or cytokine receptors. These mutations contribute to enhanced cell proliferation and survival. Alterations in these genes occur in ~5% of pediatric ALL cases (Inaba and Mullighan 2020; Downes et al. 2022).

ALL pathogenesis and genetic alterations are even more numerous than described above and heavily influence its pathogenesis, disease progression, and treatment response. Understanding this genetic landscape in ALL through the identification of these genetic alterations has led to the development of targeted therapies aimed at disrupting specific oncogenic pathways, thereby improving patient outcomes.

1.1.3) Treatment

Current treatment of ALL involves four stages of chemotherapy that are informed through a risk stratification that considers the patient's age, overall health, ALL subtype, and the presence of other factors that could increase their risk (like genetic aberrations) (DelRocco et al. 2024). The four stages of ALL treatment consist of induction, consolidation/intensification, central nervous system-directed therapy, and continuation/maintenance. In Edmonton, the current treatment protocol used for pediatric ALL is based on the Dana-Farber Cancer Institute protocol, as shown in **Figure 2**.

Figure 2: ALL treatment protocol in Alberta

ALL treatment protocols for pediatric patients using the Dana-Farber Cancer Institute protocol in Alberta. Treatment includes 4 phases: induction, central nervous system-directed therapy, consolidation/intensification, and continuation/maintenance. A variety of drugs are used in these treatment phases and vary depending on whether the patient is high or low risk. Image taken from Alberta Health Services website: https://www.albertahealthservices.ca/info/cancerguidelines.aspx

Abbreviations: HR: high risk; SR: standard risk; IV: intravenous; PO: per os (by mouth); IM: intramuscular; IT: intrathecal; CNS: central nervous system; XRT: radiotherapy; Gy: gray; PEG: polyethylene glycol

Figure 2

Phase of Therapy	Time Period	Chemotherapy
Induction	28 Days	Vincristine 1.5 mg/m2/dose IV, maximum 2 mg, days 3, 10, 17, 24; prednisone 40 mg/m2/d IV/PO for 28 days; doxorubicin 30 g/m2/dose IV, days 1 and 2 methotrexate 4 g/m2 IV for one dose on day 3 IT cytarabine, dosed by age, one dose on day 0 IT cytarabine, dosed by age, one dose on day 17
CNS Therapy	3 Weeks	SR girls: IT methotrexate/cytarabine for 4 doses during 2 weeks, then every 18 weeks SR boys and all HR patients: cranial XRT 18 Gy, randomly assigned to hyperfractionated (0.9 Gy bid) or conventional (1.8 Gy daily) with IT methotrexate/cytarabine for 4 doses during 2 weeks
Intensification	Every 3 weeks for 30 weeks	SR: vincristine (2 mg/m2 IV every 3 weeks, maximum 2 mg); dexamethasone 6 mg/m2/d PO for 5 days; methotrexate 30 mg/m2 IV or IM every week; mercaptopurine,randomly assigned to high-dose 1,000 mg/m2 IV for 20 hours, weeks 1 and 2) or conventional 50 mg/m2/d PO for 14 days Asparaginase, randomly assigned to PEG 2,500 IU/m2 IM every 2 weeks for 15 doses or *E. coli* 25,000 IU/m2 IM every week for 30 doses HR: same as SR patients except dexamethasone 18 mg/m2/d PO for 5 days; no methotrexate; doxorubicin 30 mg/m2 IV every 3 weeks, to total cumulative dose 360 mg/m2, randomly assigned to continuous infusion during 48 hours versus IV bolus
Continuation	Every 3 weeks until 2 years of continuous complete remission	SR: vincristine 2 mg/m2 IV every 3 weeks, maximum 2 mg; dexamethasone 6 mg/ m2/d PO for 5 days; methotrexate 30 mg/ m2 IV or IM every week; mercaptopurine 50 mg/m2/d PO for 14 days HR: same as SR patients except dexamethasone 18 mg/m2/d PO for 5 days

1.1.4) Relapse and 6-MP adherence

Survival rates of ALL have significantly improved over the past few decades, presently at about 90-95% in children (Inaba and Mullighan 2020). Sadly, in adults, survival is much lower at ~30% (Kantarjian et al. 2004; Katz et al. 2015). Another prominent issue is that approximately 10-15% of patients will relapse and require further treatment (Jeha et al. 2019; Larsen et al. 2016; Maloney et al. 2020; Moricke et al. 2016; Pieters et al. 2016; Place et al. 2015; Toft et al. 2018; Vora et al. 2014; Winter et al. 2018; Inaba and Mullighan 2020). Patients who relapse have lower overall survival than patients who don't (Inaba and Mullighan 2020). Although relapsed ALL is associated with poor prognosis, there have been extremely promising clinical trials that have shown an improvement in relapsed patients. One of the most notable drugs is blinatumomab, which is a bispecific T-cell engager. Initial trials showed it was safe and highly effective in treating relapsed ALL (Topp et al. 2011; Topp et al. 2014; Topp, Gockbuget, and Stein 2015; Apel et al. 2020). Further clinical trials have also shown it to be better than standard chemotherapy alone and additive when used with chemotherapy in relapsed ALL (Kantarjian et al. 2017; van der Sluis et al. 2023). Another promising therapeutic avenue that is being actively investigated is chimeric antigen receptor T-cells. Clinical trials have shown it to be highly effective in treating hematological malignancies, like ALL and chronic myelogenous leukemia (CML) (Du, Zhang, et al. 2023; Maude et al. 2014; Park et al. 2018; Porter et al. 2015).

The potential reasons for relapse are multifactorial. However, a well-known risk factor associated with relapse is adherence to chemotherapy regimens, specifically during maintenance therapy when taking 6-mercaptopurine (6-MP). Toxic side effects while taking 6-MP are a major cause of adherence issues. Changes in some of the metabolic enzymes for 6-MP have already been linked to the clinical variability of 6-MP toxicity and efficacy due to alterations in the intracellular

active metabolites that will be described below. The enzymes thiopurine methyltransferase (TPMT) and nudix hydrolase 15 (NUDT15) have been linked to changes in 6-MP therapeutic efficacy and the incidence of toxic side effects (Hartford et al. 2007; Karas-Kuzelicki and Mlinaric-Rascan 2009; Chouchana et al. 2014; Chrzanowska et al. 2012; Coulthard et al. 2002; Dervieux et al. 2001; Ebbesen et al. 2013; Gerbek et al. 2018; Karim et al. 2013; Lennard et al. 2015; Liu et al. 2017; Relling et al. 2019; Saiz-Rodriguez et al. 2019; Schmiegelow et al. 2009; Zgheib et al. 2017; Du, Huang, et al. 2023; Kodidela et al. 2020; Moriyama et al. 2016; Tanaka 2017; Yang et al. 2014). TPMTs mechanism of action is the methylation of 6-MP and its various metabolites, while NUDT15 is a hydrolase enzyme that converts nucleoside diphosphates to nucleoside monophosphates. The two enzymes and their respective mutations alter the levels of active metabolites of 6-MP, which can reduce 6-MP efficacy or increase the incidence of toxic side effects. These two enzymes have been extensively studied and are generally assessed in patients prior to initiation of 6-MP therapy. Other known potential variations have also been associated with the genes *NT5C2, NT5E, MSH6, mTORC1,* and *PRPS1* but are not clinically utilized prior to the initiation of drug therapy (Dieck et al. 2018; Evensen et al. 2018; Li et al. 2015; Li et al. 2010; Pieters et al. 1992; Tzoneva et al. 2013; Vo et al. 2017).

Furthermore, 6-MP is primarily taken daily in the outpatient setting, which solely relies on the patient's discretion in taking it. Increased toxic side effects lead to patients not taking 6-MP, thus decreasing their adherence rate. Reductions in adherence to 6-MP below 90% are associated with a 2 – 5 fold increase in the risk of relapse, which gets progressively higher depending on how low the patient’s adherence rate is (Alsous et al. 2017; Bhatia et al. 2012; Bhatia et al. 2014; Bhatia et al. 2015; Wu et al. 2018; Wadhwa et al. 2023; Kahn et al. 2023). This problem is further complicated by the fact that there is a large interindividual variability among plasma

concentrations (~11-fold; 0.12 – 1.38 micromolar (μM)) of 6-MP when given a standardized dose (Lonnerholm et al. 1986; Larsen et al. 2020). This variability in plasma levels leads to toxic side effects of 6-MP and problems associated with medication adherence among patients that increases the risk of relapse and associated outcomes.

6-MP is essential in ALL chemotherapy to ensure patients remain in remission. The variability in its plasma concentrations can lead to deleterious side effects that impact adherence and associated relapse risk. Factors like TPMT and NUDT15 are clinically utilized and important but have not explained all the variability associated with 6-MP, especially the variations in plasma concentrations. Several other factors likely remain undiscovered to address this variability.

1.2) 6-Mercaptopurine

1.2.1) Mechanism of action

6-MP is a thiopurine nucleobase analogue antimetabolite, resembling endogenous purine nucleobases like adenine, guanine, and hypoxanthine. **Figure 3** shows the structure of the endogenous nucleobases as well as 6-MP and 6-thioguanine (6-TG). 6-TG is also a purine nucleobase analog that is structurally similar to 6-MP. 6-MP is a prodrug and must be converted intracellularly by a variety of metabolic enzymes to its active forms to exert its mechanism of action (Salser and Balis 1965). The main metabolites implicated in 6-MP cytotoxicity are 6-thioguanine nucleotides (6-TGNs), 6-methylthioinosine monophosphate (6-MetIMP), and 6-thioguanosine triphosphate (6-tGTP). 6-TGNs are the primary active metabolites that can be incorporated into DNA and RNA as false-nucleotides, leading to DNA damage that eventually causes cell cycle arrest in S-phase and apoptosis (Nelson et al. 1975; Fernandez-Ramos et al. 2017). 6-MetIMP inhibits phosphoribosyl pyrophosphate (PRPP) amidotransferase, which is the

rate-limiting step of *de novo* purine synthesis, leading to a decrease in nucleotides for DNA replication (Tay et al. 1969; Fernandez-Ramos et al. 2017). Inhibition of *de novo* purine synthesis further exacerbates the effects of 6-TGNs since there will be less competition for incorporation into DNA and RNA. Finally, 6-tGTP inhibits the GTPase Rac1, which activates pro-survival pathways in ALL (Troeger et al. 2010; Freret et al. 2011; Marinkovic et al. 2014). Together, these distinct compounds impair the growth and proliferation of cells, with the most pronounced effects on rapidly dividing cells, like gastrointestinal cells, immune cells, and cancer cells.

Figure 3: Endogenous nucleobases and nucleobase analogs

Purine and pyrimidine nucleobases and the nucleobase analogs 6-mercaptopurine and 6-thioguanine. All molecular structures were taken from PubChem: ("Compound Summary for CID 190, Adenine" 2004; "Compound Summary for CID 597, Cytosine" 2004; "Compound Summary for CID 135398634, Guanine" 2004; "Compound Summary for CID 1135, Thymine" 2004; "Compound Summary for CID 1174, Uracil" 2004; "Compound Summary for CID 667490, Mercaptopurine" 2004; "Compound Summary for CID 2723601, Thioguanine" 2004)

Figure 3

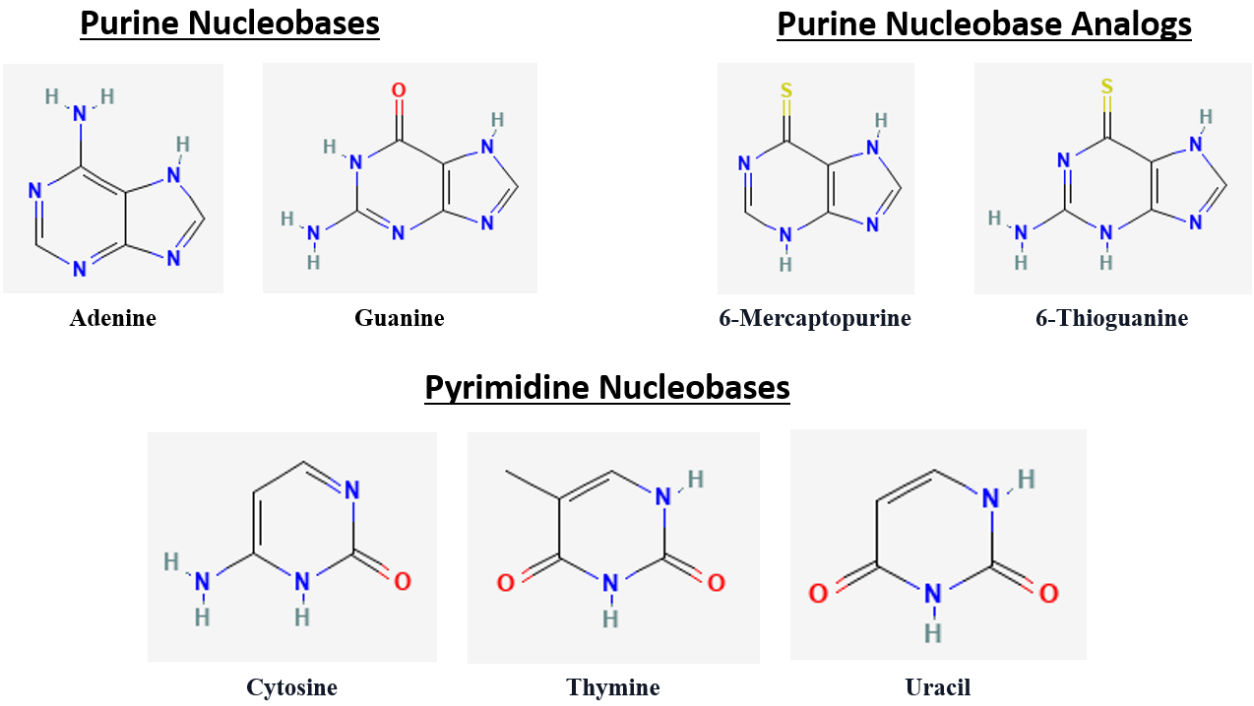
Purine Nucleobases
Purine Nucleobase Analogs
Adenine
Guanine
6-Mercaptopurine
6-Thioguanine
Pyrimidine Nucleobases
Cytosine
Thymine
Uracil

1.2.2) Intracellular metabolism

Figure 4 shows the metabolic pathway for 6-MP, which can be separated into three distinct pathways. **(1)** the hypoxanthine-guanine phosphoribosyl transferase (HPRT) pathway, **(2)** the xanthine dehydrogenase/oxidase (XDH/XO) pathway, and **(3)** the TPMT pathway.

(1): The HPRT pathway is the primary pathway for 6-MP activation. 6-MP is initially converted to 6-thioinosine monophosphate (6-tIMP) by HPRT. At this point, 6-tIMP can either be converted by TPMT or continue through the HPRT pathway. Assuming 6-tIMP remains in the HPRT pathway, inosine monophosphate dehydrogenase 1 (IMPDH1), which is the rate-limiting step of this pathway (Stet et al. 1991), followed by guanosine monophosphate synthetase (GMPS), converts 6-tIMP into 6-TGNs. 6-TGNs can be incorporated into DNA as a false nucleotide during DNA synthesis that eventually leads to apoptosis (Fernandez-Ramos et al. 2017; Nelson et al. 1975). 6-TG is another structurally similar purine nucleobase analog to 6-MP, but it has a more direct activation to active metabolites via conversion through HPRT to 6-TGNs. Although 6-TG has been noted to have slightly higher efficacy than 6-MP, it is not commonly used due to higher incidences of side effects (Escherich et al. 2011; Tu et al. 2022; Stork et al. 2010). However, a current clinical trial is currently investigating the use of low-dose 6-TG in combination with the regular maintenance therapy treatment of 6-MP and methotrexate (MTX) (Toksvang et al. 2022).

(2): The XDH/XO pathway is primarily an excretion pathway that converts 6-MP or its various metabolites to inactive forms for removal. XDH/XO converts 6-MP to 6-thiouric acid, which is excreted via the urine (Jackson 1983). Conversion of 6-MP to 6-thiouric acid primarily happens in the liver and gastrointestinal tract, where XDH/XO expression is the highest (Uhlen et al. 2015). This pathway is generally not considered important in lymphocytes/lymphoblasts, the

cancer cell associated with ALL, as XDH/XO is not expressed in lymphocytes/lymphoblasts (Uhlen et al. 2015).

(3): The TPMT pathway methylates 6-MP and various metabolites that have both active and inactive metabolites. 6-MP is methylated to 6-methylmercaptopurine (6-MeMP), a therapeutically inactive metabolite. 6-tIMP is also methylated to 6-MetIMP, a therapeutically active metabolite that has been shown to be responsible for the inhibition of *de novo* purine synthesis (Tay et al. 1969; Coulthard et al. 2002; Bokkerink et al. 1993) that can be further converted to 6-methylmercaptourine ribonucleotide. It has been well characterized that the methylated metabolites of 6-MP mentioned previously have been linked to hepatotoxicity in patients owing to the importance of the TPMT pathway in 6-MP toxicity (Choi et al. 2019; Dubinsky et al. 2000; Moon et al. 2019; Nygaard, Toft, and Schmiegelow 2004; Shaye et al. 2007; van Asseldonk et al. 2012).

The metabolism of 6-MP has been known for several decades, and various enzymes have been associated with toxic side effects. However, the transport of 6-MP into cells remained elusive and is critical for its mechanism of action. Being a nucleobase analog, 6-MP would be transported by nucleobase transporters, which were first investigated in the 1980s.

Figure 4: 6-MP metabolism

Diagram of 6-MPs metabolic pathway.

Abbreviations: ENBT1: equilibrative nucleobase transporter 1; 6-MP: 6-mercaptopurine; 6-MeMP: 6-methylmercaptopurine; TPMT: thiopurine methyltransferase; 6-TU: 6-thiouric acid; XDH/XO: xanthine dehydrogenase/oxidase; 6-tIMP: 6-thioinosine monophosphate; HPRT: hypoxanthine guanine phosphoribosyl transferase; 6-MetIMP: 6-methylthioinosine monophosphate; IMPDH: inosine monophosphate dehydrogenase; GMPS: guanosine monophosphate synthetase; 6-TGN: 6-thioguanine nucleotides; 6-TG: 6-thioguanine

Figure 4

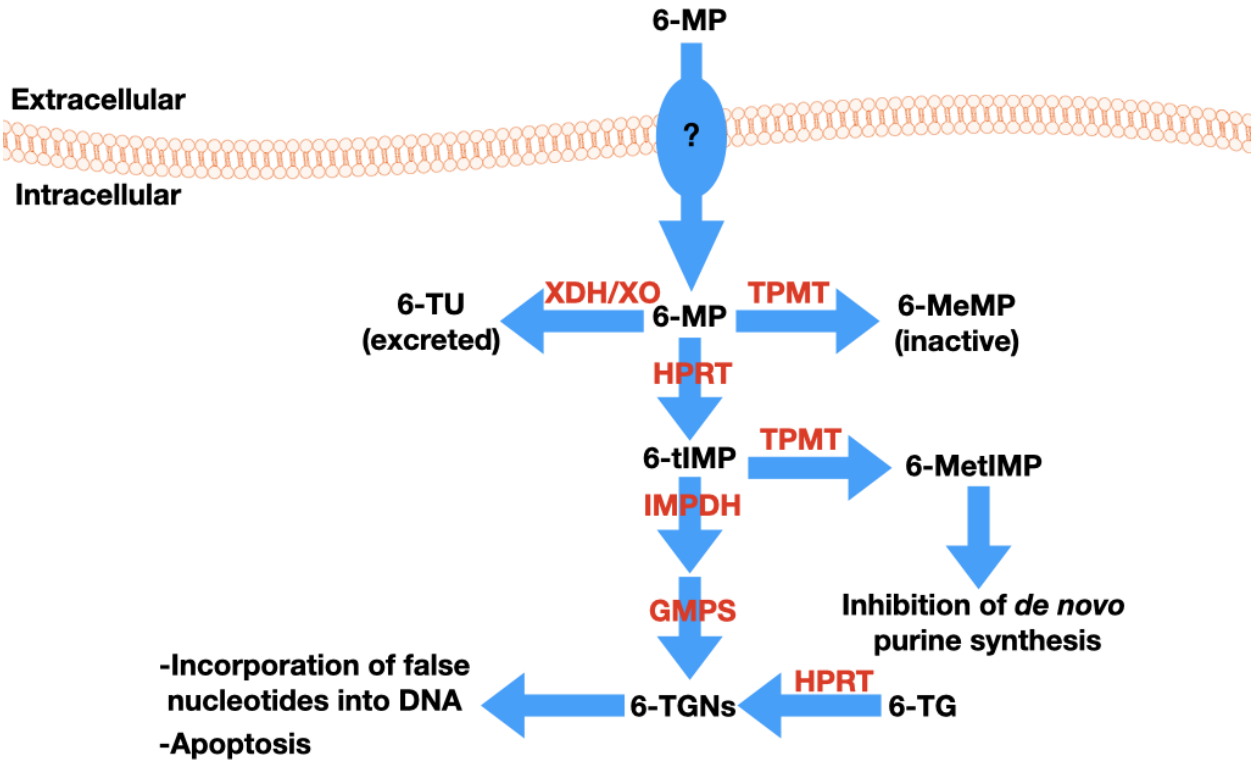
6-MP
Extracellular
?
Intracellular
6-TU
(excreted)
XDH/XO
6-MP
TPMT
6-MeMP
(inactive)
HPRT
6-tIMP
TPMT
6-MetIMP
IMPDH
GMPS
Inhibition of *de novo*
purine synthesis
-Incorporation of false
nucleotides into DNA
-Apoptosis
6-TGNs
HPRT
6-TG

1.3) Nucleobase Transporters

As noted previously, nucleobase analogs, like 6-MP, have been utilized for their therapeutic benefits for decades, but the transporters that carry them across cell membranes were not known. In the late 1980s, the initial characterization of nucleobase transport systems began. The first functional characterizations of nucleobase transport came from mutant T-lymphoblast cells and mouse S49 lymphoblast cells, in which a novel purine nucleobase transport system was described to mediate the uptake of adenine, hypoxanthine, and guanine (Aronow et al. 1986; Beck and Ullman 1987). Following up on these findings, the same group further characterized this system as being bidirectional in its method of transport and distinct from nucleoside transporters, which were investigated around the same time (Beck and Ullman 1987). Another purine-like transporter was also characterized with remarkable similarities to the one seen in S49 cells in human erythrocytes. It showed a remarkable affinity for purine nucleobases that was not inhibited by nucleosides (Domin, Mahony, and Zimmerman 1988). Further evidence supporting this same type of transporter came in the early 1990s when it was shown that the toxicity of 6-thiopurines, like 6-MP, could be prevented by purine nucleobases adenine and hypoxanthine (Hashimoto et al. 1990). Furthermore, this transporter was inhibited by purine nucleobase derivatives and not classical nucleoside transport inhibitors, like nitrobenzylthioinosine (NBMPR), dipyridamole (DY) or dilazep (Kraupp et al. 1994; Kraupp and Marz 1995). This evidence pointed to a selective purine nucleobase transporter system distinct from any other transporter being characterized at the time.

However, even at the passing of the century in 2000, there were still no known genes that were attributed to nucleobase transport, which essentially halted much of the work and interest in the systems that were described above. That being said, over the years, a few transporters of interest were characterized as being able to transport nucleobases. The sodium-dependent

nucleobase transporter 1 was characterized in Lilly Laboratories culture-porcine kidney 1 (LLC-PK1) and showed an affinity for various nucleobases in the low μM range (Griffith and Jarvis 1993). However, it was found to be a defective pseudogene in humans (*SLC23A4P*) (Yamamoto et al. 2010). Two of the organic anion transporters (OAT), OAT1 and OAT3, encoded by the *SLC22A6* and *SLC22A8* genes, respectively, were also found to transport nucleobases with low μM affinity in rats and mice. However, their affinity in humans is understudied but suggests a lower affinity (mid to high μM) (Mori et al. 2004; Ohtsuki et al. 2002; Kobayashi et al. 2004; El-Sheikh et al. 2013). Furthermore, OATs have very limited or absent expression in many body systems, including lymphoblasts, the cancer cells associated with ALL (Burckhardt 2012; Thul et al. 2017). OAT transporters may be relevant for other parts of the body that have more robust expression, such as the kidney. Finally, members of the equilibrative nucleoside transporter (ENT) family, specifically ENT1 and ENT2, encoded by the *SLC29A1* and *SLC29A2* gene, respectively, were shown to transport nucleobases, but the affinity of nucleobases for these transporters was into the millimolar (mM) range (Yao et al. 2011).

Several efflux pumps have been investigated and studied throughout the years in terms of their interaction with nucleoside and nucleobase analogs (Fukuda and Schuetz 2012). There has been a focus on the multidrug resistance protein (MRP) 4 and MRP5, encoded by the adenosine triphosphate-binding cassette (*ABC*) *C4* and *ABCC5* genes, respectively. MRP4 and MRP5 physiological functions may include the transport of cyclic guanosine monophosphate and cyclic adenosine monophosphate (cAMP), which activate a variety of intracellular pathways (Chen, Lee, and Kruh 2001). MRP4 and MRP5 are also proposed to be involved in the sensitivity and transport of 6-MP, 6-TG, and MTX. Several studies have shown that overexpression of either MRP4 or MRP5 in different cell lines leads to decreased efficacy (shift in half maximal effective

concentration (EC_{50})) of 6-MP in these cells (Chen, Lee, and Kruh 2001; Peng et al. 2008; Schuetz et al. 1999; Wijnholds et al. 2000). This supports the role of MRP4/5 in the efflux of nucleobase analogs from cells and resistance, but they are not relevant to the uptake into cells.

A large question still loomed over nucleobase uptake into cells. Is there a transporter that mediates the influx of nucleobases and their analogs at high affinity that is ubiquitously expressed throughout the body? All the above-mentioned transporters either lack the affinity for nucleobases and their analogs or are not expressed widely throughout the body. This made it hard to characterize nucleobase analogs in chemotherapy, like 6-MP and 6-TG, in terms of their efficacy and bio-distribution in patients, which can impact the therapeutic outcome for patients and the prevalence of toxic side effects.

1.4) Equilibrative Nucleobase Transporter 1

1.4.1) Discovery

In 2015, it was discovered that the gene *SLC43A3* encoded for a transporter capable of transporting nucleobases like hypoxanthine, adenine, and guanine (Furukawa et al. 2015). In this study, they showed that the transport of adenine by the *SLC43A3*-encoded transporter was inhibited by nucleobases. Specifically, the nucleobase analog 6-MP was also shown to inhibit. Prior to this discovery, the *SLC43A3* was an orphan transporter of the *SLC43A* family. The other members are *SLC43A1* and *SLC43A2*, which encode large neutral amino acid transporters 3 and 4, respectively, which transport amino acids (Bodoy et al. 2013). *SLC43A3* was found not to transport amino acids and thus was not investigated further by those in the amino acid transporter community. This led to it remaining obscure for many years. Interestingly, a study conducted in

2007, prior to the 2015 discovery, looked at a purine-selective nucleobase transporter. The authors named it equilibrative nucleobase transporter 1 (ENBT1). In the study, human microvascular endothelial cells (MVEC) displayed similar characteristics to the *SLC43A3*-encoded ENBT1 from the study in 2015 and were likely the same transporter being characterized (Bone and Hammond 2007). It is also likely that the transporter that was being characterized in the late 1980s, as covered in section **1.3**, was also likely to be ENBT1 since it was a high-affinity purine-selective transporter with similar characteristics (Aronow et al. 1986). Furthermore, *SLC43A3* is known to express two different isoforms, assessed in **Chapter 4** of this thesis, and are different by the absence (referred to herein as *SLC43A3_1* (gene); ENBT1.1 (protein) or presence (*SLC43A3_2* (gene); ENBT1.2 (protein)) of 13 amino acids in the predicted first extracellular loop of the protein **(Figure 5)**.

Figure 5: Predicted topology of ENBT1

Predicted topology of ENBT1 using Protter prediction open-source software (Omasits et al. 2014).

Figure 5

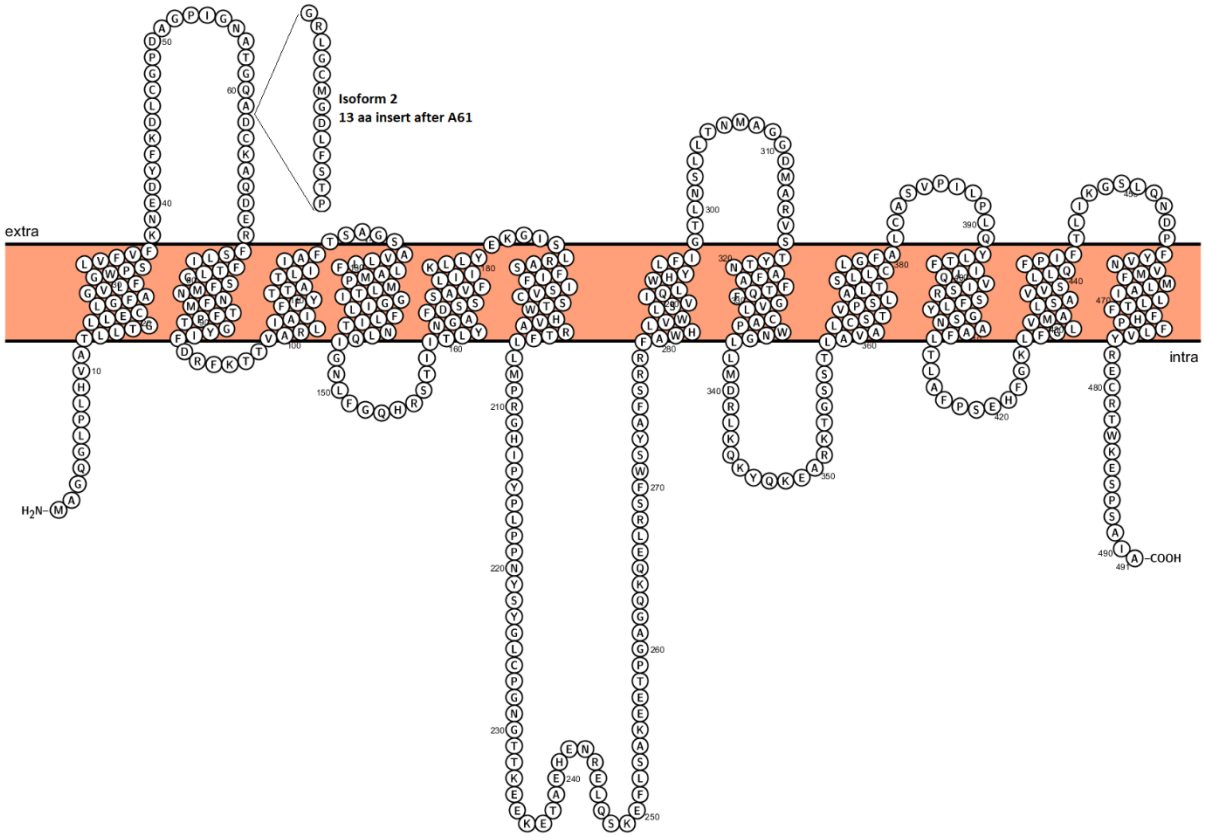

1.4.2) Expression and current studies

Based on publicly available data from the Human Protein Atlas (proteinatlas.org), the expression of *SLC43A3* is ubiquitous in humans, with the highest expression in the liver, thyroid, adipose, and bone marrow (Uhlen et al. 2015). Since 2015, *SLC43A3* has already been investigated for interactions with other cytotoxic drugs and has been implicated in the cytotoxicity of 6-thio-2'-deoxyguanosine and ganciclovir (Furukawa et al. 2017; Mender et al. 2020). Interestingly, it has also been shown to be a factor in the transport of 6-MP in brain MVECs, further supporting that it does potentially interact with 6-MP (Kurosawa et al. 2021). Outside of drug interactions, *SLC43A3* has been shown to be involved in regulating fatty acid uptake, is a novel fusion gene in angiosarcoma, and is a potential prognostic signature in glioblastoma (Hasbargen et al. 2020; Shimozono et al. 2015; Larionova and Tashireva 2023; Zhang et al. 2024). Finally, *SLC43A3*/ENBT1 has been suggested to be regulated by oxidative stress and protein kinase modulation. However, these findings were prior to the 2015 discovery and have not been fully investigated (Bone et al. 2014; Griffith and Jarvis 1996). Understanding its expression patterns, structure, drug-drug interactions, regulation, and mechanism of substrate translocation opens the opportunity for clinical applications of this transporter in the future.

1.4.3) Predicted 3D structure

Structurally, ENBT1 does not have a solved crystal structure nor do the other members of the *SLC43* family on the Protein Data Bank (Berman et al. 2000). This means we must rely on a broad characterization of its predicted 3D structure. The *SLC43* family belongs to the major facilitator superfamily (MFS) of transporters, meaning we can look at this family's predicted structural classifications for ENBT1. Proteins in the MFS typically consist of 12 transmembrane

(TM) domains, which is also what ENBT1 is predicted to have **(Figure 5)**. These 12 TMs are organized into two six-helix bundles, formed into the N (TM 1 – 6) and C (TM 7 – 12) terminal domains. These N and C-terminal domains can be further divided into two separate domains (N-terminal: TM 1 – 3 and TM 4 – 6; C-terminal: TM 7 – 9 and TM 10 – 12) that share a pseudosymmetry that is represented by a 180° rotation of TM 4 – 6 relative to TM 1 – 3 in the N-terminal and TM 10-12 relative to TM 7 – 9 in the C-terminal. This particular orientation in MFS proteins is called the "MFS fold" (Yan 2013). Furthermore, specific transmembrane domains are typically referred to in certain locations relative to other transmembrane domains that predict their overall conformation and substrate binding importance. TMs 1, 4, 7, and 10 are in the centre of the transporter and are essential for substrate recognition. TMs 2, 5, 8, and 11 are on the sides of the protein and form interdomain contacts. TMs 3, 6, 9, and 12 are just outside of the central TMs and help with the structural integrity of the protein (Yan 2013). A 3D predicted structure of ENBT1 is shown in **Figure 6** using Alpha Fold (Jumper et al. 2021). Generally speaking, the predicted 3D structure is consistent with the above characterization of predicted MFS transporter folding and organization. Although predictive, it could provide insights into the potential targeting of certain residues within ENBT1 to investigate substrate recognition motifs and potential drug-drug interactions.

Figure 6: Predicted 3D structure of ENBT1 using Alpha Fold

A) 3D predicted structure of ENBT1 from Alpha Fold (Jumper et al. 2021). Red lines indicate the approximate location of the cellular membrane with the intracellular, transmembrane, and extracellular domains labelled. The colour coding on the 3D structure is the estimated confidence of each residue on a scale of 1 - 100. Dark blue indicates a high confidence of > 90. Light blue indicates a moderate confidence of 70 – 90. Yellow indicates a low confidence of 50 – 70. Orange indicates a very low confidence of < 50. **B)** 3D predicted structure of ENBT1 from Alpha Fold using the same orientation as **Panel A** but with the N and C-terminal TM domains highlighted. The N-terminal is highlighted in red and yellow. The C-terminal is highlighted in purple and pink. White indicates every other residue that is not associated with a TM domain. **C)** 3D predicted structure of ENBT1 from Alpha Fold using a top-down point of view. Red indicates TMs 1, 4, 7, and 10. Yellow indicates TMs 2, 5, 8, and 11. Orange indicates TMs 3, 6, 9, and 12.

Figure 6

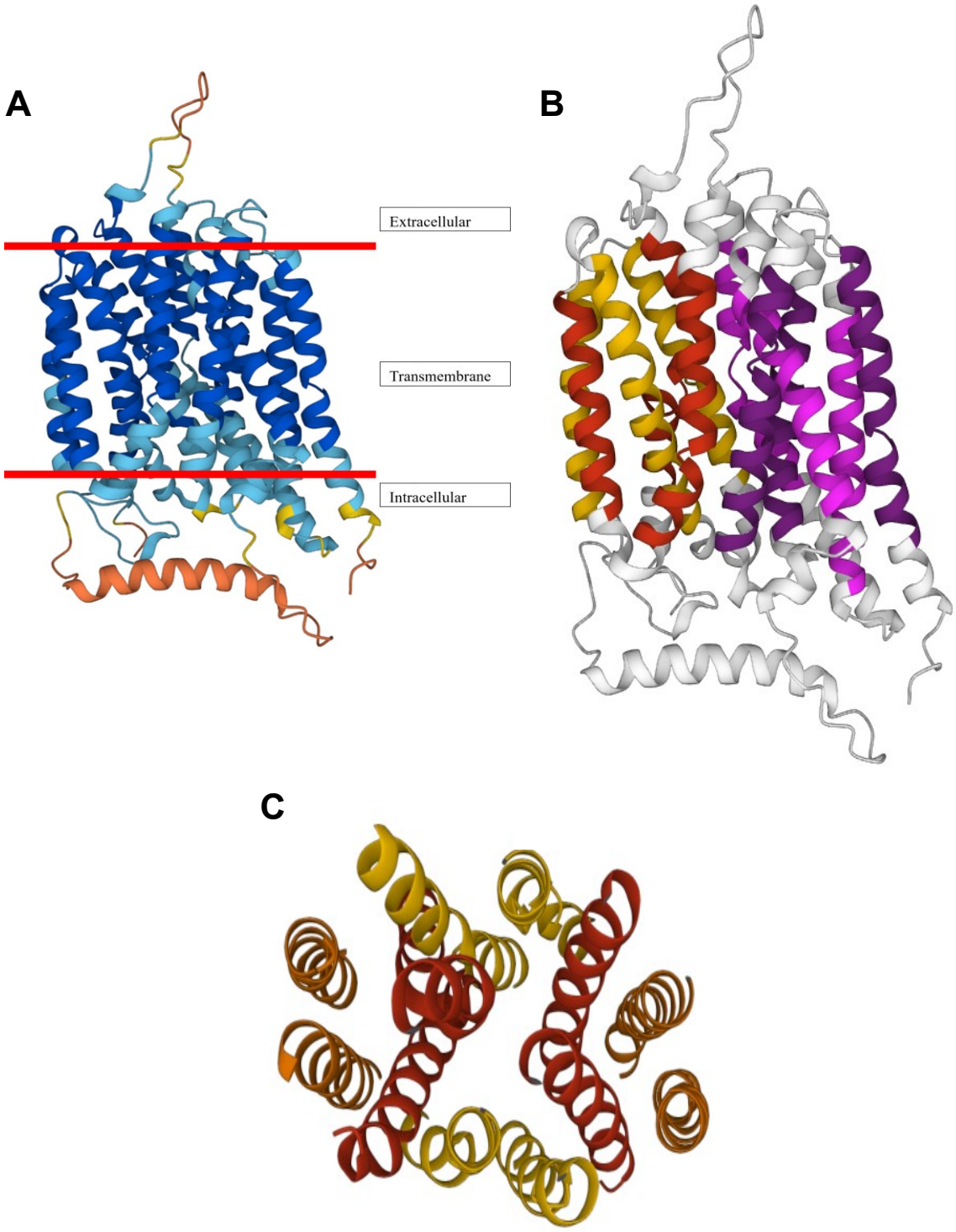

1.4.4) Predicted translocation mechanism

As mentioned above for the predicted structure, ENBT1 is novel, and no studies have investigated its translocation mechanism. Therefore, we look again at the MFS family for the predicted mechanism. Regarding substrate translocation, MFS transporters undergo a series of conformational changes within the transporter protein, alternating between three distinct transition states: outward open, occluded, and inward open, to facilitate substrate translocation. The outward open state allows substrate binding in the central cavity of the protein and is the first step in the translocation of the substrate. At this point, the conformation of the protein will change into the occluded state, wherein the protein is neither open to the inside nor outside of the cell, essentially shielding the substrate. After further conformational changes, the protein then goes into the inward open conformation, allowing the release of the substrate into the cell. This process will then be repeated for further substrates of the transporter protein; this process is called the "alternating access cycle." This model was first proposed in 1966 by Oleg Jardetzky and has been fundamental to understanding substrate translocation (uptake and export) by transporters at the plasma membrane and cell organelles (Yan 2013; Jardetzky 1966). The "alternating access cycle" has three proposed models for its movement: the rocking bundle model, the elevator model, and the rocker switch model. The rocking bundle model proposes that one protein domain (N or C-terminal) rocks back and forth to facilitate substrate translocation while the other domain is stationary. The elevator model proposes that one protein domain (N or C-terminal) actively moves from one side of the membrane to the other to facilitate substrate translocation while the other domain remains stationary. The rocker switch model proposes that both domains (N and C-terminal) of the protein rock back and forth to facilitate substrate translocation. Of these models, the rocker switch model has been the most popular model of substrate translocation by the MFS

proteins (Sauve et al. 2023). ENBT1 does not necessarily have to conform to these structural standards and translocation mechanisms. These broad characterizations serve as a starting point for further in-depth investigation of its overall structure and interactions. One such important interaction is its interaction with intracellular processes, especially metabolic processes.

1.5) Mechanistic interactions between transporters and enzymatic systems

Transporters and enzymatic systems are crucial in drug metabolism and distribution within the body. Transporters are membrane proteins that facilitate the movement of xenobiotics and endogenous compounds across biological membranes, affecting their pharmacokinetic profile. The most widely studied families of transporters that have been implicated in drug distribution are the SLC and the ABC families. The SLC family is typically responsible for the influx of compounds into cells, while the ABC family members mediate the efflux from cells. Both of these families have been extensively studied, and efforts to characterize every member of each family are ongoing (Zhou et al. 2008). For example, P-glycoprotein, a well-known ABC efflux transporter, reduces intracellular concentration of drugs by pumping them out of cells. This efflux activity mediated by transporters like P-glycoprotein can influence the bioavailability and efficacy of drugs (Liu 2019).

Transporters interact closely with drug metabolizing systems involved in drug metabolism, such as the cytochrome P450 (CYP) enzyme. CYP enzymes are major contributors to drug metabolism in the liver and intestine (Ogu and Maxa 2000). Many drugs that interact with these enzymes can be substrates, inhibitors, and inducers of these enzymes. Any of these interactions can significantly alter the bioavailability of other drugs and lead to potentially deleterious drug-drug interactions in patients (Ogu and Maxa 2000). Changes to the charge, lipophilicity, and

molecular weight of drugs have been shown to alter the potential for drug-drug interactions with CYP enzymes that can impact the clearance and bioavailability of drugs in patients (Steyn and Varma 2020). Finally, these enzymes have been associated with a plethora of mutations that can significantly alter drug metabolism and biodistribution in patients (Pandey and Sproll 2014).

The interplay between transporters and drug-metabolizing enzymes can impact drug metabolism, kinetics, and bioavailability. For example, concurrent administration of two separate drugs may interact with the same transporters and drug metabolizing enzymes, leading to competition for binding sites and ultimately altering drug concentrations throughout the body. Drugs that interact this way exhibit complicated pharmacokinetic profiles and are extremely hard to study. This is further complicated since the overall expression distribution of transporters and drug metabolizing enzymes in each patient can vary widely (Lin 2007). In general, when looking at whole-body pharmacokinetics, drug metabolizing enzymes will play a more significant role in determining drug biodistribution (with CYP enzymes playing the biggest role), while on a single-cell level, transporters will play a more significant role (Lin 2007).

On a single-cell level, it can be simplified, since within certain cell types, it is well characterized which transporters and enzymatic systems are expressed. For this thesis, the transporter system on the plasma membrane is of primary interest, and to ensure accurate characterization of the transporter, intracellular metabolism must be kept in mind. A primary concern with enzymatic intracellular metabolism is “metabolic trapping.” Metabolic trapping was first noted in 1978 and is the process by which there is an intracellular accumulation of metabolites in cells via enzymatic conversion (Gallagher et al. 1978). Metabolic trapping is especially important with equilibrative transport systems (studied in this thesis) since once the substrate has reached equilibrium, transport is at a steady state (transport in = transport out). However,

enzymatic conversion of the substrate is active. If transport is at equilibrium and there is enzymatic conversion, this will drive further transport inward since equilibrium will be lost, leading to metabolic trapping. Throughout this thesis, the timepoint used to assess transporter-mediated radioactive substrate uptake will be a time that is under five sec (typically 2 sec). This short time point ensures that the transporter of interest is being assessed and not any enzymatic systems. If time points past equilibrium were to be used, metabolic trapping would be taking place and would appear as a sustained uptake process beyond equilibrium concentrations, leading to incorrect assumptions of the transporter-mediated process. Furthermore, if a Michaelis-Menten analysis is done using a time point that is too long, rather than assessing the transporter's kinetics, enzyme kinetics would be assessed.

Chapter 2: Hypothesis and Research Aims

2.1) HYPOTHESIS

It is hypothesized that ENBT1 is responsible for the transport of 6-MP into leukemia cells. Furthermore, variations in the inter-individual cellular toxicity of 6-MP are due to variations in the expression of ENBT1 in its target cells (specifically, leukemia cells).

2.2) RATIONALE

ALL is the most common cancer in childhood that affects a significant number of patients every year. It is a multifactorial disease that has seen a huge increase in the survival of patients over the past decades. However, approximately 10 – 15% of patients will still relapse with much lower survival rates. A significant component leading to relapse is the inadequate efficacy of maintenance therapy. This is likely due to variability in plasma doses of 6-MP leading to low efficacy or high incidence of toxic side effects leading to low adherence to treatment and, thus, high rates of relapse. A new transporter, called ENBT1, has been shown to transport 6-MP and is a likely candidate for its entry into the cells, which influences the cytotoxicity of 6-MP. Furthermore, the regulation of ENBT1 expression at the plasma membrane could impact the entry of 6-MP, thus decreasing the efficacy of treatment.

2.3) RESEARCH AIMS

2.3.1) AIM 1: Characterization of recombinant ENBT1 in ENBT1-deficient human embryonic kidney cells

To investigate ENBT1, HEK293 cells will be used, which are innately deficient in ENBT1. Messenger RNA (mRNA) expression, protein expression, and function of ENBT1 in transfected

HEK293 cells will be assessed. Furthermore, a panel of inhibitors that could potentially interact with ENBT1 will be investigated. This aim will functionally characterize ENBT1 and how it handles 6-MP and changes it cytotoxicity.

2.3.2) AIM 2: Characterization of endogenous ENBT1 in a panel of leukemia cell lines

To investigate the endogenous function of ENBT1, a panel of leukemia cell lines will be assessed for their ENBT1 mRNA and protein level, as well as function, similar to what is done in **AIM 1**. The cell lines to be investigated are ALL-1, MOLT-4, RS4;11, REH, NALM-6, SUP-B15, and K562. Furthermore, short hairpin RNA interference (shRNAi) targeted against *SLC43A3* will be transfected to determine the impact of *SLC43A3*-knockdown on the mRNA, protein, and function of ENBT1, as well as the 6-MP cytotoxicity.

2.3.3) AIM 3: Determine how ENBT1 is regulated by protein kinase C and oxidative stress

If variations in the plasma membrane expression of ENBT1 affect 6-MP efficacy and toxicity, the regulation of ENBT1 should be investigated. Previous studies have implicated that ENBT1 may be regulated by protein kinase c (PKC) and oxidative stress. Broad-spectrum PKC activators and inhibitors will be used to investigate potential PKC-mediated regulation and determine its impact on ENBT1-mediated uptake. Finally, site-directed mutagenesis of *SLC43A3* will be used to determine specific residues responsible for the potential PKC-mediated effects seen. For oxidative stress, inducers of oxidative stress and several antioxidants will determine if the induction of oxidative stress alters ENBT1-mediated uptake and if antioxidants can reverse any changes seen.

Chapter 3: Materials and Methods

3.1) MATERIALS

[2,8-^{3}H] adenine (20-40 Ci/mmol), [8-^{14}C] 6-MP (50-60 mCi/mmol), [^{3}H] 6-MP (0.3 Ci/mmol), and [^{3}H] water (1 mCi/g) were from Moravek Biochemicals (Brea, CA). 6-TG, hypoxanthine, 6-MeMP, 2-chloroadenosine, adenine, adenosine, 3-(4,5-dimethyl-2thiazolyl)-2,5-diphenyl-2H-tetrazolium bromide (MTT), N-methyl-D-glucamine (NMG), dimethyl sulfoxide (DMSO) NBMPR, DY, 6-TG, geneticin (G418), Dulbecco's modified Eagle's medium, fetal bovine serum (FBS), doxycycline (Dox), menadione, tert-butyl hydroperoxide (TBHP), N-acetyl-cysteine (NAC), 4-Hydroxy-2,2,6,6-tetramethylpiperidine-1-oxyl (TEMPOL), 2-mercaptoethanol, polybrene, puromycin, mouse monoclonal anti-myelocytomatosis oncogene (MYC) tag antibody (Clone 4A6), rabbit polyclonal anti-*SLC43A3* (HPA030551), 4α-phorbol 12-myristate 13-acetate (4α-PMA), and phorbol 12-myristate 13-acetate (PMA) were purchased from Sigma-Aldrich (St. Louis, MO). StemSpan SFEM II, 10x CD34+ expansion supplement, UM729, and StemRegenin 1 were obtained from Stemcell Technologies (Vancouver, Canada). All primers were ordered through Integrated DNA Technologies (Coralville, Iowa). Agarose, oligo (dT)12–18 primer, Iscove's Modified Dulbecco's Media, 4-(2-hydroxyethyl)-1-piperazineethanesulfonic acid (HEPES), sodium pyruvate (NaPyr), D-glucose solution (200 g/L), penicillin-streptomycin, ethylenediamine tetraacetic acid (EDTA), sodium dodecyl sulfate (SDS), polyvinylidene fluoride membranes, PowerUp SYBR Green, Total Reactive Oxygen Species (ROS) Assay Kit 520 nanometer (nm), HALT Protease Inhibitor Cocktail, Lipofectamine 3000 transfection reagent, TRIzol Reagent, and Superscript III Reverse Transcriptase came from Thermo Fisher Scientific (Waltham, MA). The 100 base pair DNA Ladder was supplied by Truin Science (Edmonton, AB). Power Up SYBR Green and TRIzol Reagent were supplied by Life Technologies (Burlington, ON). Mouse monoclonal anti-β-actin (C4) (sc-47778), donkey anti-rabbit immunoglobulin G

(IgG)-horseradish peroxidase (HRP) (sc2313), and m-IgGk binding protein-HRP (sc-516102) were purchased from Santa Cruz Biotechnology (Dallas, TX). Anti-rabbit IgG-HRP-linked was purchased from Cell Signaling Technology (Danvers, MA). Roswell Park Memorial Institute (RPMI)-1640 medium and the enhanced chemiluminescence Prime western blotting system were purchased from Cytiva Life Sciences (Marlborough, MA). Leu-Fect A was purchased from RJH Biosciences (Edmonton, AB). QuikChange Lightning Site-Directed Mutagenesis Kit was purchased from Agilent (Santa Clara, CA). SMARTvector 2.0 Inducible Lentiviral shRNAi particles targeting *SLC43A3* and SMARTvector 2.0 non-targeting shRNA control particles were from GE Healthcare Dharmacon, Inc. (Lafayette, CO). Decynium-22 (D22), ceefourin-1, zaprinast, and Gö6983 were from Tocris Bioscience (Oakville, ON), and MTX was from Alfa Aesar (Tewksbury, MA). MOLT-4, NALM-6, SUP-B15, and HEK293 were purchased from ATCC (Manassas, VA). ALL-1, REH, and RS4;11 cells were generously provided by Dr. David Eisenstat (University of Alberta, Edmonton). K562 cells were generously provided by Dr. Elaine Leslie (University of Alberta, Edmonton).

Table 1: List of pharmacological agents

All pharmacological agents along with their primary mechanism of action used in this thesis.

Table 1

Pharmacological Agent	Primary Mechanism of Action
CDDO-Im	NRF2 activator
Ceefourin-1	MRP4 inhibitor
CX-4945	Casein kinase II inhibitor
Cycloheximide	Protein translation inhibitor
Dasatinib	BCR-ABL tyrosine kinase inhibitor
Decynium-22	ENT4/PMAT/ENBT1 inhibitor
Diamide	Thiol oxidizing agent
Dipyridamole	ENT1/ENT2 inhibitor
Erlotinib	EGFR tyrosine kinase inhibitor
Gefitinib	EGFR tyrosine kinase inhibitor
Gö6983	Protein Kinase C inhibitor
H89	Protein Kinase A inhibitor
Imatinib	BCR-ABL tyrosine kinase inhibitor
Menadione	Reactive oxygen species inducer
Methotrexate	Dihydrofolate reductase inhibitor
N-acetyl cysteine	Glutathione precursor/antioxidant
NBMPR	ENT1 inhibitor
Nilotinib	BCR-ABL tyrosine kinase inhibitor
4α-PMA	Inactive analog of PMA
PMA	PKC activator

TEMPOL	Free radical scavenger
tert-butyl hydroperoxide	Reactive oxygen species inducer
Zaprinast	MRP5 inhibitor

3.2) METHODS

3.2.1) Cell culture

HEK293 cells were cultured in Dulbecco's modified Eagle's medium with 10% FBS, penicillin (100 units/mL), streptomycin (100 µg/mL), and NaPyr (1 mM). G418 was added (300 µg/ml) in the transfected *SLC43A3*-HEK293 cell media to maintain selection pressure on the stable transfectants. The HEK293 cells were removed from flasks by exposure to 0.05% trypsin/EDTA for 5 min at 37°C, and the suspended cells were washed in the appropriate buffer solution (without G418) immediately prior to use in subsequent assays. Various modifiers were used either before or after the washes as relevant to individual experiments.

ALL-1, MOLT-4, RS4;11, NALM-6, K562, and REH cells were cultured in RPMI-1640 medium with 10% FBS supplemented with D-glucose (4500 mg/L), NaPyr (1 mM), penicillin (100 U/mL), streptomycin (100 mg/mL), and HEPES (10 mM). SUP-B15 cells were cultured in Iscove's Modified Dulbecco's Media with 20% FBS and 0.05 mM 2-mercaptoethanol. All leukemia cell lines utilized along with their leukemia type, donor age and sex, and documented genetic anomalies is shown in **Table 2**. Suspended cells were centrifuged and washed in appropriate assay buffer solutions prior to their use in subsequent assays. Various modifiers were used before or after the washes as relevant.

Primary ALL bone marrow aspirates were cultured in StemSpan™ II medium supplemented with CD34+ expansion supplement, UM729 (1 uM), and StemRegenin 1 (500 nanomolar (nM)). Bone marrow aspirates were only cultured for a maximum of one day to enable acclimatization to the medium and to ensure maximum viability prior to any experiments.

Table 2: Leukemia cell line information

Leukemia cell lines used with information on the type of leukemia, donor age and sex, and genetic anomalies. All data was obtained from Cellosaurus (https://www.cellosaurus.org/).

Table 2

Cell Line	Leukemia Type	Donor		Genetic Anomalies
		Sex (M/F)	Age (Years)	
MOLT-4	T-ALL	M	19	NOTCH1, NRAS, PTEN, STK11, TP53
ALL-1	B-ALL	F	7	BCR-ABL1
RS4;11	B-ALL	F	32	KMT2A-AFF1
REH	B-ALL	F	15	ETV6-RUNX1, NR3C1, PTEN, TP53
NALM-6	B-ALL	M	19	IGH-DUX4, EGFR, NRAS, RARA
SUP-B15	B-ALL	M	9	BCR-ABL1
K562	CML	F	53	BCR-ABL1, TP53

3.2.2) Stable transfection of recombinant MYC-*SLC43A3*

Oligonucleotides corresponding to the coding region of isoform 1 (NM_001278201) or isoform 2 (NM_001278206) of *SLC43A3*, with an N-terminal MYC-epitope tag, were prepared in the GeneArt Cloning pMA plasmid by Invitrogen. The MYC-*SLC43A3* sequences were transferred to the mammalian cloning vector pcDNA3.1(-) using the Xbal (5') and KpnI (3') restriction enzymes. The inserts were sequenced in both directions to confirm integrity and then used to transfect HEK293 cells using the calcium phosphate method (Kingston, Chen, and Rose 2003). Cells expressing *SLC43A3* were selected based on their resistance to 600 µg/ml G418 using standard procedures. Cells stably transfected with the 'empty' pcDNA3.1(-) vector were also tested to assess the impact of the transfection procedure and G418 on the measured parameters.

3.2.3) Transient transfection

One day prior to the transfection, HEK293 cells were plated on a T175 flask to be ~80 - 90% confluent. The following day, Lipofectamine 3000 was used per the manufacturer's protocol to transfect plasmids of interest into HEK293 cells. Cells were incubated for 72 hours before experiments were conducted on them.

3.2.4) Site-directed mutagenesis

Isoform 1-MYC-*SLC43A3* pcDNA3.1(-) plasmid was used as a template for site-directed mutagenesis at three different amino acid positions, threonine 231 (ACC) (a736g), serine 253 (TCA) (t802g), and serine 276 (TCT) (t871g), to convert each of the relevant residues to alanine. The QuikChange Lightning site-directed mutagenesis kit was used from Agilent (Santa Clara,

CA), the isoform 1-*SLC43A3* pcDNA3.1(-) plasmid was mutagenized per manufacturer protocol, and each plasmid was sequenced to confirm successful mutagenesis at each site prior to transient transfection in HEK293 cells.

3.2.5) Nucleobase uptake

Cells were suspended in nominally sodium-free buffer (to eliminate any potential contribution of sodium-dependent transporters) (NMG buffer: 140 mM NMG, 5 mM KCl, 4.2 mM $KHCO_3$, 0.36 mM K_2HPO_4, 0.44 mM KH_2PO_4, 10 mM HEPES, 0.5 mM $MgCl_2$, 1.3 mM $CaCl_2$, pH 7.4) containing 500 nM, 1 µM, or 5 µM DY (to block potential ENT1/ENT2 mediated uptake) for 15 min at room temperature prior to assay. Cellular uptake was initiated by adding 250 µl of cell suspension to 250 µl of [^{14}C] or [^{3}H] 6-MP or [^{3}H] adenine layered over 21:4 silicone: mineral oil (v:v) (200 µl) in 1.5 ml microcentrifuge tubes. [^{3}H] 6-MP was used because [^{14}C] 6-MP became unavailable from the supplier. [^{3}H] adenine was used at times since it had a higher specific activity than [^{3}H] 6-MP, leading to a better signal-to-noise ratio. The uptake reaction was terminated after specified times by centrifugation of the cells through the oil layer at ~10,000 g. The aqueous layer was aspirated, and the tube was washed with ~1 ml of NMG buffer prior to the removal of the oil layer. The resulting cell pellet was digested in 1 M sodium hydroxide (NaOH) overnight (~16 hr), with aliquots of digested cells assessed for radioactive content using standard liquid scintillation counting techniques in a Beckman Coulter LS6500 scintillation system. In the HEK293 cells, total uptake of [^{3}H] adenine was defined as [^{3}H] adenine uptake in the transfected *SLC43A3*-HEK293 cells, while non-mediated uptake of [^{3}H] adenine was defined as uptake of [^{3}H] adenine in untransfected HEK293 cells. Total uptake of [^{14}C] 6-MP was done in transfected *SLC43A3*-HEK293 cells in the absence of adenine, with non-mediated uptake defined as uptake in the

presence of 1 mM adenine. In leukemia cell models, total uptake was defined as the uptake of [^{3}H] or [^{14}C] 6-MP and [^{3}H] adenine in the absence of adenine, while non-mediated uptake was defined as [^{3}H] or [^{14}C] 6-MP, and [^{3}H] adenine in the presence of 5 mM adenine. Mediated uptake was defined as the difference between the total uptake and non-mediated uptake components. Cell volume (µl) was estimated by incubating cells with [^{3}H] water for 3 min, centrifuging the cells through the oil layer, sampling 100 µl of the supernatant and processing as above. Total cellular water volume was determined from the ratio of the decays per minute of the cell pellet to the decays per minute of the supernatant, allowing for inter-experimental normalization via calculation of pmol of substrate accumulated per µl of cell-associated water.

3.2.6) 6-MP efflux

Cells were trypsinized from confluent T175 flasks and washed in a sodium-free buffer as described for the nucleobase uptake assays. Viable cell numbers were determined using trypan blue stain (Hyclone, GE Healthcare, Logan, UT) on a BioRad TC10 Automated Cell Counter prior to loading the cells with radioactive substrate. Cells were loaded with 100 µM [^{14}C] 6-MP for 30 sec and then centrifuged at 1000 g for 30 sec to lightly pellet the cells. The supernatant was removed, and cell pellets were rapidly suspended in sodium-free buffer (± inhibitors) to initiate efflux. Aliquots (500 µl) of this cell suspension were layered over 21:4 silicone: mineral oil (v:v) in a 1.5 ml microcentrifuge tube and centrifuged at specified time points. The cell pellets were then washed and incubated in 1 M NaOH overnight and processed as described for the nucleobase uptake assays for the determination of intracellular [^{14}C] content. In experiments where 1 mM adenine was used, the initial load of [^{14}C] 6-MP (time 'zero') was determined by extrapolation of the exponential decay curve fit to the data obtained in the presence of 1 mM adenine. In

experiments where 1 mM adenine was not used, the initial load of [^{14}C] 6-MP (time 'zero') was determined by centrifuging an aliquot (500 µl) of the cells immediately following the loading step and processing as described above. No difference was noted between these two methods in the determination of the initial load for these experiments.

3.2.7) MTT cell viability

HEK293 cells: Cells were seeded into a 24-well plate at a density of 5 x 10^4 cells/well in culture media and left overnight. Culture media was removed the following day and replaced by media containing 6-MP (75 nM - 1.28 mM) and incubated for 48 hr at 37°C in a humidified 5% CO_2 atmosphere. In some cases, the ENT1/ENT2 inhibitor DY or the MRP4 and MRP5 inhibitors ceefourin-1 and zaprinast, respectively, were included in the media to assess the influence of these transporters on 6-MP cytotoxicity/sensitivity. Herein, 6-MP cytotoxicity will be referred to as 6-MP sensitivity, as it was determined by another lab member that the 48 hr incubation with 6-MP does not cause robust cell toxicity (as determined by the lactate dehydrogenase (LDH) assay) (Chan Kim, personal communication, June 27, 2023), but rather a decrease in MTT reduction, likely due to the cytostatic effect of 6-MP in effecting energy metabolism in cells (Fernandez-Ramos et al. 2017). After 48 hr the media was removed and replaced with 250 µL of Dulbecco's phosphate buffered saline (D-PBS) (137 mM NaCl, 2.7 mM KCl, 6.3 mM Na_2HPO_4, 1.5 mM KH_2PO_4, 0.5 mM $MgCl_2 \cdot 6H_20$, 0.9 mM $CaCl_2 \cdot 2H_20$, pH 7.4) containing MTT (1 mg/ml) for 90 min. Formazan crystals formed were solubilized in 450 µl of DMSO, and absorbance was measured at 570 nm in a Spectra Max i3x plate reader (Molecular Devices, Sunnyvale, CA).

Leukemia cells: Cells were seeded into a 24-well plate at a density of 5×10^4 cells/well in culture medium. Following plating, a medium containing 6-MP (75 nM – 1.28 mM) was added and incubated for 48 hr at 37°C in a humidified 5% CO_2 atmosphere. Cells were then transferred to a 1.5 mL microcentrifuge tube and centrifuged at 3000 g for 10 min. Following centrifugation, media was removed and replaced with 250 µL of D-PBS (137 mM NaCl, 2.7 mM KCl, 6.3 mM Na_2HPO_4, 1.5 mM KH_2PO_4, 0.5 mM $MgCl_2$, 0.9 mM $CaCl_2$, pH 7.4) containing MTT (1 mg/ml) for 90 min. Microcentrifuge tubes were centrifuged again at 23,500 rcf for 15 min, and the D-PBS containing MTT was removed. The resultant formazan crystals were solubilized in 450 µl of DMSO, and absorbance was measured at 570 nm in a Spectra Max i3x plate reader (Molecular Devices, Sunnyvale, CA).

3.2.8) Immunoblotting

Samples were prepared in radioimmunoprecipitation buffer (150 mM NaCl, 50 mM Tris, 1% NP40, 0.5% sodium deoxycholate, 1% SDS) containing EDTA and Halt™ Protease and Phosphatase Inhibitor Cocktail (Thermo Fisher Scientific, Waltham, MA). For determination of glycosylation, cell lysates were treated with or without 500 units of PNGase F according to the manufacturer's protocol prior to loading. Samples were adjusted to 2% (v/v) β-mercaptoethanol and resolved by SDS-polyacrylamide gel electrophoresis (PAGE) on 12.5% (w/v) acrylamide gels. Proteins were electro-transferred onto Immobilon-P polyvinylidene fluoride membranes (Millipore Corporation, MA, USA) for 1.5 hr at a constant current of 280 mA. After transfer, membranes were rinsed in Tris-buffered saline (TBS) (TBS – 150 mM NaCl, 50 mM Tris, pH 7.5) and incubated with TBS-TM (TBS containing 0.1% v/v Tween-20 and 5% w/v skim milk powder) for 1 hr at room temperature with gentle rocking to block nonspecific binding. Membranes were

then incubated overnight at 4°C with gentle rocking in the presence of either mouse anti-MYC, rabbit anti-*SLC43A3*, mouse anti-β-actin, or mouse anti-ENT1 at 1:1000, 1:250, 1:500, and 1:500 dilutions, respectively, in TBS-TM (containing 1% skim milk). After successive washes with TBS-TM (containing 1% skim milk), the membranes were incubated with a 1:2000 or 1:3000 dilution of goat anti-rabbit IgG-HRP or m-IgGk binding protein-HRP, respectively, in TBS-TM for 1 hr at room temperature and further washed with TBS-T (TBS, containing 0.2% (v/v) Tween-20). Proteins were detected using enhanced chemiluminescence western blot substrate (EMD Millipore, Canada) and visualized using an Amersham Imager AI680 (GE Healthcare, Chicago, USA).

3.2.9) Polymerase chain reaction

Cells from confluent 10 cm plates were suspended in 1 ml of TRIzol reagent and homogenized for extraction of RNA according to the manufacturer's protocol (Thermo Fisher Scientific). Total RNA concentration and purity were determined using a Nanodrop 2000 spectrophotometer (Life Technologies Inc.).

For qualitative reverse transcriptase polymerase chain reaction (RT-PCR), 1 μg of total RNA was reverse transcribed to complementary DNA (cDNA) using Oligo (dT)12–18 primer and Superscript III Reverse Transcriptase and amplified using recombinant Taq DNA Polymerase. The following conditions were used for amplification: 3 min at 95°C, followed by 40 cycles of 30 sec at 95°C, 30 sec at 56°C, and 60 sec at 72°C, followed by extension for 10 min at 72°C in a BioRad T-100 Thermocycler. Primer sequences are shown in **Table 3**.

Semiquantitative reverse transcriptase polymerase chain reaction (RT-qPCR) was conducted using cDNA (~100 ng/well) prepared as described above with the primer sets shown in **Table 3** using Power Up SYBR Green fluorescence on a Roche Light Cycler 480 System (Cardiovascular Research Centre, Edmonton, Canada). Primer efficiency and melt curves were assessed prior to their use for gene expression analysis. Semiquantitative RT-qPCR conditions were: 2 min at 50°C (uracil-DNA glycosylase activation), 2 min at 95°C (denaturation), followed by 50 cycles of 15 sec at 95°C, and 60 sec at 60°C for amplification, with a final melt curve analysis. Gene expression was normalized to either glyceraldehyde-3-phosphate dehydrogenase (*GAPDH*) alone or the geographic mean of three separate reference genes, *GAPDH*, *18S ribosomal N5 (RNA18SN5)*, and *β-actin* (*ACTB*), and analyzed relative to expression in the untransfected HEK293, ALL-1 cells, or a relevant control using the $\Delta\Delta C_t$ method.

Table 3: PCR primer sequences

Forward and reverse primer sequences are shown for various genes, along with their expected product size in base pairs. The table is broken up into two sections: one for qualitative RT-PCR primers and one for semiquantitative RT-qPCR primers.

Table 3

Gene name	Primer sequence (5' to 3')	Expected product (base pairs)
Qualitative RT-PCR		
ABCC4	Fwd – TGCAAGGGTTCTGGGATAAAG Rev – GACGAAGTGCCTTCCGATAAA	363
GAPDH	Fwd – ACATCATCCCTGCCTCTAC Rev – CCTGTTGCTGTAGCCAAAT	356
SLC43A3 [a]	Fwd – CTGTGTGGACCAGATGC Rev – TGCAGAGGTGAAGGCTA	225 – *SLC43A3_1* 264 – *SLC43A3_2*
SLC43A3_2 [b]	Fwd – GAGACCTTTTTTCTACTCC Rev – TGCAGAGGTGAAGGCTA	197
Semiquantitative RT-qPCR		
ABCB1	Fwd – TGCAGGTACCATACAGAAACTC Rev – ACCGGAAACATCCAGCATAG	105
ABCC4	Fwd – GGAGAGCCAAGATACAGAGAATG Rev – GAGCACCAGCTCTGAAGTAAT	107
ABCC5	Fwd – ACCATCCACGCCTACAATAAA Rev – GCATCGCACACGTAAACAAA	100
ACTB	Fwd – CCCTGGAGAAGAGCTACGA Rev – GAAGGAAGGCTGGAAGAGTG	95

GAPDH	Fwd – GATTCCACCCATGGCAAATTC Rev – CTGGAAGATGGTGATGGGATT	87
GMPS	Fwd – GAAGATGCTCCCTGGTTTGA Rev – TGCACAGTACCTCCAAATACC	107
HPRT1	Fwd – TGGCGTCGTGATTAGTGATG Rev – CCCATCTCCTTCATCACATCTC	156
IMPDH1	Fwd – GGTCTTACTGGCAGGTGTT Rev – GCCGCTGATCAGGTAGTC	76
NQO1	Fwd – GGGATGAGACACCACTGTAT Rev – CTCCTCATCCTGTACCTCTTT	95
NUDT15	Fwd – TGAAAGTTGGGAGTGGGTTC Rev – CCACCAGATGGTTCAGATCTTC	122
RNA18SN5	Fwd – CACGGACAGGATTGACAGATT Rev – GCCAGAGTCTCGTTCGTTATC	119
SLC29A1	Fwd – GAGCAGGCAAAGAGGAATCT Rev – GAGAAAGCCAGGACTGAGATATT	106
SLC29A2	Fwd – AAGTAGCTCTGACCCTGGAT Rev – GGAAGACAGTGAAGACTGAAGG	99
SLC29A4	Fwd – CAGACTTCGTGGGCAAGAT Rev – CAGGATGAAGAGGGGGATGAAG	107

SLC43A3 [a]	Fwd – CTTCTGGAGCTACGCTTTCT Rev – GGAGTTGAGAGTGCCAATGA	100
TPMT	Fwd – GGAACAAGGACATCAGCTATTA Rev – CTGATTTCCACACCAACTACA	150
TXNRD1	Fwd – GTAGTAGCTCAGTCCACCAATA Rev – CCTACGGTTTCTAAGCCAATTT	113
XDH/XO	Fwd – TTGGTGCTGTGGTTGCT Rev – CTTTCTCGATCTTCAGCTCAGG	150

[a] These primer pairs amplify the same sequence for both *SLC43A3_1* and *SLC43A3_2*.

[b] This primer pair amplifies the sequence for *SLC43A3_2*.

3.2.10) Trypan blue staining

Following the treatment of cells, 0.4% trypan blue stain was combined in a 1:1 ratio with cells and mixed. Afterwards, 10 uL was aliquoted onto counting slides in duplicate and placed in a BioRad TC10 Automated Cell Counter (Bio-Rad Laboratories, Hercules, USA) for determination of total cell count, live cell count, and % live cell count.

3.2.11) Suppression of *SLC43A3* by shRNAi

SMARTvector 2.0 Lentiviral shRNA particles bind to cells and deliver their shRNAi to the cytoplasm. The SMARTvector 2.0 includes a Turbo green fluorescent protein (GFP) reporter gene to facilitate the assessment and optimization of transduction efficiencies. It also contains a puromycin resistance gene for the selection and isolation of clonal cell populations.

HEK293 cells*:* The base HEK293 cells and *SLC43A3*-HEK293 cells were transduced with the SMARTvector Inducible Lentiviral shRNA vector containing *SLC43A3* shRNAi according to the manufacturer's protocol and stably selected using puromycin. To induce expression of the shRNA, Dox was added to the cells at 400 ng/mL for 48 or 72 hr before analysis. shRNA expression efficiency was assessed based on the reporter GFP fluorescence. *SLC43A3* knockdown was confirmed by immunoblots with anti-ENBT1 antibodies.

Leukemia cells: Attempts to transduce ALL-1 and RS4;11 leukemia cells with the SMARTvector Inducible Lentiviral shRNA system, using the same procedure that was used for the HEK293 cells, were unsuccessful. Therefore, transfection of RS4;11 cells with *SLC43A3* shRNAi vector lentiviral particles or non-targeting control shRNAi was done using Leu-Fect A according to the manufacturer's protocols. Cells were transfected and incubated at 37°C in a

humidified 5% CO_2 atmosphere for 48 hr in culture media, without FBS or penicillin/streptomycin, containing the Leu-FectA and shRNAi lentiviral particles. Following the 48 hr, culture media containing FBS and penicillin/streptomycin was added, and cells were grown for one week. Puromycin was then added at 2 mg/mL, and the cells were incubated until no untransfected cells (cultured in parallel) remained. Transfected cells were allowed to continue proliferating in the presence of 1 mg/mL puromycin to a density of approximately 1,000,000 cells/mL. Cells were then sorted on a BD FACS Aria III BSL2 cell sorter (BD Biosciences, San Jose, CA) (University of Alberta, Faculty of Medicine & Dentistry Flow Cytometry Facility) for GFP-positive cells and maintained in culture media with 1 µg/mL puromycin. GFP expression was assessed on each cell passage using a Zeiss inverted widefield epifluorescence Axio Observer Z1 microscope (Oberkochen, Germany) at 388 nm, and cells were resorted if expression started to decrease (this was typically done every five passages to ensure sufficient signal and knockdown of target).

3.2.12) Data analysis and statistics

Data are expressed as mean plus or minus standard deviation (SD) from independent experiments done in technical duplicate or triplicate. Nonlinear curves are fitted to the transport, and MTT data and statistical analyses were performed using GraphPad Prism 10.1.1 software. In all cases, if the *P* value determined from a statistical test was less than 0.05, the difference was considered significant, and the null hypothesis (no difference between data sets) was rejected. MTT curves were statistically determined to fit either a one-phase or biphasic curve fit using an extra sum of squares F-test. Correlation data were fit using linear regression and statistically tested using the Spearman rank correlation coefficient. Influx data were fit using a one-phase association for time course data, and Michaelis-Menten curves were fit to the concentration-dependent uptake

data for determination of the Michaelis constant (K_m) and maximum rate of velocity (V_{max}) values. Statistical differences between K_m and V_{max} values were determined using the extra sum-of-squares F test. Significant differences between multiple groups were assessed using a one-way or two-way ANOVA, corrected for multiple comparisons with the Holm-Sidak method.

Chapter 4: Characterization of recombinant ENBT1 in HEK293 cells

4.1) INTRODUCTION

Nucleobase analogue drugs are used as antiviral and anticancer agents, with one of the most established being 6-MP, used in the maintenance phase of therapy for ALL. These compounds are generally pro-drugs in that they need to be metabolized by intracellular enzymes to their active phosphorylated derivatives. The first step in this activation process is the transport of the nucleobase analogues into the target cells. A number of different mechanisms have been proposed for the cellular entry of nucleobase analogues. Early studies suggested that a sodium-dependent nucleobase transporter identified in porcine LLC-PK1 cells was the 6-MP transporter (Griffith and Jarvis 1993). However, this was found to be a defective pseudogene in humans (Yamamoto et al. 2010) and is thus not relevant to the clinical actions of these agents. OAT1 and OAT3 have also been shown to mediate the transport of nucleobase drugs such as 6-MP (Mori et al. 2004), but these transporters are limited in their expression profile and are notably absent in leukemia cells (Burckhardt 2012). The nucleoside transporters hENT1 and hENT2 can also transport nucleobases, including 6-MP, but with low affinity (K_m values greater than 1 mM; 1000-fold higher than therapeutic levels of 6-MP) (Yao et al. 2011). An earlier study using mouse ENT2 overexpressing Cos-7 cells reported that 6-MP had a 14 μM K_m for ENT2 (Nagai et al. 2007), suggesting that there may be species differences in ENT2 affinity for 6-MP.

In 2007, a novel nucleobase transport system was characterized in human MVECs and given the designation ENBT1 (Bone and Hammond 2007). Using transporter-selective inhibitors, it was determined that ENBT1 was distinct from any of the aforementioned putative nucleobase transporters and was blocked by nucleobase analogues such as 6-MP and 6-TG at concentrations in the low μM range. ENBT1 activity was also described in a variety of other cell lines, including human osteosarcoma cells (U2OS), rat osteosarcoma cells (UMR), Madin-Darby canine kidney

(MDCK) cells, PK15-nucleoside transporter deficient cells, and rat MVEC, but it was notably absent in HEK293 cells (Bone and Hammond 2007). However, the gene encoding ENBT1 was not known at that time, and other than a study that showed that ENBT1 could be modulated by oxidative stress in an ischemia-reperfusion injury model (Bone et al. 2014), no further analysis was done.

In late 2015, *SLC43A3*, an orphan member of the amino acid transporter gene family (Bodoy et al. 2013), was shown to encode a protein that led to the cellular uptake of the nucleobases adenine and hypoxanthine when expressed in MDCKII cells (Furukawa et al. 2015), with characteristics almost identical to those described previously for ENBT1 (Bone and Hammond 2007). Those investigators also found that the *SLC43A3*-encoded transporter could be inhibited by 6-MP. *SLC43A3* is expressed at low to moderate levels in most tissues, including bone marrow, and has been identified in myeloid and lymphoid cell lines (Human Protein Atlas) (Thul et al. 2017; Uhlen et al. 2015). None of the aforementioned studies, however, considered the fact that *SLC43A3* exists as multiple splice variants. Many of the variants differ in the 5'-UTR, but two encode full-length proteins that differ in the absence (*SLC43A3_1*) or presence (*SLC43A3_2*) of a 13 amino acid insert in the first predicted extracellular loop **(Figure 5)**. The study examining recombinant *SLC43A3* expression in MDCKII cells used the isoform one variant (Furukawa et al. 2015). No studies have been done on the functional characteristics of the protein encoded by *SLC43A3_2*, nor has 6-MP actually been shown to be a substrate for either of these transporter variants. If the two *SLC43A3* isoforms differ in function or substrate selectivity, their differential expression in cells may impact the effectiveness of nucleobase analogue drug substrates. This chapter will define the characteristics of adenine and 6-MP transport by the ENBT1 variants encoded by *SLC43A3_1* and *SLC43A3_2* expressed in HEK293 cells.

4.2) RESULTS

4.2.1) Transfection of HEK293 cells with *SLC43A3*

To ensure that the stable cell transfection protocol was successful, qualitative PCR was conducted using cDNA prepared from untransfected HEK293 and *SLC43A3*-transfected HEK293 cells **(Figure 7A)**. The untransfected and vector-only transfected HEK293 cells expressed minimal levels of *SLC43A3* isoform 1, and there was no detectable isoform 2 transcript, supporting prior data that these cells do not have measurable ENBT1-mediated nucleobase flux capacity (Bone and Hammond 2007). In contrast, the *SLC43A3*-transfected cell lines expressed high levels of the respective *SLC43A3* transcript **(Figure 7A)**. Both *SLC43A3* isoform-encoded proteins were also detected by immunoblotting using either anti-ENBT1 **(Figure 7B)** or anti-MYC **(Figure 7C)** antibodies, with about 6-fold more isoform 1 detected than isoform 2 (relative to β-actin). Henceforth, the encoded protein will be referred to as ENBT1.1 (isoform 1) and ENBT1.2 (isoform 2). It was also noted that the size of the band (~62 kDa) was much larger than the expected native ENBT1 based on its amino acid sequence (estimated to be ~55 kDa). It was hypothesized that it may be a result of glycosylation. Therefore, *SLC43A3_1*-transfected HEK293 cell protein lysates were extracted and treated with or without PNGase F for 1 hr at 37°C. Incubation with PNGase F showed a decrease in size relative to the untreated group that was near the estimated weight of the native ENBT1 (~55 kDa).

Figure 7: Stable transfection of HEK293 cells with *SLC43A3_1* and *SLC43A3_2*

A) Transfection of HEK293 cells with *SLC43A3* was confirmed using PCR with the RT-PCR primers specific for *SLC43A3* (top) and *GAPDH* (bottom) shown in **Table 3**. cDNA was prepared from Total RNA isolated from untransfected HEK293 cells or HEK293 cells stably transfected with *SLC43A3_1* or *SLC43A3_2*. **B)** Membranes were prepared from HEK293 cells and cells transfected with *SLC43A3_1* (ENBT1.1) and *SLC43A3_2* (ENBT1.2). Samples were resolved on SDS-PAGE gels, transferred to polyvinyl membranes and probed with anti-ENBT1 and anti-β-actin antibodies. **C)** Parallel immunoblot analyses were performed as described above but using anti-MYC and anti-β-actin antibodies. **D)** The same immunoblot (Anti-MYC) from **Panel C** was conducted, but prior to loading, cell lysates from *SLC43A3_1* (ENBT1.1) transfected cells were treated with or without PNGase F for 1 hr at 37°C.

Figure 7

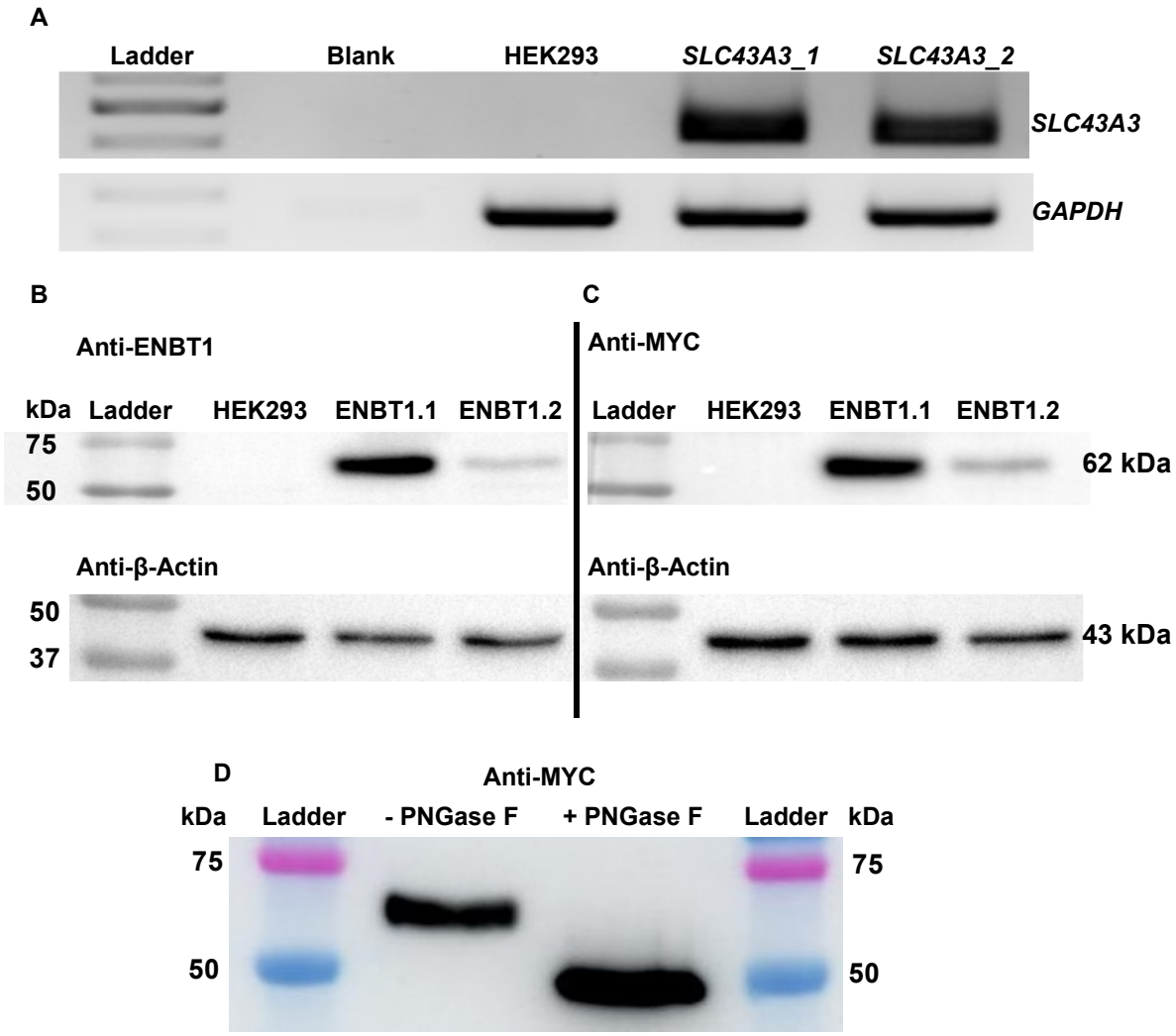
A
Ladder
Blank
HEK293
SLC43A3_1
SLC43A3_2
SLC43A3
GAPDH
B
Anti-ENBT1
kDa
Ladder
HEK293
ENBT1.1
ENBT1.2
75
50
Anti-β-Actin
50
37
C
Anti-MYC
Ladder
HEK293
ENBT1.1
ENBT1.2
62 kDa
Anti-β-Actin
43 kDa
D
Anti-MYC
kDa
Ladder
- PNGase F
+ PNGase F
Ladder
kDa
75
50
75
50

4.2.2) Gene expression analysis

The more sensitive RT-qPCR analyses indicated that HEK293 cells did express low levels of *SLC43A3*, but the *SLC43A3_1* transfected and *SLC43A3_2* transfected cells had more than 3240-fold and 840-fold higher levels of the respective transcript than untransfected HEK293 cells **(Figure 8A)**. Interestingly, cells stably transfected with the empty vector, pcDNA3.1(-), showed a 10-fold decrease in endogenous *SLC43A3* expression **(Figure 8A)**. To determine if transfection of HEK293 cells with *SLC43A3*, or the vector alone, led to compensatory changes in other relevant genes, the level of expression was examined for nucleoside transporters *SLC29A1* (ENT1), *SLC29A2* (ENT2), and *SLC29A4* (ENT4), the efflux pumps *ABCC4* (MRP4) and *ABCC5* (MRP5), and the intracellular enzymes involved in 6-MP metabolism, *TPMT* and *HPRT*. *ABCC5* was downregulated, and *TPMT* and *HPRT* were upregulated in the vector-transfected cells **(Figure 8B)**. In contrast, in cells transfected with *SLC43A3*, the transcripts for *SLC29A2, ABCC4, and ABCC5* were found to be downregulated in both the *SLC43A3_1*-transfected **(Figure 8C)** and *SLC43A3_2*-transfected **(Figure 8D)** cells relative to control HEK293 cells. In addition, the *SLC43A3_2* transfected cells displayed a significant decrease in the *SLC29A4* transcript **(Figure 8D)**. No changes were noted for the other transcripts measured.

Figure 8: Compensatory changes in gene expression upon transfection of HEK293 cells with *SLC43A3*

Gene expression, assessed by RT-qPCR, is shown relative to the amount detected in untransfected HEK293 cells. Expression was normalized to *GAPDH* transcript levels in each individual experiment. **Panel A** shows the relative expression of *SLC43A3* in HEK293 cells stably transfected with the respective *SLC43A3_1, SLC43A3_2*, or empty vector (pcDNA3.1(-)) construct (n=5). **Panels B-D** shows the relative expression of ENT1 (*SLC29A1*), ENT2 (*SLC29A2*), ENT4 (*SLC29A4*), MRP4 (*ABCC4*), MRP5 (*ABCC5*) and the enzymes *TPMT* and *HPRT* in HEK293 cells transfected with either 'empty' pcDNA3.1(-) (B), *SLC43A3_1* (**C**) or *SLC43A3_2* (**D**). Bars represent the mean ± SD of 5 independent samples. * Significant difference in expression between untransfected HEK293 cells and transfected HEK293 cells (Student's t-test, $P<0.05$, corrected for multiple comparisons with the Holm-Sidak method).

Figure 8

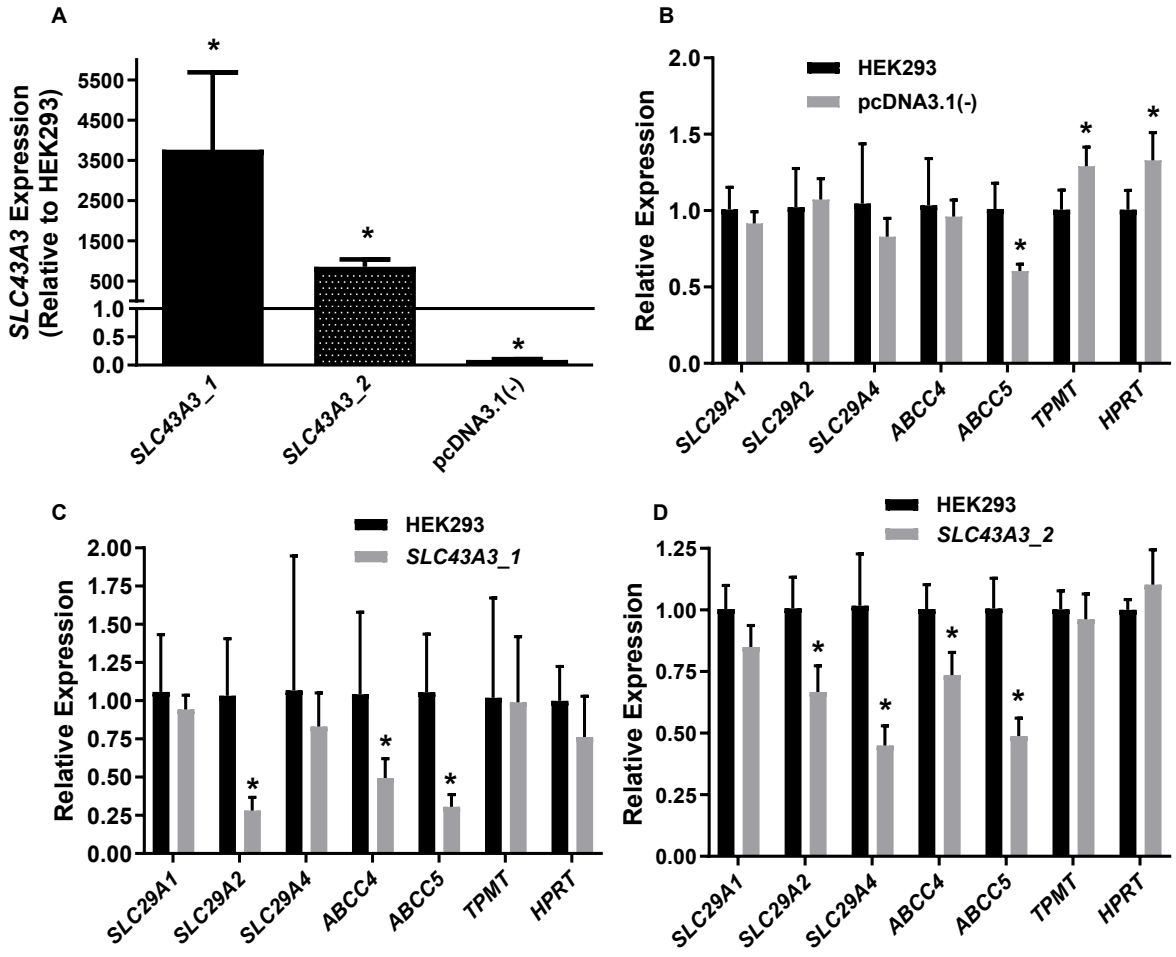
A
SLC43A3 Expression (Relative to HEK293)
5500
4500
3500
2500
1500
500
1.0
0.5
0.0
SLC43A3_1
SLC43A3_2
pcDNA3.1(-)
B
HEK293
pcDNA3.1(-)
Relative Expression
2.0
1.5
1.0
0.5
0.0
SLC29A1
SLC29A2
SLC29A4
ABCC4
ABCC5
TPMT
HPRT
C
HEK293
SLC43A3_1
Relative Expression
2.00
1.75
1.50
1.25
1.00
0.75
0.50
0.25
0.00
SLC29A1
SLC29A2
SLC29A4
ABCC4
ABCC5
TPMT
HPRT
D
HEK293
SLC43A3_2
Relative Expression
1.25
1.00
0.75
0.50
0.25
0.00
SLC29A1
SLC29A2
SLC29A4
ABCC4
ABCC5
TPMT
HPRT

4.2.3) [^{3}H] Adenine influx

Untransfected HEK293 cells, or cells transfected with empty vector, exhibited minimal time-dependent uptake of [^{3}H] adenine **(Figure 9A&B)**. In contrast, [^{3}H] adenine influx by cells transfected with *SLC43A3_1* was time-dependent with steady-state accumulation of 100 μM [^{3}H] adenine (67 ± 11 pmol/μl) achieved within 10 sec **(Figure 9A)** reflecting the high level of expression of ENBT1.1 in these cells **(see Figure 7)**. When the background (untransfected HEK293 cell-associated [^{3}H] adenine) was subtracted, an initial rate of ENBT1.1-mediated transport of 18 ± 9 pmol/μl/sec (for 100 μM [^{3}H] adenine) was estimated by extrapolation of the uptake profile to 0.5 sec. The transport efficiency of this system made it necessary to conduct full-time courses at each substrate concentration to allow the determination of transporter kinetics based on initial rates (estimated from uptake at 0.5 sec derived from curves fitted to each independent experiment). In contrast, ENBT1.2-mediated [^{3}H] adenine influx in the *SLC43A3_2* transfected cells was slower with an initial rate for 100 μM [^{3}H] adenine influx of 6 ± 2 pmol/μl/sec **(Figure 9B)** reflecting the relatively lower level of ENBT1.2 protein in the transfected HEK293 cells **(Figure 7B)**. Thus, initial rates for ENBT1.2-mediated influx were estimated from the experimentally determined 2 sec uptake time point. The results of these kinetic experiments are shown in **Figure 9C**. [^{3}H] Adenine transport by ENBT1.1 had a K_m of 37 ± 26 μM and a V_{max} of 34 ± 6 pmol/μl/sec. ENBT1.2 had a K_m for adenine (40 ± 26 μM) similar to that of ENBT1.1 and a V_{max} of 7.9 ± 1.6 pmol/μl/s.

Figure 9: [^{3}H] Adenine transport by *SLC43A3*-encoded ENBT1

HEK293 cells and cells transfected with *SLC43A3_1* **(A)**, *SLC43A3_2* or the empty pcDNA3.1(-) vector **(B)** were incubated with 100 μM [^{3}H] adenine at room temperature for the specified times and then centrifuged through oil. Cell pellets were digested overnight in 1 M NaOH and assessed for [^{3}H] content using standard liquid scintillation counting techniques to define pmol adenine accumulated per μl cell pellet. ENBT1-mediated uptake was defined as the difference in cellular accumulation by the *SLC43A3*-transfected cells (*SLC43A3*-HEK293) and that observed in the untransfected HEK293 cells assessed in parallel. Data points represent the mean ± SD of 6 **(Panel A)** or 5 **(Panel B)** experiments done in duplicate. **C)** The kinetics of ENBT1.1 (*SLC43A3_1*)- and ENBT1.2 (*SLC43A3_2*)-mediated uptake of [^{3}H] adenine were determined by assessing the uptake of a range of concentrations of [^{3}H] adenine as described for **Panels A and B**. Initial rates of influx were estimated as the transporter-mediated uptake at 0.5 sec extrapolated from time course profiles as shown in **Panel A** (ENBT1.1) or directly from the 2 sec uptake time point (**Panel B**; ENBT1.2). Data shown are the mean ± SD of n=5 experiments.

Figure 9

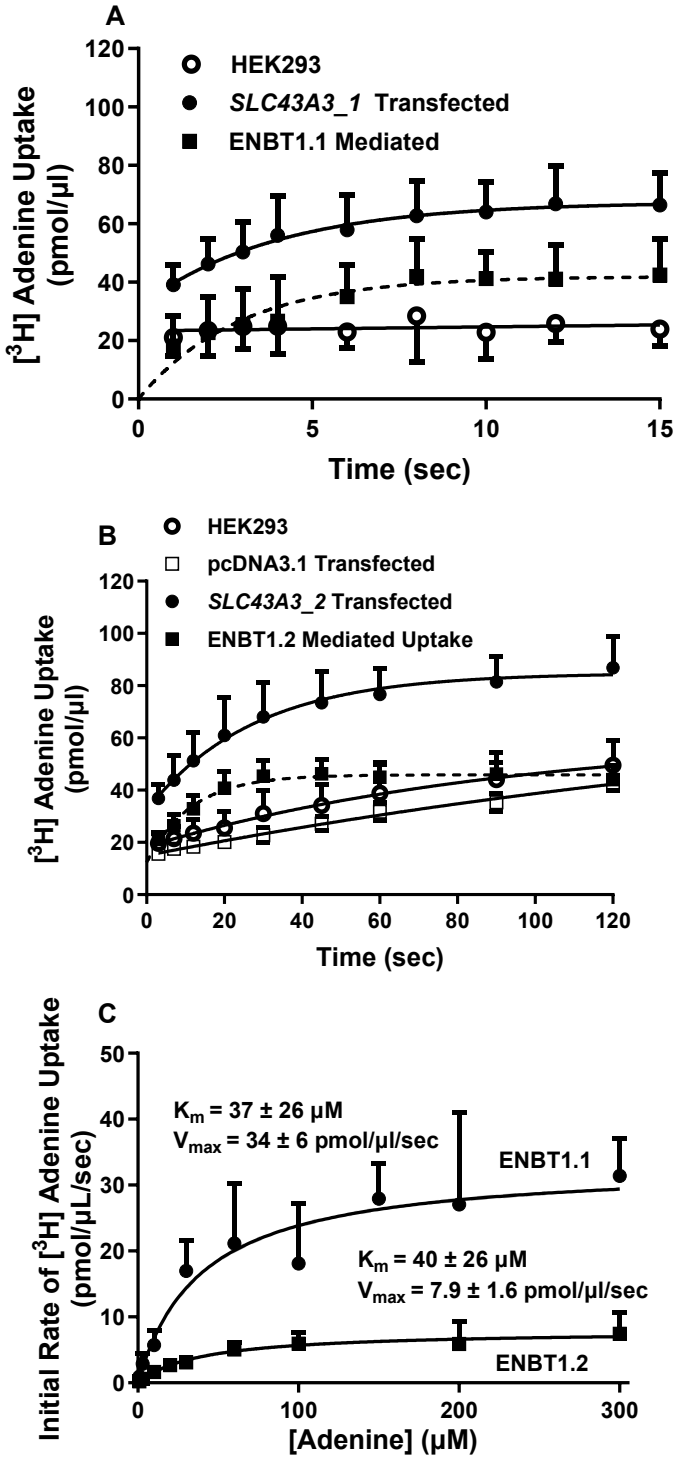
A
HEK293
SLC43A3_1 Transfected
ENBT1.1 Mediated
[3H] Adenine Uptake (pmol/µl)
Time (sec)
B
HEK293
pcDNA3.1 Transfected
SLC43A3_2 Transfected
ENBT1.2 Mediated Uptake
[3H] Adenine Uptake (pmol/µl)
Time (sec)
C
Km = 37 ± 26 µM
Vmax = 34 ± 6 pmol/µl/sec
ENBT1.1
Km = 40 ± 26 µM
Vmax = 7.9 ± 1.6 pmol/µl/sec
ENBT1.2
Initial Rate of [3H] Adenine Uptake (pmol/µL/sec)
[Adenine] (µM)

4.2.4) Inhibition of ENBT1-mediated adenine uptake by tyrosine kinase inhibitors

A previous study has demonstrated that various tyrosine kinase inhibitors may inhibit ENBT1 (Damaraju et al. 2015). Furthermore, the study noted that imatinib and dasatinib, which are used to treat Ph-positive ALL, may inhibit ENBT1. Adenine uptake was assessed in *SLC43A3_2*-HEK293 cells in the presence of 10 μM tyrosine kinase inhibitors (TKI) (imatinib, dasatinib, erlotinib, nilotinib, and gefitinib) or the absence of inhibitors. All TKIs assessed showed significant inhibition of ENBT1 **(Figure 10A)**. Gefitinib was the most effective, with ENBT1 uptake dropping to 31 ± 6% of control. Concentration-response curves were conducted in *SLC43A3_2*-HEK293 cells **(Figure 10B).** Gefitinib displayed a concentration-dependent inhibition of ENBT1 with an IC_{50} value of 5.4 ± 0.5 μM in the *SLC43A3_2*-HEK293 cells. The K_i value was calculated using the Cheng-Prusoff equation (Cheng and Prusoff 1973) and was determined to be 2.7 μM.

Figure 10: Tyrosine kinase inhibitors inhibit ENBT1-mediated adenine uptake

A) The uptake of [^{3}H] adenine in *SLC43A3_2*-HEK293 cells was assessed using a 2 sec time point in the presence and absence of 10 μM TKIs gefitinib, imatinib, nilotinib, erlotinib, and dasatinib. Data were normalized as percent of control uptake where 100% was defined as the uptake [^{3}H] adenine in the absence of inhibitor (no inhibitor) and 0% was defined as the uptake in untransfected HEK293 cells. Each bar represents the mean ± SD of 6 experiments done in duplicate. * Indicates a significant difference from no inhibitor (One-way ANOVA with the post hoc Holm-Sidak test, $P<0.05$). **B)** A range of concentrations (30 nM – 100 μM) of gefitinib was assessed for their ability to inhibit the 2 sec uptake of 30 μM [^{3}H] adenine in *SLC43A3_2*-HEK293 cells. Data was normalized as percent of control uptake with 100% defined as the uptake of adenine in the absence of inhibitor and 0% defined as the uptake in untransfected HEK293 cells. Sigmoid curves were fitted to these data for the determination of IC_{50} values, which were used to calculate the inhibitor K_i values shown in the text. Each point represents the mean ± SD of n=5 experiments done in duplicate.

Figure 10

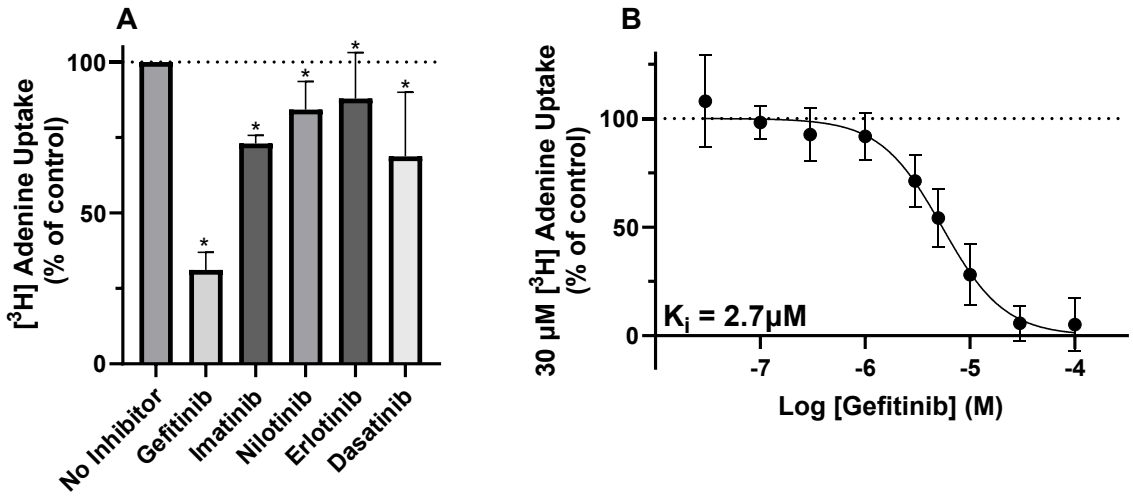
A
[3H] Adenine Uptake (% of control)
100
50
0
No Inhibitor
Gefitinib
Imatinib
Nilotinib
Erlotinib
Dasatinib
B
30 µM [3H] Adenine Uptake (% of control)
100
50
0
Ki = 2.7µM
-7
-6
-5
-4
Log [Gefitinib] (M)

4.2.5) ENBT1-mediated [^{14}C] 6-MP influx

Similar studies were then conducted using [^{14}C] 6-MP as the substrate. As seen for the [^{3}H] adenine uptake assays, the 'background' uptake of [^{14}C] 6-MP in the untransfected HEK293 cells was higher than expected for this assay protocol. However, this background was not affected by the addition of the ENT1/ENT2 inhibitor DY (1 μM) (Ward et al. 2000), the pan-nucleoside transporter substrate uridine (1 mM) (Young et al. 2013), nor the nucleobase adenine (1 mM), indicating it was not due to the operation of other nucleoside/nucleobase transporters such as ENT1, ENT2, or concentrative nucleoside transporter (CNT) 3 that others have suggested to mediate 6-MP uptake (Yao et al. 2011; Nagai et al. 2007). Nor did the OAT inhibitor novobiocin (300 μM) (Duan and You 2009; Burckhardt 2012; Mori et al. 2004) have an effect on the residual accumulation of 100 μM 6-MP (17.8 ± 1.8 pmol/μl/2sec and 17.2 ± 1.8 pmol/μl/2sec) in the absence and presence of novobiocin, respectively, n=5). Nor was the background reduced by additional washing steps, suggesting that this remaining [^{14}C] was likely cell membrane-associated [^{14}C] 6-MP or nonspecific binding of [^{14}C] 6-MP to the polypropylene centrifuge tubes. HEK293 cells expressing ENBT1.1 accumulated 100 μM 6-MP in a time-dependent manner, and this uptake could be inhibited completely by 1 mM adenine **(Figure 11A)**. **Figure 11B** shows a similar time course profile for 30 μM 6-MP uptake by untransfected and pcDNA3.1(-)-transfected HEK293 cells and ENBT1.2-expressing HEK293 cells in the presence and absence of 1 mM adenine. As for the ENBT1.1 expressing cells **(Figure 11A)**, the uptake of 6-MP by ENBT1.2 was inhibited completely by 1 mM adenine, with uptake in the presence of adenine not significantly different from 6-MP uptake by the untransfected HEK293 cells or by the vector-only transfected cells **(Figure 11B)**. Therefore, 6-MP uptake in the presence of 1 mM adenine was defined as a non-transporter-mediated background in subsequent experiments. Time courses of uptake by ENBT1.1

were constructed for a range of [^{14}C] 6-MP concentrations (1 – 300 μM), with initial rates represented by the rate of influx at 0.5 sec extrapolated from individual time course curves. ENBT1.1-mediated [^{14}C]6-MP accumulation was saturable with a K_m of 163 ± 126 μM and a V_{max} of 82 ± 30 pmol/μl/sec **(Figure 11C)**. ENBT1.2-expressing cells accumulated [^{14}C] 6-MP at less than half the rate of ENBT1.1-transfected cells (V_{max} = 32 ± 8 pmol/μl/sec), again reflecting the lower expression level of ENBT1.2, relative to ENBT1.1. However, the K_m of [^{14}C] 6-MP for ENBT1.2 mediated transport (188 ± 68 μM) was not significantly different from that determined for ENBT1.1.

Figure 11: [^{14}C] 6-MP transport by *SLC43A3*-encoded ENBT1

HEK293 cells and cells transfected with *SLC43A3_1* **(A)**, *SLC43A3_2* or empty pcDNA3.1(-) **(B)** were incubated with 100 μM **(A)** or 30 μM **(B)** [^{14}C] 6-MP at room temperature, in the presence and absence of 1 mM adenine, for the specified times and then centrifuged through oil. Cell pellets were digested overnight in 1 M NaOH and assessed for [^{14}C] content using standard liquid scintillation counting techniques to define pmol 6-MP accumulated per μl cell pellet. Data points represent the mean ± SD of 7 **(Panel A)** or 5 **(Panel B)** experiments done in duplicate. **C)** The kinetics of ENBT1.1 (*SLC43A3_1*)- and ENBT1.2 (*SLC43A3_2*)-mediated [^{14}C] 6-MP uptake were determined by assessing the uptake of a range of concentrations of [^{14}C] 6-MP as described for **Panels A and B**. Initial rates of influx were estimated as the transporter-mediated uptake (calculated as the difference in cellular uptake ± adenine) at 0.5 sec interpolated from time course profiles as shown in **Panel A** (ENBT1.1), or directly from the 2 sec uptake time point (ENBT1.2). Data shown are the mean ± SD of n=5 experiments.

Figure 11

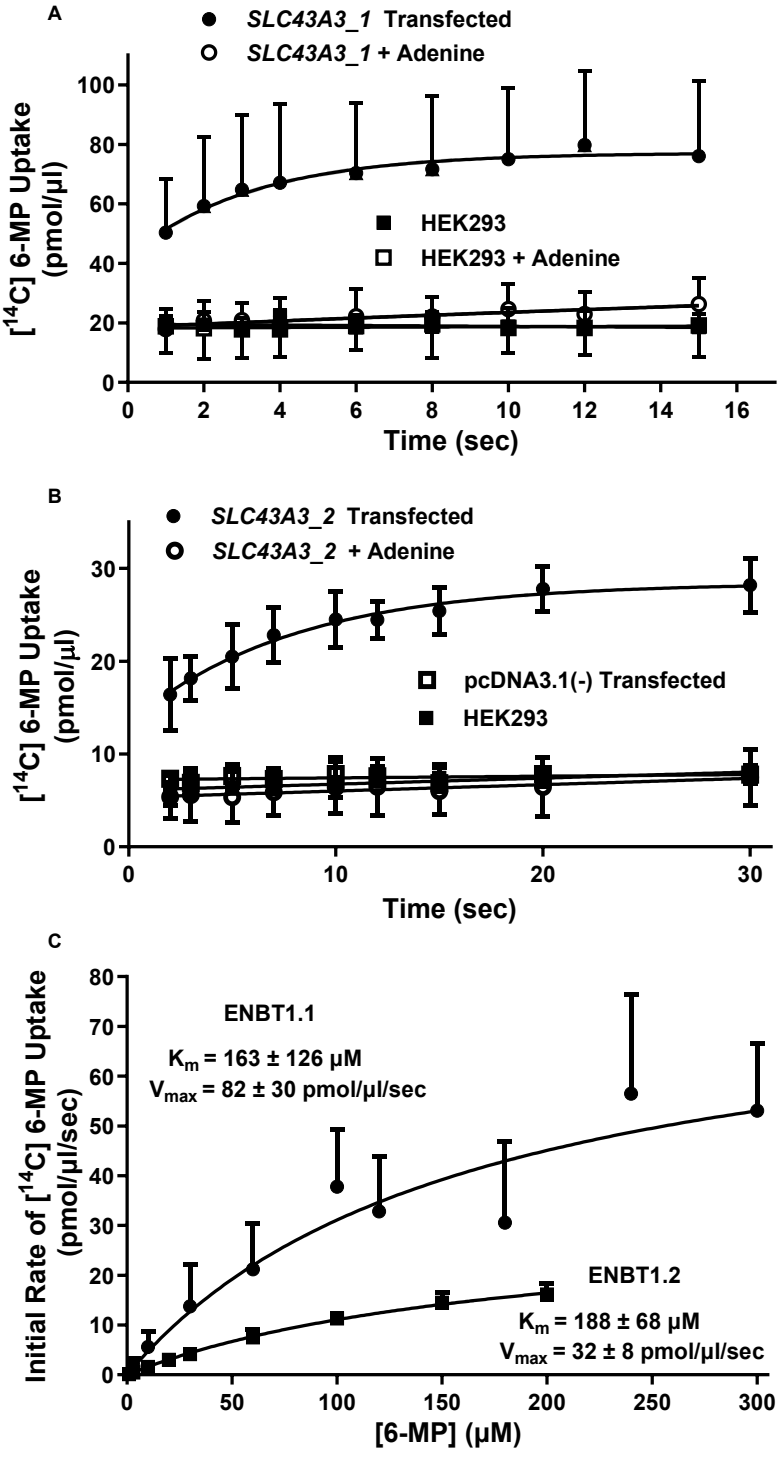
A
SLC43A3_1 Transfected
SLC43A3_1 + Adenine
HEK293
HEK293 + Adenine
[14C] 6-MP Uptake (pmol/µl)
Time (sec)
B
SLC43A3_2 Transfected
SLC43A3_2 + Adenine
pcDNA3.1(-) Transfected
HEK293
[14C] 6-MP Uptake (pmol/µl)
Time (sec)
C
ENBT1.1
Km = 163 ± 126 µM
Vmax = 82 ± 30 pmol/µl/sec
ENBT1.2
Km = 188 ± 68 µM
Vmax = 32 ± 8 pmol/µl/sec
Initial Rate of [14C] 6-MP Uptake (pmol/µl/sec)
[6-MP] (µM)

4.2.6) Inhibition of ENBT1-mediated 6-MP uptake

Several compounds were screened initially at a single concentration for their ability to inhibit the 2 sec influx of [^{14}C] 6-MP in the ENBT1.1 **(Figure 12A)** and ENBT1.2 **(Figure 12B)** expressing HEK293 cells. All inhibitors tested affected ENBT1.1 and ENBT1.2 mediated 6-MP uptake similarly. The nucleoside adenosine (1 mM) did not affect 6-MP uptake. Nor did MTX, a folate analogue that is used concurrently with 6-MP in the treatment of ALL. However, the adenosine analogue 2-chloroadenosine (2-ClAdo) did produce a significant inhibition of 6-MP uptake (58 ± 6% inhibition of ENBT1.1 at 1 mM). NBMPR, the selective ENT1 nucleoside transport inhibitor, inhibited ENBT1.1-mediated 6-MP uptake by 41% at 100 μM. As has been shown previously (Furukawa et al. 2015), D22, an ENT4 inhibitor, was a relatively effective inhibitor of ENBT1, achieving 71 ± 6% inhibition of ENBT1.1 at 10 μM. The nucleobases 6-TG and hypoxanthine, at 1 mM, inhibited 100 μM [^{14}C] 6-MP uptake by ENBT1.1 by 86 ± 14% and 61 ± 6%, respectively. The 6-MP metabolite 6-MeMP also inhibited ENBT1.1-mediated 6-MP uptake by 91 ± 6% at 1 mM. 6-TG is a nucleobase analogue similar in structure to 6-MP. Therefore, it is anticipated that 6-TG may also be a substrate for ENBT1 and, as such, should act as a competitive inhibitor of 6-MP for the substrate recognition site. To test this, uptake was examined over a range of concentrations of [^{3}H] adenine by ENBT1.1 in the presence of 750 μM 6-TG **(Figure 12)**. [^{3}H] Adenine uptake in the presence of 6-TG had a significantly higher apparent K_m with no significant difference in V_{max} relative to data obtained in the absence of 6-TG **(see Figure 9C)**, indicative of competitive inhibition kinetics. Full concentration-inhibition profiles were then constructed for 6-TG, 6-MeMP, and D22 **(Figure 12D)**, allowing the calculation of the inhibitory constant (K_i) values of 67 ± 30, 73 ± 20, and 1.0 ± 0.4 μM, respectively, for their inhibition of 6-MP uptake by ENBT1.1.

Figure 12: Inhibition of [^{14}C] 6-MP transport in *SLC43A3*-transfected HEK293 cells

The uptake of [^{14}C] 6-MP by ENBT1.1 (100 μM; **Panel A**) and ENBT1.2 (30 μM; **Panel B**) was assessed using a 2 sec time point in the presence and absence of the indicated concentration of MTX, 6-TG, 6-MeMP, 2Cl-Ado, adenosine, 2-deoxyadenosine (Deoxy-Adenosine), hypoxanthine, uridine, NBMPR, D22. Data were normalized as percent of control uptake where 100% was defined as the uptake [^{14}C] 6-MP in the absence of inhibitor and 0% was defined as the uptake in the presence of 1 mM adenine. Each bar represents the mean ± SD of 5 experiments done in duplicate. *Significantly different from 100% control (Student's t-test, $P<0.05$, corrected for multiple comparisons with the Holm-Sidak method). **C)** Time courses were constructed at various concentrations of [^{3}H] adenine, as described in **Figure 9C**, in the presence of 750 μM 6-TG. Initial rates of transport were derived from the rate of uptake at 0.5 sec as extrapolated from the time course profiles. The dashed line indicates the analogous data obtained in the absence of 6-TG **(from Figure 9C)**. Data points represent the mean ± SD of 5 experiments done in duplicate. **D)** A range of concentrations of 6-TG, 6-MeMP, and D22 were assessed for their ability to inhibit the 2 sec uptake of 100 μM [^{14}C] 6-MP by the ENBT1.1. Data was normalized as percent of control uptake with 100% defined as the uptake of 100 μM [^{14}C] 6-MP in the absence of inhibitor and 0% defined as that in the presence of 1 mM adenine. Sigmoid curves were fitted to these data for the determination of IC_{50} values, which were used to calculate the inhibitor K_i values shown in the text. Each point represents the mean ± SD of n=5 experiments done in duplicate.

Figure 12

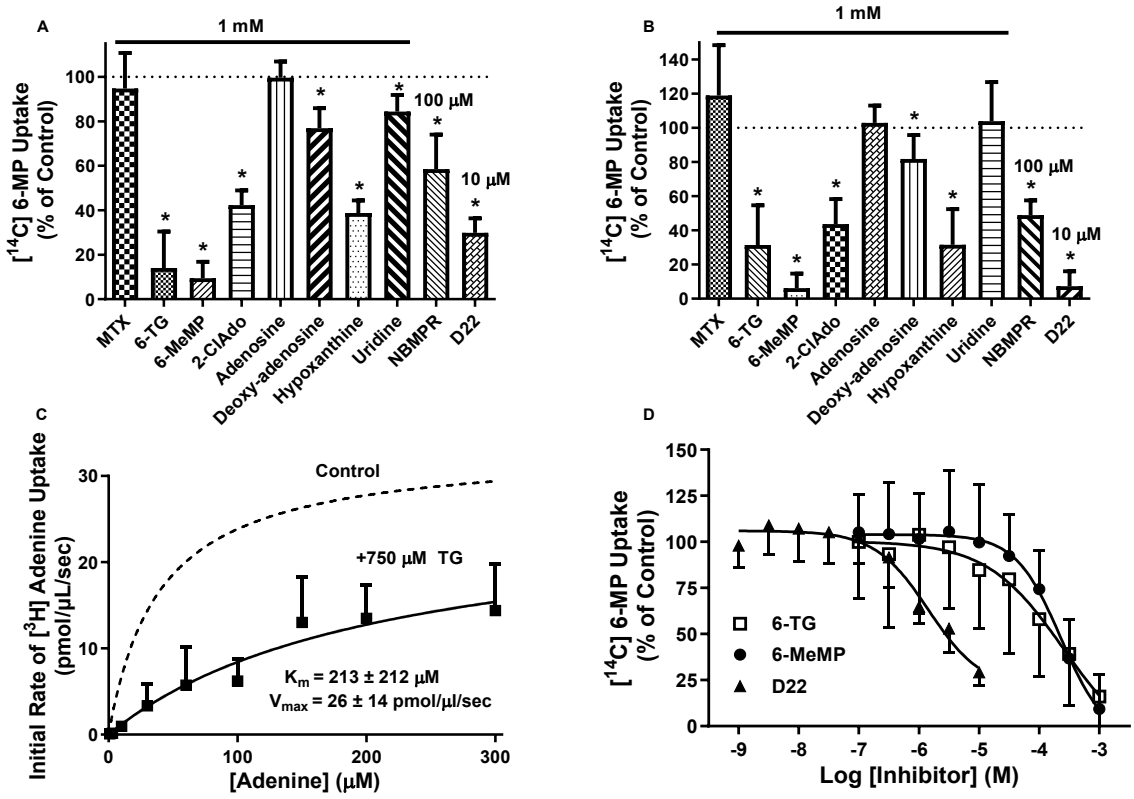
A
1 mM
100 µM
10 µM
[14C] 6-MP Uptake (% of Control)
MTX
6-TG
6-MeMP
2-ClAdo
Adenosine
Deoxy-adenosine
Hypoxanthine
Uridine
NBMPR
D22
B
1 mM
100 µM
10 µM
[14C] 6-MP Uptake (% of Control)
C
Control
+750 µM TG
Km = 213 ± 212 µM
Vmax = 26 ± 14 pmol/µl/sec
Initial Rate of [3H] Adenine Uptake (pmol/µL/sec)
[Adenine] (µM)
D
6-TG
6-MeMP
D22
[14C] 6-MP Uptake (% of Control)
Log [Inhibitor] (M)

4.2.7) ENBT1-mediated 6-MP efflux

To determine whether ENBT1 was bidirectional with respect to the transport of 6-MP, *SLC43A3_1*-transfected HEK293 cells were loaded with 100 μM [^{14}C] 6-MP for 30 sec and assessed for the rate of release of [^{14}C] upon resuspension of cells in substrate-free media. The change in intracellular 6-MP was measured with time after resuspension **(Figure 13)**. Due to the handling time required for this experimental procedure, the minimum efflux time that could be attained reliably was 10 sec. From the data shown in **Figure 13**, it is apparent that, in the absence of any competing compound, a new steady-state was achieved prior to the first recordable time point of 10 sec (estimated rate constant of at least 0.35 sec^{-1}). This rapid rate of efflux was not unexpected, given the rapid rate of 6-MP influx by ENBT1.1 in this recombinant transfection model **(see Figure 11A)**. The presence of extracellular adenine decreased the rate of 6-MP efflux significantly. The efflux time course in the presence of 1 mM adenine fits best to a one-phase decay profile, allowing the calculation of an efflux rate constant of 0.020 ± 0.004 sec^{-1}. Efflux in the presence of 100 μM adenine fits best to a two-phase decay profile, with the first phase having a rate constant of 0.15 ± 0.10 sec^{-1} and the second phase having a rate constant of 0.014 ± 0.016 sec^{-1}, which is not significantly different from the rate of efflux in the presence of 1 mM adenine. When the same type of analysis was done using untransfected HEK293 cells, it was necessary to use a 10 min loading time for [^{14}C] 6-MP to achieve comparable intracellular concentrations to those seen using the 30 sec loading time in the *SLC43A3*-transfected cells. The efflux of 6-MP from the HEK293 cells was dramatically slower than that observed in the *SLC43A3*-transfected cells, with over 70% of the initial load still retained within the cell after 3 min. Adenine (1 mM) had a slight but significant inhibitory effect on [^{14}C] 6-MP efflux from the untransfected HEK293

cells (rate constants of 0.14 ± 0.08 sec^{-1} and 0.07 ± 0.04 sec^{-1} in the absence and presence of adenine, respectively) suggesting that it was mediated by endogenous nucleobase transporters.

Figure 13: 6-MP efflux by ENBT1.1

Cells were loaded with 100 μM [^{14}C] 6-MP for 30 sec (*SLC43A3_1* transfected) or 10 min (untransfected HEK293), pelleted and then, to initiate efflux, suspended in either NMG buffer (Control) or buffer containing either 1 mM or 100 μM adenine. Aliquots of cell suspension were centrifuged through an oil layer at the specified times and processed to assess intracellular [^{14}C] content. Data are expressed as % of initial [^{14}C] 6-MP load with 100% defined as [^{14}C] 6-MP content at zero time extrapolated from curves fit (one phase exponential decay) to the 1 mM adenine data. One-phase or two-phase decay profiles were fitted to the data depending on which fit was determined to be statistically superior ($P<0.05$; extra sum of squares F-test). Each point represents the mean ± SD of 5 (Control and 100 μM adenine) or 10 (1 mM adenine) experiments.

Figure 13

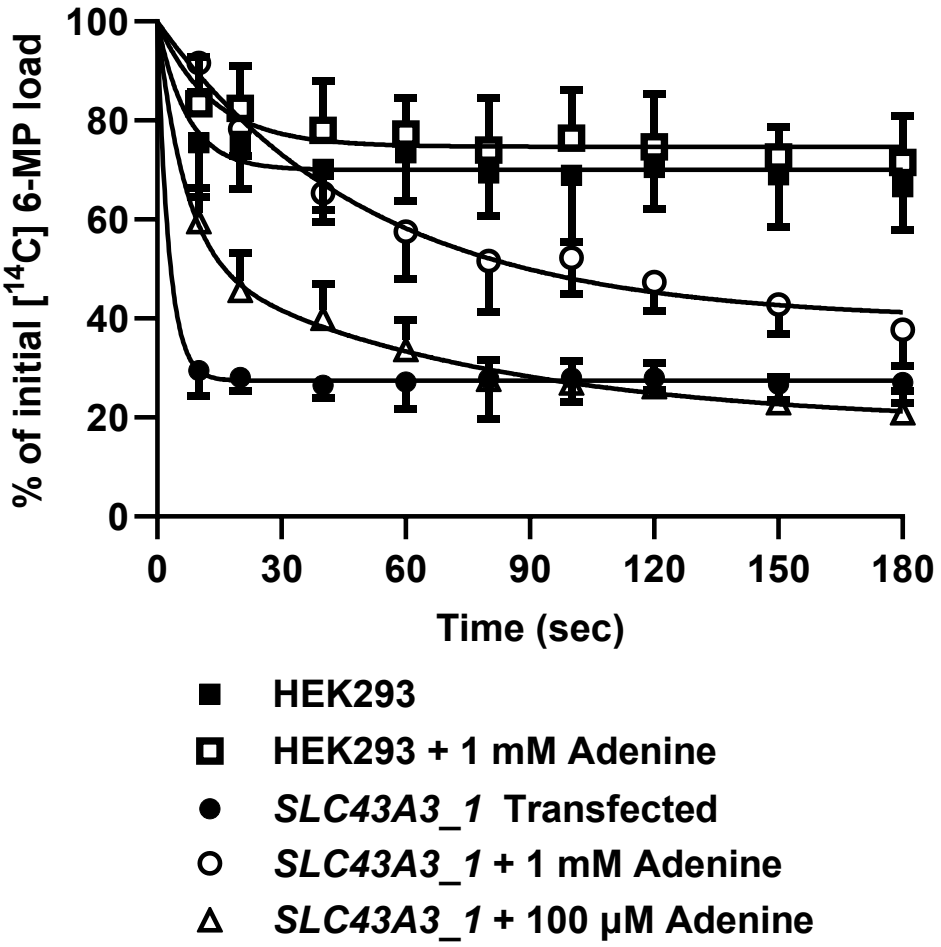
% of initial [14C] 6-MP load
100
80
60
40
20
0
0
30
60
90
120
150
180
Time (sec)
HEK293
HEK293 + 1 mM Adenine
SLC43A3_1 Transfected
SLC43A3_1 + 1 mM Adenine
SLC43A3_1 + 100 µM Adenine

4.2.8) Contribution of ENT2 and MRP4/5 on 6-MP efflux

Given the two-phase decay profile observed in the presence of 100 μM adenine and the finding that *ABCC4*, *ABCC5*, and *SLC29A2* expression all declined concomitantly with the increased expression of *SLC43A3_1* by the HEK293 cells **(Figure 8C)**, the effect of the MRP4 inhibitor ceefourin-1, the MRP5 inhibitor zaprinast, and the ENT2 inhibitor DY were assessed on the efflux of 6-MP from the *SLC43A3_1* transfected cells **(Figure 14)**. Ceefourin-1 had no significant effect on the initial rate of 6-MP efflux in the absence of adenine (0.29 ± 0.16 sec^{-1} and 0.38 ± 0.86 sec^{-1}, in the absence and presence of ceefourin-1, respectively**) (Figure 14A)**. However, ceefourin-1 did reveal a second slower phase of efflux with a rate constant of 0.02 ± 0.04 sec^{-1}. The rapidity of the efflux in the absence of adenine made these data difficult to interpret due to the large errors in the calculated parameters. Therefore, the effect of ceefourin-1 was also assessed in combination with 100 μM adenine. Efflux in the presence of 100 μM adenine was monophasic in this case with a rate constant of 0.16 ± 0.04 sec^{-1}, similar to the first phase of efflux in the presence of 100 μM adenine seen previously, as reported in **Figure 13**. The addition of ceefourin-1 led to a biphasic efflux profile with the initial fast component having a rate constant of 0.26 ± 0.24 sec^{-1} (which is not significantly different from that seen in the absence of ceefourin-1) and a significantly larger slower component with a rate constant of 0.014 ± 0.014 sec^{-1}. In the absence of ceefourin-1, $75 \pm 2\%$ of the efflux occurred at the faster rate in the presence of 100 μM adenine. However, in the presence of ceefourin-1, this initial fast component represented only 42 ± 18 % of the total efflux. In contrast, the MRP5 inhibitor zaprinast had no significant effect on 6-MP efflux in either the presence or absence of 100 μM adenine **(Figure 14B)**. Likewise, the combination of ceefourin-1 and zaprinast **(Figure 14C)** affected 6-MP efflux in a manner similar

to that seen using ceefourin-1 alone. The *SLC29A2* inhibitor DY also had no effect on the efflux of 6-MP **(Figure 14D)**.

Figure 14: Effect of ceefourin-1, zaprinast, and DY on 6-MP efflux

SLC43A3_1 transfected HEK293 cells were loaded with 100 μM [^{14}C] 6-MP for 30 sec pelleted and then, to initiate efflux, suspended in either NMG buffer (Control) or buffer containing either 1 mM or 100 μM adenine, as indicated, in the presence and absence of the MRP4 inhibitor ceefourin-1 (50 μM; **A**), the MRP5 inhibitor zaprinast (100 μM; **B**), a combination of 50 μM ceefourin-1 and 100 μM zaprinast (**C**), or the ENT2 inhibitor DY (1 μM; **D**). Aliquots of cell suspension were centrifuged through an oil layer at the specified times and processed to assess intracellular [^{14}C] content. Data are expressed as % of initial [^{14}C] 6-MP load, and either a one-phase or two-phase decay profile was fitted to the data based on which fit was determined to be statistically superior ($P<0.05$; extra sum of squares F-test). Each point represents the mean ± SD of 5 experiments.

Figure 14

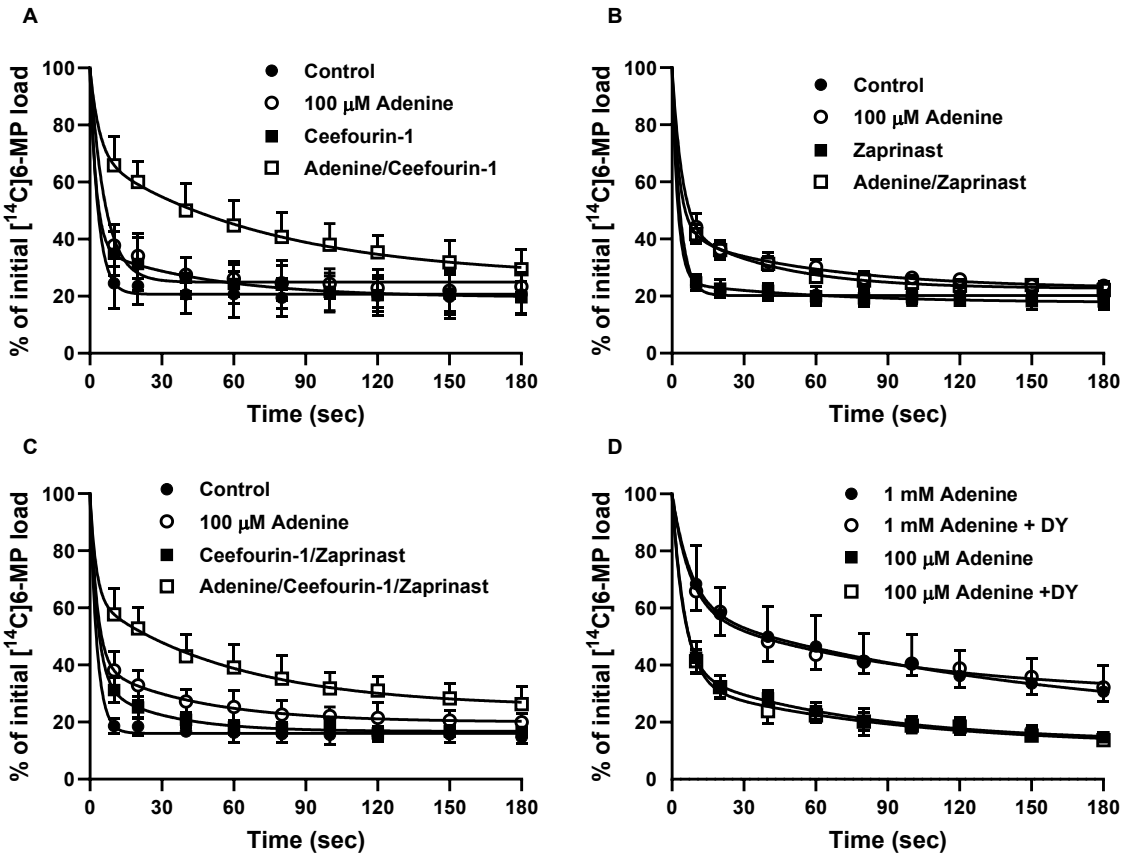
A
% of initial [14C]6-MP load
Time (sec)
Control
100 μM Adenine
Ceefourin-1
Adenine/Ceefourin-1
B
% of initial [14C]6-MP load
Time (sec)
Control
100 μM Adenine
Zaprinast
Adenine/Zaprinast
C
% of initial [14C]6-MP load
Time (sec)
Control
100 μM Adenine
Ceefourin-1/Zaprinast
Adenine/Ceefourin-1/Zaprinast
D
% of initial [14C]6-MP load
Time (sec)
1 mM Adenine
1 mM Adenine + DY
100 μM Adenine
100 μM Adenine +DY

4.2.9) *SLC43A3* expression and cell viability

If ENBT1 is critical to the cellular accumulation of 6-MP, and hence its sensitivity, then one might predict that the *SLC43A3*-transfected HEK293 cells would be more sensitive to the toxic effects of 6-MP than untransfected HEK293 cells. In untransfected HEK293 cells, 6-MP had a biphasic effect on cell viability with 51 ± 16% of the cells impacted by 6-MP with an EC_{50} of 5.6 μM ($logEC_{50}$ = -5.25 ± 0.16), while the remaining cells were relatively resistant to 6-MP with 35 ± 8% remaining even after 48 hr exposure to 1 mM 6-MP **(Figure 15A)**. Cells transfected with the 'empty' pcDNA3.1(-) plasmid had a similar biphasic profile with an EC_{50} of 13.2 μM ($LogEC_{50}$ = -4.878 ± 0.064) for 6-MP mediated sensitivity, which is slightly, but significantly higher (Extra sum-of-squares F test, $P<0.05$), higher than that seen for the untransfected HEK293 cells **(Figure 15A)**. Cells transfected with *SLC43A3_1* and *SLC43A3_2* also had biphasic responses to 6-MP. However, in both cases, there was a significantly lower proportion of 6-MP resistant cells after transfection with *SLC43A3* (50 ± 26% and 23 ± 8% for untransfected and *SLC43A3_1* transfected cells, and 44 ± 14% and 28 ± 6% for untransfected and *SLC43A3_2* transfected HEK293 cells, respectively). Transfection of HEK293 cells with *SLC43A3* also enhanced the sensitivity of the cells to the toxic effects of 6-MP by 7-fold **(Figure 15A)** and 15-fold **(Figure 15B)** for the *SLC43A3_1* and *SLC43A3_2* transfected cells, respectively. $LogEC_{50}$ values for 6-MP-mediated sensitivity of -6.05 ± 0.22 and -6.29 ± 0.06 were calculated from these data for the *SLC43A3_1* and *SLC43A3_2* transfected cells, respectively. To assess the contribution of the nucleoside/nucleobase transporters ENT1 and ENT2 to the actions of 6-MP, similar analyses were conducted in the presence and absence of DY **(Figure 15C)**. DY, at concentrations sufficient to completely block ENT1 and ENT2 (1 μM), did not change the sensitivity profile of 6-MP in either the untransfected or *SLC43A3_1*-transfected HEK293 cells. In addition, the inclusion of G418 in

the media during the 48 hr MTT assay did not affect the sensitivity of either the *SLC43A3_1* or the *SLC43A3_2*-transfected cells to 6-MP **(Figure 15D)**.

Figure 15: *SLC43A3* transfection of HEK293 cells significantly enhances the sensitivity of 6-MP

HEK293 cells and cells transfected with 'empty' pcDNA3.1(-) plasmid or *SLC43A3_1* (**A**) or *SLC43A3_2* (**B**) were plated at a density of 5 x 10^4 cells/well in 24-well plates and incubated with a range of concentrations of 6-MP for 48 hr at 37°C in a humidified incubator (5% CO_2/95% air). Cell viability was assessed using the MTT assay and expressed as a percent of the cell viability measured at 48 hr in the absence of 6-MP (% of control). Biphasic dose-response curves were fitted to these data, and each point represent the mean ± SD of 5 experiments. *Significant difference between HEK293 cells and *SLC43A3*-transfected cells (Student's t-test, $P<0.05$, corrected for multiple comparisons with the Holm-Sidak method). **C)** Effect of DY on the sensitivity to 6-MP. HEK293 cells and cells transfected with *SLC43A3_1* were incubated with a range of concentrations 6-MP in the absence and presence of the ENT1/ENT2 blocker DY (1 μM). Cell viability was assessed, and data was presented as described for **Panels A & B** (n=5). **D**) Effect of G418 on the sensitivity to 6-MP in *SLC43A3_1*- and *SLC43A3_2*-transfected HEK293 cells. Cell viability was assessed upon incubation with the indicated concentrations of 6-MP for 48 hr, as described for **Panels A & B**, in the presence and absence of G418 (n=5).

Figure 15

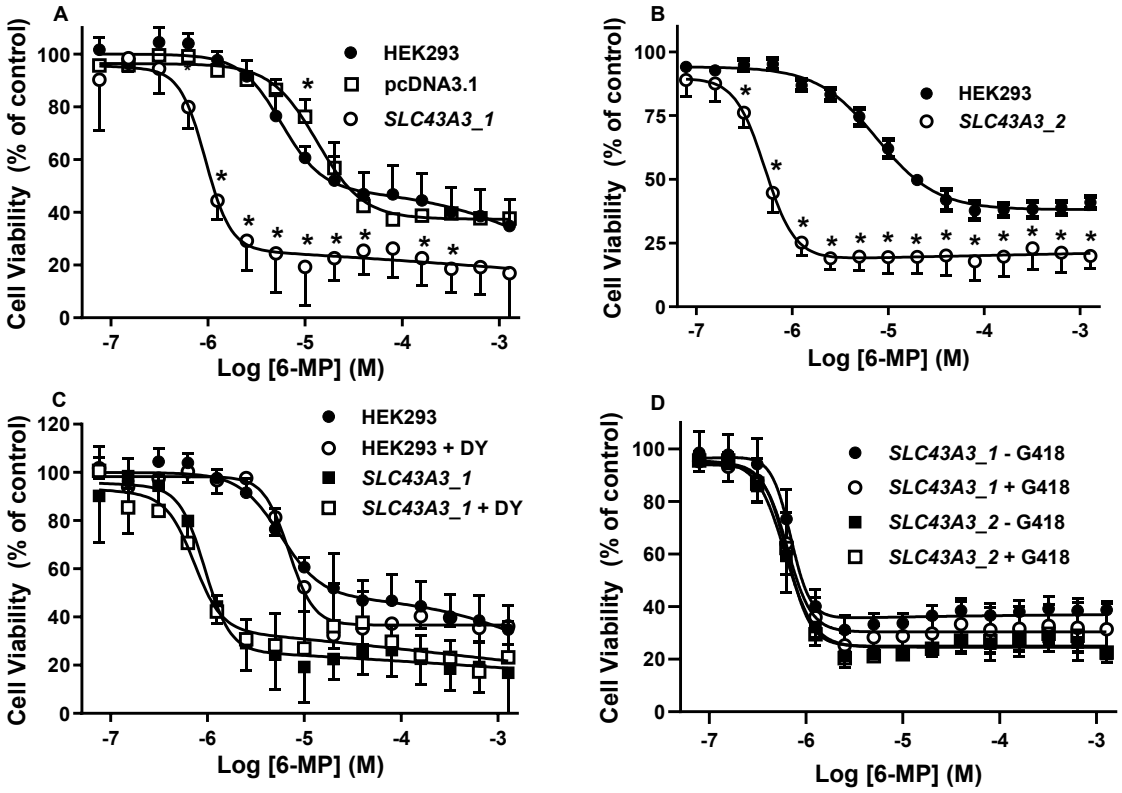
A
Cell Viability (% of control)
HEK293
pcDNA3.1
SLC43A3_1
Log [6-MP] (M)
B
Cell Viability (% of control)
HEK293
SLC43A3_2
Log [6-MP] (M)
C
Cell Viability (% of control)
HEK293
HEK293 + DY
SLC43A3_1
SLC43A3_1 + DY
Log [6-MP] (M)
D
Cell Viability (% of control)
SLC43A3_1 - G418
SLC43A3_1 + G418
SLC43A3_2 - G418
SLC43A3_2 + G418
Log [6-MP] (M)

4.2.10) Contribution of MRP4/5 on 6-MP sensitivity

To confirm that the increased sensitivity to 6-MP was due to the *SLC43A3* transfection and not the concomitant decrease in *ABCC4* (MRP4) and *ABCC5* (MRP5) expression observed in the *SLC43A3* isoform 1 transfected HEK293 cells **(see Figure 8)**, the sensitivity to 6-MP were repeated in the presence of the MRP4 and MRP5 inhibitors ceefourin-1 and zaprinast. These inhibitors, alone or in combination, had no significant effect on the EC_{50} of 6-MP in untransfected HEK293 cells **(Figure 16A)** or cells transfected with *SLC43A3_1* **(Figure 16B)**. However, ceefourin-1 alone or in combination with zaprinast did cause a significant increase in the relative proportion of 6-MP-resistant cells in the untransfected HEK293 cells **(Figure 16A)** (29 ± 2% and 40 ± 2% of the cells were resistant to 6-MP in the absence and presence of ceefourin/zaprinast, respectively). For the *SLC43A3_1* transfected cells, a similarly significant shift in the resistant cell population upon treatment with the combination of ceefourin-1 and zaprinast was observed (38 ± 2% and 49 ± 2% resistant cells in the absence and presence of the inhibitors, respectively) **(Figure 16B)**. Suppression of *ABCC4* expression (by ~60%; **Figure 16D**) by stable transfection of cells with *ABCC4*-targeted short interfering RNA (siRNA) also led to a significant enhancement in the proportion of *SLC43A3_1* transfected HEK293 cells resistant to 6-MP (26 ± 8% and 37 ± 6% without and with siRNA, respectively) **(Figure 16C)**, but had no effect on the cytotoxic EC_{50} of 6-MP. However, siRNA suppression of *ABCC4* in the untransfected HEK293 cells led to a significant decrease in the proportion of cells resistant to 6-MP (44 ± 2% and 34 ± 2% without and with siRNA, respectively). There was also a significant enhancement in the sensitivity to 20 μM and 30 μM 6-MP in the siRNA transfected cells. However, there was no change in the overall EC_{50} of 6-MP for the sensitive population of cells (due to the increase in the relative percentage of 6-MP sensitive cells after siRNA transfection).

Figure 16: Effect of MRP4 and MRP5 inhibition on the sensitivity to 6-MP

HEK293 cells **(A)** and cells transfected with *SLC43A3_1* **(B)** were exposed to a range of concentrations of 6-MP for 48 hr in the absence (control) and presence of ceefourin-1 (50 μM), zaprinast (100 μM), or a combination of both, and then assessed for cell viability as described for Figure 9. * Significant difference between control and ceefourin-1 + zaprinast. # Significant difference between control and ceefourin-1 alone (Student's t-test, $P<0.05$, corrected for multiple comparisons with the Holm-Sidak method, n=6). **C)** HEK293 cells and cells transfected with *SLC43A3_1* were stably transfected with *ABCC4* (MRP4)-targeted siRNA. The sensitivity to a range of concentrations of 6-MP was then assessed in these cell lines, as described in **Figure 15**. * Significant effect of siRNA in *SLC43A3_1* transfected HEK293 cells. # Significant effect of siRNA in untransfected HEK293 cells (Student's t-test, $P<0.05$, corrected for multiple comparisons with the Holm-Sidak method, n=5). **D)** *ABCC4* transcript levels (± siRNA transfection) in the untransfected and *SLC43A3_1*-transfected HEK293 cells used for the experiments shown in **Panel C**. *GAPDH* transcript levels were determined in parallel for each cell line to correct for loading differences. Densitometry analysis indicates that *ABCC4* transcript was suppressed by ~60% in the siRNA-transfected cells.

Figure 16

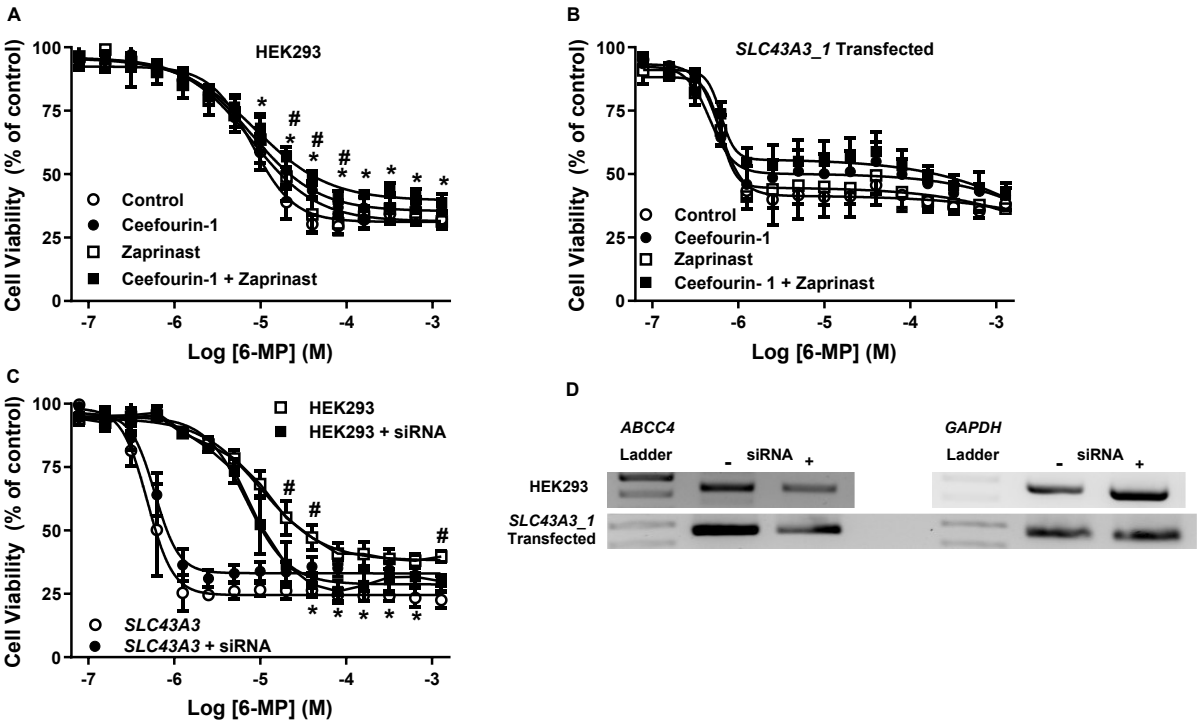
A
HEK293
Cell Viability (% of control)
Control
Ceefourin-1
Zaprinast
Ceefourin-1 + Zaprinast
Log [6-MP] (M)
B
SLC43A3_1 Transfected
Cell Viability (% of control)
Control
Ceefourin-1
Zaprinast
Ceefourin- 1 + Zaprinast
Log [6-MP] (M)
C
HEK293
HEK293 + siRNA
Cell Viability (% of control)
SLC43A3
SLC43A3 + siRNA
Log [6-MP] (M)
D
ABCC4
Ladder
- siRNA +
GAPDH
Ladder
- siRNA +
HEK293
SLC43A3_1 Transfected

4.3) DISCUSSION

Both isoforms of *SLC43A3* encode proteins (ENBT1.1 and ENBT1.2) that mediate the uptake of the endogenous nucleobase adenine and the nucleobase analogue 6-MP with comparable K_m values **(Figure 9C** and **Figure 11C)**. Therefore, the 13 amino acid insert in the first extracellular loop of ENBT1.2 does not directly affect substrate affinity or transporter function. The K_m for adenine determined herein was similar to that reported for the *SLC43A3_1*-encoded ENBT1 expressed in MDCKII cells (Furukawa et al. 2015) and is also similar to that which was reported for an ENBT1-like transporter in human MVECs (Bone and Hammond 2007). ENBT1 is predicted to contain an N-linked glycosylation site within the first extracellular loop of the protein (Hornbeck et al. 2015). A large shift in band size on the western blot was noted using PNGase F, an endoglycosidase that cleaves N-linked oligosaccharide bonds, thus confirming that ENBT1 is glycosylated **(Figure 7D)**. It is unclear if glycosylation is required for ENBT1 function or translocation to the plasma membrane and would be of interest to study in the future. Transfection of HEK293 cells with *SLC43A3* (either isoform) resulted in a dramatic enhancement in the ability of 6-MP to decrease cell viability **(Figure 15)**. This indicates that ENBT1 activity has a direct impact on the decrease in cell viability caused by 6-MP and that variations in *SLC43A3* expression may modify the therapeutic effectiveness of 6-MP. It is notable, however, that cells transfected with *SLC43A3_2* had a similar shift in cell viability caused by 6-MP as cells transfected with *SLC43A3_1*, even though the level of transfection with *SLC43A3_1* was 6-fold higher than that seen for *SLC43A3_2* **(Figure 7)**, and the *SLC43A3_1* cells had an ~2.5-fold higher rate of uptake of 6-MP than the *SLC43A3_2* cells **(Figure 11C)**. This may indicate that ENBT1-mediated 6-MP transport is rate limiting for 6-MP sensitivity only up to a certain point, after which the intracellular metabolic pathways are saturated, and the rate of intracellular 6-MP metabolism becomes limiting.

Stable transfection of HEK293 cells with *SLC43A3* (either isoform) decreased the expression of *SLC29A2* (ENT2), *ABCC4* (MRP4) and *ABCC5* (MRP5) **(Figure 8C** and **D)**. Transfection with *SLC43A3_2* also caused a downregulation of *SLC29A4* (ENT4). The downregulation of *ABCC5* may be due to the transfection or the influence of chronic exposure to G418, as a similar downregulation was seen in vector-only transfected cells **(Figure 8B)**. The vector controls did not exhibit downregulation of the other genes assessed in the *SLC43A3*-transfected cells. The downregulation of ENT2 and MRP4 may reflect compensation by the cells to the enhanced availability of nucleobases via ENBT1 to support intracellular metabolism (Senyavina and Tonevitskaya 2015). Both of these transporters are proposed to mediate the flux of 6-MP (Yao et al. 2011; Ansari et al. 2009; Peng et al. 2008; Janke et al. 2008; Tanaka et al. 2015). However, in terms of 6-MP sensitivity, a decrease in ENT2 activity would actually lead to reduced cellular uptake of 6-MP and, consequently, decreased sensitivity – opposite to that observed in the present study. hENT2 has a very low affinity for 6-MP (> 1 mM K_m) relative to ENBT1 (Yao et al. 2011), making it unlikely to contribute to 6-MP uptake at clinically relevant concentrations. Furthermore, the ENT1/ENT2 inhibitor DY impacted neither the uptake nor the efflux of 6-MP, nor did it affect the 6-MP sensitivity curve. The reason for the downregulation of ENT4 in the *SLC43A3_2* transfected cells is obscure. ENT4 is predominantly a monoamine transporter at neutral pH and transports adenosine under acidic pH conditions (Zhou et al. 2010; Zhou et al. 2007), and nucleobases are not substrates for ENT4 (Engel, Zhou, and Wang 2004). On the other hand, the efflux pumps MRP4 and MRP5 are proposed to be associated with 6-MP resistance (Chen, Lee, and Kruh 2001; Fukuda and Schuetz 2012; Reid et al. 2003), and their decreased expression was thus considered a potential factor in the increased 6-MP sensitivity

observed. The MRP5 inhibitor zaprinast had no effect on 6-MP uptake, efflux, or sensitivity, suggesting that MRP5 does not contribute to the 6-MP activity in this model. The MRP4 inhibitor ceefourin-1, however, significantly decreased the rate of efflux of 6-MP from *SLC43A3*-transfected HEK293 cells **(Figure 14A)**, suggesting that MRP4 does contribute to 6-MP efflux in this model. This conjecture is supported by the finding that transfection of the HEK293 cells with siRNA for *ABCC4* led to an increase in their sensitivity to 6-MP at higher concentrations **(Figure 16C)**. However, MRP4-mediated efflux of 6-MP is slower than that mediated by ENBT1 and only has an impact at lower levels of ENBT1 activity (such as when ENBT1 is partially inhibited with 100 μM adenine). The dominance of ENBT1 in this model is also apparent from the finding that ceefourin-1 had no effect on the sensitivity to 6-MP in *SLC43A3*-transfected cells **(Figure 16)**. These data indicate that the compensatory downregulation of *ABCC4* in the *SLC43A3*-transfected cells is not contributing to the enhanced sensitivity of the *SLC43A3*-transfected cells to 6-MP. Interestingly, incubation of the untransfected HEK293 cells with MRP4 inhibitors resulted in a significant increase in the relative proportion of 6-MP resistant cells **(Figure 16A)**. A similar trend was seen for the *SLC43A3_1* transfected cells. One could speculate that MRP4 inhibition may lead to increased intracellular cAMP (an endogenous substrate for MRP4), causing cell cycle arrest in the HEK293 cells, as has been reported in other cell lines (Copsel et al. 2011; Zhao et al. 2014), such that more of the cells enter a quiescent phase where they are not affected by 6-MP.

The significant contribution of ENBT1 to the cellular accumulation of 6-MP suggests that changes in the expression of this transporter may impact the therapeutic effectiveness of 6-MP. Little is known about the regulation of *SLC43A3* expression. However, the striking downregulation (10-fold) of *SLC43A3* expression in cells transfected with pcDNA3.1(-) only (vector control;

Figure 8A) suggests that it is transcriptionally regulated. This decrease in expression also impacts the cellular sensitivity to 6-MP, as evidenced by a decrease in 6-MP EC_{50} (2-fold) in the vector-transfected cells **(Figure 15A)**. It is possible that metabolic stress associated with the expression of aminoglycoside phosphotransferase (mediating the G418 resistance) in the transfected cells (Yallop and Svendsen 2001; Veraitch and Al-Rubeai 2005) and/or chronic exposure to G418, may be responsible for this downregulation. A previous study has shown that the uptake of hypoxanthine by ENBT1 in human MVECs is decreased by oxidative stress associated with hypoxia (Bone et al. 2014). This may have ramifications for the use of nucleobase analogues in cancer therapy, as there is a strong association between oxidative stress and cancer progression (Sosa et al. 2013).

Given the importance of ENBT1 to the cellular uptake of 6-MP, this system may be a target for drug-drug interactions which impact 6-MP therapeutic activity. Both isoforms (ENBT1.1 and ENBT1.2) had comparable sensitivities to the inhibitors tested **(Figure 12)**. **Figure 12** confirmed that MTX and adenosine do not have an affinity for ENBT1. MTX, as a folate analogue, would not be expected to inhibit ENBT1, but the confirmation of no direct drug-drug interactions via ENBT1 is important, given that MTX is used in conjunction with 6-MP for chemotherapy. Likewise, the ENT1 blocker NBMPR was relatively ineffective against 6-MP uptake by ENBT1. The finding that adenosine and uridine had no inhibitory activity also confirms that ENT1, ENT2, CNT1, CNT2 and CNT3 are not involved in 6-MP uptake in our model. However, 2-ClAdo did significantly inhibit 6-MP uptake. This adenosine analog can induce apoptosis in B-cells and is resistant to metabolism by adenosine deaminase (Bastin-Coyette et al. 2008), making it more metabolically stable than adenosine. 2-ClAdo has also been reported to inhibit an ENBT1-like

transporter in PK15-NTD (nucleoside transport deficient) cells (Hoque et al. 2008). It is possible that the addition of the halogen group leads to enhanced recognition by nucleobase transporters. In this regard, 2-ClAdo has a higher affinity for the nucleoside transporter ENT2 than it does for ENT1 (Hammond 1991), and ENT2 has a higher affinity for nucleobases than ENT1 (Yao et al. 2011). This chemical characteristic may be something to consider in the search for selective inhibitors of ENBT1. Also of interest is the finding that the 6-MP metabolite generated through the methylation of 6-MP by TPMT, 6-MeMP, inhibits ENBT1. ENBT1.1 is bidirectional in that it can also mediate the efflux of 6-MP from cells. Therefore, it is possible that the removal of 6-MeMP from cells via ENBT1 may contribute to cellular resistance to 6-MP, depending on the relative affinity of 6-MeMP for the transporter compared with subsequent intracellular enzymatic processes. It may be of value in future studies to determine how intracellular 6-MeMP affects the rate of uptake of 6-MP. A complex interplay between these two systems may explain some of the variability seen in the assessment of TPMT-mediated metabolism of 6-MP (Karas-Kuzelicki and Mlinaric-Rascan 2009; Chouchana et al. 2014). It was also determined that 6-TG inhibits 6-MP uptake and is itself a likely substrate for ENBT1. 6-TG is not as commonly used in the therapy of ALL due to the greater toxicity associated with its use (Vora et al. 2006; Stork et al. 2010), but it is used for the treatment of inflammatory bowel diseases such as Crohn's disease (Bar, Sina, and Fellermann 2013). Finally, TKIs were found to inhibit ENBT1, with gefitinib being the most effective, with a Ki value of 2.7 μM **(Figure 10)**. This supports a previous study that showed inhibition of an ENBT1-like transporter in human renal proximal tubule epithelial cells (Damaraju et al. 2015). Gefitinib is an epidermal growth factor receptor (EGFR) TKI utilized in the treatment of non-small cell lung cancer (Maemondo et al. 2010; Lynch et al. 2004; Shepherd et al. 2005). Notably, 6-MP is not utilized in non-small cell lung cancer, nor is gefitinib used in leukemia, and

thus would not lead to drug-drug interactions. However, the TKIs, imatinib and dasatinib, are used in conjunction with 6-MP in ALL patients who possess the Ph chromosome (BCR-ABL1) (Ottmann 2012). Imatinib is a first-generation BCR-ABL1 TKI typically used for first-line treatment of Ph-positive ALL, while dasatinib is a second-generation BCR-ABL1 TKI used when patients become resistant to imatinib due to mutations in the BCR-ABL1 (Kantarjian et al. 2010; Talpaz et al. 2006; Weisberg et al. 2007). This is because dasatinib can bind to both the active and inactive forms of BCR-ABL1, increasing its affinity relative to imatinib (Bradeen et al. 2006; Shah et al. 2004). However, dasatinib is less selective than imatinib and has been shown to interact with other receptor tyrosine kinases (Lombardo et al. 2004). Co-treatment with imatinib or dasatinib and 6-MP could result in an interaction and the inhibition of ENBT1 uptake of 6-MP, which could negatively impact the efficacy of treatment.

4.4) CONCLUSIONS

In summary, both variants of ENBT1 can mediate the transport of 6-MP and increased *SLC43A3* expression enhances the ability of 6-MP to induce a loss of cell viability. There are no apparent differences in the ENBT1 variants in terms of their affinity for adenine or 6-MP. Further studies examining whether differences in *SLC43A3* expression contribute to the variability in 6-MP effectiveness when used in the treatment of leukemia and inflammatory bowel disorders are clearly warranted.

4.5) LIMITATIONS

4.5.1) Recombinant expression model

Data from this study suggest an important role for ENBT1 in 6-MP transport and sensitivity in HEK293 cells. However, the above results were obtained using a recombinantly expressed model system, which is not necessarily representative of ENBT1 under endogenous regulation. It is well known that overexpression model systems lead to vast overexpression and thus lack clinical relevance. Furthermore, overexpression can lead to a depletion of cellular resources required for normal cell function, which leads to imbalances in protein levels across the board and, thus, an exaggeration of cellular effects (Moriya 2015). This burden on the cells can negatively impact protein translation, post-translational modifications, protein folding, trafficking, and degradation.

To address this, the endogenous function and regulation of ENBT1 in leukemia cells is assessed in **Chapters 5, 6, and 7**. Leukemia cells express high levels of ENBT1 and are under endogenous cellular regulation.

4.5.2) 6-MP efflux

The data above shows that ENBT1 can mediate the bidirectional transport of 6-MP in transfected HEK293 cells with potential contributions from MRP4. It was determined in **Figure 14** that ceefourin-1, an inhibitor of MRP4, altered the cellular efflux of 6-MP in the transfected cell line. Due to the dominant nature of ENBT1 in the efflux process, it is challenging to ascertain the true contribution MRP4 played in 6-MP efflux in the experiments. A follow-up experiment examining the efflux of other MRP4 substrates, like cAMP, cyclic guanosine monophosphate, or estradiol 17 beta-D-glucuronide, could clarify this issue (Chen, Lee, and Kruh 2001).

4.5.3) 6-MP cell viability

As noted above in **3.2.7**, the MTT assay was used to determine the sensitivity of cells to 6-MP. However, the reliance on the MTT assay throughout is a potential limitation, and another similar method should have been used to confirm the results of the MTT assay. Assays like the MTS, XTT, and WST-1, which have mechanisms similar to MTT by assessing the cells metabolic activity, could have been used for confirmation (Riss et al. 2004). Although 6-MP does have cytostatic effects that would be more sensitive in the MTT assay, 6-MP is also well known to induce cell death via the induction of apoptosis (Salser and Balis 1965). To determine this, the LDH assay would be useful for determining the proportion of cellular toxicity following treatment with 6-MP in the transfected HEK293 cells (Kumar, Nagarajan, and Uchil 2018). A preliminary study by another member of the Hammond Lab showed that using the LDH assay following treatment with 6-MP did cause cell toxicity (~20% total cellular toxicity after 48 hr with 100 μM 6-MP) (Chan Kim, personal communication, April 9, 2023). This is in stark contrast to the MTT assay, which had an ~80% loss in cell viability after 48 hr with 100 μM 6-MP **(Figure 15)**. This limitation is recognized for all future chapters in this thesis, which rely heavily on the MTT assay to determine 6-MP sensitivity, which measures the mitochondrial reduction of MTT to assess the cell's metabolic activity and, by extension, cell viability.

4.5.4) Mechanism of various inhibitors

The data above supports that several compounds interact with ENBT1 and can inhibit adenine and 6-MP uptake into cells. However, the mechanism of inhibition is unclear and rather than being just an inhibitor, it could also be a substrate for ENBT1. To confirm this, studies on the [^{3}H] or [^{14}C] uptake of the various compounds would be required to determine if they are truly a

substrate for ENBT1. This is important since several of the compounds are therapeutically active, like the TKIs, meaning that ENBT1 may also be a factor in their efficacy.

If they are not substrates of ENBT1, the mechanism of their inhibition would also be helpful to determine. By determining if they interact directly with the active site of ENBT1 or an allosteric site, we can further our understanding of ENBT1 structural recognition motifs to develop selectively targeted compounds against ENBT1.

Chapter 5: Characterization of endogenous ENBT1 in leukemia cells

5.1) INTRODUCTION

The nucleobase analog 6-MP, in combination with other drugs such as MTX, is a mainstay of maintenance protocols for the treatment of ALL (Pui et al. 2015; Toft et al. 2018), the most common malignancy in children and adolescents. Although the survival rate of pediatric patients with ALL has increased in recent decades, there are still about 15% of patients who do not respond adequately to treatment and experience relapses with far lower survival rates (Chouchana et al. 2015). A complicating factor in the use of 6-MP to treat ALL is the wide variability in its plasma concentration (Lonnerholm et al. 1986; Larsen et al. 2020), as well as in the levels of active intracellular thionucleotide metabolites, achieved with a standard dose (Lennard 1992; Estlin 2001; Schmiegelow et al. 2014). This suggests extensive inter-individual variability in factors that influence 6-MP metabolism and biodistribution. 6-MP must be metabolized by intracellular enzymes to its phosphorylated derivatives in the target cells to exert its cytotoxic effects. Changes in the activity of intracellular enzymes such as TPMT contribute to clinical variability in thioguanine nucleotide levels (Lennard et al. 2015; Abaji and Krajinovic 2017). However, *TPMT* polymorphisms do not explain all of the therapeutic variability observed, and particularly not the variable plasma concentrations (Chouchana et al. 2015; Patel and Papachristos 2015), nor do changes in other genes/proteins that have been linked with variations in 6-MP activity, such as *PRPS1, NUDT15, mTORC1, MSH6,* and *NT5C2* (Tzoneva et al. 2013; Li et al. 2015; Liu et al. 2017; Tanaka et al. 2015; Vo et al. 2017; Zgheib et al. 2017; Dieck et al. 2018; Evensen et al. 2018). Further understanding of factors that influence 6-MP activity is still required to optimize treatment protocols.

Hydrophilic drugs such as 6-MP require specific transporter proteins to enter and exit cells. Variations in transporter expression/activity are well known to impact both the clinical

effectiveness of drugs and their off-target toxicities (Nakanishi 2007; Colas, Ung, and Schlessinger 2016; Wu and Li 2018). Since 6-MP produces its therapeutic effects via interference with intracellular processes, the very first step in 6-MP action, prior to conversion to its therapeutic cytotoxic form, is its transfer into leukemic cells across the plasma membrane. The ABC transporters MRP4 (*ABCC4*) and MRP5 (*ABCC5*) are proposed to mediate the efflux of 6-MP and metabolites from cells (Wijnholds et al. 2000; Wielinga et al. 2002; Janke et al. 2008; Tanaka et al. 2015; Liu et al. 2017). However, the mechanism by which 6-MP gets into cells, especially lymphoblasts (the target in ALL treatment), remained elusive until the recent identification of ENBT1 encoded by the gene *SLC43A3*. There are two alternative splice variants of *SLC43A3* that have been shown in **Chapter 4** to encode transport proteins that are functionally similar with respect to their ability to transport 6-MP and adenine (Ruel et al. 2019). Furthermore, **Chapter 4** established that ENBT1, heterologously expressed in HEK293 cells, can transport 6-MP at concentrations within the therapeutic range and that changes in ENBT1 activity directly impact the ability of 6-MP to reduce cell viability. Given these findings, it is hypothesized that endogenous ENBT1 expression may be an important variable in 6-MP accumulation by ALL cells, and variations in ENBT1 activity may modify the therapeutic effectiveness of 6-MP. In the present chapter, for the first time, it is shown that ALL cells express *SLC43A3* and exhibit robust ENBT1-mediated 6-MP transport activity. Furthermore, the rate of 6-MP accumulation by these cell lines correlates directly with the level of expression of *SLC43A3*.

5.2) RESULTS

5.2.1) *SLC43A3* expression

All of the cell lines tested expressed both isoforms of *SLC43A3*, with isoform 1 being dominant in all cases **(Figure 17A & B)**. Immunoreactivity using an ENBT1-selective antibody was also detected at the molecular mass expected for both the native (~ 55 kDa) and glycosylated version (~62 kDa) of the ENBT1 protein in all cell lines **(Figure 17C)**. Most of the cell lines had similar levels of expression of *SLC43A3* transcript and ENBT1 protein **(Table 4)**, with the exception of NALM-6, SUP-B15, and MOLT-4, which had about a 2-fold lower expression relative to the other cell lines tested.

Figure 17: *SLC43A3* isoform expression and ENBT1 protein levels

cDNA was prepared from mRNA isolated from ALL-1, MOLT-4, REH, RS4;11, NALM-6, SUP-B15, and K562 human leukemia cell lines. Qualitative RT-PCR was used to screen for the two known isoforms of *SLC43A3* (*SLC43A3_1* and *SLC43A3_2)* using primers that flanked the region that differs between the two isoforms (to amplify both isoforms; **Panel A**) and a primer set where the forward primer was designed against the region that is unique to *SLC43A3_2* (to specifically amplify isoform 2; **Panel B)** (See **Table 3** for primer sequences). **Panel C** shows a representative immunoblot for ENBT1 in these cell lines. Samples were resolved on SDS-PAGE gels, transferred to polyvinyl membranes and probed with anti-ENTB1 (upper) and anti-β-actin (lower) antibodies. 'Ladder' indicates the respective DNA **(Panel A and B)** and protein **(Panel C)** molecular size ladders.

Figure 17

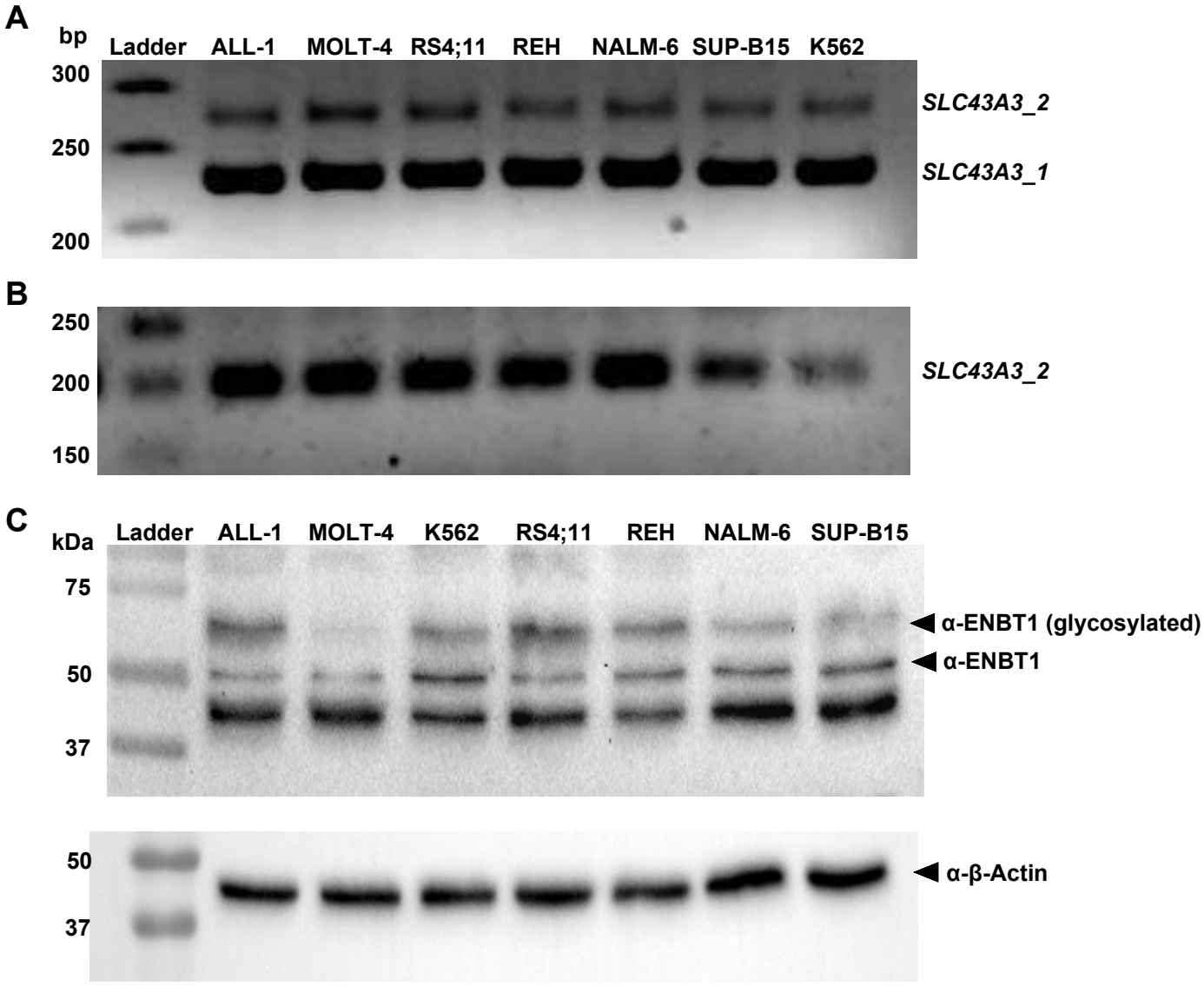
A
bp
Ladder
ALL-1
MOLT-4
RS4;11
REH
NALM-6
SUP-B15
K562
300
250
200
SLC43A3_2
SLC43A3_1
B
250
200
150
SLC43A3_2
C
kDa
Ladder
ALL-1
MOLT-4
K562
RS4;11
REH
NALM-6
SUP-B15
75
50
37
α-ENBT1 (glycosylated)
α-ENBT1
50
37
α-β-Actin

5.2.2) Expression of other transporters/enzymes

The expression of transcripts encoding enzymes involved in 6-MP metabolism (*HPRT, TPMT*) and other transporters (i.e., *ABCC4, ABCC5, SLC29A1, SLC29A2, SLC29A4*) that have been implicated in nucleoside/nucleobase flux are shown in **Figure 18**. Of all the genes tested, only *SLC29A4,* which encodes for ENT4, varied significantly among the cell lines with the SUP-B15 cells having zero expression. Furthermore, NALM-6 cells have ~50-fold lower expression than the ALL-1 cells.

Figure 18: Transcript levels of various enzymes and transporters potentially associated with 6-MP metabolism

Gene expression was assessed by semi-quantitative PCR and is shown relative to the ALL-1 cell line. Expression was normalized to 3 separate reference genes (*GAPDH, RNA18SN5, and ACTB*) and quantified using the ΔΔCt method. **(A-H)** Relative expression of *SLC43A3, TPMT, SLC29A1, SLC29A2, SLC29A4, HPRT1, ABCC4,* and *ABCC5* as compared to ALL-1 cell line. Lines represent the mean ± SD of 7 independent samples done in triplicate.

Figure 18

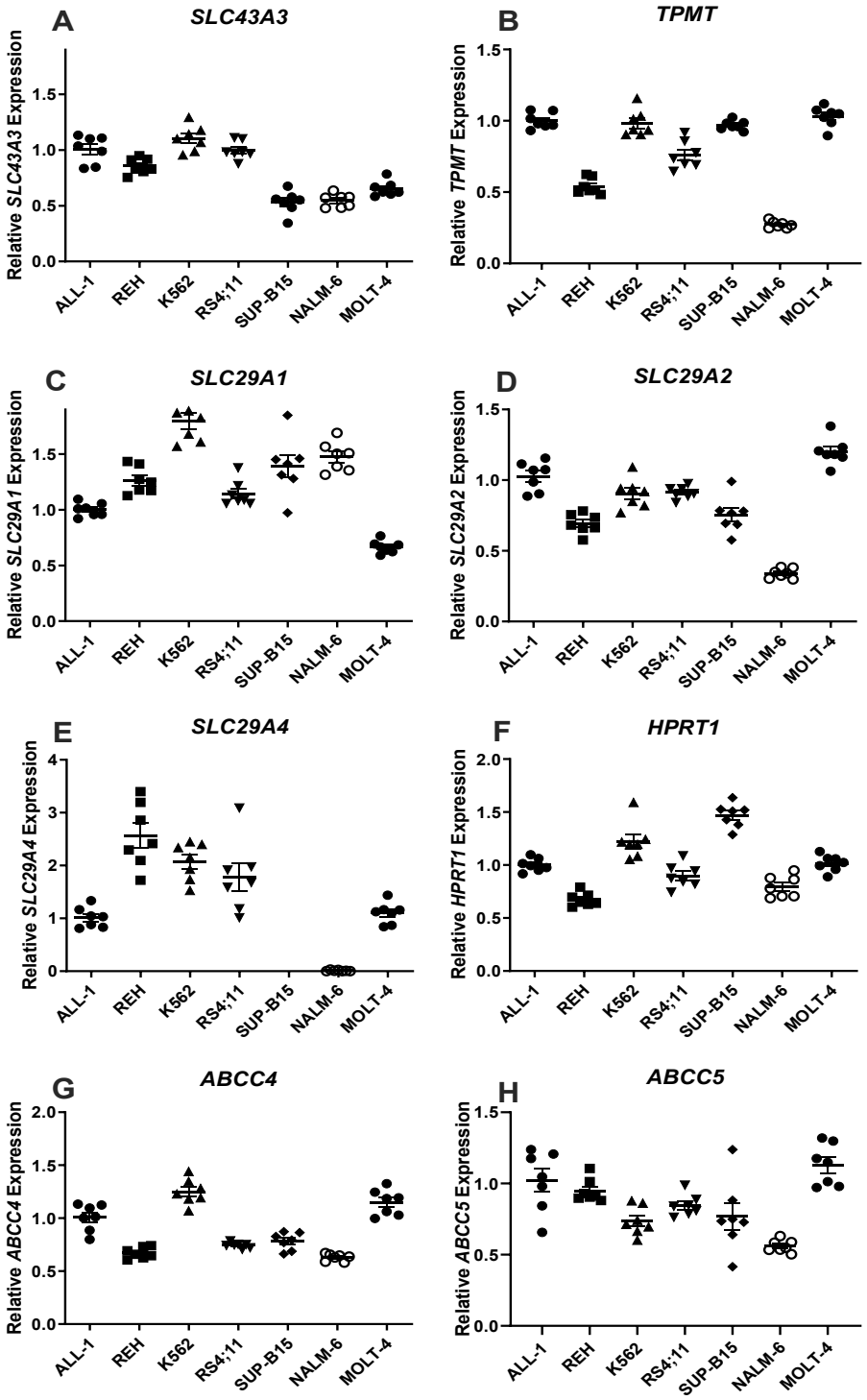
A
SLC43A3
Relative SLC43A3 Expression
B
TPMT
Relative TPMT Expression
C
SLC29A1
Relative SLC29A1 Expression
D
SLC29A2
Relative SLC29A2 Expression
E
SLC29A4
Relative SLC29A4 Expression
F
HPRT1
Relative HPRT1 Expression
G
ABCC4
Relative ABCC4 Expression
H
ABCC5
Relative ABCC5 Expression
ALL-1
REH
K562
RS4;11
SUP-B15
NALM-6
MOLT-4

5.2.3) 6-MP uptake

Initial studies were done to assess the rate of uptake of 6-MP by the ALL-1 and SUP-B15 cell lines using either 1 μM (which reflects its therapeutic plasma concentration (Lonnerholm et al. 1986)) or 100 μM 6-MP. [^{14}C] 6-MP uptake was very rapid with a $t_{1/2}$ of ENBT1-mediated uptake (adenine inhibitable) of ~4.0 sec and ~2.3 sec at 1 μM and 100 μM, respectively for the ALL-1 cells, and ~1.6 sec and ~3.5 sec, respectively, for the SUP-B15 cells **(Figure 19)**. Based on these time-course profiles, a 2 sec time point was chosen to estimate the initial rate of influx; this is the shortest incubation time that can be practically achieved using this method. When initial rates were derived in this manner over a range of [^{14}C]6-MP concentrations, a classic Michaelis-Menten relationship was observed with a V_{max} of 69 ± 10 pmol/μl/s and a K_m of 141 ± 40 μM for ALL-1 cells. In the SUP-B15 cells, a significantly lower V_{max} was observed for ENBT1-mediated 6-MP uptake of 22 ± 5 pmol/μl/s and a K_m of 133 ± 53 μM **(Figure 19E)**. These K_m values for 6-MP transport by ENBT1 are similar to those determined previously for *SLC43A3*-transfected HEK293 cells (K_m = 163 ± 26 μM; **Figure *11***), providing strong evidence that we are assessing the same transporter (Ruel et al. 2019). Several other leukemia cell lines (RS4;11, REH, NALM-6, MOLT-4, K562) were also examined for their adenine-inhibitable (ENBT1-mediated) uptake of [^{14}C] 6-MP, revealing a similar affinity across cell lines. They did, however, vary significantly in the V_{max} of 6-MP transport; these data are summarized in **Table 4**.

Figure 19: [^{14}C] 6-MP transport by ENBT1

ALL-1 and SUP-B15 cells were incubated at room temperature with 1 μM **(A, B)** and 100 μM **(C, D)** [^{14}C] 6-MP for the indicated times in the absence (Total uptake) and presence (Non-mediated uptake) of 1 mM adenine. Transport was terminated by centrifugation of the cells through an oil layer. Cell pellets were digested overnight in 1 M NaOH, and their [^{14}C] content was assessed via liquid scintillation counting. ENBT1-mediated uptake is defined as the difference between the total uptake and the non-mediated uptake. Data are represented as the mean ± SD of 5 experiments done in duplicate. **E)** The kinetics of ENBT1-mediated transport of 6-MP in ALL-1 and SUP-B15 cells were determined by incubating the cells in a range of concentrations of [^{14}C] 6-MP for 2 sec (ALL-1) or 3 sec (SUP-B15) in the presence and absence of 1 mM adenine with ENBT1-mediated transport calculated as the adenine sensitive transport component. Data are shown as the pmol of 6-MP accumulated by the cells/μl of cell volume/sec. Data points are the mean ± SD of 5 experiments done in duplicate.

Figure 19

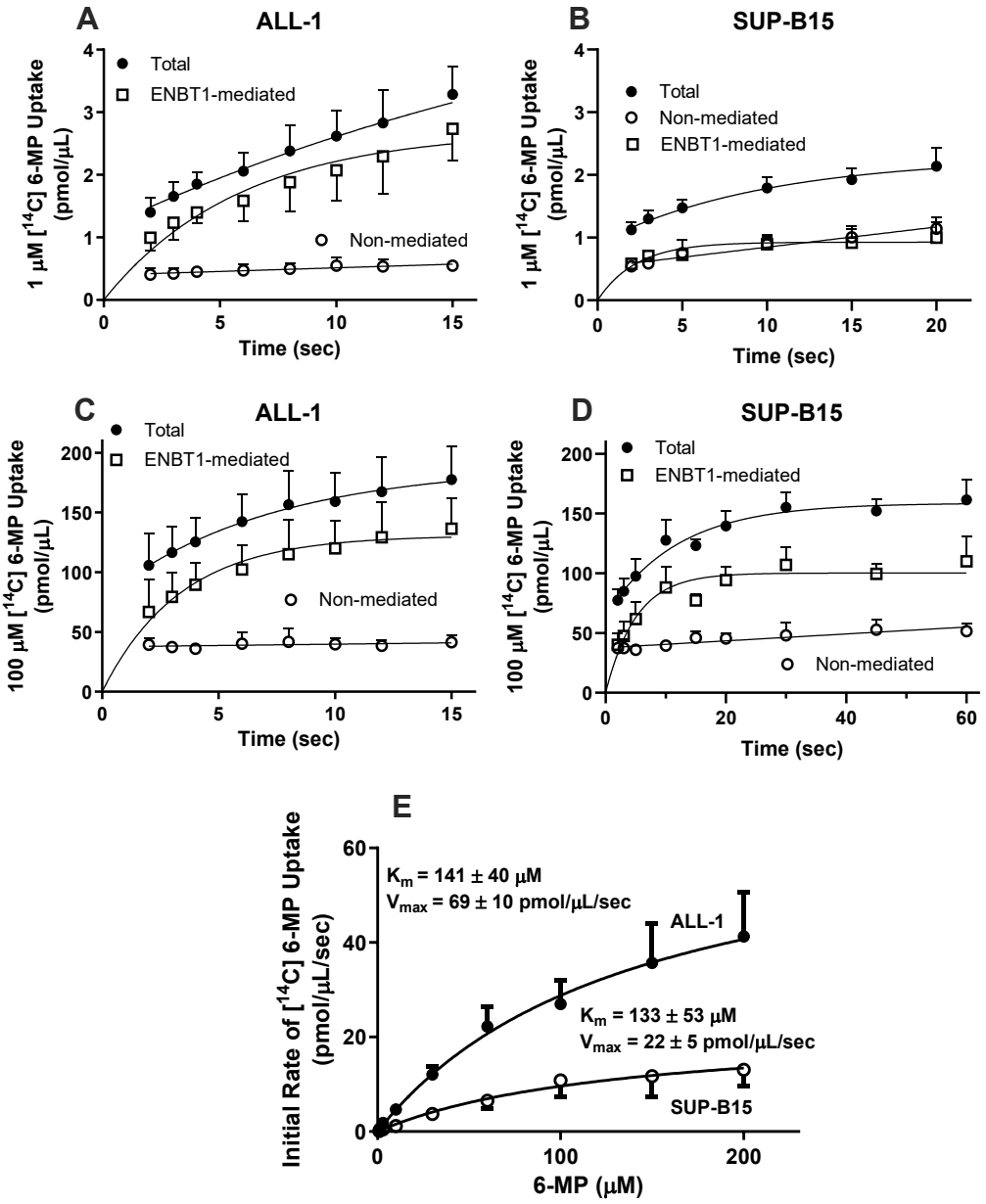
A
ALL-1
Total
ENBT1-mediated
Non-mediated
1 μM [14C] 6-MP Uptake (pmol/μL)
Time (sec)
B
SUP-B15
Total
Non-mediated
ENBT1-mediated
1 μM [14C] 6-MP Uptake (pmol/μL)
Time (sec)
C
ALL-1
Total
ENBT1-mediated
Non-mediated
100 μM [14C] 6-MP Uptake (pmol/μL)
Time (sec)
D
SUP-B15
Total
ENBT1-mediated
Non-mediated
100 μM [14C] 6-MP Uptake (pmol/μL)
Time (sec)
E
Km = 141 ± 40 μM
Vmax = 69 ± 10 pmol/μL/sec
ALL-1
Km = 133 ± 53 μM
Vmax = 22 ± 5 pmol/μL/sec
SUP-B15
Initial Rate of [14C] 6-MP Uptake (pmol/μL/sec)
6-MP (μM)

5.2.4) Inhibition of 6-MP uptake by gefitinib

In **4.2.4**, **Figure 10** demonstrates that gefitinib potently inhibits ENBT1 in a concentration-dependent manner in transfected *SLC43A3_2*-HEK293 cells. However, this was done in a recombinantly expressed ENBT1 cell model. To determine if this interaction is also present in a cell model that endogenously expresses ENBT1, K562 cells were used since they have the highest expression of ENBT1. Similar to the recombinant model, gefitinib displayed a concentration-dependent inhibition of ENBT1 with an IC_{50} value of 3.4 ± 0.6 μM in the K562 cells **(Figure 20)**. The K_i value was calculated using the Cheng-Prusoff equation (Cheng and Prusoff 1973) and was determined to be 2.8 μM. This is identical to that determined in the recombinant model.

Figure 20: Gefitinib inhibits ENBT1-mediated 6-MP uptake in K562 cells

A range of concentrations (30 nM – 100 μM) of gefitinib was assessed for their ability to inhibit the 2 sec uptake of 30 μM [^{14}C] 6-MP in K562 cells. Data was normalized as percent of control uptake, with 100% defined as the uptake of 6-MP in the absence of gefitinib and 0% defined as the uptake in the presence of 5 mM adenine. Sigmoid curves were fitted to these data for the determination of IC_{50} values, which were used to calculate the inhibitor K_i values shown in the text. The dashed line indicates the analogous data obtained in the recombinant model (from **Figure 10B**). Each point represents the mean ± SD of n=6 experiments done in duplicate.

Figure 20

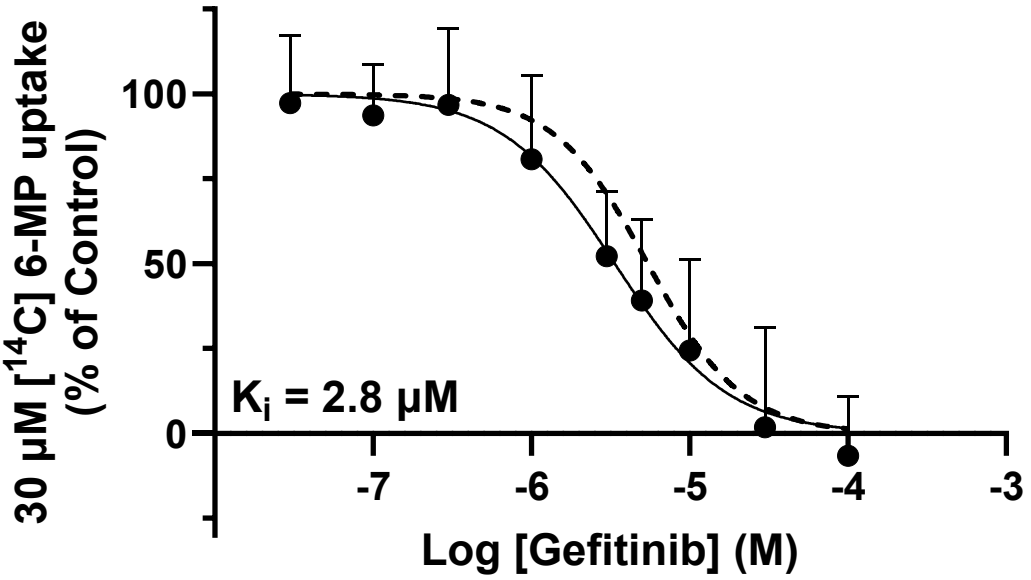
30 µM [14C] 6-MP uptake
(% of Control)
100
50
0
Ki = 2.8 µM
-7
-6
-5
-4
-3
Log [Gefitinib] (M)

5.2.5) 6-MP sensitivity

Each of the cell lines tested displayed a biphasic sensitivity to 6-MP, with ~45% of the cells sensitive to 6-MP with an EC_{50} of ~1 μM (sensitive cell component) and the remainder requiring concentrations greater than 500 μM to affect cell viability (resistant cell component) **(Figure 21)**. Given that the therapeutic concentrations of 6-MP are in the range of 1 μM, cell lines were compared with respect to the EC_{50} of 6-MP for the sensitive component. MOLT-4 cells were the most sensitive to 6-MP (EC_{50} = 0.56 ± 0.28 μM) and the SUP-B15 cells were the least sensitive (EC_{50} = 2.06 ± 0.49 μM). Sensitivity data for all cell lines is compiled in **Table 4**.

Figure 21: Sensitivity to 6-MP

The leukemia cell lines indicated in **Panels A-G** were plated at a density of $5x10^4$ cells/well in 24-well plates and incubated with a range of concentrations of 6-MP for 48 hr at 37°C in a humidified incubator (5% CO2/95% air). Cell viability was assessed using the MTT assay and expressed as a percentage of the cell viability measured at 48 hr in the absence of 6-MP. Data were fitted with a biphasic concentration-response curve, and each point represents the mean ± SD from the number of experiments (n) indicated on each panel.

Figure 21

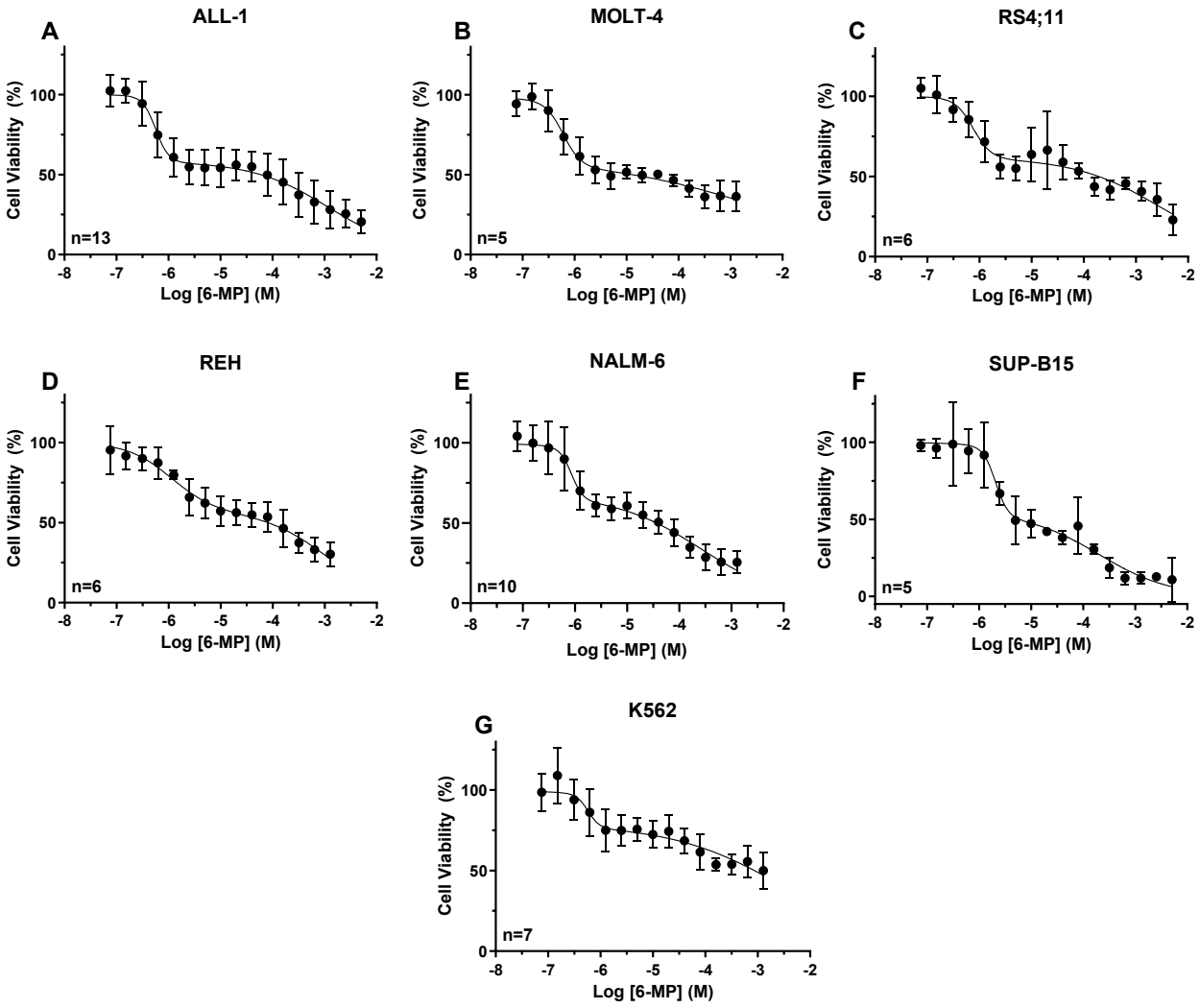
A
ALL-1
B
MOLT-4
C
RS4;11
D
REH
E
NALM-6
F
SUP-B15
G
K562
Cell Viability (%)
Log [6-MP] (M)
n=13
n=5
n=6
n=6
n=10
n=5
n=7

5.2.6) Correlation of 6-MP uptake, sensitivity, and gene expression

All of the independent measures made in this study were compared to reveal any significant correlations. This analysis led to only one significant correlation. The rate of 6-MP uptake (V_{max}) positively correlated with *SLC43A3* mRNA expression (Spearman r = 0.85) **(Figure 22)**. However, there was no significant correlation between 6-MP uptake (V_{max}) and the sensitivity to 6-MP in the 'sensitive' cell populations (1st phase of the sensitivity profiles) (Spearman r = -0.32) when comparing the full panel of cell lines. No other parameters had any other significant correlations to any other parameter investigated.

Table 4: Summary of experimental parameters measured

Data collected from the panel of leukemia cells was compiled and put into a table. The table displays data on the cell line, *SLC43A3* transcript, ENBT1 protein expression, ENBT1-mediated transport, and 6-MP sensitivity.

Table 4

Cell Line	*SLC43A3* transcript [b]	ENBT1 protein [c]	ENBT1-mediated transport	6-MP sensitivity [d]		
			V_{max} (pmol/μL/sec)	% Sensitive	EC_{50}_1 (μM)	EC_{50}_2 (mM)
K562	1.09 ± 0.13 (7) [a]	0.84 ± 0.38 (13)	66 ± 9 (6)	49 ± 46 (5)	0.74 ± 0.38 (5)	0.11 ± 0.12 (5)
ALL-1	1.01 ± 0.13 (7)	0.74 ± 0.38 (13)	69 ± 10 (5)	44 ± 10 (14)	0.66 ± 0.23 (14)	1.71 ± 1.55 (14)
RS4;11	1.01 ± 0.09 (7)	0.91 ± 0.42 (13)	52 ± 8 (5)	39 ± 8 (6)	0.96 ± 0.39 (6)	3.73 ± 2.21 (6)
REH	0.86 ± 0.09 (7)	1.19 ± 0.78 (13)	65 ± 2 (5)	28 ± 12 (6)	1.21 ± 0.42 (6)	0.72 ± 0.93 (6)
MOLT-4	0.64 ± 0.08 (7)	0.83 ± 0.34 (13)	30 ± 10 (5)	38 ± 27 (5)	0.56 ± 0.28 (5)	0.16 ± 0.21 (5)
NALM-6	0.59 ± 0.07 (7)	0.48 ± 0.24 (6)	15 ± 2 (5)	37 ± 7 (9)	0.92 ± 0.42 (9)	0.49 ± 0.46 (9)
SUP-B15	0.52 ± 0.11 (7)	0.65 ± 0.37 (12)	22 ± 5 (5)	44 ± 12 (5)	2.06 ± 0.49 (5)	0.25 ± 0.21 (5)

[a] Mean ± SD from the number of independent experiments shown in parentheses.

[b] Expression relative to ALL-1 (see **Figure 18**)

[c] Expression relative to β-actin (see **Figure 17C** for representative immunoblot), both the glycosylated and the non-glycosylated bands were combined for ENBT1 protein expression

[d] Data derived from the biphasic 6-MP sensitivity profiles shown in **Figure 21**. % Sensitive refers to the proportion of cells that were sensitive to low μM concentrations of 6-MP. EC50_1 and EC50_2 refer to the concentrations of 6-MP that reduced the viability of the 6-MP sensitive and resistant cell populations, respectively.

Figure 22: *SLC43A3* expression correlates to ENBT1-mediated 6-MP uptake

Correlation of the various independent variables measured in this study revealed one significant ($P<0.05$) correlation among the cell lines between *SLC43A3* expression and the rate (V_{max}) of ENBT1-mediated 6-MP uptake. No other correlations appeared between any of the other observed data sets. Data points represent the mean ± SD for each independent measure. Data was analyzed using simple linear regression, and correlations were assessed using the Spearman rank-order correlation method. * Indicates significance at $P<0.05$ using a Spearman rank-order correlation.

Figure 22

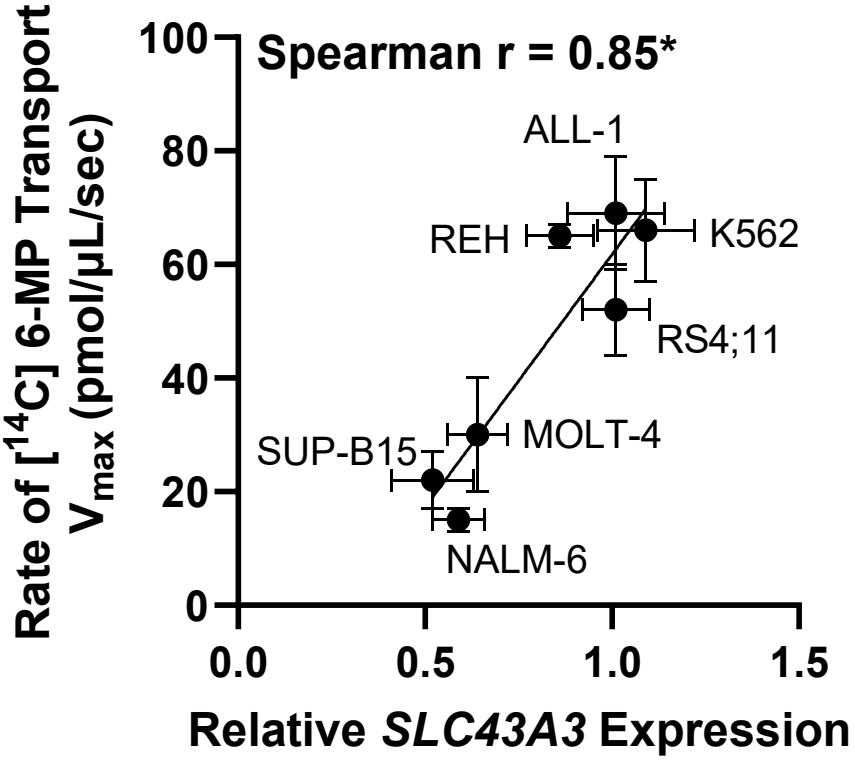
Spearman r = 0.85*
Rate of [^{14}C] 6-MP Transport
V_{max} (pmol/µL/sec)
100
80
60
40
20
0
0.0
0.5
1.0
1.5
Relative *SLC43A3* Expression
ALL-1
REH
K562
RS4;11
MOLT-4
SUP-B15
NALM-6

5.2.7) 6-MP resistant cells

To further examine the 6-MP-resistant cell population that was apparent from the sensitivity profiles shown in **Figure 21**, ALL-1 cells were grown in the presence of 640 μM 6-MP for 48 hr (concentration selected to ensure complete elimination of the 6-MP-sensitive cell population; see **Figure 21A**) and then sub-cultured for at least 10 passages. These cells retained their relative insensitivity to 6-MP. The resistant ALL-1 cells (ALL-1R) still showed a biphasic sensitivity profile to 6-MP **(Figure 23A)**, but with only ~20% of the cell population being relatively sensitive to 6-MP induced cell death (EC_{50} = 1.41 ± 0.63 μM; not significantly different than that obtained for the parent ALL-1 cell line). However, these ALL-1R cells had a reduced rate of uptake of 6-MP (determined using the ~K_m concentration of 100 μM) relative to the parent cell line **(Figure 23B)**. In terms of gene expression, the ALL-1R cells had reduced expression of *TPMT* and *SLC43A3* and an increased expression of *SLC29A4* and *ABCC5* **(Figure 23C)**. Immunoblotting confirmed a decrease in ENBT1 protein expression in ALL-1R cells when normalized to β-actin levels **(Figure 23D)**.

Figure 23: ALL-1 cells resistant to 6-MP have decreased *SLC43A3* expression

6-MP resistant ALL-1 cells (ALL-1R) were derived by incubating the cells with 640 μM 6-MP for 48 hr and sub-culturing the surviving cells for 10 passages. **(A)** Cells were assessed for their viability via the MTT assay after exposure to a range of concentrations of 6-MP, as described in **Figure 21.** Data points are expressed as the mean ± SD of 6 (ALL-1) and 5 (ALL-1R) experiments and fitted to a biphasic concentration-response relationship. * Indicates a significant difference between the ALL-1R and ALL-1 cells using a 2-way ANOVA with a Holm-Sidak post hoc test ($P<0.0001$ for all points). **(B)** The rate of 6-MP accumulation by the ALL-1 and ALL-1R cells was determined as described in **Figure 19**. Bars represent the mean ± SD of 8 experiments. * Indicates a significant difference in the rate of influx (Student's t-test, $P=0.049$) **(C)** Transcripts levels were determined as described in **Figure 18** with the exception that *GAPDH* alone was used as the reference gene. Bars represent the mean ± SD of 5 - 7 independent samples done in triplicate. * Indicates a significant difference in gene expression between the ALL-1 and ALL-1R cells based on an unpaired t-test ($P=0.032$, 0.019, <0.0001, 0.0037 for *TPMT, SLC43A3, SLC29A4,* and *ABCC5,* respectively). **(D)** ENBT1 protein levels in ALL-1 and ALL-1R cell lines. Samples were resolved on SDS-PAGE gels, transferred to polyvinyl membranes and probed with anti-ENBT1 (upper) and anti-β-actin (lower) antibodies.

Figure 23

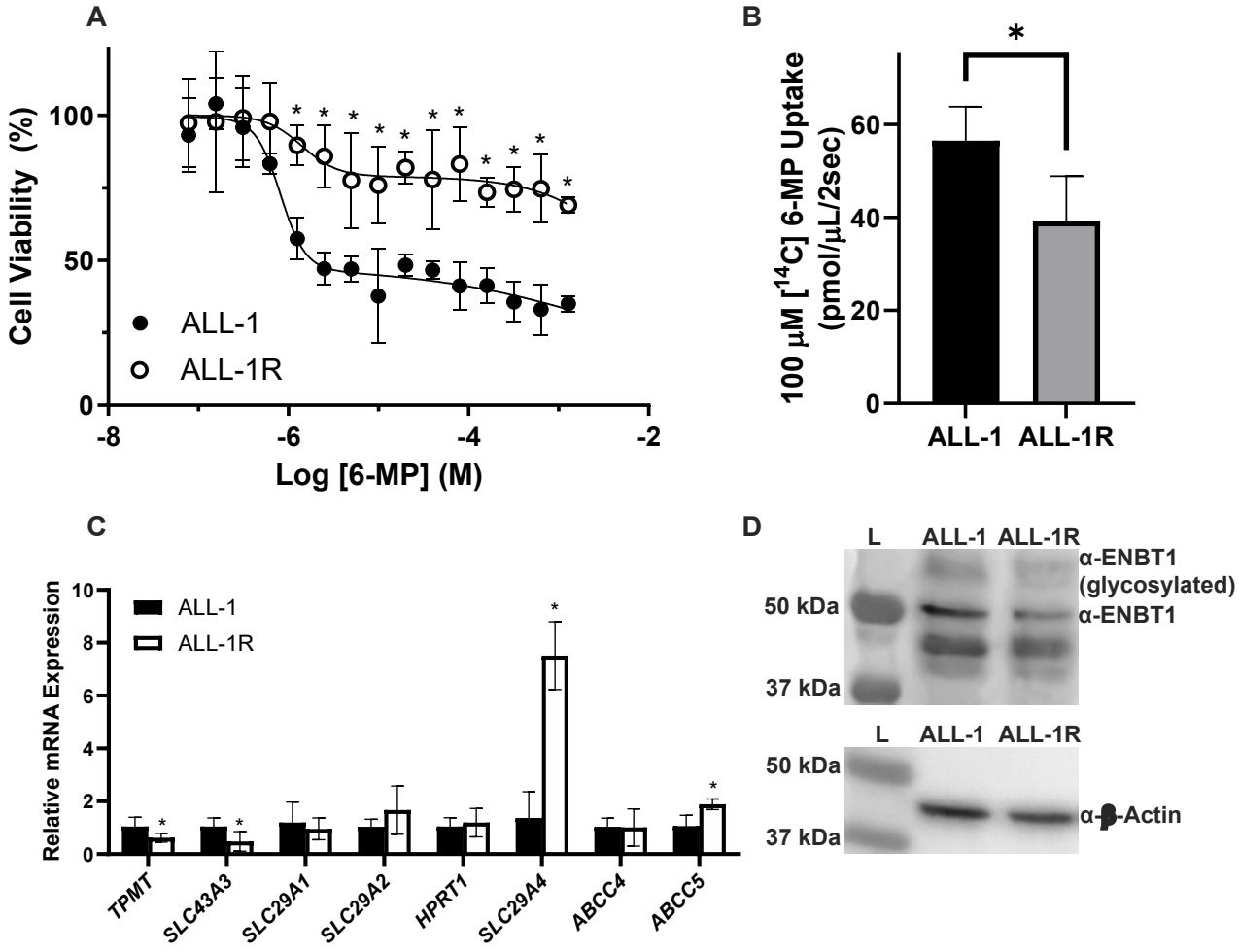
A
Cell Viability (%)
100
50
0
-8
-6
-4
-2
Log [6-MP] (M)
ALL-1
ALL-1R
B
100 μM [14C] 6-MP Uptake (pmol/μL/2sec)
60
40
20
0
ALL-1
ALL-1R
C
Relative mRNA Expression
10
8
6
4
2
0
ALL-1
ALL-1R
TPMT
SLC43A3
SLC29A1
SLC29A2
HPRT1
SLC29A4
ABCC4
ABCC5
D
L
ALL-1
ALL-1R
50 kDa
37 kDa
α-ENBT1 (glycosylated)
α-ENBT1
α-β-Actin

5.2.8) shRNAi suppression of *SLC43A3* in transfected HEK293 cells

The initial shRNAi suppression studies were done using the *SLC43A3*-HEK293 cells that were created and reported on previously in **Chapter 4** (Ruel et al. 2019). *SLC43A3*-HEK293 cells were stably transduced with a lentiviral vector containing *SLC43A3*-targeting shRNAi under the control of a Dox-sensitive promoter **(Figure 24A)**. Immunoblotting and PCR indicated that *SLC43A3* transcript was suppressed upon incubation of these cells with Dox for 72 hr **(Figure 24B** and **C),** with a ~5-fold reduction in expression observed. This is corroborated by the uptake data, which showed a 5-fold reduction in the rate of 6-MP uptake upon treatment with Dox to induce the shRNAi expression (K: -Dox: 0.77 ± 0.08 sec^{-1}; +Dox: 0.14 ± 0.02 sec^{-1} **(Figure 24D)**. Furthermore, upon activation of the shRNAi expression, the *SLC43A3*-HEK293 cells were significantly less sensitive to 6-MP (EC_{50}: -Dox: 0.54 ± 0.05 μM; +Dox: 1.58 ± 0.07 μM) **(Figure 24E)**. Interestingly, exposure of the untransfected HEK293 cells to Dox for 72 hr actually enhanced their sensitivity to 6-MP **(Figure 24E)**. This finding indicates that the decrease in 6-MP sensitivity upon activation of the *SLC43A3*-shRNAi expression was due to the knockdown of *SLC43A3* and not a non-specific effect of the Dox exposure.

Figure 24: shRNAi suppression of *SLC43A3* decreases uptake and sensitivity to 6-MP in *SLC43A3*-transfected HEK293 cells

MYC-tagged-*SLC43A3*-HEK293 cells stably transfected with an inducible shRNAi vector targeting *SLC43A3* were treated with or without 400 ng/μL Dox for 48 or 72 hr to induce shRNAi expression (with concomitant GFP). **(A)** Expression of the GFP indicator without and with 72 hr exposure to Dox. Scale bars represent 100 microns. **(B)** MYC-ENBT1 levels before and after exposure to Dox for 72 hr. Samples were resolved on SDS-PAGE gels, transferred to polyvinyl membranes and probed with anti-MYC (upper) and anti-β-actin (lower) antibodies. **(C)** *SLC43A3* transcript levels were quantified by semi-quantitative PCR using *GAPDH* as the reference gene in shRNAi-transfected *SLC43A3*-HEK293 cells following incubation with and without Dox for 48 and 72 hr. Expression levels in *SLC43A3*-HEK293 cells (no shRNAi/no Dox) are shown for comparison. Bars represent the mean ± SD of 4 - 6 independent samples done in triplicate. * Indicates a significant difference using a 1-way ANOVA with a Holm-Sidak post hoc test (P=0.0027). **(D)** Time course of the cellular uptake of 30 μM [^{14}C] 6-MP by *SLC43A3*-targeting shRNAi transfected *SLC43A3*-HEK293 cells with and without exposure to Dox for 72 hr. Data are expressed as the mean ± SD of 5 experiments done in duplicate. * Indicates a significant difference ± Dox (multiple t-tests with a Holm-Sidak post hoc test, P=0.00016, 0.00011, <0.0001, <0.0001 for 2, 4, 6, and 8 sec timepoints, respectively). **(E)** Effect of 6-MP on cell viability for HEK293 cells, HEK293 cells stably transfected with *SLC43A3* (*SLC43A3*-HEK293) and *SLC43A3*-HEK293 cells stably transfected with *SLC43A3*-targeting shRNAi, with and without incubation of cells with Dox for 72 hr. Points represent the mean ± SD of 5 – 7 independent experiments. * Indicates a significant different ± Dox (2-way ANOVA with a Holm-Sidak post hoc test, P=<0.0001, <0.0001, 0.0005, 0.0281 for -5.9, -6.2, -6.5, and -6.8 (log molar 6-MP), respectively).

Figure 24

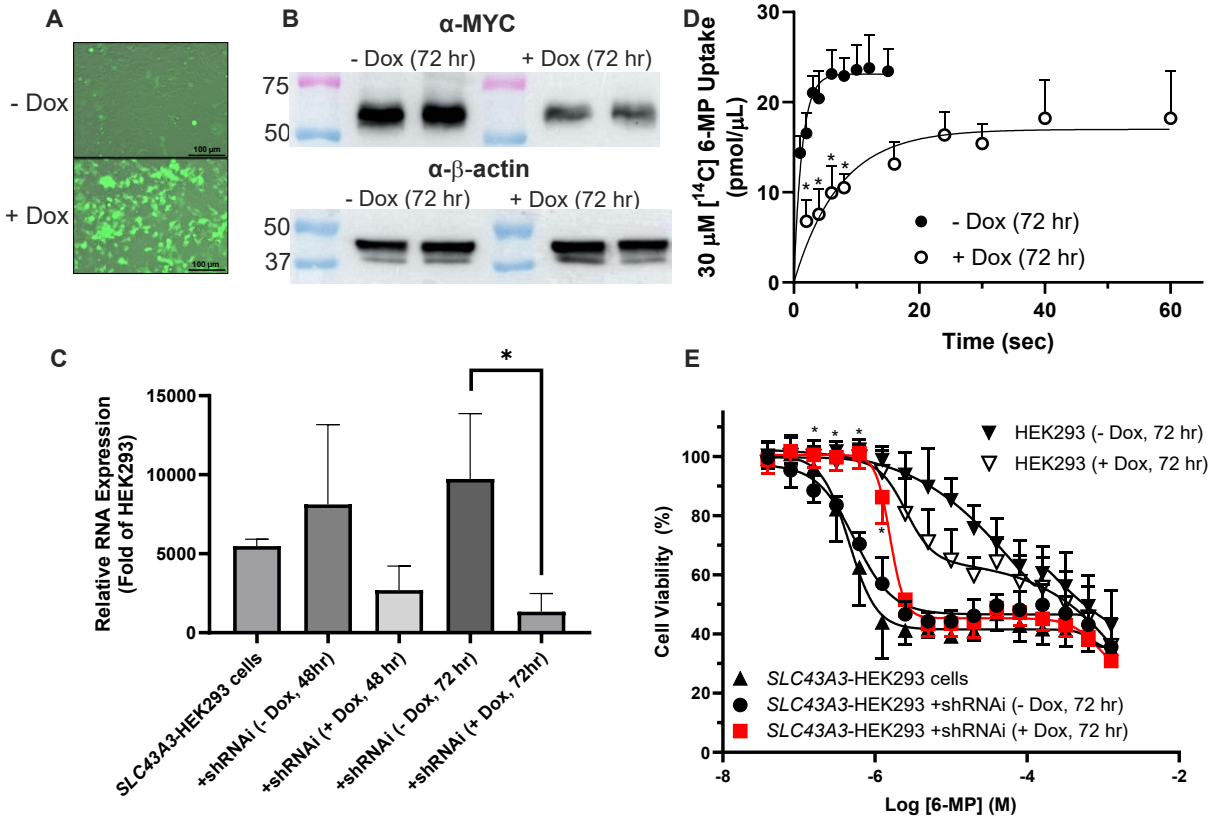
A
- Dox
+ Dox
B
α-MYC
- Dox (72 hr)
+ Dox (72 hr)
75
50
α-β-actin
- Dox (72 hr)
+ Dox (72 hr)
50
37
D
30 μM [14C] 6-MP Uptake (pmol/μL)
- Dox (72 hr)
+ Dox (72 hr)
Time (sec)
C
Relative RNA Expression (Fold of HEK293)
SLC43A3-HEK293 cells
+shRNAi (- Dox, 48hr)
+shRNAi (+ Dox, 48 hr)
+shRNAi (- Dox, 72 hr)
+shRNAi (+ Dox, 72hr)
E
HEK293 (- Dox, 72 hr)
HEK293 (+ Dox, 72 hr)
Cell Viability (%)
SLC43A3-HEK293 cells
SLC43A3-HEK293 +shRNAi (- Dox, 72 hr)
SLC43A3-HEK293 +shRNAi (+ Dox, 72 hr)
Log [6-MP] (M)

5.2.9) shRNAi suppression of *SLC43A3* in RS4;11 cells

For reasons that remain obscure, this same stable inducible knockdown approach that was successful for the HEK293 cells was not successful in the leukemia cell lines. Therefore, the RS4;11 cell line was transiently transfected with the shRNAi containing vectors (*SLC43A3* targeting and control) as described in **3.2.11**. This resulted in robust expression of the shRNAi, based on GFP reporter levels, as well as a significant reduction in ENBT1 immunoreactivity **(Figure 25A)**. Cells transfected with the *SLC43A3*-shRNAi containing vector displayed a 35% reduction in ENBT1-mediated 6-MP uptake (V_{max}: RS4;11 - 40 ± 4 pmol/µl/s; RS4;11 shRNAi - 26 ± 3 pmol/µl/s) **(Figure 25B)**. The *SLC43A3*-shRNAi expressing cells were also significantly less sensitive to the cytotoxic effects of 6-MP (EC_{50}: RS4;11 - 0.58 ± 0.05 µM; RS4;11 shRNAi - 1.44 ± 0.59 µM) **(Figure 25C)**. Gene expression analysis showed a significant paradoxical (in spite of the decrease in ENBT1 protein and function) 2-fold increase in *SLC43A3* transcript and also a 4-fold increase in *SLC29A2* (ENT2) transcript **(Figure 25D)**.

Figure 25: shRNAi knockdown of *SLC43A3* in RS4;11 leukemia cells decreases both ENBT1-mediated uptake of 6-MP and 6-MP sensitivity

(A) ENBT1 protein expression in non-targeting shRNAi transfected (control) and *SLC43A3*-targeting shRNAi (*SLC43A3*-shRNAi) transfected RS4;11 cells. Cell membrane samples from two independent experiments were resolved on SDS-PAGE gels, transferred to polyvinyl membranes and probed with anti-ENBT1 (upper) and anti-β-actin (lower) antibodies. **(B)** Kinetic analysis of [^{14}C] 6-MP uptake by RS4;11 cells transfected with non-targeting shRNAi (control) or with *SLC43A3*-targeted shRNAi was conducted as described in **Figure 19**. Points represent the mean ± SD of 6 - 10 experiments done in duplicate. * Indicates a significant effect ± shRNAi (2-way Anova with a Holm-Sidak post hoc test, P=0.021, 0.021, 0.0003, <0.0001, <0.0001, 0.0174 for 60, 100, 120, 180, 240, and 300 μM 6-MP, respectively). **(C)** Sensitivity to 6-MP in RS4;11 cells transfected with non-targeting shRNAi (Control) or *SLC43A3*-targeting shRNAi. Assays were conducted as described in **Figure 21**. Points represent the mean ± SD of 6 – 9 experiments. * Indicates a significant effect of *SLC43A3* knockdown (2-way Anova with a Holm-Sidak post hoc test, P=0.039, 0.028, <0.0001 for -5.3, -5.6, and -5.9 (log molar 6-MP), respectively). **(D)** Gene expression profiles of enzymes and transporters associated with 6-MP metabolism in RS4;11 cells transfected with non-targeting shRNAi (Control) or with *SLC43A3*-targeted shRNAi. Bars represent the mean ± SD of 5 – 6 independent samples done in triplicate. * Indicates a significant effect of shRNAi suppression of *SLC43A3* (unpaired t-Test, P<0.05).

Figure 25

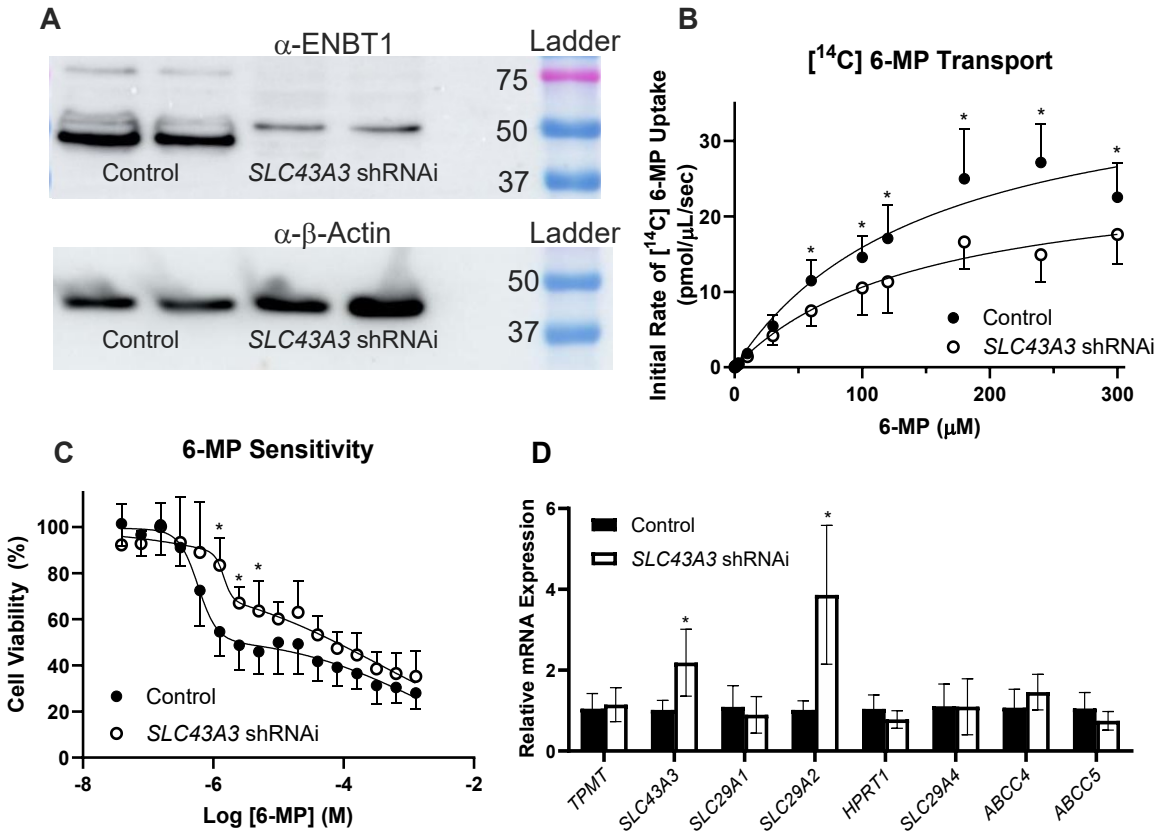
A
α-ENBT1
Ladder
75
50
37
Control
SLC43A3 shRNAi
α-β-Actin
Ladder
50
37
Control
SLC43A3 shRNAi
B
[14C] 6-MP Transport
Initial Rate of [14C] 6-MP Uptake (pmol/μL/sec)
6-MP (μM)
Control
SLC43A3 shRNAi
C
6-MP Sensitivity
Cell Viability (%)
Log [6-MP] (M)
Control
SLC43A3 shRNAi
D
Relative mRNA Expression
Control
SLC43A3 shRNAi
TPMT
SLC43A3
SLC29A1
SLC29A2
HPRT1
SLC29A4
ABCC4
ABCC5

5.3) DISCUSSION

This study clearly shows that *SLC43A3* is expressed in acute lymphoblastic leukemia cell lines and mediates the uptake of 6-MP by these cells. This is consistent with the relatively high expression of *SLC43A3* in bone marrow and lymphoid tissues, as reported by the Human Protein Atlas (proteinatlas.org) (Uhlen et al. 2015). There is a strong correlation between the expression of *SLC43A3* and the rate of 6-MP uptake among these cell lines **(Figure 22)**. This suggests that the protein encoded by *SLC43A3* is a major player in the cellular accumulation of 6-MP by leukemic lymphoblasts. While 6-MP uptake correlated with the expression of *SLC43A3*, this did not translate to a correlation with 6-MP-mediated sensitivity in the cell panel studied. This suggests that relatively small changes (~2-fold in this case) in *SLC43A3*/ENBT1 activity may not be sufficient to be a factor in 6-MP sensitivity. The difference in 6-MP sensitivity among cell lines was likely more dependent on differences in the activity of intracellular metabolic enzymes such as HPRT or TPMT. Nevertheless, larger changes in *SLC43A3* expression may be clinically relevant. Over 1600 coding sequence variants (non-synonymous SNPs) and 26 splice variants have been identified to date for *SLC43A3* (Cunningham et al. 2022). Many of these are predicted to affect protein function (Poly-Phen score >0.9) (Adzhubei et al. 2010). However, none have been characterized, and there is limited information on allele frequency in human populations.

Chapter 4 demonstrated that there was a significant enhancement of 6-MP sensitivity when *SLC43A3* was recombinantly expressed in a HEK293 cell model **(Figure 15)**, which normally has low endogenous levels of *SLC43A3* (Ruel et al. 2019). Furthermore, in the results above, the knockdown of *SLC43A3* via transfection of these *SLC43A3*-HEK293 cells with shRNAi targeting *SLC43A3* led to a dramatic reduction in 6-MP uptake and sensitivity **(Figure 24)**. A similar result was obtained when RS4;11 leukemia cells were transfected with this same *SLC43A3*

shRNAi expression vector. The *SLC43A3* shRNAi transfected RS4;11 cells showed a dramatic decrease in the rate of ENBT1-mediated 6-MP uptake, the amount of ENBT1 protein, as well as a significant decrease in their sensitivity to the cytotoxic activity of 6-MP, relative to cells transfected with the non-targeting control shRNAi **(Figure 25)**. However, in the RS4;11 cells, the shRNAi was expressed, based on the GFP reporter, even in the absence of Dox. This may reflect the higher level of the construct internalized in the RS4;11 cells (likely due to the inclusion of Leu-Fect-A in the transfection media). Therefore, *SLC43A3*-encoded ENBT1 is clearly a major contributor to the sensitivity and uptake of 6-MP in the RS4;11 cell line. The paradoxical increase in *SLC43A3* expression levels observed in the *SLC43A3* shRNA transfected RS4;11 cells may be due to an effect of the high level of expression of the shRNAi in this model, which can result in a compensatory increase in the target mRNA with the shRNAi suppressing mRNA translation (Neumeier and Meister 2020). There was also a significant increase in the expression of *SLC29A2.* This gene encodes for ENT2, which can transport nucleobases with low affinity. So, this may be a compensatory response in these cells to the loss of the primary purine nucleobase transporter ENBT1.

To examine the potential contribution of *SLC43A3* downregulation to the development of cellular resistance to 6-MP, a 6-MP resistant subclone was selected (ALL-1R) from the ALL-1 cells by incubation with 640 μM 6-MP for 48 hr. The resistant cell line showed a modest reduction in the expression of *SLC43A3* as well as a reduced rate of uptake of 6-MP **(Figure 23)**. However, the ALL-1R cells also had a reduced expression of *TPMT*, which would contribute to a reduced cellular accumulation of 6-MP metabolites and an upregulation of the efflux pump *ABCC5* (MRP5). These combined changes, and likely further metabolic alterations not assessed in this study, led to the observed profound level of resistance of the ALL-1R cells to 6-MP. The 6-MP

resistant cells also had a dramatic upregulation of *SLC29A4* **(Figure 23C)**. *SLC29A4* encodes for ENT4, an acidic pH-activated adenosine and monoamine transporter (Barnes et al. 2006; Tandio, Vilas, and Hammond 2019). ENT4 does not transport nucleobases, and the role of ENT4 in lymphoblasts has not been investigated. While there is no known direct link between 6-MP and ENT4, it has been noted in the literature that 5-HT2A receptor stimulation and/or serotonin uptake have been attributed to the activation of Rac1 in certain conditions (Saponara et al. 2018; Dai et al. 2008). Rac1 is known to be inhibited by 6-MP. Therefore, one may speculate that *SLC29A4* upregulation could be a novel resistance mechanism, and further investigation is clearly warranted.

5.4) CONCLUSION

In summary, this study shows that *SLC43A3*-encoded ENBT1 is highly expressed in acute lymphoblastic leukemia cells and is the predominant mechanism for 6-MP accumulation by these cells. While minor differences in *SLC43A3*/ENBT1 expression do not appear to affect 6-MP sensitivity, major changes in the expression of *SLC43A3* due to, for example, down regulation of ENBT1 from long term use of 6-MP or gain/loss of function polymorphisms, may significantly impact 6-MP therapeutic efficacy in ALL and other clinical indications.

5.5) LIMITATIONS

5.5.1) Cell lines

The data above shows that *SLC43A3*/ENBT1 plays an important role in mediating 6-MP uptake and sensitivity in a panel of leukemia cells. However, it is of note that all the cell lines tested are cancer cell lines and are not representative of normal cells. It is well known that cancer

cell lines, including the ones looked at above, can have many aberrations related to cell cycle, cell proliferation, and cell metabolism (Suski et al. 2021).

Furthermore, one of the cell lines tested, K562, is not an ALL-cell model but is instead a model of CML. This limits the applicability of the study to ALL but is still valuable for the overall screen of ENBT1 activity relative to the loss of cell viability to 6-MP in cells.

5.5.2) Western blots

Notably, the mRNA expression correlated to the uptake of 6-MP **(Figure 22)**. However, the protein expression, as determined by western blotting, did not display any correlation to the uptake of 6-MP or mRNA expression. This was unexpected, as the ENBT1 protein itself is responsible for mediating 6-MP uptake, as opposed to the mRNA. As shown in **Figure 17C,** the western blot of the leukemia cells has multiple bands when probing with the ENBT1 antibody. The most noteworthy bands are at ~55 kDa and ~62 kDa, representative of the non-glycosylated and glycosylated versions of ENBT1, respectively. These bands were combined to quantify the western blots since these bands were shown to correspond to ENBT1 in the recombinant model **(Figure 7)**. An in-depth analysis of potential post-translational modifications (PTMs), like glycosylation, that could impact the trafficking or function of ENBT1 at the plasma membrane has not been conducted, and it could impact the densitometry analysis of the western blots. It is well known that PTMs can significantly alter how proteins run on a western blot (Mishra, Tiwari, and Gomes 2017). Finally, when running ENBT1 on the western blot, whole cell lysates are utilized. This means that all the ENBT1 protein is being captured from the entirety of the cell and not just the plasma membrane component of ENBT1, which would be more relevant to its function. In the

future, determining the membrane content of ENBT1 through cell surface biotinylating assays would be a more suitable approach (Huang 2012).

These factors could explain why the western blot data does not correlate to the measured parameters and would require a deeper dive into potential PTMs of ENBT1 that impact the measurement of protein expression in these cell lines.

5.5.3) Correlation analysis

After conducting all the analyses on the cell lines tested, looking at expression, 6-MP sensitivity, and function of ENBT1, only one correlation was found (between mRNA and uptake (V_{max})). Of note is that nothing correlated to the EC_{50} value of 6-MP in the cell lines tested. It is well documented in the literature that many factors influence the sensitivity to 6-MP, including TPMT, NUDT15, MRP4, MRP5, and XDH/XO (Chouchana et al. 2014; Du, Huang, et al. 2023; Ansari et al. 2009; Sampath et al. 2002; de Lemos et al. 2007). However, none of these correlated to 6-MP sensitivity. A significant limitation of these correlations is that they use mRNA expression for the correlations, and it is well known that mRNA expression does not always translate to protein expression (Guo et al. 2008). Conducting correlations with protein levels would have been more appropriate to accurately assess any interactions.

Alternatively, given that none of these factors influence 6-MP sensitivity across the cell lines, it is likely that given the heterogeneous mixture of cell lines tested, not just one factor is impacting 6-MP sensitivity. Rather, it could be a multifactorial effect within each cell line that will alter 6-MP sensitivity individually in each cell line. Furthermore, the differences between the cell

lines tested were relatively small; extending our analysis to include a broader range of expression in more cell lines would enhance the potential correlations found.

Chapter 6: Regulation of ENBT1 by oxidative stress

6.1) INTRODUCTION

Two previous studies have examined how oxidative stress impacts ENBT1 function. Both studies looked at human MVECs and found that induction of oxidative stress, either by simulated ischemia and reperfusion or via the compound menadione, decreased ENBT1-mediated activity (Bone et al. 2014; Bone et al. 2015). This is important because if oxidative stress in leukemia cells decreases ENBT1-mediated 6-MP uptake, it could lead to a decrease in the efficacy of 6-MP and thus lead to resistance to therapy. Another study examined large-scale proteomic changes following treatment with 2-cyano-3,12-dioxooleana-1,9(11)-dien-28-oic acid (CDDO)-Me, an activator of the nuclear factor erythroid 2-related factor 2 (Nrf2). Nrf2 is a transcription factor and master regulator of oxidative stress pathways. In the study, K562 cells showed a modest decrease in *SLC43A3* expression (Wang, Zhang, et al. 2017). This suggests that Nrf2 may regulate *SLC43A3*/ENBT1 levels. This is further supported by the Gene Cards database, which suggests a potential transcription factor binding site for Nrf2 (Fishilevich et al. 2017).

Oxidative stress is characterized by an imbalance between free radical production and cellular antioxidant defence mechanisms in cells but is a fundamental physiological process with implications across various cellular functions (Pizzino et al. 2017). Free radicals are comprised of two separate categories: ROS, including superoxide radical ($O_2^{\bullet -}$), the hydroxyl radical (OH•), and hydrogen peroxide (H_2O_2), and reactive nitrogen species (RNS), which include nitric oxide (NO•) and peroxynitrite ($ONOO^-$). Free radicals are natural byproducts of cellular metabolism that are primarily generated in mitochondria and peroxisomes (Valko et al. 2007). A prime example of a fundamental physiological process involving ROS is the oxidative burst, which is a component of our immune defence mechanism, wherein neutrophils and macrophages generate controlled amounts of ROS and RNS to kill pathogens (Chen and Junger 2012; Slauch 2011). Free radicals

are also produced in the electron transport chain in the mitochondria. Electrons can react with oxygen in Complexes I and III, leading to the generation of superoxide radicals (Cadenas et al. 1977; Hirst, King, and Pryde 2008). Furthermore, free radicals are produced within our body by several enzymes as well as environmental stimuli such as ultraviolet radiation, pollutants, and pesticides (Lakey et al. 2016). Two notable enzymes in our body are the nicotinamide adenine dinucleotide phosphate hydrogen (NADPH) oxidase and XDH/XO. NADPH oxidase uses NADPH to convert oxygen into superoxide (Babior 2004). XDH/XO can produce multiple free radicals from the purine analog hypoxanthine, ranging from superoxide, H_2O_2, and peroxynitrite when in the presence of nitric oxide (Granger 1988; Houston et al. 1998; Millar et al. 2002). Although free radicals are integral to regular cell function, excessive ROS accumulation can lead to oxidative damage of lipids, proteins, and nucleic acids, thereby disrupting cellular homeostasis (Stadtman and Levine 2003; Sallmyr, Fan, and Rassool 2008). For this reason, excessive oxidative stress has been implicated in many diseases such as cancer, diabetes, Parkinson's, and many more (Abou-Seif, Rabia, and Nasr 2000; Chugh et al. 1999; Huang, Sheu, and Lin 1999; Medeiros et al. 2016; Suzuki et al. 1999).

To counteract ROS-induced damage, cells use antioxidant defence mechanisms to limit the effects of free radicals by enzymatic conversion to harmless byproducts. The main enzymes involved in antioxidant defence are superoxide dismutase (SOD), catalase, and glutathione peroxidase (Trachootham, Alexandre, and Huang 2009). SOD converts superoxide radicals into the less reactive H_2O_2 and oxygen (McCord and Fridovich 1969). Catalase functions to convert H_2O_2 into water and oxygen (Aebi 1984). Finally, glutathione peroxidase uses the antioxidant glutathione (GSH) to reduce H_2O_2 into water (Flohe, Gunzler, and Schock 1973). These enzymes limit the damaging effects of excessive ROS and RNS and protect cells from oxidative stress.

In leukemia, a heterogeneous hematologic malignancy, oxidative stress-mediated DNA damage and impaired antioxidant defence mechanisms have been implicated in leukemogenesis, promoting genomic instability, and aberrant cell proliferation (Sallmyr, Fan, and Rassool 2008; Storz 2005). In multiple studies, leukemia cells have been observed to have significantly increased levels of free radicals in acute and chronic leukemia patients compared to controls (Devi et al. 2000; Battisti et al. 2008; Oltra et al. 2001; Al-Tonbary et al. 2011; Al-Gayyar et al. 2007; Chaudhary et al. 2023). Increased ROS production and altered redox balance can contribute to leukemic cell survival and drug resistance (Szatrowski and Nathan 1991). However, the picture is not too clear when it comes to the levels of antioxidants in leukemia cells. Antioxidants have been seen to both be increased (Devi et al. 2000; Al-Gayyar et al. 2007; Maung et al. 1994; Yamanaka, Nishida, and Ota 1979) and decreased (Battisti et al. 2008; Oltra et al. 2001; Al-Tonbary et al. 2011; Chaudhary et al. 2023), relative to controls. However, there is agreement that chemotherapy treatment leads to a decrease in antioxidants and an overall increase in ROS levels (Kennedy et al. 2005; Battisti et al. 2008; Chaudhary et al. 2023). This duality of ROS and antioxidants displays the fine line that is at play in the development and progression of leukemia, as well as the benefits it has on treatment outcomes and the destruction of cancer cells (Udensi and Tchounwou 2014).

Another central defence mechanism against oxidative stress is Nrf2, a transcription factor that orchestrates the expression of antioxidant and detoxifying enzymes (Moi et al. 1994). Nrf2 operates through a complex mechanism of action primarily centred on its regulation by Kelch-like ECH-associated protein 1 (KEAP1) and its subsequent translocation into the nucleus (Itoh et al. 1999). Under basal conditions, KEAP1 is bound to Nrf2 in the cytoplasm, facilitating its ubiquitination and proteasomal degradation. However, in response to oxidative stress, cysteine residues within KEAP1 undergo modification, leading to the dissociation of Nrf2 from KEAP1

and its subsequent stabilization and translocation to the nucleus. In the nucleus, Nrf2 dimerizes with small musculoaponeurotic fibrosarcoma proteins and binds to antioxidant response elements in the promoter regions of target genes (Igarashi et al. 1994; Motohashi et al. 2004). A myriad of genes have been shown to be targets of Nrf2 with the most studied being heme oxygenase 1, NADPH quinone oxidoreductase 1 (*NQO1*), glutamate cysteine ligase, glutathione s-transferases, and thioredoxin reductase 1 (*TXNRD1*) (He, Ru, and Wen 2020; Inamdar, Ahn, and Alam 1996). These enzymes are responsible for the detoxification and defence against various insults the cell will encounter.

Nrf2 dysregulation has been implicated in various pathological conditions, including cancer and, specific to this thesis, leukemia. In leukemia, Nrf2 displays primarily oncogenic properties. Higher expression of Nrf2 in leukemia has been shown to be associated with poorer prognosis for patients and decreased overall survival (Villa-Morales et al. 2023). Nrf2 overexpression has also been associated with chemoresistance for various drugs used in leukemia treatment (Wang et al. 2022; Wang, Li, et al. 2017; Ma et al. 2015; Xu et al. 2019). Furthermore, several variants have been noted within the Nrf2 pathway, mainly for the *KEAP1* and small musculoaponeurotic fibrosarcoma (*MAFF, MAFG, MAFK*) genes, that have been associated with the development of leukemia (Martinez-Hernandez et al. 2014; Akin-Bali et al. 2020). The aberrant activation of Nrf2 in leukemia leads to the uncontrolled proliferation of leukemia cells and the ability to withstand toxic insults due to the detoxification enzymes upregulated by Nrf2.

This chapter will explore the role of oxidative stress and how it impacts the functional uptake of 6-MP via ENBT1. The oxidants used will be TBHP, menadione, and diamide, and the antioxidants used will be NAC and TEMPOL. K562 cells will be the primary cell line used for the experiments in this chapter as they display the highest expression of *SLC43A3*/ENBT1 **(Table 4)**.

6.2) RESULTS

6.2.1) Effect on cell viability with the oxidants menadione, TBHP, and diamide

Using the MTT assay, the effect on cell viability of each oxidant was assessed to determine a concentration that could be used that would not adversely impact the cell's viability and thus complicate subsequent interactions. Menadione and TBHP were assessed at 15 min **(Figure 26A)**, 30 min **(Figure 26B)**, and 24 hr **(Figure 26C).** Fifteen- and 30-min incubations displayed minimal loss of cell viability except at the two highest concentrations. 24 hr incubation with either compound yielded a much more robust loss of cell viability. TBHP displayed a monophasic relationship with an EC_{50} of 73 ± 5 μM. Menadione displayed a biphasic relationship with first phase EC_{50} of 1.3 ± 0.8 μM **(Figure 26C)**. Menadione was further assessed at 48 hr; it displayed a monophasic relationship with an EC_{50} of 13 ± 1 μM, while the control treatment displayed no loss of cell viability **(Figure 26D**). The loss of cell viability due to diamide was determined in K562 **(Figure 26E)**, MOLT-4 **(Figure 26F)**, and SUP-B15 cells **(Figure 26G)** following a 1 hr treatment. Diamide had a monophasic profile with an EC_{50} of 2.1 ± 0.4, 2.5 ± 0.3, and 1.2 ± 0.1 mM for K562, MOLT-4, and SUP-B15 cells, respectively. From these data, treatment with 100 μM TBHP and menadione for 30 min was deemed suitable for further study. For diamide, the concentrations used for the 1 hr treatment in each cell was 150 μM. These concentrations and time points display minimal loss of cell viability.

Figure 26: The oxidative stress inducers menadione, TBHP, and diamide decrease cell viability in K562, MOLT-4, and SUP-B15 cells

K562 cells were plated at a density of 5 x 10^4 cells/well in 24-well plates and incubated with a range of menadione or TBHP concentrations (195 nM – 400 μM) for 15 min **(A)**, 30 min **(B),** or 24 hr **(C)**, at 37°C in a humidified incubator (5% CO_2/95% air). Cell viability was assessed using the MTT assay and expressed as a percent of the cell viability measured at each time point in the absence of menadione or TBHP (% of control). Sigmoidal concentration-response curves were fit to the data except in the 24 hr menadione data, which was fit using a biphasic concentration-response curve. Each point represents the mean ± SD of 5 **(A)** or 4 **(B, C)** experiments. **D)** K562 cells were plated at a density of 5 x 10^4 cells/well in 24-well plates and incubated with a range of menadione concentrations (586 nM – 200 μM) for 48 hr at 37°C in a humidified incubator (5% CO_2/95% air). Cell viability was assessed in the same as way as in **Panel A**. Each point represents the mean ± SD of 5 experiments. K562 **(E)**, MOLT-4 **(F)**, and SUP-B15 **(G)** cells were plated at a density of 5 x 10^4 cells/well in 24-well plates and incubated with a range of diamide concentrations (**E, F**: 305 nM – 5 mM; **G**: 39 μM – 5 mM) for 1 hr at 37°C in a humidified incubator (5% CO_2/95% air). Cell viability was assessed in the same as way as in **Panel A**. Each point represents the mean ± SD of 5 **(E, G)** or 6 **(F)** experiments.

Figure 26

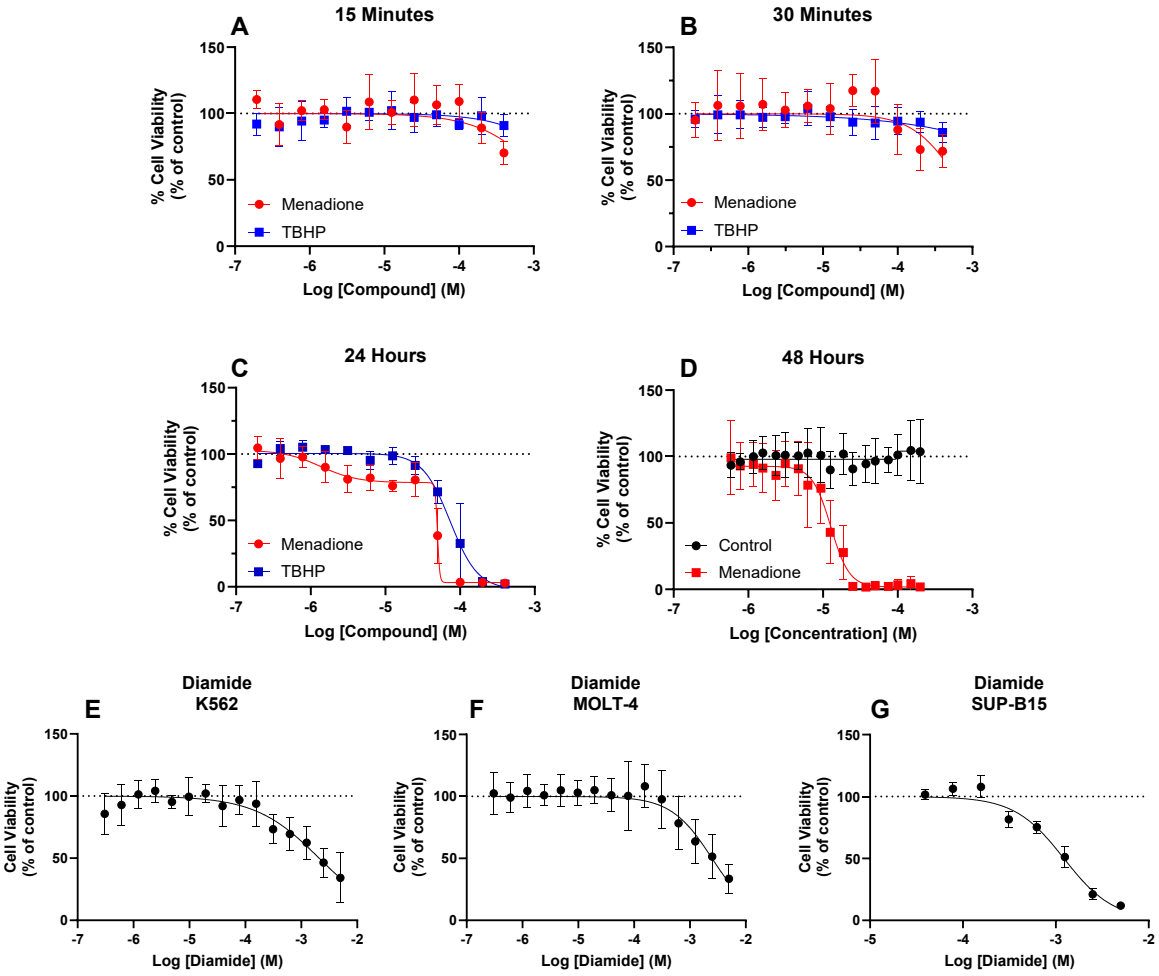
A
15 Minutes
% Cell Viability (% of control)
Menadione
TBHP
Log [Compound] (M)
B
30 Minutes
% Cell Viability (% of control)
Menadione
TBHP
Log [Compound] (M)
C
24 Hours
% Cell Viability (% of control)
Menadione
TBHP
Log [Compound] (M)
D
48 Hours
% Cell Viability (% of control)
Control
Menadione
Log [Concentration] (M)
E
Diamide
K562
Cell Viability (% of control)
Log [Diamide] (M)
F
Diamide
MOLT-4
Cell Viability (% of control)
Log [Diamide] (M)
G
Diamide
SUP-B15
Cell Viability (% of control)
Log [Diamide] (M)

6.2.2) Effect of diamide on ENBT1-mediated 6-MP uptake

As determined above for diamide, the concentration of 150 μM for a 1 hr treatment does not significantly alter the cell viability of the cell lines. K562, MOLT-4, and SUP-B15 cells were treated with 150 μM diamide for 1 hr and then assessed their ENBT1 function by looking at the 2 sec uptake of [^{3}H] 6-MP at 1 μM (**Figure 27A, C, E**) and 150 μM (**Figure 27B, D, F**) in each cell line. There was no significant change in ENBT1 function in either of the concentrations or cell lines tested.

Figure 27: Diamide does not affect ENBT1-mediated 6-MP uptake in K562, MOLT-4, and SUP-B15 cells

K562 **(A, B),** MOLT-4 **(C, D),** and SUP-B15 **(E, F)** cells were incubated at 37°C with either control (D-PBS) or 150 μM diamide for 1 hr. Cells were then washed twice in NMG buffer before determining their uptake of [^{3}H] 6-MP at 1 μM **(A, C, E)** and 150 μM **(B, D, F)** at room temperature for 2 sec. Transport was terminated by centrifugation of the cells through an oil layer. Cell pellets were digested overnight in 1 M NaOH, and their [^{3}H] content was assessed via liquid scintillation counting. Bars represent the ENBT1-mediated uptake, defined as the difference between the total uptake (absence of 5 mM adenine) and the non-mediated uptake (presence of 5 mM adenine). Data are shown as the pmols of 6-MP accumulated by the cells/μl of cell volume/sec. Data are represented as the mean ± SD of 5 **(A, B)** or 4 **(C - F)** experiments done in duplicate.

Figure 27

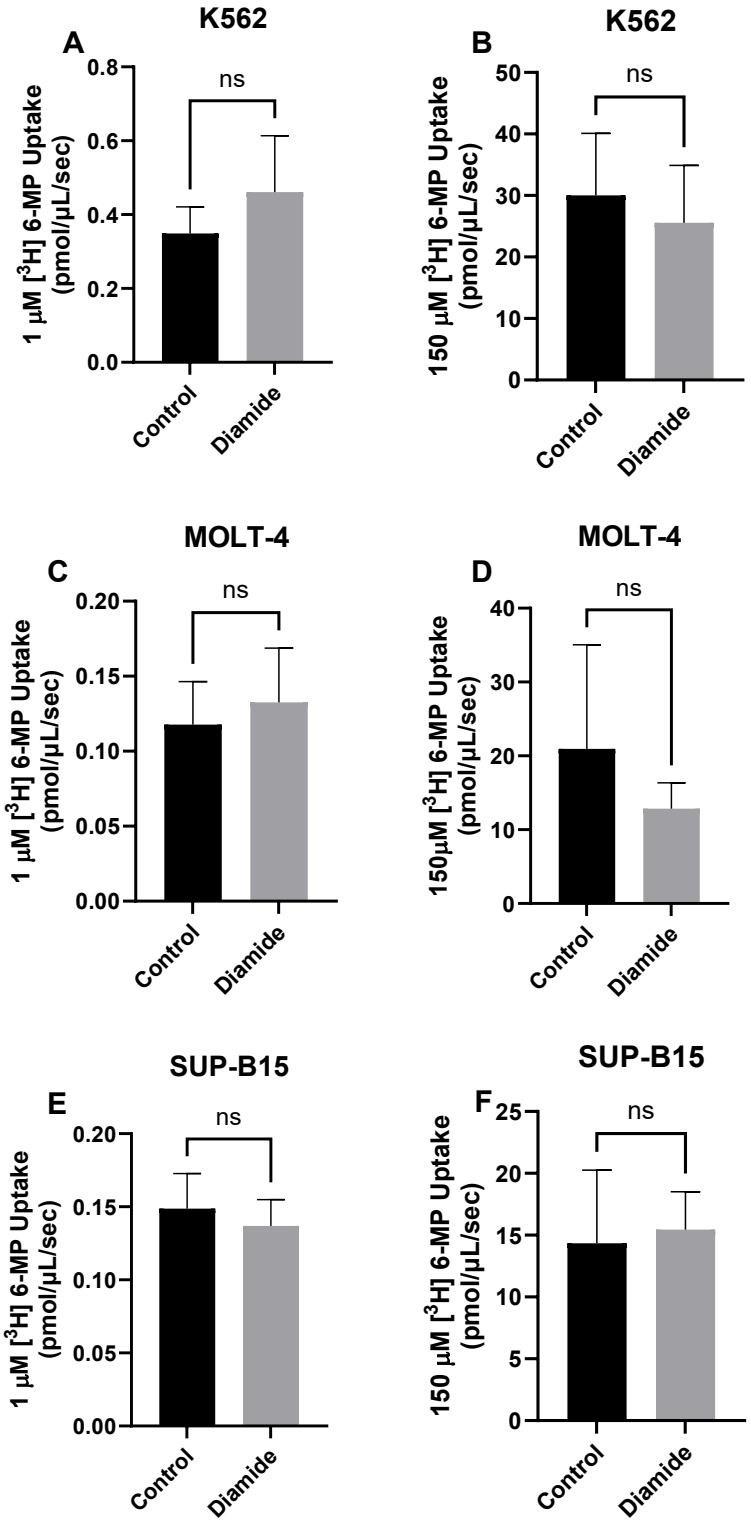
A
K562
1 μM [3H] 6-MP Uptake (pmol/μL/sec)
0.8
0.6
0.4
0.2
0.0
ns
Control
Diamide
B
K562
150 μM [3H] 6-MP Uptake (pmol/μL/sec)
50
40
30
20
10
0
ns
Control
Diamide
C
MOLT-4
1 μM [3H] 6-MP Uptake (pmol/μL/sec)
0.20
0.15
0.10
0.05
0.00
ns
Control
Diamide
D
MOLT-4
150μM [3H] 6-MP Uptake (pmol/μL/sec)
40
30
20
10
0
ns
Control
Diamide
E
SUP-B15
1 μM [3H] 6-MP Uptake (pmol/μL/sec)
0.20
0.15
0.10
0.05
0.00
ns
Control
Diamide
F
SUP-B15
150 μM [3H] 6-MP Uptake (pmol/μL/sec)
25
20
15
10
5
0
ns
Control
Diamide

6.2.3) Effect of menadione and TBHP on ENBT1-mediated 6-MP uptake

Similar to diamide, menadione and TBHP were determined to cause minimal loss of cell viability when treated with 100 μM for 30 min in K562 cells. This is also the same concentration and time that was used in the previous study in human MVECs (Bone et al. 2014). Treatment with TBHP showed no significant change in the V_{max} value for ENBT1 (V_{max}: Control - 83 ± 18 pmol/μL/sec; TBHP – 135 ± 43 pmol/μL/sec) **(Figure 28A)**. Treatment with menadione also had no significant decrease in V_{max} (V_{max}: Control - 98 ± 16 pmol/μL/sec; Menadione – 74 ± 11 pmol/μL/sec) **(Figure 28C)**. However, it was noted that there was a trend to a decrease in V_{max}, and four data points were significantly lower for the menadione group as compared to the control group (2-way ANOVA with a post-hoc Holm-Sidak, $P<0.05$).

Total ROS levels were also detected using flow cytometry to determine the degree to which the TBHP and menadione increased ROS levels in the cells. TBHP significantly increased the total ROS levels by ~19-fold over the control **(Figure 28B)**. Menadione also significantly increased total ROS levels by around ~1.3-fold over the control **(Figure 28D)**.

Figure 28: Menadione decreases ENBT1-mediated 6-MP uptake in K562 cells

K562 cells were incubated with 100 μM of menadione **(A)** or TBHP **(C)** for 30 min at 37°C. Cells were then washed twice in NMG buffer before determining the uptake kinetics of [^{14}C] 6-MP at room temperature. The kinetics of ENBT1-mediated [^{14}C] 6-MP uptake were determined by assessing the uptake of a range of concentrations of [^{14}C] 6-MP (1 – 300 μM) estimated by the transporter-mediated uptake at 2 sec (calculated as the difference in cellular uptake ± 5 mM adenine). Cells were then centrifuged through oil, and the cell pellets were digested overnight in 1 M NaOH and assessed for [^{14}C] content using standard liquid scintillation counting techniques to define pmol 6-MP accumulated per μl/second in the cell pellet. Data points represent the mean ± SD of 7 **(A)** or 14 **(C)** experiments done in duplicate. * Represents a significant difference between control and menadione using a 2-way ANOVA with a post-hoc Holm-Sidak test. **B, D)** K562 cells were loaded with a fluorescent dye before being treated with control or 100 μM of either TBHP **(B)** and menadione **(D)** for 30 min. Afterwards, fluorescent intensity was measured using an Attune NxT flow cytometer (Flow Cytometry Facility, University of Alberta) to determine total ROS in the cells. 10,000 events were captured and graphed as the median fluorescent intensity for each individual experiment. Data are represented as the mean ± SD of 6 experiments done in duplicate. * Represents a significant difference from D-PBS **(B)** or DMSO **(D)** using a student's T-test, $P<0.05$.

Figure 28

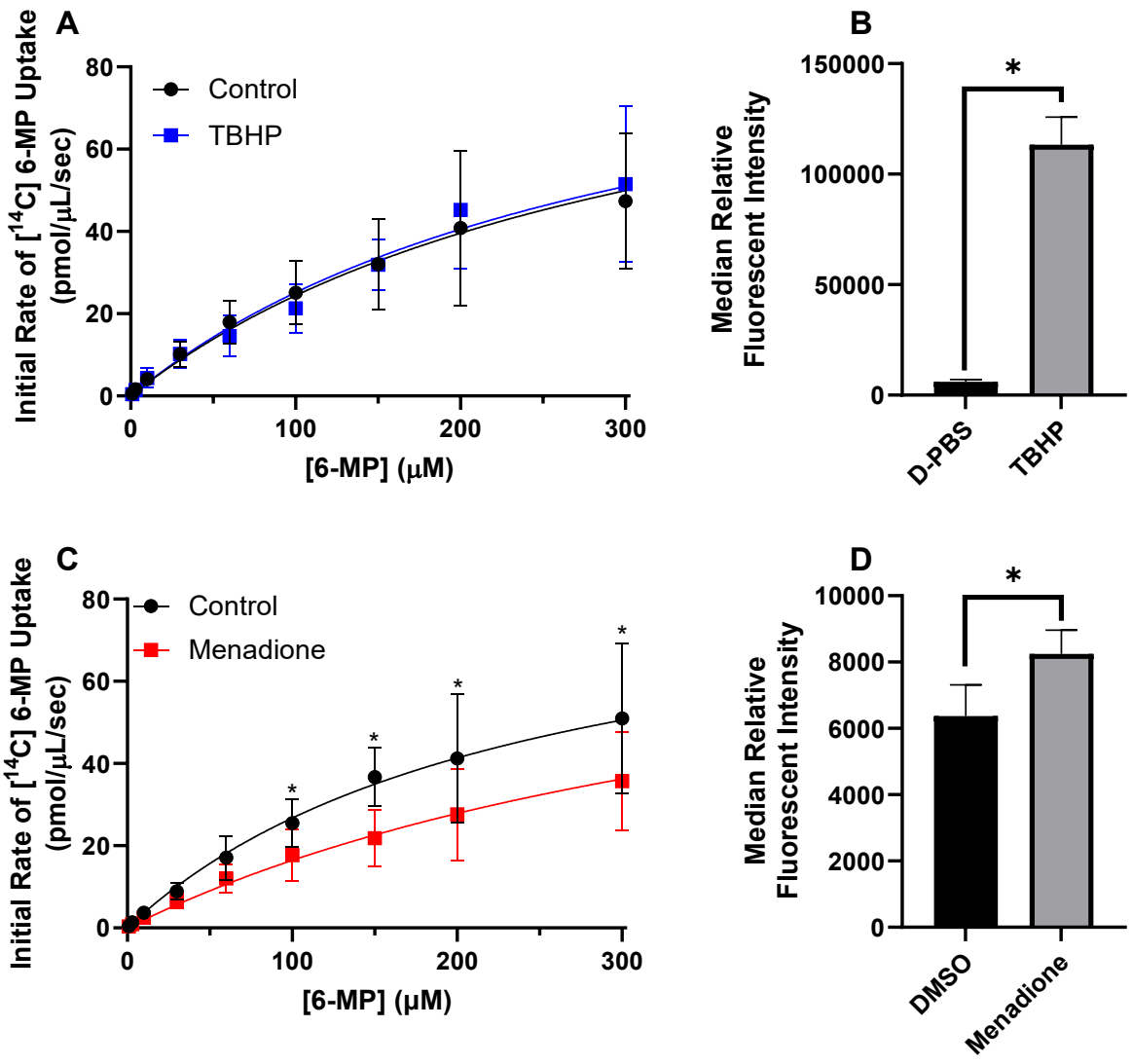
A
Initial Rate of [14C] 6-MP Uptake (pmol/µL/sec)
Control
TBHP
[6-MP] (µM)
B
Median Relative Fluorescent Intensity
D-PBS
TBHP
C
Initial Rate of [14C] 6-MP Uptake (pmol/µL/sec)
Control
Menadione
[6-MP] (µM)
D
Median Relative Fluorescent Intensity
DMSO
Menadione

6.2.4) Effect of the antioxidants NAC and TEMPOL on ENBT1-mediated uptake after menadione treatment

As shown above, menadione treatment at 100 μM for 30 min in K562 cells appears to cause a decrease in ENBT1 function. To attenuate the effect seen, the antioxidants NAC and TEMPOL were investigated. In **Figure 29B**, the antioxidant NAC was tested, and none of the treatments were different from the control (V_{max}: Control - 73 ± 10 pmol/μL/sec; NAC – 82 ± 13 pmol/μL/sec; Menadione – 89 ± 11 pmol/μL/sec; Menadione + NAC – 83 ± 8 pmol/μL/sec). With TEMPOL, the kinetics of [^{3}H] adenine were determined instead of 6-MP. TEMPOL alone did not have a significantly different V_{max} from control. Treatment with menadione alone was significantly different from control (extra sum of squares F-test, $P<0.05$), while the combination of TEMPOL and menadione was not significantly different from control (V_{max}: Control - 22 ± 4 pmol/μL/sec; TEMPOL – 16 ± 1 pmol/μL/sec; Menadione – 12 ± 1 pmol/μL/sec; Menadione + TEMPOL – 17 ± 2 pmol/μL/sec) **(Figure 29C)**.

TEMPOL reversed the decrease in V_{max} caused by menadione treatment in K562 cells. Similar to what was done above for the determination of total ROS in **Figure 28**, ROS levels were determined using the treatment protocol for TEMPOL. TEMPOL alone and the combination of menadione and TEMPOL had a significant increase in the total ROS levels in the cells, ~3.5-fold and ~9.5-fold for TEMPOL alone and menadione + TEMPOL, respectively (1-way ANOVA with a post-hoc Holm-Sidak test, $P<0.05$). Although menadione did not have a significant increase in ROS in this analysis, it showed a similar ~1.4-fold increase in total ROS levels, which matches what was seen in **Figure 28**.

Figure 29: Pre-incubation with TEMPOL reverses the decrease in ENBT1-mediated uptake following menadione treatment

A) K562 cells were pre-incubated with 5 mM NAC (NAC and Menadione + NAC) for 48 hr before adding either DMSO (Control and NAC) or 100 µM menadione (Menadione and Menadione + NAC) for an additional 30 min at 37°C. Cells were then washed twice in NMG buffer before determining the uptake kinetics of [^{14}C] 6-MP at room temperature. The kinetics of ENBT1-mediated [^{14}C] 6-MP uptake were determined by assessing the uptake of a range of concentrations of [^{14}C] 6-MP (1 – 300 µM) estimated by the transporter-mediated uptake at 2 sec (calculated as the difference in cellular uptake ± 5 mM adenine). Cells were then centrifuged through oil and the cell pellets were digested overnight in 1 M NaOH and assessed for [^{14}C] content using standard liquid scintillation counting techniques to define pmol 6-MP accumulated per µl/second in the cell pellet. Data points represent the mean ± SD of 4 experiments done in duplicate. **B)** K562 cells were pre-incubated with 5 mM TEMPOL (TEMPOL and Menadione + TEMPOL) for 15 min before adding either DMSO (Control and TEMPOL) or 100 µM menadione (Menadione and Menadione + TEMPOL) for an additional 30 min at 37°C. The kinetics of ENBT1-mediated [^{3}H] adenine uptake were determined by assessing the uptake of a range of concentrations of [^{3}H] adenine (1 – 150 µM) estimated by the transporter-mediated uptake at 2 sec (calculated as the difference in cellular uptake ± 5 mM adenine). Cells were then centrifuged through oil, and cell pellets were digested overnight in 1 M NaOH and assessed for [^{3}H] content using standard liquid scintillation counting techniques to define pmol adenine accumulated per µl/second in the cell pellet. Data points represent the mean ± SD of 5 experiments done in duplicate. **C)** K562 cells were loaded with a fluorescent dye before being treated with D-PBS (Control and Menadione) or 5 mM TEMPOL (TEMPOL and TEMPOL + Menadione) for 15 min. Afterwards, cells were

treated with either DMSO (Control and TEMPOL) or 100 μM menadione (Menadione and Menadione + TEMPOL) for 30 min. Fluorescent intensity was measured using an Attune NxT flow cytometer (Flow Cytometry Facility, University of Alberta) for the determination of total ROS in the cells. 10,000 events were captured and graphed as the median fluorescent intensity for each individual experiment. Data are represented as the mean ± SD of 6 experiments. * Represents a significant difference from control using a 1-way ANOVA with a post-hoc Holm-Sidak test, $P<0.05$.

Figure 29

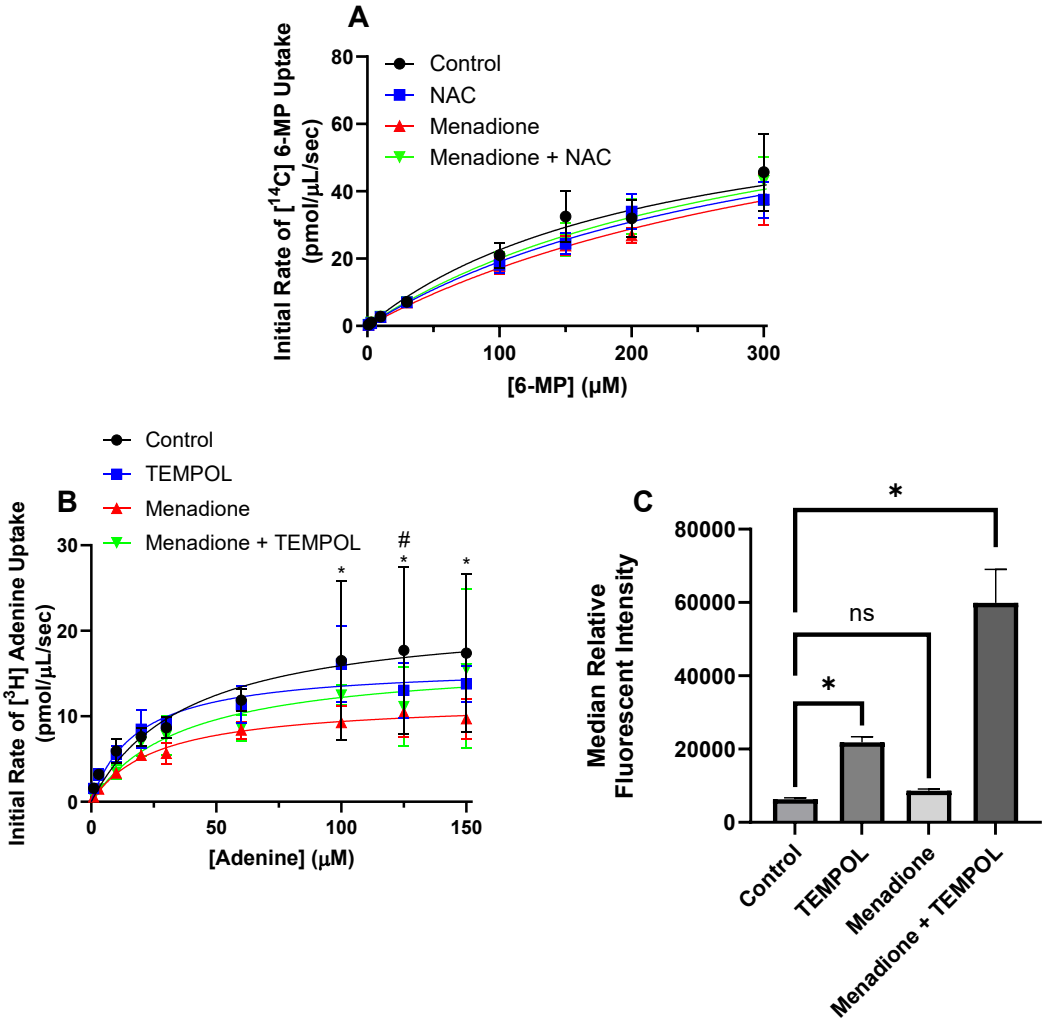
A
Control
NAC
Menadione
Menadione + NAC
Initial Rate of [14C] 6-MP Uptake (pmol/µL/sec)
[6-MP] (µM)
B
Control
TEMPOL
Menadione
Menadione + TEMPOL
Initial Rate of [3H] Adenine Uptake (pmol/µL/sec)
[Adenine] (µM)
C
Median Relative Fluorescent Intensity
ns
Control
TEMPOL
Menadione
Menadione + TEMPOL

6.2.5) Effect of the Nrf2 activator CDDO-Im in MOLT-4 and SUP-B15 cells

Nrf2 activation was studied via the activator CDDO-Im. 100 nM of CDDO-Im was incubated with MOLT-4 **(Figure 30)** and SUP-B15 **(Figure 31)** cells for 24 hr prior to RNA extraction, cDNA synthesis and subsequent qPCR analysis. Both cell lines displayed similar changes relative to the control treatment, with some exceptions. Both cell lines had significant increases in the positive controls *TXNRD1* and *NQO1*. An increase was also seen in *TPMT* expression for both cell lines. Both cells saw a decrease in *SLC43A3*, *SLC29A1*, *HPRT1*, and *ABCC4* expression. MOLT-4 cells showed no change in *SLC29A2* and *SLC29A4* expression. SUP-B15 cells showed a significant decrease in *SLC29A2* expression. Notably, SUP-B15 cells do not express *SLC29A4*, similar to what was shown in **Figure 18**.

qPCR analysis from **Figure 30** and **Figure 31** noted that *SLC43A3* expression is decreased following CDDO-Im incubation (~1.4 fold). To see whether the CDDO-Im-induced decrease in mRNA translates to a loss of ENBT1 function, CDDO-Im was incubated in MOLT-4 and SUP-B15 cells for 24 hr before the determination of ENBT1 function. MOLT-4 cells showed no significant change in ENBT1-mediated 6-MP **(Figure 32A)** or adenine **(Figure 32B)** uptake following incubation with CDDO-Im. In SUP-B15 cells, the V_{max} of adenine transport was significantly increased relative to DMSO-treated cells (V_{max}: DMSO – 6 ± 1 pmol/μL/sec; CDDO-Im – 11 ± 2 pmol/μL/sec) **(Figure 32C)**.

Figure 30: qPCR analysis following 24 hr incubation with CDDO-Im in MOLT-4 cells

MOLT-4 cells were treated with either DMSO or 100 nM CDDO-Im for 24 hr at 37°C in a humidified incubator (5% CO_2/95% air). RNA was extracted via TRIzol using the manufacturer's protocol, and cDNA was made. Gene expression was assessed by semi-quantitative RT-qPCR and is shown relative to the control treatment (DMSO). Expression was normalized to 3 separate reference genes (*GAPDH, RNA18SN5, and ACTB*) and quantified using the ΔΔCt method. **(A-I)** Relative expression of *TXNRD1, NQO1, SLC43A3, SLC29A1, SLC29A2, SLC29A4, HPRT1, TPMT, and ABCC4,* as compared to DMSO-treated cells. Bars represent the mean ± SD of 6 independent samples done in triplicate. * Represents a significant difference from DMSO using a student's T-test, $P<0.05$.

Figure 30

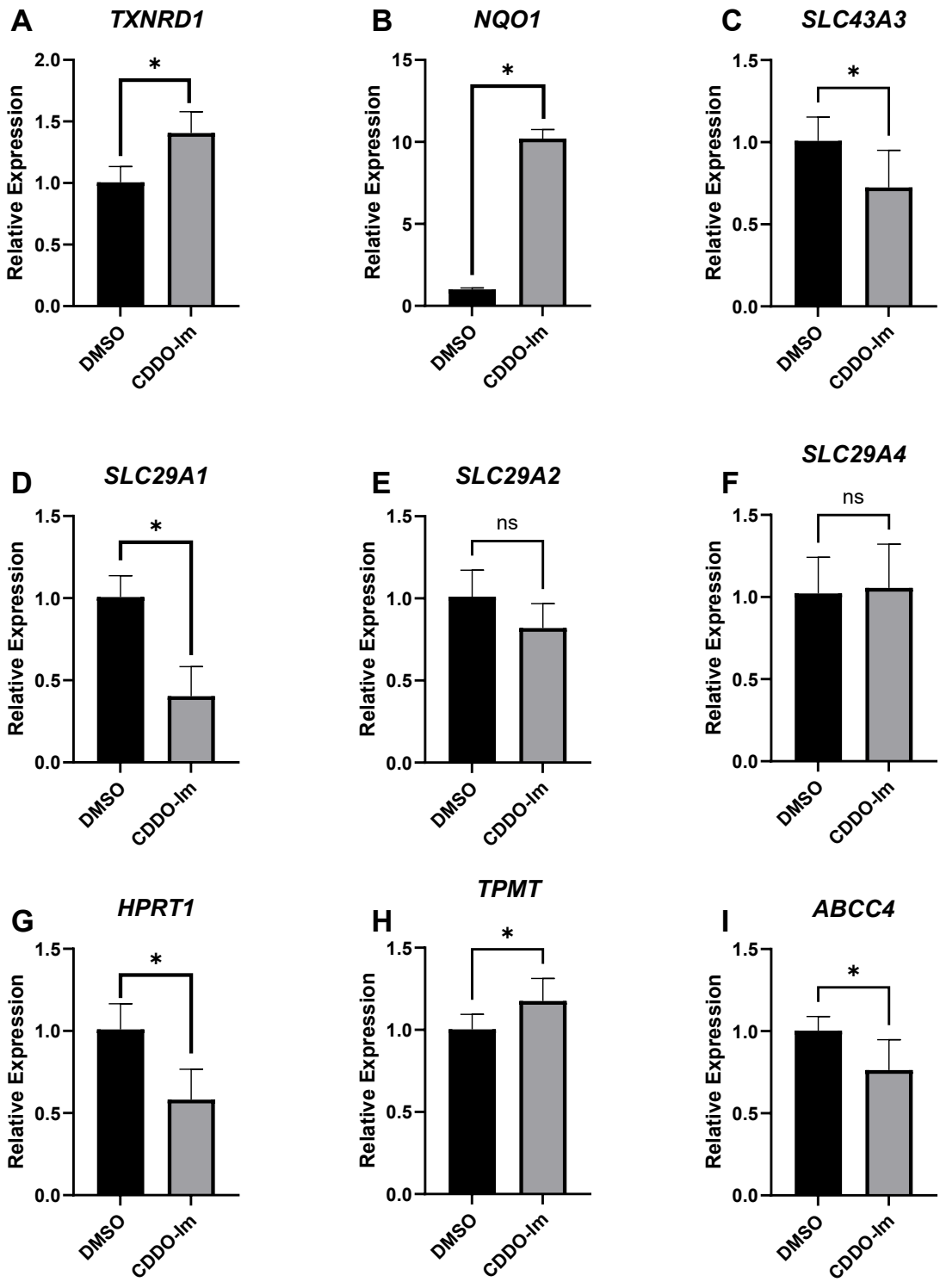
A
TXNRD1
B
NQO1
C
SLC43A3
D
SLC29A1
E
SLC29A2
F
SLC29A4
G
HPRT1
H
TPMT
I
ABCC4
Relative Expression
DMSO
CDDO-Im
*
ns

Figure 31: qPCR analysis following 24 hr incubation with CDDO-Im in SUP-B15 cells

SUP-B15 cells were treated with either DMSO or 100 nM CDDO-Im for 24 hr at 37°C in a humidified incubator (5% CO_2/95% air). RNA was extracted via TRIzol using the manufacturer's protocol, and cDNA was made. Gene expression was assessed by semi-quantitative RT-qPCR and is shown relative to the control treatment (DMSO). Expression was normalized to 3 separate reference genes (*GAPDH, RNA18SN5, and ACTB*) and quantified using the ΔΔCt method. **(A-I)** Relative expression of *TXNRD1, NQO1, SLC43A3, SLC29A1, SLC29A2, SLC29A4, HPRT1, TPMT, and ABCC4,* as compared to DMSO-treated cells. Bars represent the mean ± SD of 6 independent samples done in triplicate. * Represents a significant difference from DMSO using a student's T-test, $P<0.05$.

Figure 31

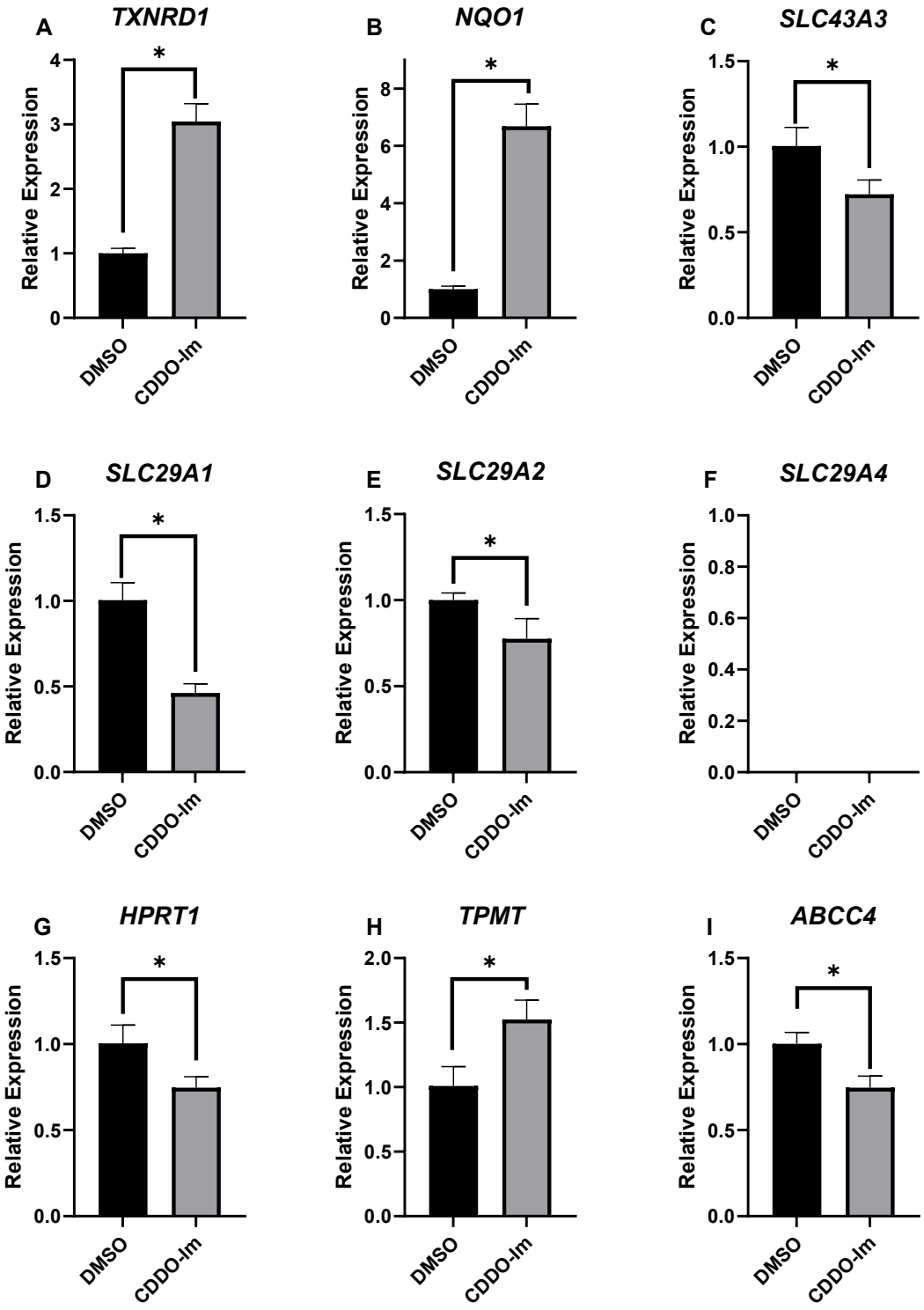
A
TXNRD1
Relative Expression
DMSO
CDDO-Im
B
NQO1
C
SLC43A3
D
SLC29A1
E
SLC29A2
F
SLC29A4
G
HPRT1
H
TPMT
I
ABCC4

Figure 32: ENBT1-mediated uptake following 24 hr incubation with CDDO-Im in MOLT-4 and SUP-B15 cells

A) MOLT-4 cells were incubated with either DMSO or 100 nM CDDO-Im for 24 hr at 37°C in a humidified incubator (5% CO_2/95% air). Cells were then washed twice in NMG buffer before determining the uptake kinetics of [^{14}C] 6-MP at room temperature. The kinetics of ENBT1-mediated [^{14}C] 6-MP uptake were determined by assessing the uptake of a range of concentrations of [^{14}C] 6-MP (1 – 300 μM) estimated by the transporter-mediated uptake at 2 sec (calculated as the difference in cellular uptake ± 5 mM adenine). Cells were then centrifuged through oil, and cell pellets were digested overnight in 1 M NaOH and assessed for [^{14}C] content using standard liquid scintillation counting techniques to define pmol 6-MP accumulated per μl/second in the cell pellet. Data points represent the mean ± SD of 5 experiments done in duplicate. MOLT-4 **(B)** and SUP-B15 cells **(C)** were incubated with either DMSO or 100 nM CDDO-Im for 24 hr at 37°C in a humidified incubator (5% CO_2/95% air). The kinetics of ENBT1-mediated [^{3}H] adenine uptake were determined by assessing the uptake of a range of concentrations of [^{3}H] adenine (1 – 150 μM) estimated by the transporter-mediated uptake at 2 sec (calculated as the difference in cellular uptake ± 5 mM adenine). Cells were then centrifuged through oil, and the cell pellets were digested overnight in 1 M NaOH and assessed for [^{3}H] content using standard liquid scintillation counting techniques to define pmol adenine accumulated per μl/second in the cell pellet. Data points represent the mean ± SD of 6 **(C)** or 7 **(B)** experiments done in duplicate. * Represents a significant difference from DMSO using a 2-way ANOVA with a post-hoc Holm-Sidak test, $P<0.05$.

Figure 32

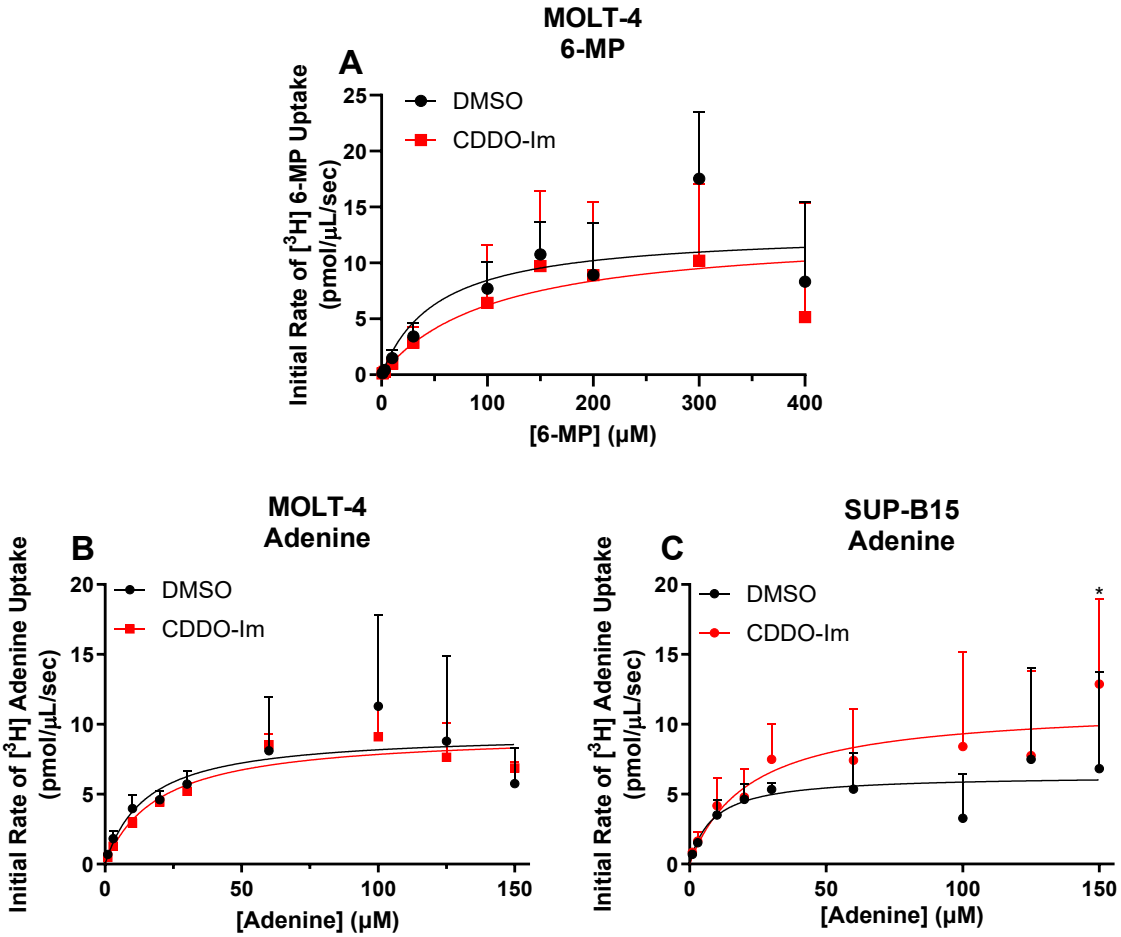
MOLT-4
6-MP
A
DMSO
CDDO-Im
Initial Rate of [3H] 6-MP Uptake (pmol/µL/sec)
[6-MP] (µM)
MOLT-4
Adenine
B
DMSO
CDDO-Im
Initial Rate of [3H] Adenine Uptake (pmol/µL/sec)
[Adenine] (µM)
SUP-B15
Adenine
C
DMSO
CDDO-Im
*
Initial Rate of [3H] Adenine Uptake (pmol/µL/sec)
[Adenine] (µM)

6.3) DISCUSSION

These data demonstrate that incubation with the oxidative stress inducer, menadione, leads to a decrease in ENBT1-mediated uptake of substrates, which can be reversed via the introduction of the antioxidant TEMPOL. However, it is noted that the menadione effect was quite variable throughout. **Figure 28C** shows a decrease in the menadione-treated cells, which does not reach statistical significance, while **Figure 29A** has no effect. This difference could be due to the internal variability of the performed uptake assay, which is known to be highly variable based on previous experience (Ruel et al. 2019; Ruel et al. 2022). This variability is due to the nature of the performed uptake assays, which, in the case of ENBT1, uses a time point of 2 sec. This time point is incredibly challenging to do consistently and causes high variability. Another reason could be the actual proposed mechanism of action of menadione. **Figure 28B** shows that menadione only increased total ROS levels in the cells by ~1.3-fold over control, which, relative to the increase seen by TBHP (~19-fold, **Figure 28D**), is quite small, and if the menadione increase in ROS varies even slightly between different experiments, this could explain the variability in the menadione response in the uptake assays.

The difference between TBHP and menadione is also interesting and speaks to the potential mechanism of action of the two compounds relative to their effects on ENBT1. Menadione, also known as Vitamin K_3, due to its structural similarity to Vitamin K, produces oxidative stress via a mechanism known as "redox cycling," which results in the formation of superoxide anion within the cells ($O_2^{\bullet-}$) (Hassan 2013; Loor et al. 2010). On the other hand, TBHP has been shown to produce peroxyl (ROO•) and alkoxyl radicals (RO•) and decrease cellular GSH content (Davies 1989; Crane et al. 1983). The decrease in ENBT1 function is unlikely to be the result of decreased glutathione since diamide, a radiosensitizer whose mechanism of action is the oxidation of

reducing agents in cells (Harris and Power 1978), like glutathione, has no impact on ENBT1 function **(Figure 27)**. This would suggest that the type of oxidant being produced by these compounds is important to the overall effect seen. As stated above, menadione primarily produces superoxide anion, while TBHP produces peroxyl and alkoxyl radicals. More specifically, TBHP will produce more alkoxyl radicals than peroxyl radicals due to the presence of NADPH oxidase enzymes (Davies 1989). Chemically, any of the radicals mentioned above can react with any cellular component, like DNA, lipids, and proteins. However, superoxide anion has a larger variety of other reactions in cells that can lead to the formation of other reactive compounds like the hydroxyl radical (HO•) (via the Haber-Weiss reaction), peroxynitrite ($ONOO^-$) (via a reaction with nitric oxide), and hydrogen peroxide (H_2O_2), in which, the hydroxyl radical is the most reactive of all known reactive species to induce oxidative stress (Collin 2019). Conversely, peroxyl and alkoxyl radicals primarily interact with cellular components instead of creating further reactive compounds. It is unclear whether this difference is important in the context of the experiments above and would need to be investigated in more detail to determine which individual species of ROS are being produced.

Another potential explanation for the difference is the localization of the compounds within the cells. Menadione is ~10-fold more lipophilic (based on Log P values) than TBHP and thus is expected to associate with membranes more readily ("Compound Summary for CID 4055, Menadione" 2004; "Compound Summary for CID 6410, tert-Butyl Hydroperoxide" 2004). The incorporation of menadione into membranes has been shown to impact membrane fluidity and lipid organization (Monteiro et al. 2013), which could heavily impact protein function. It is speculated that preferential menadione localization over TBHP to the plasma membrane leads to

localized increases in reactive oxidative species where ENBT1 is located, leading to oxidative damage of ENBT1, causing a decrease in cellular uptake.

The antioxidants NAC and TEMPOL were assessed to try attenuating the decrease seen with menadione incubation, of which only TEMPOL was successful. TEMPOL is a SOD mimetic which mimics the action of SOD that converts superoxide anion to hydrogen peroxide, which then gets converted to water and oxygen by the action of catalase (Lewandowski and Gwozdzinski 2017). On the other hand, NAC is a precursor to glutathione and has been shown to enhance glutathione levels and protect against chemical oxidants in leukemia cells (Mlejnek and Dolezel 2014). The experiment with NAC incubation for 48 hr in **Figure 29A** did not work as expected, and neither of the conditions had any significant difference in V_{max} from the other. This suggests that the experiment itself was unsuccessful as menadione did not induce a decrease in function, as seen in the other experiments. Therefore, it is highly unlikely that NAC was the issue in this experiment as extensive literature supports its reversal of oxidative stress, including in leukemia cell lines (Hu, Hirano, and Oka 2003), but rather a human error. In contrast, a decrease with menadione was noted in the TEMPOL experiment. Menadione decreased the V_{max} of ENBT1 by ~25%, similar to that seen in **Figure 28C** and TEMPOL preincubation prior to the addition of menadione reversed the decrease up to near control values **(Figure 29B)**. This is in line with a previous study on ENBT1 and oxidative stress in 2014, which showed the menadione-induced decrease in ENBT1 function was partially reversed by the antioxidant, Mn(III)tetrakis(1-methyl-4-pyridyl)porphyrin, which is also a SOD mimetic (Bone et al. 2014). Successful reversal with Mn(III)tetrakis(1-methyl-4-pyridyl)porphyrin (literature) and TEMPOL (these data) suggests that superoxide is the central player in mediating menadiones effects and would be in line with its mechanism of action. The levels of total ROS species were determined for this experimental set in

Figure 29C, and it was noted that TEMPOL alone and menadione + TEMPOL had significantly higher levels of ROS over control, ~3.5-fold and ~9.5-fold, respectively. This is at odds with the suggestion that ROS decreases ENBT1 function since, based on that assertion, the combination of menadione and TEMPOL should have drastically impacted ENBT1. TEMPOL is a nitroxide compound that contains a nitroxyl group with an unpaired electron, allowing it to interact with other reactive species and work as an antioxidant (Lewandowski and Gwozdzinski 2017). It is speculated that due to the nature of the kit used for ROS detection, which assesses the total ROS species present, regardless of type, the kit also picked up TEMPOL itself. Furthermore, TEMPOL has been shown to both decrease and increase ROS levels at high concentrations depending on the cell line used (Gariboldi et al. 2000; Park 2021).

A notable parameter, the K_m, which was determined for all of the Michaelis-Menten graphs above, was not shown since there were no statistical differences between K_m values for all of the experimental sets. Plus, all the K_m values were close to the expected K_m for both adenine (~30 μM) and 6-MP (~150 μM) in the experiments. This means that none of the treatments used in the experiments interacted with ENBT1 and changed how it handled adenine or 6-MP, suggesting the change was independent of alterations to ENBT1 substrate recognition.

Finally, the transcription factor Nrf2 was investigated to determine if ENBT1 was transcriptionally regulated by Nrf2. **Figure 30** and **Figure 31** assessed changes in qPCR expression of factors that can impact 6-MP transport and enzymatic conversion. The positive controls, *NQO1* and *TXNRD1*, showed robust increases in transcript levels, suggesting the activation of Nrf2 was successful and agreed with previous literature (Rooney et al. 2020; Wang, Zhang, et al. 2017; Shen et al. 2017; Suvorova et al. 2009). Most of the other genes (*SLC43A3, SLC29A1, HPRT1*) were in agreement with a previously published study (Wang, Zhang, et al.

2017), while others have not been assessed previously (*SLC29A2, SLC29A4, TPMT*). However, our experiments showed a decrease in *ABCC4* expression, in contrast to the literature, which typically shows an increase (Aleksunes et al. 2008; Aleksunes et al. 2010). It is unclear why this one differed, but it may be specific to ALL cell lines since the MOLT-4 and SUP-B15 cells were used in the experiments. As for *SLC43A3*/ENBT1, there was a small but notable decrease in the mRNA transcript. To determine if this small decrease impacted ENBT1 plasma membrane expression, ENBT1 function was assessed. **Figure 32** shows that MOLT-4 cells had no change in ENBT1-mediated uptake. However, SUP-B15 had a significantly increased uptake relative to control (~1.8-fold). This contrasts with the qPCR results, which showed decreased transcript levels. It is speculated that it may be an interaction with the DMSO over 24 hr. DMSO is known to alter membrane bilayer properties and fluidity (Gironi et al. 2020). Further experiments are needed to determine this, by determining if DMSO incubation for 24 hr is truly disrupting ENBT1 before determining the impact CDDO-Im, and by extension, Nrf2, have on ENBT1 in cells.

6.4) CONCLUSION

In summary, our study shows that ENBT1 function is decreased following incubation with menadione, which can be reversed with TEMPOL. This suggests that oxidative stress could contribute to a loss of ENBT1 function, leading to decreased uptake of 6-MP into leukemic cells, thus decreasing its efficacy. Antioxidant therapy has been shown to be promising in reducing toxic side effects during the intensification phase of ALL therapy but has not been tested for maintenance therapy (Al-Tonbary et al. 2009). Therefore, antioxidant treatment in ALL maintenance treatment with 6-MP could be a viable therapeutic application for future investigation.

6.5) LIMITATIONS

6.5.1) ROS species

The results above speculate on the species and mechanism of action of the ROS-generating compounds and antioxidants when assessing their impact on ENBT1 function. The kit used to quantify ROS indicates that it is measuring the "Total ROS species" but does not specifically state what ROS species it is measuring. Contacting the company to determine the compound used to quantify the ROS species was unfruitful (personal communication, March 29, 2024). It is assumed with this limited information that the word "Total" implies that all ROS species are being quantified, regardless of type, which limits the interpretation of the results above. Quantification of specific ROS species would be useful in determining the exact species being produced by the oxidants and provide mechanistic insights. The compound lucigenin is a specific compound that has been shown to specifically detect superoxide and, based on the mechanism of action of menadione, which primarily produces superoxide anion, would be more useful in this case (Afanas'ev 2001; Loor et al. 2010). This would clarify the issue around the ROS species being detected in various experiments to determine what species of ROS is most likely to impact ENBT1 function.

6.5.2) GSH measurements

Another important factor that was not assessed was the determination of the levels of GSH within the cells tested. Diamide and TBHP are known to impact the levels of GSH in cells and are integral to their mechanism of action (Harris and Power 1978; Kucera et al. 2014). Although neither of these compounds altered ENBT1 function, suggesting that decreases in cellular GSH does not have an impact on ENBT1 function this cannot be said definitively. Using an established

method for GSH quantification could make these statements more definitive (Rahman, Kode, and Biswas 2006).

6.5.3) Variability in menadione and antioxidant effects

Only one of the two antioxidants that have been tested reversed the effects seen by menadione, which was TEMPOL. On top of that, menadione showed a lot of variation in its overall effect between experiments. NAC did not work, but it was noted from the graph in **Figure 29A** that menadione showed no change from control, suggesting that the overall experimental set was not successful, likely due to high variability in the assay and human error, as mentioned in the discussion. The overall discrepancies and variability in both menadione and the antioxidant treatments required tighter control and consistency for more solid conclusions.

6.5.4) Nrf2 activation

Nrf2 activation was determined by the incubation with the activator, CDDO-Im, and confirmed via induction of the positive control genes, *NQO1* and *TXNRD1*. This is standard in the literature (Rooney et al. 2020; Wang, Zhang, et al. 2017; Shen et al. 2017; Suvorova et al. 2009); however, a more robust method could also have been used to specifically determine if the *SLC43A3* gene expression was targeted. A simple luciferase reporter assay that is commercially available from most companies could determine if Nrf2 is transcriptionally repressing or enhancing *SLC43A3* expression (Smale 2010).

Chapter 7: Regulation of ENBT1 by protein kinase C

7.1) INTRODUCTION

To investigate whether protein kinases potentially regulate ENBT1, an *in-silico* analysis was conducted to determine whether ENBT1 contained potential consensus sites for protein kinase-mediated phosphorylation. Using NetPhos 3.1 (Blom et al. 2004), potential sites for phosphorylation on several residues in ENBT1 were noted, with the majority being on the largest predicted intracellular loop of ENBT1. PKC, protein kinase A (PKA), and casein kinase 2 (CK2) had predicted consensus sites in ENBT1. Of note is that PKC showed the highest probability associated with its predicted sites on ENBT1 and will be the primary focus. These potential sites are shown in **Figure 33** with their predicted probabilities.

Phosphorylation is a fundamental biochemical process that involves the addition of a phosphate group to specific amino acid residues, such as serine, threonine, or tyrosine, on protein molecules by protein kinases. This post-translational modification serves as a crucial mechanism for regulating cellular signalling pathways and modulating various physiological responses within cells (Manning et al. 2002). By altering the structure and function of proteins, phosphorylation acts as a molecular switch, influencing cellular processes such as metabolism, cell cycle progression, gene expression, and cell signalling. Dysregulation of phosphorylation events is implicated in numerous diseases, including cancer, neurodegenerative disorders, and metabolic syndromes, highlighting its importance in cellular homeostasis and disease pathogenesis (Cohen 2001).

PKC, a family of serine/threonine protein kinases, has pivotal roles in cellular signalling networks, governing diverse processes such as cell proliferation, differentiation, apoptosis, and metabolism. There are several PKC isoforms that are categorized into three separate groups: conventional (cPKCs: α, β, γ), novel (nPKCs: δ, ε, η, θ), and atypical (aPKCs: ζ, ι), each exhibiting distinct activation requirements and cellular functions (Newton 2018). cPKCs are activated by

phospholipids, calcium ions, and diacylglycerol (DAG). Conversely, nPKCs are activated by DAG but do not require calcium ions for activation, while aPKCs are insensitive to both calcium and DAG but are activated by phosphatidyl serine (Newton 2018; Steinberg 2008). The signalling pathways mediated by PKC are involved in numerous physiological and pathological processes, making them attractive targets for therapeutic interventions in various diseases.

One such disease that has extensively investigated the role of PKC is in the pathogenesis and treatment of ALL. Evidence suggests an interplay between PKC and the pathogenesis of ALL. Firstly, it was noted that PKC and its various isoforms are expressed in ALL cells (Komada et al. 1991). Several studies have highlighted aberrant PKC signalling pathways in leukemic cells, contributing to their uncontrolled growth, survival, and chemoresistance to treatment (Lutzny et al. 2013; Jiffar et al. 2004; Loi et al. 2016). Furthermore, PKC expression has been noted to be upregulated in leukemic cells and leukemic cells that are resistant to chemotherapeutic drugs (Sutherland et al. 1992; Beck et al. 2001).

Based on this upregulation, targeting PKC emerged as a promising therapeutic strategy in the management of ALL. Various preclinical and clinical studies have explored the efficacy of PKC inhibitors in suppressing leukemic cell growth and enhancing treatment outcomes. Several studies have noted that PKC expression is prognostic of relapse in leukemia patients (Volm, Sauerbrey, and Zintl 1994; Volm et al. 1997; Volm et al. 2002). Also, a multitude of studies have delineated the efficacy of PKC inhibitors in sensitizing ALL cells to conventional chemotherapeutic agents, thereby augmenting their cytotoxic effects and potentially being a viable therapeutic approach (Weisenthal et al. 1987; Sakurada et al. 1989; Zhu et al. 1998; Zhu et al. 1999; Guzman et al. 2007; Saba and Levy 2011; Alexander et al. 2017; Ruiz-Aparicio et al. 2020; Ruiz-Aparicio et al. 2021; Franciosa et al. 2021). Although most of the evidence appears to suggest

PKC as pro-oncogenic, it is not completely clear. A study looking at the expression of PKCα in T-ALL patients showed that lower expression of this PKC isozyme was associated with a higher incidence of relapse and worse overall survival and event-free survival (Milani et al. 2014). These differences display the complexity of PKC and its multitude of biological effects that are dependent on cell type, interacting proteins and modulators, and isozyme-dependent expression in cells (Griner and Kazanietz 2007; Nakashima 2002).

In terms of the potential interaction of PKC and the use of 6-MP in ALL, there has been little work in this area. It has been noted that PKC is associated with the activity of TPMT and, therefore, could impact 6-MP toxicity (Stocco et al. 2012). Another study in a subset of ALL patients investigated the PKCζ isozyme. This study noted higher levels of PKCζ expression and overall phosphorylation within the cells that was associated with a higher sensitivity to 6-MP (Hartsink-Segers et al. 2015). The study notes that the sensitivity is likely due to the expression of MSH2, which is involved in the DNA mismatch repair (Diouf et al. 2011). Only one study has investigated how the activation of PKC can impact nucleobase uptake following activation with PMA, a broad-spectrum PKC activator. The study looked at LLC-PK1 cells after incubation with PMA for 24 hr and showed increased sodium-independent hypoxanthine uptake into the cells (Griffith and Jarvis 1996). At the time, the nucleobase transporter in question was not clear. However, based on the kinetic analyses from this study, it is possible that the transporter in question could be ENBT1. Therefore, the activation of PKC by PMA could be directly responsible for the trafficking of ENBT1 and could impact 6-MP uptake in ALL cells, leading to changes in its efficacy.

This chapter will explore the role of protein kinases, primarily PKC, and how it impacts the functional uptake of 6-MP via ENBT1. Activators and inhibitors of protein kinases will be

utilized to investigate this. Similar to **Chapter 6**, K562 cells will be the primary cell line used for the experiments in this chapter as they display the highest expression of *SLC43A3*/ENBT1 **(Table 4)**.

Figure 33: Predicted probability of consensus sites for protein kinase phosphorylation on ENBT1

The predicted topology of ENBT1 using Protter (Omasits et al. 2014) is shown. The arrows point out predicted phosphorylation sites by PKC, PKA, and CKII with there respective probabilities as determined using NetPhos 3.1 (Blom et al. 2004).

Figure 33

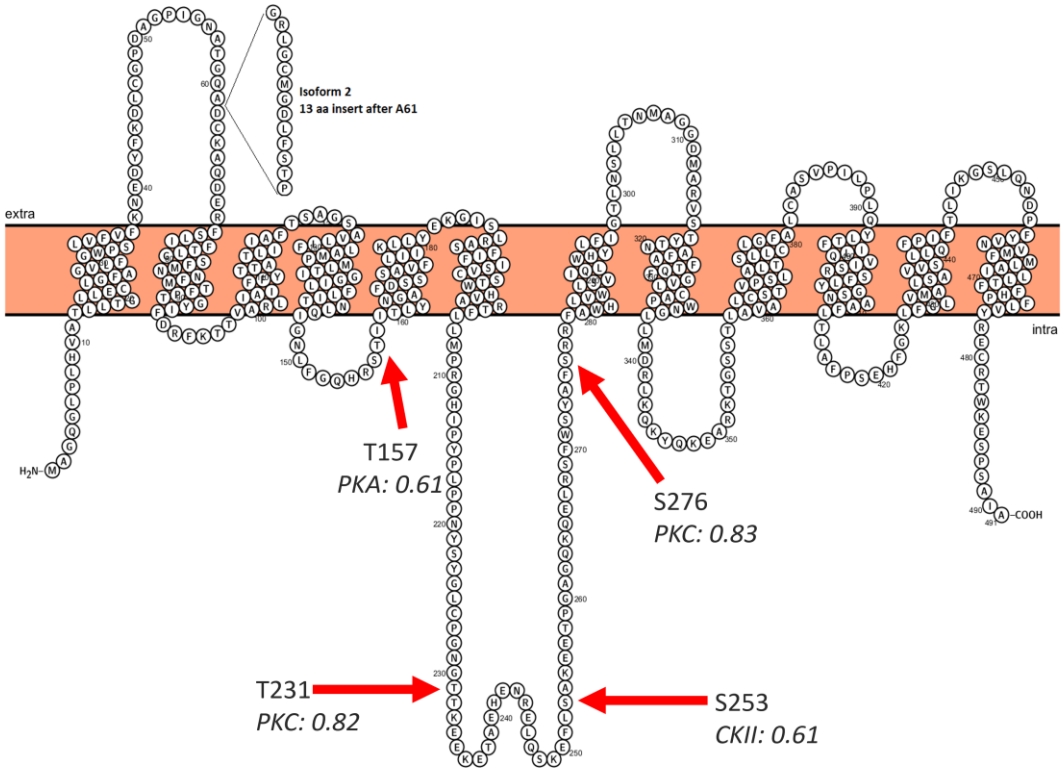
extra
intra
Isoform 2
13 aa insert after A61
T157
PKA: 0.61
S276
PKC: 0.83
T231
PKC: 0.82
S253
CKII: 0.61
H2N-
-COOH

7.2) RESULTS

7.2.1) Effect of the PKC activator PMA in K562 cells

ENBT1 has several predicted high-probability residues for PKC phosphorylation. To determine if PKC activation alters ENBT1 function, the broad-spectrum PKC activator PMA was used in K562 cells. As a control, a structurally identical inactive analog of PMA (binds to PKC but does not activate it), 4α-PMA, was used. PMA was incubated with cells at two different time points, 15 min and 30 min, in D-PBS. PMA was also incubated at various stages of the uptake assay, centred specifically around the two washes in the NMG buffer **(Figure 34)**. This was done because it was unclear whether the effect of PMA would still be apparent after the successive washes and incubation in DY prior to the assay (it takes ~ 30 min to wash cells and incubate in DY prior to the uptake assay). Doing it in this method also assesses whether PMA has a direct impact on ENBT1 since if it is incubated after washes are complete, it will be present in the uptake assay. This is in contrast to incubation before the washes since the washes will essentially dilute out the PMA and, therefore, would not be present in the assay. For **Panels A and B,** PMA was incubated for a total of 15 min either before the NMG washes **(Panel A)** or after the NMG washes **(Panel B)** prior to the uptake. In both experiments, PMA did not change ENBT1 function relative to control treatment (**Panel A**: V_{max}: DMSO - 76 ± 9 pmol/µL/sec; PMA – 58 ± 5 pmol/µL/sec) (**Panel B**: V_{max}: 4α-PMA - 57 ± 8 pmol/µL/sec; PMA – 46 ± 5 pmol/µL/sec). However, it is noted that PMA treatment is slightly decreasing the ENBT1-mediated 6-MP uptake, indicated by the significant difference in the final concentration of 6-MP in the kinetic analysis (2-way ANOVA with a post-hoc Holm-Sidak test, $P<0.05$). For the 30 min incubations, PMA was incubated for 15 min before the wash and 15 min after the wash (30 min total) **(Panel C)** or 30 min before the wash step **(Panel D)** in D-PBS prior to the uptake. In both 30 min incubations, PMA showed a

significantly decreased V_{max} value for ENBT1 (**Panel C**: V_{max}: 4α-PMA - 63 ± 9 pmol/μL/sec; PMA – 41 ± 5 pmol/μL/sec; extra sum of squares F-test, $P<0.05$) (**Panel D**: V_{max}: 4α-PMA - 74 ± 13 pmol/μL/sec; PMA – 47 ± 5 pmol/μL/sec; extra sum of squares F-test, $P<0.05$). Finally, the effect of PMA was determined in the same fashion as in **Panel D,** except that the incubation with PMA was done in serum-free media as opposed to D-PBS. There was no difference seen between 4α-PMA and PMA in this experiment (V_{max}: 4α-PMA - 62 ± 5 pmol/μL/sec; PMA – 86 ± 15 pmol/μL/sec) **(Panel E)**. All subsequent experiments with PMA were conducted in D-PBS, as shown in **Panel D**.

Figure 34: Incubation with PMA in D-PBS for 30 min decreases ENBT1-mediated 6-MP uptake in K562 cells

K562 cells were incubated with either DMSO **(A)**, 100 nM of 4α-PMA **(B)**, or PMA **(A, B)** for 15 min at 37°C in D-PBS either before **(A)** or after **(B)** the cells were washed in NMG buffer. Cells are washed twice in NMG-buffer before determining the uptake kinetics of [^{14}C] 6-MP at room temperature. The kinetics of ENBT1-mediated [^{14}C] 6-MP uptake were determined by assessing the uptake of a range of concentrations of [^{14}C] 6-MP (1 – 300 μM) estimated by the transporter-mediated uptake at 2 sec (calculated as the difference in cellular uptake ± 5 mM adenine). Cells were then centrifuged through oil, and the cell pellets were digested overnight in 1 M NaOH and assessed for [^{14}C] content using standard liquid scintillation counting techniques to define pmol 6-MP accumulated per μl/second in the cell pellet. Data points represent the mean ± SD of 4 **(A)** or 7 **(B)** experiments done in duplicate. * Represents a significant difference from PMA using a 2-way ANOVA with a post-hoc Holm-Sidak test, $P<0.05$. **C, D)** K562 cells were incubated with either 100 nM of 4α-PMA or PMA for 30 min at 37°C. The total 30 min incubation was done by incubating for 15 min before and 15 min after **(B)** or 30 min before **(C)** the cells were washed in NMG buffer. Cells are washed twice in the NMG buffer before determining the uptake kinetics of [^{14}C] 6-MP at room temperature. The kinetics of ENBT1-mediated [^{14}C] 6-MP uptake were determined by assessing the uptake of a range of concentrations of [^{14}C] 6-MP (1 – 300 μM **(C)** or 1 – 400 μM **(D)**). Radioactive content was determined as described above for **Panel A and B**. Data points represent the mean ± SD of 6 **(C)** or 5 **(D)** experiments done in duplicate. * Represents a significant difference from PMA using a 2-way ANOVA with a post-hoc Holm-Sidak test, $P<0.05$. **E)** K562 cells were treated and assessed the same as **Panel D** except that the cells were

treated with 100 nM 4α-PMA or PMA in serum-free media instead of D-PBS. Data points represent the mean ± SD of 8 experiments done in duplicate.

Figure 34

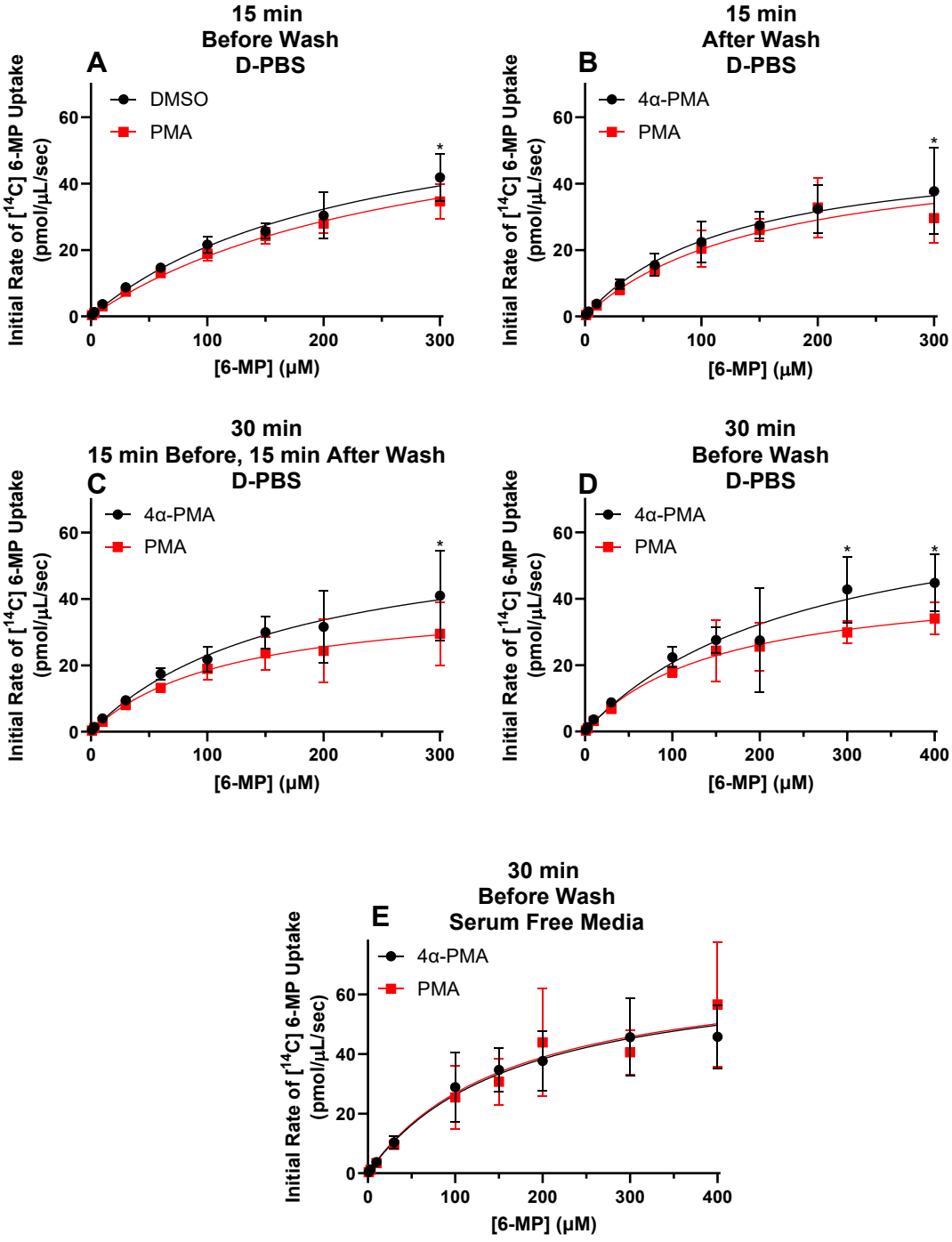
A
15 min
Before Wash
D-PBS
DMSO
PMA
B
15 min
After Wash
D-PBS
4α-PMA
PMA
C
30 min
15 min Before, 15 min After Wash
D-PBS
4α-PMA
PMA
D
30 min
Before Wash
D-PBS
4α-PMA
PMA
E
30 min
Before Wash
Serum Free Media
4α-PMA
PMA
Initial Rate of [14C] 6-MP Uptake (pmol/µL/sec)
[6-MP] (µM)

7.2.2) Effect of the PKC activator PMA in MOLT-4 and SUP-B15 cells

As determined in **Figure 34**, PMA induced a significant decrease in the V_{max} value for ENBT1 in K562 cells. MOLT-4 and SUP-B15 cells were tested in the same way to determine if incubation with PMA would also induce a decrease in these cell lines **(Figure 35)**. Both cell lines showed a significant decrease in the V_{max} value for ENBT1 following treatment with PMA relative to control (**Panel A (MOLT-4)**: V_{max}: 4α-PMA - 49 ± 9 pmol/µL/sec; PMA – 28 ± 4 pmol/µL/sec; extra sum of squares F-test, $P<0.05$) (**Panel B (SUP-B15)**: V_{max}: 4α-PMA - 42 ± 7 pmol/µL/sec; PMA – 24 ± 4 pmol/µL/sec; extra sum of squares F-test, $P<0.05$).

Figure 35: Incubation with PMA in D-PBS for 30 min decreases ENBT1-mediated 6-MP uptake in MOLT-4 and SUP-B15 cells

MOLT-4 **(A)** or SUP-B15 **(B)** cells were incubated with either 100 nM of 4α-PMA or PMA for 30 min at 37°C in D-PBS. Cells were then washed twice in an NMG buffer before determining the uptake kinetics of [^{14}C] 6-MP at room temperature. The kinetics of ENBT1-mediated [^{14}C] 6-MP uptake were determined by assessing the uptake of a range of concentrations of [^{14}C] 6-MP (1 – 400 μM) estimated by the transporter-mediated uptake at 2 sec (calculated as the difference in cellular uptake ± 5 mM adenine). Cells were then centrifuged through oil, and the cell pellets were digested overnight in 1 M NaOH and assessed for [^{14}C] content using standard liquid scintillation counting techniques to define pmol 6-MP accumulated per μl/second in the cell pellet. Data points represent the mean ± SD of 5 **(A)** or 7 **(B)** experiments done in duplicate. * Represents a significant difference from PMA using a 2-way ANOVA with a post-hoc Holm-Sidak test, $P<0.05$.

Figure 35

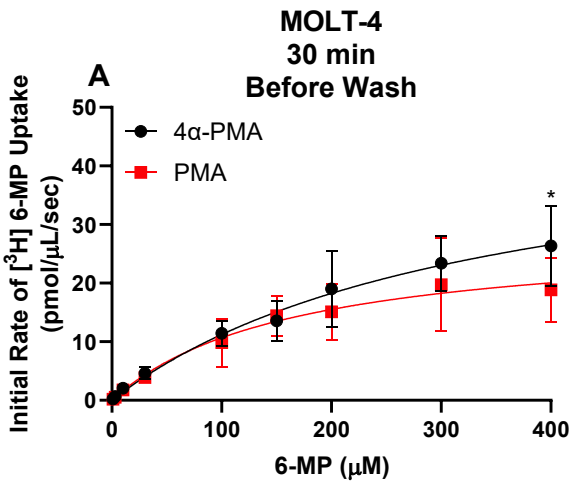
MOLT-4
30 min
Before Wash
A
4α-PMA
PMA
Initial Rate of [3H] 6-MP Uptake (pmol/µL/sec)
6-MP (µM)
0
10
20
30
40
50
0
100
200
300
400
*

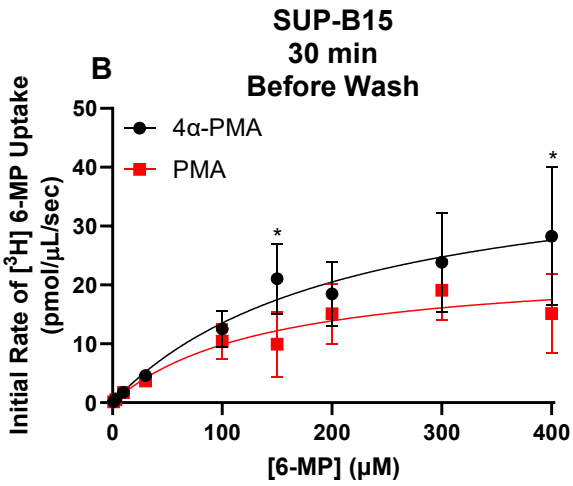
SUP-B15
30 min
Before Wash
B
4α-PMA
PMA
Initial Rate of [3H] 6-MP Uptake (pmol/µL/sec)
[6-MP] (µM)
0
10
20
30
40
50
0
100
200
300
400
*
*

7.2.3) Inhibition of PMA-mediated effect by the PKC inhibitor Gö6983

PMA induced a decrease in ENBT1 function, as displayed by a decrease in the V_{max} value in K562, MOLT-4, and SUP-B15. To ensure that the effect of PMA was a direct consequence of PKC activation, the broad-spectrum PKC inhibitor Gö6983 was used in K562 cells **(Figure 36)**. Cells incubated with Gö6983 alone showed no change from control. PMA incubation caused a significant decrease in the V_{max} value relative to the control (extra sum of squares F-test, $P<0.05$). Finally, the combination of PMA and Gö6983 was not different from the control (V_{max}: 4α-PMA - 22 ± 2 pmol/µL/sec; Gö6983 – 17 ± 1 pmol/µL/sec; PMA – 13 ± 1 pmol/µL/sec; PMA + Gö6983 – 20 ± 2 pmol/µL/sec).

Figure 36: Pre-incubation with Gö6983 reverses the decrease in ENBT1-mediated adenine uptake following incubation with PMA in K562 cells

K562 cells were pre-incubated with either DMSO (4α-PMA and PMA) or 1 μM Gö6983 (Gö6983 and PMA + Gö6983) for 15 min at 37°C before adding 100 nM 4α-PMA (4α-PMA and Gö6983) or PMA (PMA and PMA + Gö6983) for an additional 30 min at 37°C in D-PBS. Cells were then washed twice in NMG buffer before determining the uptake kinetics of [^{3}H] adenine at room temperature. The kinetics of ENBT1-mediated [^{3}H] adenine uptake were determined by assessing the uptake of a range of concentrations of [^{3}H] adenine (1 – 150 μM) estimated by the transporter-mediated uptake at 2 sec (calculated as the difference in cellular uptake ± 5 mM adenine). Cells were then centrifuged through oil, and the cell pellets were digested overnight in 1 M NaOH and assessed for [^{3}H] content using standard liquid scintillation counting techniques to define pmol adenine accumulated per μl/second in the cell pellet. Data points represent the mean ± SD of 6 experiments done in duplicate. * Represents a significant difference between 4α-PMA and PMA using a 2-way ANOVA with a post-hoc Holm-Sidak test, $P<0.05$. # Represents a significant difference between 4α-PMA and PMA + Gö6983 using a 2-way ANOVA with a post-hoc Holm-Sidak test, $P<0.05$.

Figure 36

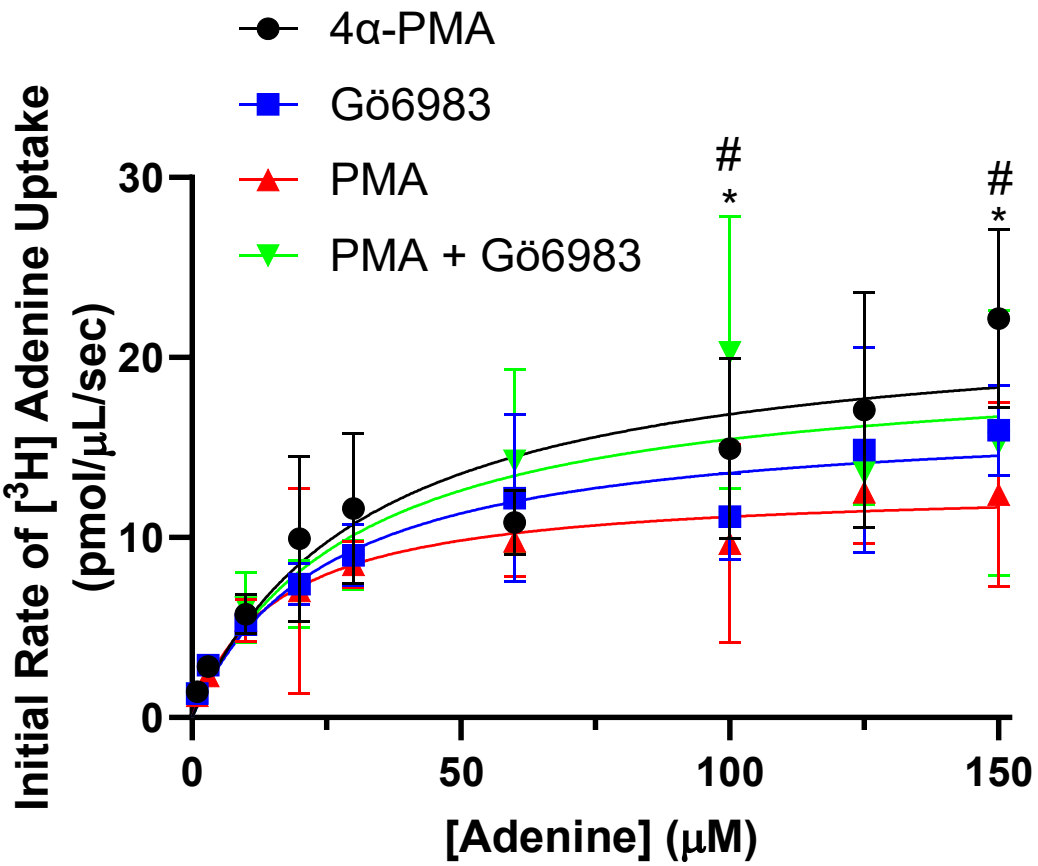
4α-PMA
Gö6983
PMA
PMA + Gö6983
Initial Rate of [3H] Adenine Uptake (pmol/µL/sec)
[Adenine] (µM)
0
10
20
30
0
50
100
150
#
*
#
*

7.2.4) Inhibition of casein kinase 2 and protein kinase A and C

An open question was whether ENBT1 was constitutively phosphorylated by various protein kinases in the cells, leading to a basal tone of phosphorylation of ENBT1 that could impact its trafficking. **Figure 33** shows ENBT1 contains predicted consensus sites for PKA, PKC and CKII. To investigate this, three separate protein kinase inhibitors, Gö6983, H89, and CX-4945, which are PKC, PKA, and CK2 inhibitors, respectively, were assessed **(Figure 37)**. Firstly, a concentration that would not decrease cell viability over a 24-hr period and would be high enough to have robust inhibition of each separate kinase was determined. Using the MTT assay, neither of the kinase inhibitors caused any great decrease in cell viability except at the higher end of the concentrations used **(Panel A, B, C)**. Of note, none of the kinase inhibitors showed a loss of viability at 1 μM, which is the concentration that was used for the determination of its impact on ENBT1 function. This concentration is also sufficient to completely inhibit each separate protein kinase based on the reported literature values (Gschwendt et al. 1996; Chijiwa et al. 1990; Pierre et al. 2011). K562 cells were incubated for 24 hr with 1 μM of each separate inhibitor prior to determining the uptake of 1 μM **(Panel D)** and 150 μM **(Panel E)** [^{3}H] 6-MP. These concentrations were used since they represent the clinical concentration of 6-MP (1 μM) (Lonnerholm et al. 1986) and are near the K_m of 6-MP (~150 μM) for ENBT1. A 24 hr incubation was used as a starting point as the median protein half-life is around 9 hr, but membrane proteins are generally more stable than the median, so a longer time point was used (Chen, Smeekens, and Wu 2016; Hare and Taylor 1991). None of the inhibitors tested at either concentration of 6-MP showed any change in uptake relative to treatment with control (DMSO).

Figure 37: 24 hr incubation with protein kinase inhibitors does not vastly effect cell viability and ENBT1-mediated 6-MP uptake in K562 cells

K562 cells were plated at a density of 5 x 10^4 cells/well in 24-well plates and incubated with a range of concentrations (1.2 nM – 20 μM) of the protein kinase inhibitors Gö6983 **(A)**, H89 **(B),** and CX-4945 **(C)**, at 37°C in a humidified incubator (5% CO_2/95% air). Cell viability was assessed using the MTT assay and expressed as a percent of the cell viability measured at each time point in the absence of the inhibitor (% of control). Sigmoidal concentration-response curves were fit to the data. Each point represents the mean ± SD of 5 experiments done in duplicate. **D, E)** K562 cells were incubated with either DMSO or 1 μM of each protein kinase inhibitor for 24 hr at 37°C in a humidified incubator (5% CO_2/95% air). Cells were then washed twice in an NMG buffer before determining their uptake of [^{3}H] 6-MP at 1 μM **(D)** and 150 μM **(E)** at room temperature for 2 sec. Transport was terminated by centrifugation of the cells through an oil layer. Cell pellets were digested overnight in 1 M NaOH, and their [^{3}H] content was assessed via liquid scintillation counting. Bars represent the ENBT1-mediated uptake and are defined as the difference between the total uptake (absence of 5 mM adenine) and the non-mediated uptake (presence of 5 mM adenine). Data are shown as the pmols of 6-MP accumulated by the cells/μl of cell volume/second. Data are represented as the mean ± SD of 6 experiments done in duplicate.

Figure 37

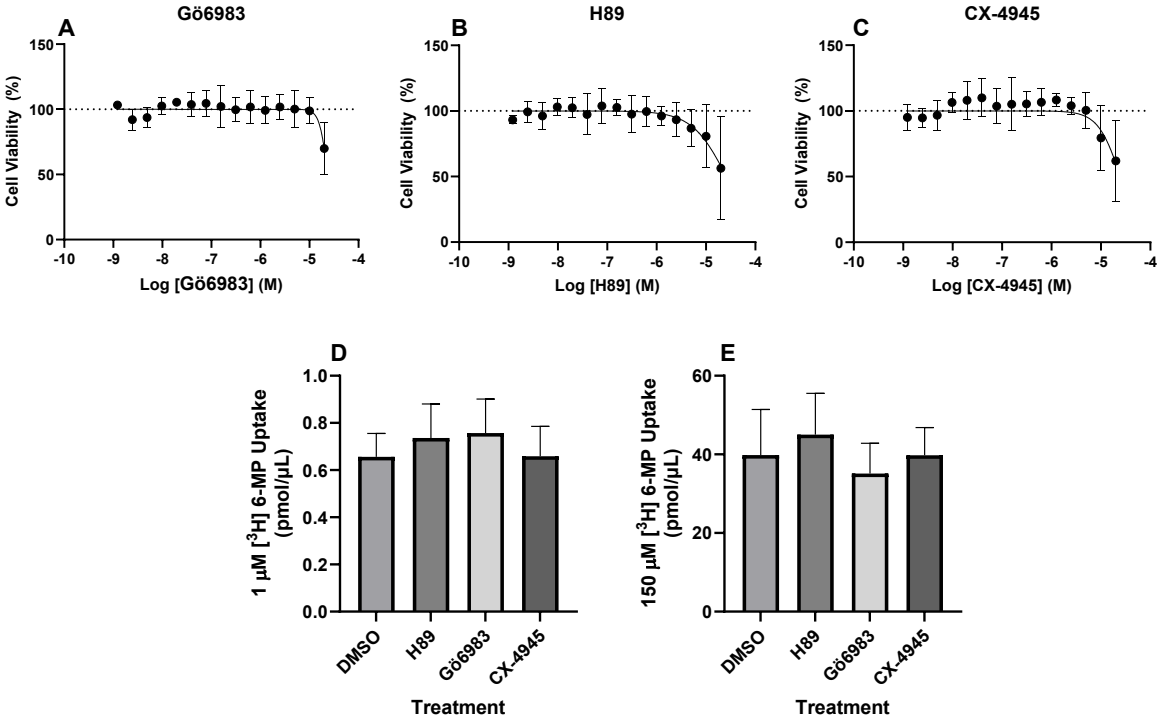
A
Gö6983
Cell Viability (%)
Log [Gö6983] (M)
B
H89
Cell Viability (%)
Log [H89] (M)
C
CX-4945
Cell Viability (%)
Log [CX-4945] (M)
D
1 µM [3H] 6-MP Uptake (pmol/µL)
DMSO
H89
Gö6983
CX-4945
Treatment
E
150 µM [3H] 6-MP Uptake (pmol/µL)
DMSO
H89
Gö6983
CX-4945
Treatment

7.2.5) Treatment with cycloheximide in MOLT-4 and SUP-B15 cells

Figure 37 determined that there was no change in ENBT1 function following treatment with various protein kinase inhibitors, suggesting that ENBT1 does not contain constitutive basal phosphorylation that impacts its trafficking. However, the experiment used a 24-hr incubation period that assumes the ENBT1 protein would undergo complete turnover. To determine the turnover rate of ENBT1, cycloheximide (a protein synthesis inhibitor) was used to estimate the ENBT1 turnover rate in MOLT-4 and SUP-B15 cells **(Figure 38)**. The toxicity of cycloheximide was first investigated over a 24-hr period at different concentrations (5 μg/mL, 10 μg/mL, 25 μg/mL, 50 μg/mL, and 100 μg/mL) **(Panel A and B)**. All concentrations of cycloheximide decreased % of live cells in a dose-dependent manner, with higher concentrations being more toxic than lower concentrations. MOLT-4 cells appear to be more susceptible to cycloheximide than SUP-B15 cells. Thus, SUP-B15 cells were used for the western blot analysis. SUP-B15 cells were incubated with 100 μg/mL cycloheximide over a 24-hr period with protein extracted every 4 hr. Densitometric analysis shows that ENBT1 protein is slightly increased at each timepoint assessed relative to time zero.

Figure 38: Cycloheximide decreases live cells and slightly increases ENBT1 protein levels in MOLT-4 and SUP-B15 cells

SUP-B15 **(A)** and MOLT-4 **(B)** cells were plated at a density of 1 x 10^6 cells/plate in 10 cm plates and incubated with DMSO or different concentrations (5 µg/mL, 10 µg/mL, 25 µg/mL, 50 µg/mL, 100 µg/mL) of cycloheximide for 24 hr, at 37°C in a humidified incubator (5% CO_2/95% air). Cell viability was assessed using the trypan blue assay and expressed as a percent of live cells. Bars represent the mean ± SD of 5 experiments done in duplicate. * Represents a significant difference from DMSO using a 1-way ANOVA with a post-hoc Holm-Sidak test, $P<0.05$. **C)** SUP-B15 cells were treated with 100 µg/mL cycloheximide, and ENBT1 protein was extracted every 4 hr over a 24-hr treatment period. ENBT1 expression levels were assessed using a western blot. Samples were resolved on SDS-PAGE gels, transferred to polyvinyl membranes and probed with anti-ENBT1 (upper) and anti-β-actin (lower) antibodies. The arrows indicate the bands for ENBT1 protein and was used for densitometry analysis. The numbers displayed below the ENBT1 blot represent the densitometry analysis of ENBT1 relative to time zero using β-actin as a loading control.

Figure 38

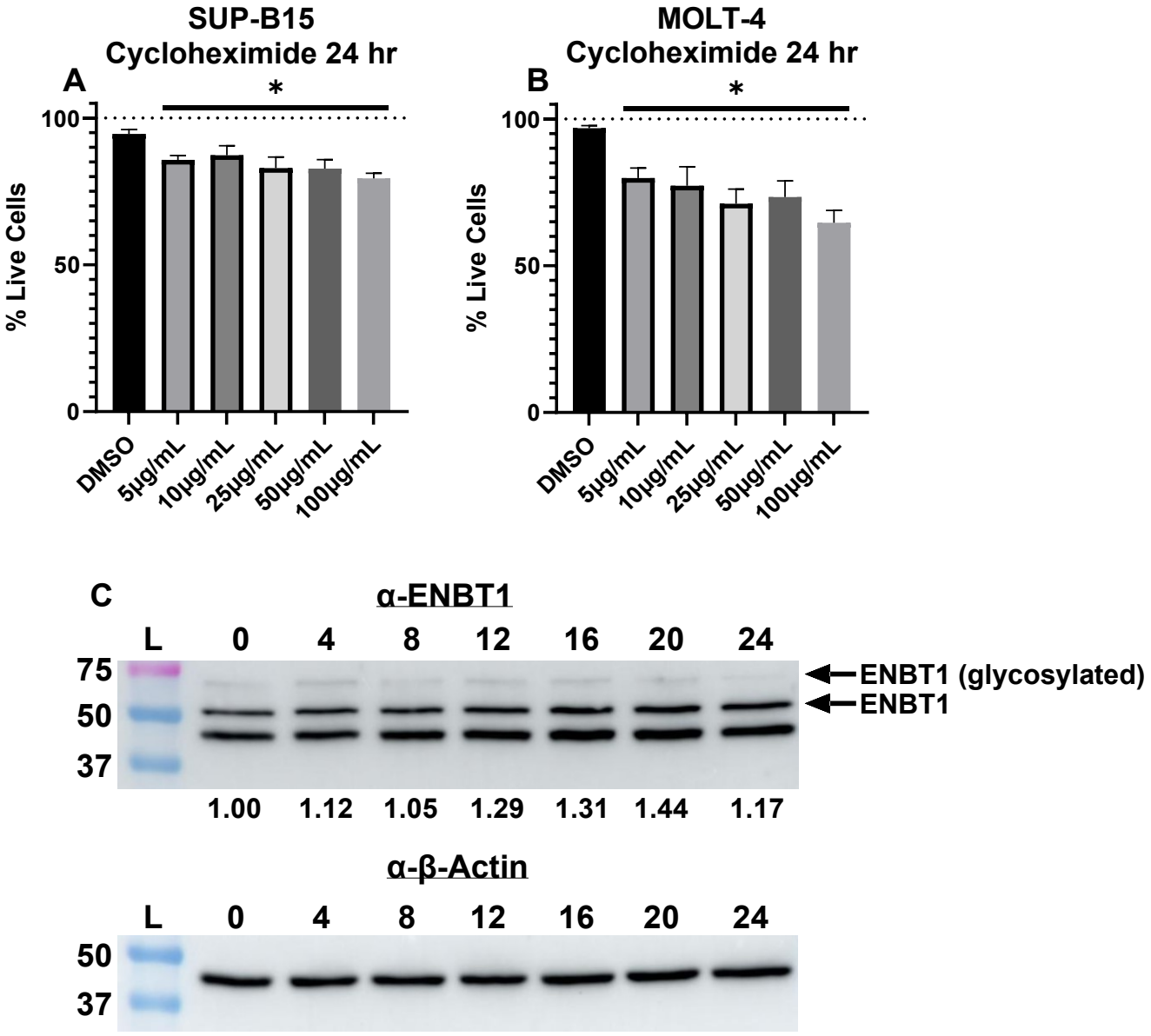
SUP-B15
Cycloheximide 24 hr
A
*
100
50
0
% Live Cells
DMSO
5µg/mL
10µg/mL
25µg/mL
50µg/mL
100µg/mL
MOLT-4
Cycloheximide 24 hr
B
*
100
50
0
% Live Cells
DMSO
5µg/mL
10µg/mL
25µg/mL
50µg/mL
100µg/mL
C
α-ENBT1
L
0
4
8
12
16
20
24
75
50
37
ENBT1 (glycosylated)
ENBT1
1.00
1.12
1.05
1.29
1.31
1.44
1.17
α-β-Actin
L
0
4
8
12
16
20
24
50
37

7.2.6) Treatment with cycloheximide in K562 cells

Based on the data from **Figure 38** that noted there was a slight increase in ENBT1 protein after 24 hr in SUP-B15 cells, the analysis was extended to determine the turnover of ENBT1 in a longer time frame but also to ensure the cycloheximide was working as expected. The longer-term incubation was done in K562 cells, as opposed to SUP-B15 cells, because they were less sensitive to cell death caused by cycloheximide, which could be a potentially confounding variable. Firstly, as was done in the MOLT-4 and SUP-B15 cells, the toxicity of 100 μg/mL cycloheximide was determined over a 96 hr period and assessed every 24 hr. Cycloheximide displayed a time-dependent decrease in % of live cells **(Figure 39A)**. At the same time, the total cell count was determined, and cells treated with control (DMSO) showed rapid proliferation of the cells that stopped when the cells got confluent (reached by 48 hr). In contrast, cells treated with cycloheximide appeared to be senescent and did not proliferate after 24 hr of cycloheximide treatment **(Figure 39B)**. Similar to what was done in **Figure 38C**, a western blot was conducted on cells with protein extracted every 24 hr over the 96-hr period for determination of ENBT1 protein expression. Densitometric analysis shows that ENBT1 protein appears to be increased at each timepoint assessed relative to time zero. To ensure that the cycloheximide was working as expected, ENT1 protein expression was also assessed as a control. ENT1 protein levels remained relatively unchanged for the first 48 hr, but by 96 hr of treatment, ENT1 protein expression was decreased by 4-fold relative to time zero **(Figure 39D)**. Finally, the impact of cycloheximide on ENBT1 function was determined following a 24 hr incubation; cycloheximide showed no difference to treatment with control (DMSO) (V_{max}: DMSO - 12 ± 1 pmol/μL/sec; Cycloheximide – 10 ± 1 pmol/μL/sec) **(Figure 39C)**.

Figure 39: Cycloheximide decreases live cells and halts cell proliferation with little impact on ENBT1 in K562 cells

A, B) K562 cells were plated at a density of 5 x 10^5 cells/plate in 10cm plates and incubated with DMSO or 100 µg/mL of cycloheximide for 96 hr, at 37°C in a humidified incubator (5% CO_2/95% air). % of live cells **(A)** and total cell count **(B)** were determined every 24 hr over the 96-hr period using the trypan blue assay. **Panel A** bars represent the mean ± SD of 5 experiments done in duplicate. * Represents a significant difference from DMSO using a 1-way ANOVA with a post-hoc Holm-Sidak test, $P<0.05$ **Panel B** points represent the mean ± SD of 5 experiments done in duplicate. * Represents a significant difference from DMSO using a 2-way ANOVA with a post-hoc Holm-Sidak test, $P<0.05$ **C)** K562 cells were incubated with either DMSO or 100 µg/mL of cycloheximide for 24 hr at 37°C in a humidified incubator (5% CO_2/95% air). Cells are washed twice in NMG buffer before determining the uptake kinetics of [^{3}H] adenine at room temperature. The kinetics of ENBT1-mediated [^{3}H] adenine uptake were determined by assessing the uptake of a range of concentrations of [^{3}H] adenine (1 -150 µM) estimated by the transporter-mediated uptake at 2 sec (calculated as the difference in cellular uptake ± 5 mM adenine). Cells were then centrifuged through oil, and the cell pellets were digested overnight in 1 M NaOH and assessed for [^{3}H] content using standard liquid scintillation counting techniques to define pmol adenine accumulated per µl/second in the cell pellet. Data points represent the mean ± SD of 5 experiments done in duplicate. **D)** K562 cells were treated with 100 µg/mL cycloheximide, and ENBT1 protein was extracted every 24 hr over a 96-hr treatment period. ENBT1 and ENT1 expression levels were assessed using a western blot. Samples were resolved on SDS-PAGE gels, transferred to polyvinyl membranes and probed with anti-ENBT1 (top-left), anti-ENT1 (top-right), and anti-β-actin (lower left and right) antibodies. The arrows indicate the bands for the approximate sizes of the proteins,

which was used for densitometry analysis. The numbers displayed below the ENBT1 and ENT1 blot represent the densitometry analysis of the protein relative to time zero using β-actin as a loading control.

Figure 39

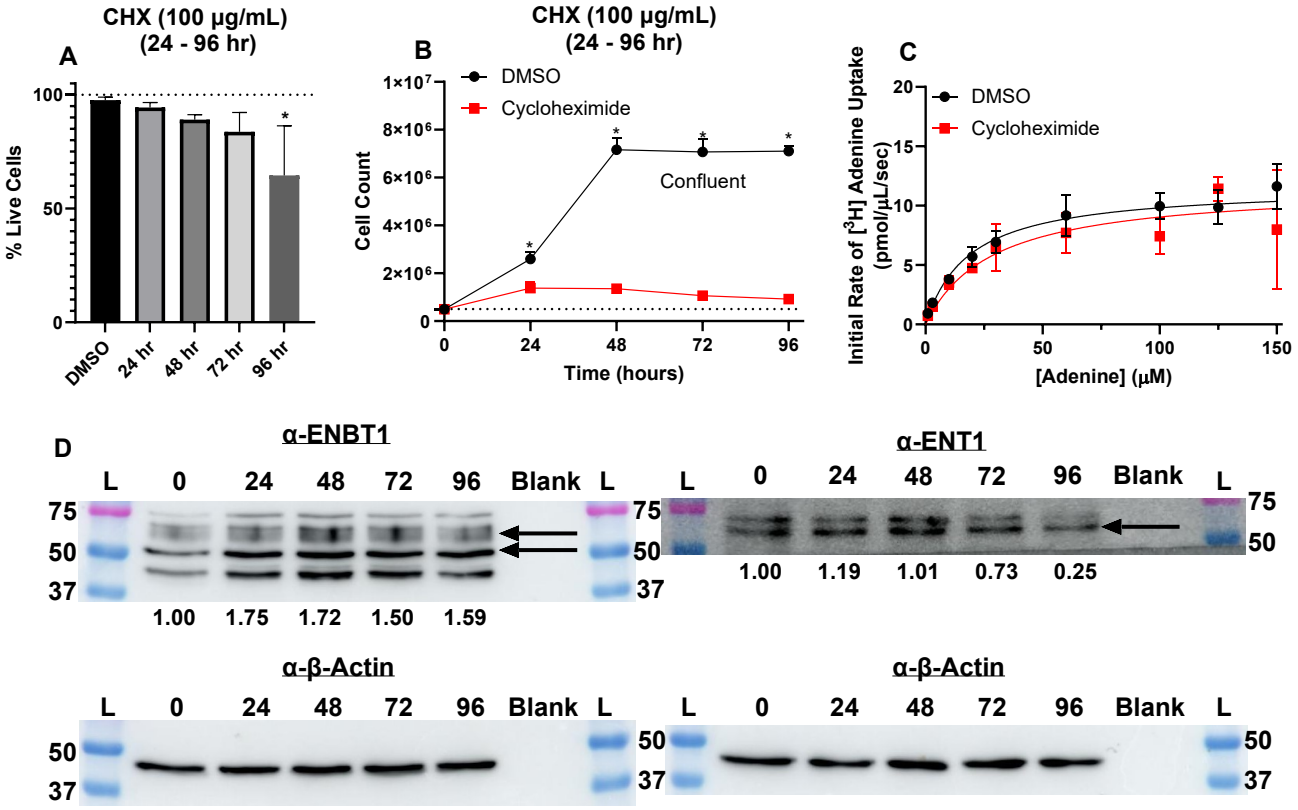
A
CHX (100 µg/mL)
(24 - 96 hr)
% Live Cells
100
50
0
DMSO
24 hr
48 hr
72 hr
96 hr
B
CHX (100 µg/mL)
(24 - 96 hr)
DMSO
Cycloheximide
Cell Count
1×10⁷
8×10⁶
6×10⁶
4×10⁶
2×10⁶
0
Confluent
0
24
48
72
96
Time (hours)
C
DMSO
Cycloheximide
Initial Rate of [³H] Adenine Uptake
(pmol/µL/sec)
20
15
10
5
0
0
50
100
150
[Adenine] (µM)
D
α-ENBT1
L
0
24
48
72
96
Blank
L
75
50
37
1.00
1.75
1.72
1.50
1.59
α-ENT1
L
0
24
48
72
96
Blank
L
75
50
1.00
1.19
1.01
0.73
0.25
α-β-Actin
L
0
24
48
72
96
Blank
L
50
37
α-β-Actin
L
0
24
48
72
96
Blank
L
50
37

7.2.7) Site-directed mutagenesis of ENBT1

As shown in **Figure 36**, it was determined that the decrease caused by PMA was a direct result of PKC activation. As noted from the introduction, ENBT1 contains several predicted consensus sites for PKC phosphorylation **(Figure 33)**, with three strong candidates being in the largest intracellular loop of ENBT1. Plasmids were mutagenized according to the method in **3.2.4** prior to transfection in HEK293 cells. The uptake of 30 μM [^{3}H] adenine was determined using a 2 sec time point following treatment with control (4α-PMA) or PMA as above. ENBT1_WT, ENBT1_S253A, and ENBT1_S276A had a significant decrease relative to control following treatment with PMA, while the ENBT1_T231A showed no change from control. (1-way ANOVA with a post-hoc Holm-Sidak test, $P<0.05$) **(Figure 40)**.

Figure 40: T231A mutant of ENBT1 is resistant to the PMA induced decrease in ENBT1-mediated adenine uptake in transfected HEK293 cells

Wild-type or site-directed mutants (T231A, S253A, S276A) of ENBT1 were transiently transfected in HEK293 cells and left for 72 hr. Afterwards, cells were harvested and treated with either 100 nM of 4α-PMA or PMA for 30 min at 37°C in D-PBS. Cells are washed twice in NMG buffer before determining the uptake of 30 μM [^{3}H] adenine at room temperature estimated by the transporter-mediated uptake at 2 sec (calculated as the difference in cellular uptake ± 5 mM adenine). Cells were then centrifuged through oil, and cell pellets were digested overnight in 1 M NaOH and assessed for [^{3}H] content using standard liquid scintillation counting techniques. Data is represented as the % of control relative to each individual transfected WT or mutant ENBT1 treated with 4α-PMA. Bars represent the mean ± SD of 4 experiments done in duplicate. * Represents a significant difference from control using a 1-way ANOVA with a post-hoc Holm-Sidak test, $P<0.05$.

Figure 40

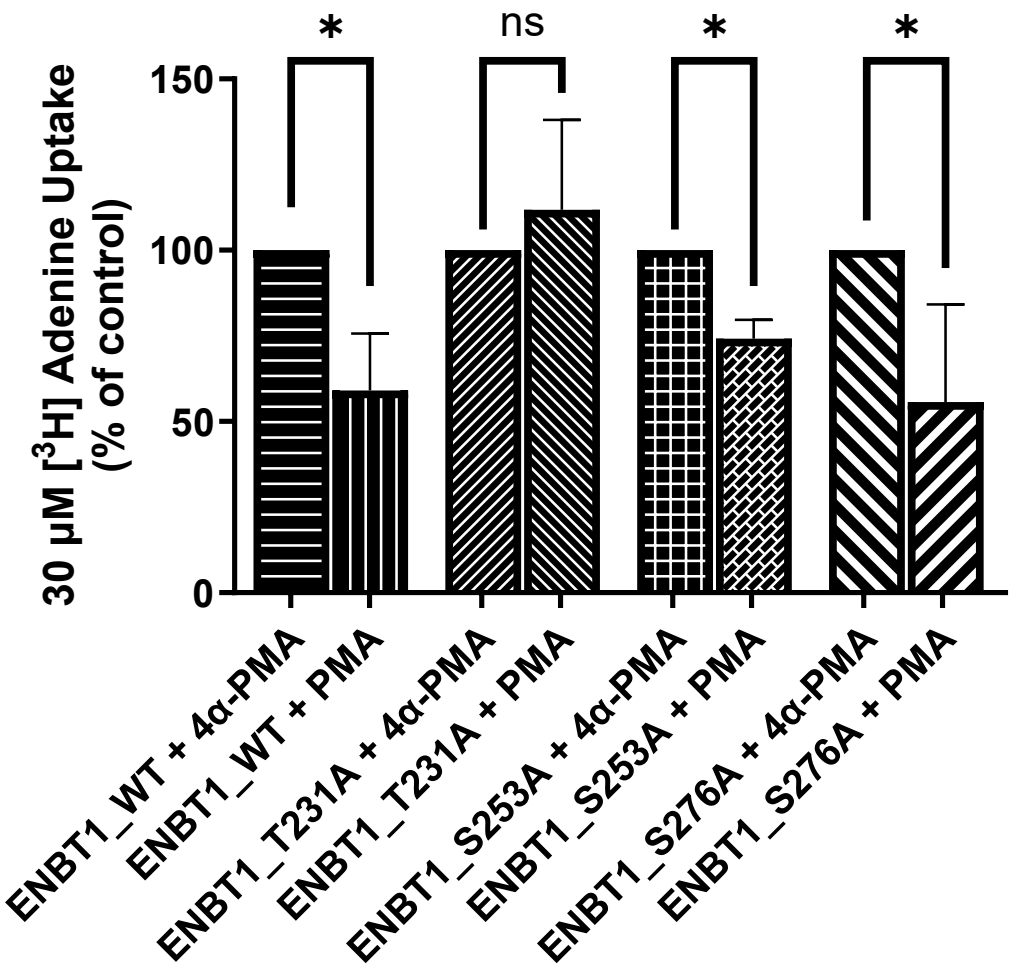
*
ns
*
*
150
100
50
0
30 µM [3H] Adenine Uptake
(% of control)
ENBT1_WT + 4α-PMA
ENBT1_WT + PMA
ENBT1_T231A + 4α-PMA
ENBT1_T231A + PMA
ENBT1_S253A + 4α-PMA
ENBT1_S253A + PMA
ENBT1_S276A + 4α-PMA
ENBT1_S276A + PMA

7.3) DISCUSSION

These data suggest that incubation with the PKC activator, PMA, decreases ENBT1 function via the phosphorylation of threonine 231. **Figure 34** and **Figure 35** demonstrate that regardless of the cell type, whether it be an ALL (MOLT-4, SUP-B15) or CML (K562) cell line, PMA induces a decrease in ENBT1 V_{max} values. A notable difference that was determined early in the experiments looking at PMA was that the PMA-induced decrease in ENBT1 uptake was consistent in D-PBS but ineffective when using serum-free media. **Figure 34E** shows that incubation of PMA for 30 min in serum-free media did not impact ENBT1-mediated uptake; this is in contrast to all the studies done in D-PBS, which always have a decrease. The difference between serum-free media and D-PBS is a matter of different salts and mainly amino acids present in the serum-free media that would not be in the D-PBS. There is no literature that suggests the base composition of the two would have an impact. It is speculated that rather than being the composition of the D-PBS and the serum-free media, it may be a result of the cell line being in a different proliferative state or cell cycle stage as a result of being in the two separate mediums. PKC has been shown to be entwined with the cell cycle at various stages and thus could depend on the cell cycle status while in the D-PBS or serum-free media (Black and Black 2012). The exact mechanism is unclear and would require further investigation.

As noted above in a separate study described in **7.1**, incubation of PMA for 24 hr in LLC-PK1 cells led to an increase in sodium-independent hypoxanthine uptake, and based on the characteristics described in the study, implies the transporter in question is ENBT1 (Griffith and Jarvis 1996). This contrasts with the results above, which always have a clear decrease in ENBT1-mediated uptake following PMA incubation. The differences between the literature and the results above can be explained by looking at the incubation time for PMA in the cells. In the results above,

all incubations are done at 100 nM for either 15 or 30 min at 37°C, with the majority being 30 min, which has been shown in the literature to be a standard methodology used for achieving maximal activation of PKC (Hipkin, Wang, and Schonbrunn 2000; Montero et al. 2016; Rybin et al. 2004). Incubation with PMA for much longer time points, like 24 hr (as done in the study by Griffith and Jarvis), has been shown to decrease PKC levels in cells and thus its activity (Montero et al. 2016; Rybin et al. 2004). The decreased expression and activity has been reported to be due to the enhanced degradation of PKC in PMA-treated cells over longer time periods compared to cells not treated with PMA (Young et al. 1987). Therefore, at 30 min with maximal PKC activation, ENBT1 function decreases, whereas, at 24 hr, when PKC activity is assumably decreased, Griffith and Jarvis have shown that an ENBT1-like transporter function is increased. This suggests that PKC controls either the transcriptional regulation of ENBT1 or that constitutive phosphorylation of ENBT1 in cells by PKC regulates the trafficking and membrane content of ENBT1.

To investigate the potential constitutive control of ENBT1 by protein kinases, the impact of various protein kinase inhibitors, namely H89 (PKA inhibitor), Gö6983 (PKC inhibitor), and CX-4945 (CK2 inhibitor), was assessed. In **Figure 37**, incubation with either of the inhibitors for the protein kinases had no change in cell viability or ENBT1 function. Although this suggests that ENBT1 is not under the basal control of any of these protein kinases, the potential stability of ENBT1 in the membrane is not taken into account. Cycloheximide was used to assess the stability of ENBT1 according to standard protocols over a 24 hr period (Kao et al. 2015). Initial experiments conducted in MOLT-4 and SUP-B15 cells in **Figure 38** showed slight decreases in cell viability but notably, following a 24-hr incubation with cycloheximide, appeared to have an increase in ENBT1 protein levels. It is speculated that inhibition of protein synthesis by cycloheximide causes a cascading effect. Firstly, all short-lived proteins will be degraded, and within a few hours, cell

division is halted due to the loss of critical proteins for cell cycle progression (Liu et al. 2010). It is speculated that within these few hours, the increase in ENBT1 protein will occur. Cells typically require a 2-fold increase in nucleotides to perform cell division (Lane and Fan 2015), and it is speculated that ENBT1 protein levels will increase to accommodate this need. The cell will ultimately not be able to divide due to cycloheximide, but it will likely still try to. This is apparent from the data in **Figure 38C**, which displays a slight increase in ENBT1 protein even at the 4 hr timepoint, which is sustained throughout. Since SUP-B15 cells did not appear to have a decrease in ENBT1 protein and a half-life could not be determined, a longer incubation period (96 hr) was conducted in K562 cells, as shown in **Figure 39**. Cycloheximide completely slowed cell proliferation, likely due to cycloheximide's ability to block mitotic entry (Lockhead et al. 2020), but still displayed an increase in ENBT1 protein levels even after incubation for 96 hr, similar to that seen for the SUP-B15 cells. It is speculated that a mechanism similar to the one described above for the SUP-B15 cells is at play, along with the fact that the ENBT1 protein stability in the membrane is very high. ENT1 protein level was used as a positive control and showed a decrease of 75% by the 96-hr time point. This supports that cycloheximide was working but does not completely match the literature since ENT1 has a reported half-life of ~7 hr (Nivillac, Bacani, and Coe 2011). In contrast, the results above suggest ENT1 has a half-life of somewhere between 72 – 96 hr. However, it should be noted that the study by Nivillac, Bacani, and Coe mentioned above used a transient transfection protocol to look at ENT1 half-life. Due to the unstable nature and variability associated with transiently expressed proteins, this is unlikely to reflect endogenously expressed protein half-lives. In fact, protein half-life is a much more dynamic process and varies widely between different cell types. For example, using stable isotope labelling in cell culture followed by mass spectrometry (that can capture large-scale proteomic changes), previous studies

have shown that both ENT1 and ENBT1 have different half-lives (ENT1: 14 – 97 hr; ENBT1: 40 – 60 hr) depending on the cell line that is being looked at (Chen, Smeekens, and Wu 2016; Mathieson et al. 2018; Zecha et al. 2018). Furthermore, it has been noted that membrane-associated proteins are generally more stable (i.e. longer half-life) than non-membrane-associated proteins (Hare and Taylor 1991). This is in line with the data obtained in **Figure 38** and **Figure 39** which shows ENBT1 half-life in K562 cells exceeding 96 hr. Overall, it cannot be concluded what the half-life of ENBT1 protein in K562 cells is; therefore, the basal control by protein kinases in these cells cannot be assessed accurately with the current methods utilized.

Further evidence for the direct role of PKC on the PMA-induced decrease in ENBT1 function is that it could be reversed via the broad-spectrum PKC inhibitor, Gö6983, suggesting a causative effect **(Figure 36)**. However, it should be noted that this combination of activator and inhibitor gives little information on the exact PKC isoform that is responsible. The activator, PMA, activates both the conventional (α, β, γ) and novel (δ, ε, η, θ) isoforms of PKC, while the inhibitor, Gö6983, inhibits the conventional (α, β, γ) as well as the novel isoform PKCδ and the atypical isoform PKCζ (Castagna et al. 1982; Young, Balin, and Weis 2005). By the process of elimination, this means that the potential isoform responsible for the effect could be any of the conventional PKC isoforms (α, β, γ) or PKCδ. More specific inhibitors or shRNAi would need to be used to confirm the precise isoform. To confirm the exact residues of ENBT1 that are possibly phosphorylated by PKC, site-directed mutagenesis was used to mutate three separate residues with the highest predicted probability from **Figure 33**. **Figure 40** shows that changing threonine 231 to an alanine resulted in a loss of the PMA-induced decrease in ENBT1 function. It is speculated that phosphorylation of threonine 231 by PKC induces the internalization of ENBT1, leading to a decrease in its uptake of 6-MP or adenine. However, further investigation is needed to determine

this. As noted above in **6.3** for the oxidative stress section, the K_m was also determined for the graphs in **7.2**. Again, the expected K_m for both adenine (~30 μM) and 6-MP (~150 μM) in the experiments involving the PKC activators and inhibitors were similar. This means that similar to the work on oxidative stress, none of the treatments used in the experiments interacted with ENBT1 and changed how it handled adenine or 6-MP, suggesting the change was independent of alterations to ENBT1 substrate recognition.

A final note is the potential interplay between oxidative stress and phosphorylation by PKC in cells. It has been shown that activation with PMA leads to transcriptional activation of Nrf2 target genes (Huang, Nguyen, and Pickett 2000). Furthermore, oxidative stress has also been linked to the activation of PKC and its subsequent downstream effectors (Rybin et al. 2004). From the studies above in **Chapters 6 and 7**, it cannot be concluded whether these pathways were mutually exclusive of each other or if an interplay was at play. A more focused approach would need to be used to assess any contributions from these intertwined signalling pathways.

7.4) CONCLUSION

Activation of PKC by PMA leads to a decrease in ENBT1 function, which is mediated through the phosphorylation of threonine 231 on the large central intracellular loop of ENBT1. This suggests that aberrant upregulation of PKC activity in leukemia could decrease ENBT1 protein levels at the membrane, thus decreasing 6-MP efficacy. Targeting the PKC-mediated ENBT1 effect could potentially be a therapeutically viable option to increase 6-MP efficacy in ALL.

7.5) LIMITATIONS

7.5.1) Specific PKC isoform and activity

The study above focused primarily on the conventional and novel isoforms of PKC due to the choice of activator (PMA) and inhibitor (Gö6983) used. However, this still doesn't answer the question of which specific isoform is mediating the decrease in ENBT1 function. This is important because each isoform of PKC has been separately implicated in various leukemia pathogenic features, and their expression and activity can vary from patient to patient. To address this, the use of more specific inhibitors could have been employed, such as Gö6976, which specifically targets PKCα and β (Martiny-Baron et al. 1993), or Ro 32-0432, which specifically targets PKC α, β, and γ, but not PKCδ (Wilkinson, Parker, and Nixon 1993). More specifically, shRNAi methods could be deployed to individually investigate the specific conventional (α, β, γ) and novel (δ, ε, η, θ) isoform to determine the specific isoform. This would allow an exact determination of the specific isoform at play.

The data above strongly suggests that PKC mediates the effect seen, but it would be better if PKC activity was determined. PKC activity can be determined either by commercially available PKC activity kits or western blot analysis by looking at the activation of downstream signalling effectors such as ERK1/2 in the MAPK pathway (Zhao, Zhang, and Longo 2005; Muraleedharan et al. 2021). Confirmation of the PKC isoform and PKC activation would further strengthen the conclusions and allow more specific targeted treatments to be investigated.

7.5.2) Cycloheximide

Cycloheximide decreased cell viability and appeared to stop cell proliferation beyond 24 hr, as noted in **Figure 39**. A limitation of the study looking at cycloheximide is using ENT1 as the

control since its potential half-life is wide depending on the source you look at. An alternative would be using a short-lived protein with a half-life of less than 2 hr, like PRELID3B, or one with an intermediate half-life of 8 hr, like CDKN3 (Li et al. 2021). Although this would have to be confirmed for the specific cell line used, it would add another layer to confirm the effectiveness of the cycloheximide treatment working as intended.

Another noticeable effect that cycloheximide had on the cells was the decreased cell viability and the inhibition of cell proliferation after 24 hr **(Figure 39)**. Cell count was used as a surrogate for inhibition of cell proliferation. However, a cell cycle analysis could have been done to determine the extent to which cycloheximide was impacting the cell cycle stages. This can be done in many ways, but the most common method is flow cytometry, using propidium iodide staining for DNA content (Pozarowski and Darzynkiewicz 2004). This would have provided further evidence of cycloheximide working as intended and that the cell's lack of proliferation is due to the halt in the cell cycle, which is expected based on cycloheximide's mechanism of action (Liu et al. 2010).

Chapter 8: Summary

8.1) SUMMARY

We initially hypothesized that ENBT1 is responsible for the transport of 6-MP into leukemia cells and that the variability of inter-individual cellular toxicity of 6-MP is due to variation in the expression of ENBT1 in leukemia cells. The work above supports this hypothesis.

In **Chapter 4: Characterization of recombinant ENBT1 in HEK293 cells**, it was shown that ENBT1 mediates the uptake **(Figure 11)** and efflux **(Figure 13)** of 6-MP from cells in recombinantly transfected HEK293 cells (which are innately deficient in ENBT1). The major finding was that the overexpression of ENBT1 in HEK293 cells led to a significant enhancement of 6-MP sensitivity in cells **(Figure 15)**. This shows that ENBT1 transports 6-MP and is implicated in its efficacy.

In **Chapter 5: Characterization of endogenous ENBT1 in leukemia cells**, leukemia cells were shown to express varying levels of endogenous ENBT1 **(Figure 17)** and transport 6-MP **(Figure 19)**. Furthermore, the mRNA expression of *SLC43A3* correlated to the ENBT1-mediated 6-MP uptake in leukemia cells **(Figure 22)**. Finally, the knockdown of ENBT1 led to a decrease in the sensitivity to 6-MP in leukemia cells **(Figure 25)**. These data supported the strong notion that endogenous ENBT1 expression at the plasma membrane in leukemia cells can profoundly determine the efficacy of 6-MP. Based on this, the regulation of ENBT1 plasma membrane expression was investigated.

Chapter 6: Regulation of ENBT1 by oxidative stress, explored how oxidative stress regulates ENBT1 function. Incubation of cells with the oxidative stress inducer menadione decreased ENBT1-mediated uptake **(Figure 28)**. This decrease could be attenuated by the antioxidant TEMPOL **(Figure 29)**. These data strongly suggest the involvement of oxidative stress

in decreasing ENBT1-mediated 6-MP uptake at the plasma membrane, which could impact its therapeutic efficacy.

Chapter 7: Regulation of ENBT1 by protein kinase C, explored how PKC regulates ENBT1 function. Incubation of cells with the PKC activator PMA decreased ENBT1-mediated uptake in leukemia cells **(Figure 34 and Figure 35)**. This decrease could be reversed by the broad-spectrum PKC inhibitor Gö6983 **(Figure 36)**. Finally, the mutation of threonine 231 to alanine on ENBT1 was unaffected by PMA, suggesting a causative role of that residue in the phosphorylation and subsequent decrease in ENBT1-mediated uptake **(Figure 40)**. These data strongly suggest the involvement of PKC in decreasing ENBT1-mediated 6-MP uptake at the plasma membrane, which could impact its therapeutic efficacy.

8.2) FUTURE DIRECTIONS

These data clearly demonstrate the importance of ENBT1 on 6-MP efficacy in ALL chemotherapy. To address the gaps and build on these data, it is crucial that we pursue the following areas of interest:

1. **Investigate how 6-MP absorption is impacted in an ENBT1-knockout mouse model.** The data collected in this thesis demonstrate that decreases and increases in ENBT1 expression impact the sensitivity to 6-MP. However, since 6-MP is given orally to patients, ENBT1 expression in the intestinal tract could impact the absorption of 6-MP and potentially its efficacy. Using an ENBT1-knockout mouse model, mice can be given 6-MP via oral gavage and tissues extracted at specific time points to determine the extent to which 6-MP absorption is impacted in the knockout mouse compared to the wild type.

2. **Determine if ENBT1 expression correlates to the efficacy or toxicity of 6-MP in ALL patients**. Preliminary data has been collected for this, shown in the **Appendix**. However, the data collected is currently limited and needs to be built upon. Accessing more samples and the associated clinical correlates would strengthen the power of the analysis. Furthermore, a prospective study should be conducted to follow ALL patients from diagnosis to potentially relapsing to determine changes in ENBT1 expression and function and how it may impact the efficacy and toxicity of 6-MP.
3. **Investigate potential polymorphisms of *SLC43A3*/ENBT1 in ALL patients and determine their impact on ENBT1 function.** The data shown above clearly demonstrates that significant changes in ENBT1 expression or function can significantly impact 6-MP sensitivity in ALL cell lines. Gain/loss of function polymorphisms of *SLC43A3* in patients that impact how ENBT1 handles 6-MP could significantly alter the efficacy and toxicity of 6-MP in ALL patients. Studies should be conducted to investigate any polymorphisms of *SLC43A3* in patients that may impact ENBT1-mediated 6-MP transport. These can then be followed up by characterizing the impact of these polymorphisms on ENBT1 function in transfected cell lines.

These studies would help to further elucidate the role of ENBT1 in the overall pharmacokinetic profile of 6-MP and determine its potential therapeutic applications for 6-MP ALL chemotherapy.

8.3) CONCLUDING REMARKS

Prior to 2015, 6-MP variability in patients was simply an accepted situation that oncology patients had to live with, leading to toxic side effects and the unknown potential of relapse without

explanation. Certain variations were known but did not ultimately explain a large portion of the variability to 6-MP. The characterization of ENBT1 provides a new target with extremely high therapeutic potential. This novel mechanism assesses how 6-MP is getting into the leukemia cells and not on its metabolism, which has been a primary focus for several years. The data collected in this thesis is a foundational step to larger steps in further personalized approaches in patients with leukemia to increase efficacy and decrease the risk of adverse events.

REFERENCES

Abaji, R., and M. Krajinovic. 2017. 'Thiopurine S-methyltransferase polymorphisms in acute lymphoblastic leukemia, inflammatory bowel disease and autoimmune disorders: influence on treatment response', *Pharmgenomics Pers Med*, 10: 143-56.

Abou-Seif, M. A., A. Rabia, and M. Nasr. 2000. 'Antioxidant status, erythrocyte membrane lipid peroxidation and osmotic fragility in malignant lymphoma patients', *Clin Chem Lab Med*, 38: 737-42.

Adzhubei, I. A., S. Schmidt, L. Peshkin, V. E. Ramensky, A. Gerasimova, P. Bork, A. S. Kondrashov, and S. R. Sunyaev. 2010. 'A method and server for predicting damaging missense mutations', *Nat Methods*, 7: 248-9.

Aebi, H. 1984. 'Catalase in vitro', *Methods Enzymol*, 105: 121-6.

Afanas'ev, I. B. 2001. 'Lucigenin chemiluminescence assay for superoxide detection', *Circ Res*, 89: E46.

Akin-Bali, D. F., S. H. Aktas, M. A. Unal, and T. Kankilic. 2020. 'Identification of novel Nrf2/Keap1 pathway mutations in pediatric acute lymphoblastic leukemia', *Pediatr Hematol Oncol*, 37: 58-75.

Al-Gayyar, M. M., L. A. Eissa, A. M. Rabie, and A. M. El-Gayar. 2007. 'Measurements of oxidative stress status and antioxidant activity in chronic leukaemia patients', *J Pharm Pharmacol*, 59: 409-17.

Al-Tonbary, Y., M. Al-Haggar, R. El-Ashry, S. El-Dakroory, H. Azzam, and A. Fouda. 2009. 'Vitamin e and N-acetylcysteine as antioxidant adjuvant therapy in children with acute lymphoblastic leukemia', *Adv Hematol*, 2009: 689639.

Al-Tonbary, Y., S. A. Al-Hasan, M. Zaki, A. Hammad, S. Kandil, and A. Fouda. 2011. 'Impact of anti-oxidant status and apoptosis on the induction phase of chemotherapy in childhood acute lymphoblastic leukemia', *Hematology*, 16: 14-9.

Aleksunes, L. M., M. J. Goedken, C. E. Rockwell, J. Thomale, J. E. Manautou, and C. D. Klaassen. 2010. 'Transcriptional regulation of renal cytoprotective genes by Nrf2 and its potential use as a therapeutic target to mitigate cisplatin-induced nephrotoxicity', *J Pharmacol Exp Ther*, 335: 2-12.

Aleksunes, L. M., A. L. Slitt, J. M. Maher, L. M. Augustine, M. J. Goedken, J. Y. Chan, N. J. Cherrington, C. D. Klaassen, and J. E. Manautou. 2008. 'Induction of Mrp3 and Mrp4 transporters during acetaminophen hepatotoxicity is dependent on Nrf2', *Toxicol Appl Pharmacol*, 226: 74-83.

Alexander, P. M., D. L. Caudell, G. L. Kucera, K. M. Pladna, and T. S. Pardee. 2017. 'The novel phospholipid mimetic KPC34 is highly active against preclinical models of Philadelphia chromosome positive acute lymphoblastic leukemia', *PLoS One*, 12: e0179798.

Alsous, M., R. Abu Farha, E. Alefishat, S. Al Omar, D. Momani, A. Gharabli, J. McElnay, R. Horne, and R. Rihani. 2017. 'Adherence to 6-Mercaptopurine in children and adolescents with Acute Lymphoblastic Leukemia', *PLoS One*, 12: e0183119.

Ansari, M., G. Sauty, M. Labuda, V. Gagne, C. Laverdiere, A. Moghrabi, D. Sinnett, and M. Krajinovic. 2009. 'Polymorphisms in multidrug resistance-associated protein gene 4 is associated with outcome in childhood acute lymphoblastic leukemia', *Blood*, 114: 1383-6.

Apel, A., Y. Ofran, O. Wolach, S. Shimony, R. Ram, I. Levi, M. Zektser, and M. Koren-Michowitz. 2020. 'Safety and efficacy of blinatumomab: a real world data', *Ann Hematol*, 99: 835-38.

Aronow, B., D. Toll, J. Patrick, P. Hollingsworth, K. McCartan, and B. Ullman. 1986. 'Expression of a novel high-affinity purine nucleobase transport function in mutant mammalian T lymphoblasts', *Mol Cell Biol*, 6: 2957-62.

Babior, B. M. 2004. 'NADPH oxidase', *Curr Opin Immunol*, 16: 42-7.

Bar, F., C. Sina, and K. Fellermann. 2013. 'Thiopurines in inflammatory bowel disease revisited', *World J Gastroenterol*, 19: 1699-706.

Barnes, K., H. Dobrzynski, S. Foppolo, P. R. Beal, F. Ismat, E. R. Scullion, L. Sun, J. Tellez, M. W. Ritzel, W. C. Claycomb, C. E. Cass, J. D. Young, R. Billeter-Clark, M. R. Boyett, and S. A. Baldwin. 2006. 'Distribution and functional characterization of equilibrative nucleoside transporter-4, a novel cardiac adenosine transporter activated at acidic pH', *Circ Res*, 99: 510-9.

Bastin-Coyette, L., C. Smal, S. Cardoen, P. Saussoy, E. Van den Neste, and F. Bontemps. 2008. 'Mechanisms of cell death induced by 2-chloroadenosine in leukemic B-cells', *Biochem Pharmacol*, 75: 1451-60.

Battisti, V., L. D. Maders, M. D. Bagatini, K. F. Santos, R. M. Spanevello, P. A. Maldonado, A. O. Brule, C. Araujo Mdo, M. R. Schetinger, and V. M. Morsch. 2008. 'Measurement of oxidative stress and antioxidant status in acute lymphoblastic leukemia patients', *Clin Biochem*, 41: 511-8.

Beck, J. F., D. Brugger, K. Brischwein, C. Liu, P. Bader, D. Niethammer, and V. Gekeler. 2001. 'Anticancer drug-mediated induction of multidrug resistance-associated genes and protein kinase C isozymes in the T-lymphoblastoid cell line CCRF-CEM and in blasts from patients with acute lymphoblastic leukemias', *Jpn J Cancer Res*, 92: 896-903.

Beck, J., and B. Ullman. 1987. 'Genetic demonstration that the mutationally expressed nucleobase transporter of mouse S49 cells is nonconcentrative', *Exp Cell Res*, 171: 254-8.

Berman, H. M., J. Westbrook, Z. Feng, G. Gilliland, T. N. Bhat, H. Weissig, I. N. Shindyalov, and P. E. Bourne. 2000. 'The Protein Data Bank', *Nucleic Acids Res*, 28: 235-42.

Bhatia, S., W. Landier, L. Hageman, Y. Chen, H. Kim, C. L. Sun, N. Kornegay, W. E. Evans, A. L. Angiolillo, B. Bostrom, J. Casillas, G. Lew, K. W. Maloney, L. Mascarenhas, A. K. Ritchey, A. M. Termuhlen, W. L. Carroll, F. L. Wong, and M. V. Relling. 2015. 'Systemic Exposure to Thiopurines and Risk of Relapse in Children With Acute Lymphoblastic Leukemia: A Children's Oncology Group Study', *JAMA Oncol*, 1: 287-95.

Bhatia, S., W. Landier, L. Hageman, H. Kim, Y. Chen, K. R. Crews, W. E. Evans, B. Bostrom, J. Casillas, D. S. Dickens, K. W. Maloney, J. P. Neglia, Y. Ravindranath, A. K. Ritchey, F. L. Wong, and M. V. Relling. 2014. '6MP adherence in a multiracial cohort of children with acute lymphoblastic leukemia: a Children's Oncology Group study', *Blood*, 124: 2345-53.

Bhatia, S., W. Landier, M. Shangguan, L. Hageman, A. N. Schaible, A. R. Carter, C. L. Hanby, W. Leisenring, Y. Yasui, N. M. Kornegay, L. Mascarenhas, A. K. Ritchey, J. N. Casillas, D. S. Dickens, J. Meza, W. L. Carroll, M. V. Relling, and F. L. Wong. 2012. 'Nonadherence to oral mercaptopurine and risk of relapse in Hispanic and non-Hispanic white children with acute lymphoblastic leukemia: a report from the children's oncology group', *J Clin Oncol*, 30: 2094-101.

Black, A. R., and J. D. Black. 2012. 'Protein kinase C signaling and cell cycle regulation', *Front Immunol*, 3: 423.

Blom, N., T. Sicheritz-Ponten, R. Gupta, S. Gammeltoft, and S. Brunak. 2004. 'Prediction of post-translational glycosylation and phosphorylation of proteins from the amino acid sequence', *Proteomics*, 4: 1633-49.

Bodoy, S., D. Fotiadis, C. Stoeger, Y. Kanai, and M. Palacin. 2013. 'The small SLC43 family: facilitator system l amino acid transporters and the orphan EEG1', *Mol Aspects Med*, 34: 638-45.

Bokkerink, J. P., E. H. Stet, R. A. De Abreu, F. J. Damen, T. W. Hulscher, M. A. Bakker, and J. A. van Baal. 1993. '6-Mercaptopurine: cytotoxicity and biochemical pharmacology in human malignant T-lymphoblasts', *Biochem Pharmacol*, 45: 1455-63.

Bone, D. B., M. Antic, D. Quinonez, and J. R. Hammond. 2015. 'Hypoxanthine uptake by skeletal muscle microvascular endothelial cells from equilibrative nucleoside transporter 1 (ENT1)-null mice: effect of oxidative stress', *Microvasc Res*, 98: 16-22.

Bone, D. B., M. Antic, G. Vilas, and J. R. Hammond. 2014. 'Oxidative stress modulates nucleobase transport in microvascular endothelial cells', *Microvasc Res*, 95: 68-75.

Bone, D. B., and J. R. Hammond. 2007. 'Nucleoside and nucleobase transporters of primary human cardiac microvascular endothelial cells: characterization of a novel nucleobase transporter', *Am J Physiol Heart Circ Physiol*, 293: H3325-32.

Bradeen, H. A., C. A. Eide, T. O'Hare, K. J. Johnson, S. G. Willis, F. Y. Lee, B. J. Druker, and M. W. Deininger. 2006. 'Comparison of imatinib mesylate, dasatinib (BMS-354825), and nilotinib (AMN107) in an N-ethyl-N-nitrosourea (ENU)-based mutagenesis screen: high efficacy of drug combinations', *Blood*, 108: 2332-8.

Burckhardt, G. 2012. 'Drug transport by Organic Anion Transporters (OATs)', *Pharmacol Ther*, 136: 106-30.

Cadenas, E., A. Boveris, C. I. Ragan, and A. O. Stoppani. 1977. 'Production of superoxide radicals and hydrogen peroxide by NADH-ubiquinone reductase and ubiquinol-cytochrome c reductase from beef-heart mitochondria', *Arch Biochem Biophys*, 180: 248-57.

Castagna, M., Y. Takai, K. Kaibuchi, K. Sano, U. Kikkawa, and Y. Nishizuka. 1982. 'Direct activation of calcium-activated, phospholipid-dependent protein kinase by tumor-promoting phorbol esters', *J Biol Chem*, 257: 7847-51.

Chaudhary, P., S. Kumari, P. Dewan, S. Gomber, R. S. Ahmed, and M. Kotru. 2023. 'Chemotherapy-Induced Oxidative Stress in Pediatric Acute Lymphoblastic Leukemia', *Cureus*, 15: e35968.

Chen, W., J. M. Smeekens, and R. Wu. 2016. 'Systematic study of the dynamics and half-lives of newly synthesized proteins in human cells', *Chem Sci*, 7: 1393-400.

Chen, Y., and W. G. Junger. 2012. 'Measurement of oxidative burst in neutrophils', *Methods Mol Biol*, 844: 115-24.

Chen, Z. S., K. Lee, and G. D. Kruh. 2001. 'Transport of cyclic nucleotides and estradiol 17-beta-D-glucuronide by multidrug resistance protein 4. Resistance to 6-mercaptopurine and 6-thioguanine', *J Biol Chem*, 276: 33747-54.

Cheng, Y., and W. H. Prusoff. 1973. 'Relationship between the inhibition constant (K1) and the concentration of inhibitor which causes 50 per cent inhibition (I50) of an enzymatic reaction', *Biochem Pharmacol*, 22: 3099-108.

Chijiwa, T., A. Mishima, M. Hagiwara, M. Sano, K. Hayashi, T. Inoue, K. Naito, T. Toshioka, and H. Hidaka. 1990. 'Inhibition of forskolin-induced neurite outgrowth and protein phosphorylation by a newly synthesized selective inhibitor of cyclic AMP-dependent protein kinase, N-[2-(p-bromocinnamylamino)ethyl]-5-isoquinolinesulfonamide (H-89), of PC12D pheochromocytoma cells', *J Biol Chem*, 265: 5267-72.

Choi, R., I. Sohn, M. J. Kim, H. I. Woo, J. W. Lee, Y. Ma, E. S. Yi, H. H. Koo, and S. Y. Lee. 2019. 'Pathway genes and metabolites in thiopurine therapy in Korean children with acute lymphoblastic leukaemia', *Br J Clin Pharmacol*, 85: 1585-97.

Chouchana, L., A. A. Fernandez-Ramos, F. Dumont, C. Marchetti, I. Ceballos-Picot, P. Beaune, D. Gurwitz, and M. A. Loriot. 2015. 'Molecular insight into thiopurine resistance: transcriptomic signature in lymphoblastoid cell lines', *Genome Med*, 7: 37.

Chouchana, L., C. Narjoz, D. Roche, J. L. Golmard, B. Pineau, G. Chatellier, P. Beaune, and M. A. Loriot. 2014. 'Interindividual variability in TPMT enzyme activity: 10 years of experience with thiopurine pharmacogenetics and therapeutic drug monitoring', *Pharmacogenomics*, 15: 745-57.

Chrzanowska, M., M. Kuehn, D. Januszkiewicz-Lewandowska, M. Kurzawski, and M. Drozdzik. 2012. 'Thiopurine S-methyltransferase phenotype-genotype correlation in children with acute lymphoblastic leukemia', *Acta Pol Pharm*, 69: 405-10.

Chugh, S. N., R. Kakkar, S. Kalra, and A. Sharma. 1999. 'An evaluation of oxidative stress in diabetes mellitus during uncontrolled and controlled state and after vitamin E supplementation', *J Assoc Physicians India*, 47: 380-3.

Cohen, P. 2001. 'The role of protein phosphorylation in human health and disease. The Sir Hans Krebs Medal Lecture', *Eur J Biochem*, 268: 5001-10.

Colas, C., P. M. Ung, and A. Schlessinger. 2016. 'SLC Transporters: Structure, Function, and Drug Discovery', *Medchemcomm*, 7: 1069-81.

Collin, F. 2019. 'Chemical Basis of Reactive Oxygen Species Reactivity and Involvement in Neurodegenerative Diseases', *Int J Mol Sci*, 20.

"Compound Summary for CID 190, Adenine." In. 2004. PubChem: National Center for Biotechnology Information.

"Compound Summary for CID 597, Cytosine." In. 2004. PubChem: National Center for Biotechnology Information.

"Compound Summary for CID 1135, Thymine." In. 2004. PubChem: National Center for Biotechnology Information.

"Compound Summary for CID 1174, Uracil." In. 2004. PubChem: National Center for Biotechnology Information.

"Compound Summary for CID 4055, Menadione." In. 2004. PubChem: National Center for Biotechnology Information.

"Compound Summary for CID 6410, tert-Butyl Hydroperoxide." In. 2004. PubChem: National Center for Biotechnology Information.

"Compound Summary for CID 667490, Mercaptopurine." In. 2004. PubChem: National Center for Biotechnology Information.

"Compound Summary for CID 2723601, Thioguanine." In. 2004. PubChem: National Center for Biotechnology Information.

"Compound Summary for CID 135398634, Guanine." In. 2004. PubChem: National Center for Biotechnology Information.

Copsel, S., C. Garcia, F. Diez, M. Vermeulem, A. Baldi, L. G. Bianciotti, F. G. Russel, C. Shayo, and C. Davio. 2011. 'Multidrug resistance protein 4 (MRP4/ABCC4) regulates cAMP cellular levels and controls human leukemia cell proliferation and differentiation', *J Biol Chem*, 286: 6979-88.

Coulthard, S. A., L. A. Hogarth, M. Little, E. C. Matheson, C. P. Redfern, L. Minto, and A. G. Hall. 2002. 'The effect of thiopurine methyltransferase expression on sensitivity to thiopurine drugs', *Mol Pharmacol*, 62: 102-9.

Crane, D., D. Haussinger, P. Graf, and H. Sies. 1983. 'Decreased flux through pyruvate dehydrogenase by thiol oxidation during t-butyl hydroperoxide metabolism in perfused rat liver', *Hoppe Seylers Z Physiol Chem*, 364: 977-87.

Cunningham, F., J. E. Allen, J. Allen, J. Alvarez-Jarreta, M. R. Amode, I. M. Armean, O. Austine-Orimoloye, A. G. Azov, I. Barnes, R. Bennett, A. Berry, J. Bhai, A. Bignell, K. Billis, S. Boddu, L. Brooks, M. Charkhchi, C. Cummins, L. Da Rin Fioretto, C. Davidson, K. Dodiya, S. Donaldson, B. El Houdaigui, T. El Naboulsi, R. Fatima, C. G. Giron, T. Genez, J. G. Martinez, C. Guijarro-Clarke, A. Gymer, M. Hardy, Z. Hollis, T. Hourlier, T. Hunt, T. Juettemann, V. Kaikala, M. Kay, I. Lavidas, T. Le, D. Lemos, J. C. Marugan, S. Mohanan, A. Mushtaq, M. Naven, D. N. Ogeh, A. Parker, A. Parton, M. Perry, I. Pilizota, I. Prosovetskaia, M. P. Sakthivel, A. I. A. Salam, B. M. Schmitt, H. Schuilenburg, D. Sheppard, J. G. Perez-Silva, W. Stark, E. Steed, K. Sutinen, R. Sukumaran, D. Sumathipala, M. M. Suner, M. Szpak, A. Thormann, F. F. Tricomi, D. Urbina-Gomez, A. Veidenberg, T. A. Walsh, B. Walts, N. Willhoft, A. Winterbottom, E. Wass, M. Chakiachvili, B. Flint, A. Frankish, S. Giorgetti, L. Haggerty, S. E. Hunt, I. Isley GR, J. E. Loveland, F. J. Martin, B. Moore, J. M. Mudge, M. Muffato, E. Perry, M. Ruffier, J. Tate, D. Thybert, S. J. Trevanion, S. Dyer, P. W. Harrison, K. L. Howe, A. D. Yates, D. R. Zerbino, and P. Flicek. 2022. 'Ensembl 2022', *Nucleic Acids Res*, 50: D988-D95.

Dai, Y., N. L. Dudek, T. B. Patel, and N. A. Muma. 2008. 'Transglutaminase-catalyzed transamidation: a novel mechanism for Rac1 activation by 5-hydroxytryptamine2A receptor stimulation', *J Pharmacol Exp Ther*, 326: 153-62.

Damaraju, V. L., M. Kuzma, C. E. Cass, and M. B. Sawyer. 2015. 'Inhibition of sodium-independent and sodium-dependent nucleobase transport activities by tyrosine kinase inhibitors', *Cancer Chemother Pharmacol*, 76: 1093-8.

Davies, M. J. 1989. 'Detection of peroxyl and alkoxyl radicals produced by reaction of hydroperoxides with rat liver microsomal fractions', *Biochem J*, 257: 603-6.

de Lemos, M. L., L. Hamata, S. Jennings, and T. Leduc. 2007. 'Interaction between mercaptopurine and milk', *J Oncol Pharm Pract*, 13: 237-40.

DelRocco, N. J., M. L. Loh, M. J. Borowitz, S. Gupta, K. R. Rabin, P. Zweidler-McKay, K. W. Maloney, L. A. Mattano, E. Larsen, A. Angiolillo, R. J. Schore, M. J. Burke, W. L. Salzer, B. L. Wood, A. J. Carroll, N. A. Heerema, S. C. Reshmi, J. M. Gastier-Foster, R. Harvey, I. M. Chen, K. G. Roberts, C. G. Mullighan, C. Willman, N. Winick, W. L.

Carroll, R. E. Rau, D. T. Teachey, S. P. Hunger, E. A. Raetz, M. Devidas, and J. A. Kairalla. 2024. 'Enhanced Risk Stratification for Children and Young Adults with B-Cell Acute Lymphoblastic Leukemia: A Children's Oncology Group Report', *Leukemia*, 38: 720-28.

Dervieux, T., J. G. Blanco, E. Y. Krynetski, E. F. Vanin, M. F. Roussel, and M. V. Relling. 2001. 'Differing contribution of thiopurine methyltransferase to mercaptopurine versus thioguanine effects in human leukemic cells', *Cancer Res*, 61: 5810-6.

Devi, G. S., M. H. Prasad, I. Saraswathi, D. Raghu, D. N. Rao, and P. P. Reddy. 2000. 'Free radicals antioxidant enzymes and lipid peroxidation in different types of leukemias', *Clin Chim Acta*, 293: 53-62.

Dieck, C. L., G. Tzoneva, F. Forouhar, Z. Carpenter, A. Ambesi-Impiombato, M. Sanchez-Martin, R. Kirschner-Schwabe, S. Lew, J. Seetharaman, L. Tong, and A. A. Ferrando. 2018. 'Structure and Mechanisms of NT5C2 Mutations Driving Thiopurine Resistance in Relapsed Lymphoblastic Leukemia', *Cancer Cell*, 34: 136-47 e6.

DiGiuseppe, J. A., and J. L. Cardinali. 2019. 'Immunophenotyping of Acute Lymphoblastic Leukemia', *Methods Mol Biol*, 2032: 297-310.

Diouf, B., Q. Cheng, N. F. Krynetskaia, W. Yang, M. Cheok, D. Pei, Y. Fan, C. Cheng, E. Y. Krynetskiy, H. Geng, S. Chen, W. E. Thierfelder, C. G. Mullighan, J. R. Downing, P. Hsieh, C. H. Pui, M. V. Relling, and W. E. Evans. 2011. 'Somatic deletions of genes regulating MSH2 protein stability cause DNA mismatch repair deficiency and drug resistance in human leukemia cells', *Nat Med*, 17: 1298-303.

Domin, B. A., W. B. Mahony, and T. P. Zimmerman. 1988. 'Purine nucleobase transport in human erythrocytes. Reinvestigation with a novel "inhibitor-stop" assay', *J Biol Chem*, 263: 9276-84.

Downes, C. E., B. J. McClure, D. P. McDougal, S. L. Heatley, J. B. Bruning, D. Thomas, D. T. Yeung, and D. L. White. 2022. 'JAK2 Alterations in Acute Lymphoblastic Leukemia: Molecular Insights for Superior Precision Medicine Strategies', *Front Cell Dev Biol*, 10: 942053.

Du, M. Y., Y. Q. Zhang, D. Y. Liao, W. Xie, W. Xiong, H. Mei, and Y. Hu. 2023. '[Long-term follow-up of humanized and murine CD19 CAR-T-cell therapy for B-cell acute lymphoblastic leukemia]', *Zhonghua Xue Ye Xue Za Zhi*, 44: 793-99.

Du, S., X. Huang, X. He, M. Mao, M. Chen, R. Zhang, H. Shao, Z. Lv, X. Liu, and J. Chuan. 2023. 'Association of NUDT15 gene polymorphism with adverse reaction, treatment efficacy, and dose of 6-mercaptopurine in patients with acute lymphoblastic leukemia: a systematic review and meta-analysis', *Haematologica*.

Duan, P., and G. You. 2009. 'Novobiocin is a potent inhibitor for human organic anion transporters', *Drug Metab Dispos*, 37: 1203-10.

Dubinsky, M. C., S. Lamothe, H. Y. Yang, S. R. Targan, D. Sinnett, Y. Theoret, and E. G. Seidman. 2000. 'Pharmacogenomics and metabolite measurement for 6-mercaptopurine therapy in inflammatory bowel disease', *Gastroenterology*, 118: 705-13.

Ebbesen, M. S., J. Nersting, J. H. Jacobsen, T. L. Frandsen, K. Vettenranta, J. Abramsson, F. Wesenberg, and K. Schmiegelow. 2013. 'Incorporation of 6-thioguanine nucleotides into DNA during maintenance therapy of childhood acute lymphoblastic leukemia-the influence of thiopurine methyltransferase genotypes', *J Clin Pharmacol*, 53: 670-4.

El-Sheikh, A. A., R. Greupink, H. M. Wortelboer, J. J. van den Heuvel, M. Schreurs, J. B. Koenderink, R. Masereeuw, and F. G. Russel. 2013. 'Interaction of immunosuppressive drugs with human organic anion transporter (OAT) 1 and OAT3, and multidrug resistance-associated protein (MRP) 2 and MRP4', *Transl Res*, 162: 398-409.

Engel, K., M. Zhou, and J. Wang. 2004. 'Identification and characterization of a novel monoamine transporter in the human brain', *J Biol Chem*, 279: 50042-9.

Escherich, G., S. Richards, L. C. Stork, A. J. Vora, and Group Childhood Acute Lymphoblastic Leukaemia Collaborative. 2011. 'Meta-analysis of randomised trials comparing thiopurines in childhood acute lymphoblastic leukaemia', *Leukemia*, 25: 953-9.

Estlin, E. J. 2001. 'Continuing therapy for childhood acute lymphoblastic leukaemia: clinical and cellular pharmacology of methotrexate, 6-mercaptopurine and 6-thioguanine', *Cancer Treat Rev*, 27: 351-63.

Evensen, N. A., P. P. Madhusoodhan, J. Meyer, J. Saliba, A. Chowdhury, D. J. Araten, J. Nersting, T. Bhatla, T. L. Vincent, D. Teachey, S. P. Hunger, J. Yang, K. Schmiegelow, and W. L. Carroll. 2018. 'MSH6 haploinsufficiency at relapse contributes to the development of thiopurine resistance in pediatric B-lymphoblastic leukemia', *Haematologica*, 103: 830-39.

Fernandez-Ramos, A. A., C. Marchetti-Laurent, V. Poindessous, S. Antonio, P. Laurent-Puig, S. Bortoli, M. A. Loriot, and N. Pallet. 2017. '6-mercaptopurine promotes energetic failure in proliferating T cells', *Oncotarget*, 8: 43048-60.

Fishilevich, S., R. Nudel, N. Rappaport, R. Hadar, I. Plaschkes, T. Iny Stein, N. Rosen, A. Kohn, M. Twik, M. Safran, D. Lancet, and D. Cohen. 2017. 'GeneHancer: genome-wide integration of enhancers and target genes in GeneCards', *Database (Oxford)*, 2017.

Flohe, L., W. A. Gunzler, and H. H. Schock. 1973. 'Glutathione peroxidase: a selenoenzyme', *FEBS Lett*, 32: 132-4.

Foa, R., and S. Chiaretti. 2022. 'Philadelphia Chromosome-Positive Acute Lymphoblastic Leukemia', *N Engl J Med*, 386: 2399-411.

Franciosa, G., J. G. A. Smits, S. Minuzzo, A. Martinez-Val, S. Indraccolo, and J. V. Olsen. 2021. 'Proteomics of resistance to Notch1 inhibition in acute lymphoblastic leukemia reveals targetable kinase signatures', *Nat Commun*, 12: 2507.

Freret, M., F. Gouel, C. Buquet, E. Legrand, J. P. Vannier, M. Vasse, and I. Dubus. 2011. 'Rac-1 GTPase controls the capacity of human leukaemic lymphoblasts to migrate on fibronectin in response to SDF-1alpha (CXCL12)', *Leuk Res*, 35: 971-3.

Fukuda, Y., and J. D. Schuetz. 2012. 'ABC transporters and their role in nucleoside and nucleotide drug resistance', *Biochem Pharmacol*, 83: 1073-83.

Furukawa, J., K. Inoue, J. Maeda, T. Yasujima, K. Ohta, Y. Kanai, T. Takada, H. Matsuo, and H. Yuasa. 2015. 'Functional identification of SLC43A3 as an equilibrative nucleobase transporter involved in purine salvage in mammals', *Sci Rep*, 5: 15057.

Furukawa, J., K. Inoue, K. Ohta, T. Yasujima, Y. Mimura, and H. Yuasa. 2017. 'Role of Equilibrative Nucleobase Transporter 1/SLC43A3 as a Ganciclovir Transporter in the Induction of Cytotoxic Effect of Ganciclovir in a Suicide Gene Therapy with Herpes Simplex Virus Thymidine Kinase', *J Pharmacol Exp Ther*, 360: 59-68.

Gallagher, B. M., J. S. Fowler, N. I. Gutterson, R. R. MacGregor, C. N. Wan, and A. P. Wolf. 1978. 'Metabolic trapping as a principle of oradiopharmaceutical design: some factors resposible for the biodistribution of [18F] 2-deoxy-2-fluoro-D-glucose', *J Nucl Med*, 19: 1154-61.

Gariboldi, M. B., V. Rimoldi, R. Supino, E. Favini, and E. Monti. 2000. 'The nitroxide tempol induces oxidative stress, p21(WAF1/CIP1), and cell death in HL60 cells', *Free Radic Biol Med*, 29: 633-41.

Gerbek, T., M. Ebbesen, J. Nersting, T. L. Frandsen, M. L. Appell, and K. Schmiegelow. 2018. 'Role of TPMT and ITPA variants in mercaptopurine disposition', *Cancer Chemother Pharmacol*, 81: 579-86.

Gironi, B., Z. Kahveci, B. McGill, B. D. Lechner, S. Pagliara, J. Metz, A. Morresi, F. Palombo, P. Sassi, and P. G. Petrov. 2020. 'Effect of DMSO on the Mechanical and Structural Properties of Model and Biological Membranes', *Biophys J*, 119: 274-86.

Granger, D. N. 1988. 'Role of xanthine oxidase and granulocytes in ischemia-reperfusion injury', *Am J Physiol*, 255: H1269-75.

Griffith, D. A., and S. M. Jarvis. 1993. 'High affinity sodium-dependent nucleobase transport in cultured renal epithelial cells (LLC-PK1)', *J Biol Chem*, 268: 20085-90.

———. 1996. 'Regulation of nucleobase transport in LLC-PK1 renal epithelia by protein kinase C', *Biochim Biophys Acta*, 1284: 213-20.

Griner, E. M., and M. G. Kazanietz. 2007. 'Protein kinase C and other diacylglycerol effectors in cancer', *Nat Rev Cancer*, 7: 281-94.

Gschwendt, M., S. Dieterich, J. Rennecke, W. Kittstein, H. J. Mueller, and F. J. Johannes. 1996. 'Inhibition of protein kinase C mu by various inhibitors. Differentiation from protein kinase c isoenzymes', *FEBS Lett*, 392: 77-80.

Guo, Y., P. Xiao, S. Lei, F. Deng, G. G. Xiao, Y. Liu, X. Chen, L. Li, S. Wu, Y. Chen, H. Jiang, L. Tan, J. Xie, X. Zhu, S. Liang, and H. Deng. 2008. 'How is mRNA expression predictive for protein expression? A correlation study on human circulating monocytes', *Acta Biochim Biophys Sin (Shanghai)*, 40: 426-36.

Guzman, M. L., X. Li, C. A. Corbett, R. M. Rossi, T. Bushnell, J. L. Liesveld, J. Hebert, F. Young, and C. T. Jordan. 2007. 'Rapid and selective death of leukemia stem and progenitor cells induced by the compound 4-benzyl, 2-methyl, 1,2,4-thiadiazolidine, 3,5 dione (TDZD-8)', *Blood*, 110: 4436-44.

Hammond, J. R. 1991. 'Comparative pharmacology of the nitrobenzylthioguanosine-sensitive and -resistant nucleoside transport mechanisms of Ehrlich ascites tumor cells', *J Pharmacol Exp Ther*, 259: 799-807.

Hare, J. F., and K. Taylor. 1991. 'Mechanisms of plasma membrane protein degradation: recycling proteins are degraded more rapidly than those confined to the cell surface', *Proc Natl Acad Sci U S A*, 88: 5902-6.

Harris, J. W., and J. A. Power. 1978. 'Diamide: mechanisms of action and interactions with other sensitizers', *Br J Cancer Suppl*, 3: 84-9.

Hartford, C., E. Vasquez, M. Schwab, M. J. Edick, J. E. Rehg, G. Grosveld, C. H. Pui, W. E. Evans, and M. V. Relling. 2007. 'Differential effects of targeted disruption of thiopurine methyltransferase on mercaptopurine and thioguanine pharmacodynamics', *Cancer Res*, 67: 4965-72.

Hartsink-Segers, S. A., J. J. Beaudoin, M. W. Luijendijk, C. Exalto, R. Pieters, and M. L. Den Boer. 2015. 'PKCzeta and PKMzeta are overexpressed in TCF3-rearranged paediatric acute lymphoblastic leukaemia and are associated with increased thiopurine sensitivity', *Leukemia*, 29: 304-11.

Hasbargen, K. B., W. J. Shen, Y. Zhang, X. Hou, W. Wang, Q. Shuo, D. A. Bernlohr, S. Azhar, and F. B. Kraemer. 2020. 'Slc43a3 is a regulator of free fatty acid flux', *J Lipid Res*, 61: 734-45.

Hashimoto, H., M. Kubota, T. Shimizu, T. Takimoto, T. Kitoh, Y. Akiyama, and H. Mikawa. 1990. 'Biochemical basis of the prevention of 6-thiopurine toxicity by the nucleobases, hypoxanthine and adenine', *Leuk Res*, 14: 1061-6.

Hassan, G. S. 2013. 'Menadione', *Profiles Drug Subst Excip Relat Methodol*, 38: 227-313.

He, F., X. Ru, and T. Wen. 2020. 'NRF2, a Transcription Factor for Stress Response and Beyond', *Int J Mol Sci*, 21.

Hipkin, R. W., Y. Wang, and A. Schonbrunn. 2000. 'Protein kinase C activation stimulates the phosphorylation and internalization of the sst2A somatostatin receptor', *J Biol Chem*, 275: 5591-9.

Hirst, J., M. S. King, and K. R. Pryde. 2008. 'The production of reactive oxygen species by complex I', *Biochem Soc Trans*, 36: 976-80.

Hoque, K. M., L. Chen, G. P. Leung, and C. M. Tse. 2008. 'A purine-selective nucleobase/nucleoside transporter in PK15NTD cells', *Am J Physiol Regul Integr Comp Physiol*, 294: R1988-95.

Hornbeck, P. V., B. Zhang, B. Murray, J. M. Kornhauser, V. Latham, and E. Skrzypek. 2015. 'PhosphoSitePlus, 2014: mutations, PTMs and recalibrations', *Nucleic Acids Res*, 43: D512-20.

Houston, M., P. Chumley, R. Radi, H. Rubbo, and B. A. Freeman. 1998. 'Xanthine oxidase reaction with nitric oxide and peroxynitrite', *Arch Biochem Biophys*, 355: 1-8.

Hrusak, O., V. de Haas, J. Stancikova, B. Vakrmanova, I. Janotova, E. Mejstrikova, V. Capek, J. Trka, M. Zaliova, A. Luks, K. Bleckmann, A. Moricke, J. Irving, B. Konatkowska, T. B. Alexander, H. Inaba, K. Schmiegelow, S. Stokley, Z. Zemanova, A. V. Moorman, J. G. Rossi, M. S. Felice, L. Dalla-Pozza, J. Morales, M. Dworzak, B. Buldini, G. Basso, M. Campbell, M. E. Cabrera, N. Marinov, S. Elitzur, S. Izraeli, D. Luria, T. Feuerstein, A. Kolenova, P. Svec, O. Kreminska, K. R. Rabin, S. Polychronopoulou, E. da Costa, H. V. Marquart, A. Kattamis, R. Ratei, D. Reinhardt, J. K. Choi, M. Schrappe, and J. Stary. 2018. 'International cooperative study identifies treatment strategy in childhood ambiguous lineage leukemia', *Blood*, 132: 264-76.

Hu, X. M., T. Hirano, and K. Oka. 2003. 'Arsenic trioxide induces apoptosis in cells of MOLT-4 and its daunorubicin-resistant cell line via depletion of intracellular glutathione, disruption of mitochondrial membrane potential and activation of caspase-3', *Cancer Chemother Pharmacol*, 52: 47-58.

Huang, G. N. 2012. 'Biotinylation of Cell Surface Proteins', *Bio Protoc*, 2.

Huang, H. C., T. Nguyen, and C. B. Pickett. 2000. 'Regulation of the antioxidant response element by protein kinase C-mediated phosphorylation of NF-E2-related factor 2', *Proc Natl Acad Sci U S A*, 97: 12475-80.

Huang, Y. L., J. Y. Sheu, and T. H. Lin. 1999. 'Association between oxidative stress and changes of trace elements in patients with breast cancer', *Clin Biochem*, 32: 131-6.

Igarashi, K., K. Kataoka, K. Itoh, N. Hayashi, M. Nishizawa, and M. Yamamoto. 1994. 'Regulation of transcription by dimerization of erythroid factor NF-E2 p45 with small Maf proteins', *Nature*, 367: 568-72.

Inaba, H., and C. G. Mullighan. 2020. 'Pediatric acute lymphoblastic leukemia', *Haematologica*, 105: 2524-39.

Inamdar, N. M., Y. I. Ahn, and J. Alam. 1996. 'The heme-responsive element of the mouse heme oxygenase-1 gene is an extended AP-1 binding site that resembles the recognition

sequences for MAF and NF-E2 transcription factors', *Biochem Biophys Res Commun*, 221: 570-6.

Itoh, K., N. Wakabayashi, Y. Katoh, T. Ishii, K. Igarashi, J. D. Engel, and M. Yamamoto. 1999. 'Keap1 represses nuclear activation of antioxidant responsive elements by Nrf2 through binding to the amino-terminal Neh2 domain', *Genes Dev*, 13: 76-86.

Jackson, P. J. 1983. 'Determination of 6-thiouric acid in human urine', *Clin Biochem*, 16: 285-6.

Janke, D., S. Mehralivand, D. Strand, U. Godtel-Armbrust, A. Habermeier, U. Gradhand, C. Fischer, M. R. Toliat, P. Fritz, U. M. Zanger, M. Schwab, M. F. Fromm, P. Nurnberg, L. Wojnowski, E. I. Closs, and T. Lang. 2008. '6-mercaptopurine and 9-(2-phosphonyl-methoxyethyl) adenine (PMEA) transport altered by two missense mutations in the drug transporter gene ABCC4', *Hum Mutat*, 29: 659-69.

Jardetzky, O. 1966. 'Simple allosteric model for membrane pumps', *Nature*, 211: 969-70.

Jeha, S., D. Pei, J. Choi, C. Cheng, J. T. Sandlund, E. Coustan-Smith, D. Campana, H. Inaba, J. E. Rubnitz, R. C. Ribeiro, T. A. Gruber, S. C. Raimondi, R. B. Khan, J. J. Yang, C. G. Mullighan, J. R. Downing, W. E. Evans, M. V. Relling, and C. H. Pui. 2019. 'Improved CNS Control of Childhood Acute Lymphoblastic Leukemia Without Cranial Irradiation: St Jude Total Therapy Study 16', *J Clin Oncol*, 37: 3377-91.

Jiffar, T., S. Kurinna, G. Suck, D. Carlson-Bremer, M. R. Ricciardi, M. Konopleva, M. Andreeff, and P. P. Ruvolo. 2004. 'PKC alpha mediates chemoresistance in acute lymphoblastic leukemia through effects on Bcl2 phosphorylation', *Leukemia*, 18: 505-12.

Jumper, J., R. Evans, A. Pritzel, T. Green, M. Figurnov, O. Ronneberger, K. Tunyasuvunakool, R. Bates, A. Zidek, A. Potapenko, A. Bridgland, C. Meyer, S. A. A. Kohl, A. J. Ballard, A. Cowie, B. Romera-Paredes, S. Nikolov, R. Jain, J. Adler, T. Back, S. Petersen, D. Reiman, E. Clancy, M. Zielinski, M. Steinegger, M. Pacholska, T. Berghammer, S. Bodenstein, D. Silver, O. Vinyals, A. W. Senior, K. Kavukcuoglu, P. Kohli, and D. Hassabis. 2021. 'Highly accurate protein structure prediction with AlphaFold', *Nature*, 596: 583-89.

Kahn, J. M., K. Stevenson, M. Beauchemin, V. B. Koch, P. D. Cole, J. J. G. Welch, E. Gage-Bouchard, C. Karsenty, L. B. Silverman, K. M. Kelly, and K. Bona. 2023. 'Oral Mercaptopurine Adherence in Pediatric Acute Lymphoblastic Leukemia: A Survey Study From the Dana-Farber Cancer Institute Acute Lymphoblastic Leukemia Consortium', *J Pediatr Hematol Oncol Nurs*, 40: 17-23.

Kantarjian, H., N. P. Shah, A. Hochhaus, J. Cortes, S. Shah, M. Ayala, B. Moiraghi, Z. Shen, J. Mayer, R. Pasquini, H. Nakamae, F. Huguet, C. Boque, C. Chuah, E. Bleickardt, M. B. Bradley-Garelik, C. Zhu, T. Szatrowski, D. Shapiro, and M. Baccarani. 2010. 'Dasatinib versus imatinib in newly diagnosed chronic-phase chronic myeloid leukemia', *N Engl J Med*, 362: 2260-70.

Kantarjian, H., A. Stein, N. Gokbuget, A. K. Fielding, A. C. Schuh, J. M. Ribera, A. Wei, H. Dombret, R. Foa, R. Bassan, O. Arslan, M. A. Sanz, J. Bergeron, F. Demirkan, E. Lech-Maranda, A. Rambaldi, X. Thomas, H. A. Horst, M. Bruggemann, W. Klapper, B. L. Wood, A. Fleishman, D. Nagorsen, C. Holland, Z. Zimmerman, and M. S. Topp. 2017. 'Blinatumomab versus Chemotherapy for Advanced Acute Lymphoblastic Leukemia', *N Engl J Med*, 376: 836-47.

Kantarjian, H., D. Thomas, S. O'Brien, J. Cortes, F. Giles, S. Jeha, C. E. Bueso-Ramos, S. Pierce, J. Shan, C. Koller, M. Beran, M. Keating, and E. J. Freireich. 2004. 'Long-term follow-up results of hyperfractionated cyclophosphamide, vincristine, doxorubicin, and dexamethasone (Hyper-CVAD), a dose-intensive regimen, in adult acute lymphocytic leukemia', *Cancer*, 101: 2788-801.

Kao, S. H., W. L. Wang, C. Y. Chen, Y. L. Chang, Y. Y. Wu, Y. T. Wang, S. P. Wang, A. I. Nesvizhskii, Y. J. Chen, T. M. Hong, and P. C. Yang. 2015. 'Analysis of Protein Stability by the Cycloheximide Chase Assay', *Bio Protoc*, 5.

Karas-Kuzelicki, N., and I. Mlinaric-Rascan. 2009. 'Individualization of thiopurine therapy: thiopurine S-methyltransferase and beyond', *Pharmacogenomics*, 10: 1309-22.

Karim, H., A. Ghalali, P. Lafolie, S. Vitols, and A. K. Fotoohi. 2013. 'Differential role of thiopurine methyltransferase in the cytotoxic effects of 6-mercaptopurine and 6-thioguanine on human leukemia cells', *Biochem Biophys Res Commun*, 437: 280-6.

Katz, A. J., V. M. Chia, W. M. Schoonen, and M. A. Kelsh. 2015. 'Acute lymphoblastic leukemia: an assessment of international incidence, survival, and disease burden', *Cancer Causes Control*, 26: 1627-42.

Kennedy, D. D., E. J. Ladas, S. R. Rheingold, J. Blumberg, and K. M. Kelly. 2005. 'Antioxidant status decreases in children with acute lymphoblastic leukemia during the first six months of chemotherapy treatment', *Pediatr Blood Cancer*, 44: 378-85.

Kingston, R. E., C. A. Chen, and J. K. Rose. 2003. 'Calcium phosphate transfection', *Curr Protoc Mol Biol*, Chapter 9: Unit 9 1.

Kobayashi, Y., N. Ohshiro, A. Tsuchiya, N. Kohyama, M. Ohbayashi, and T. Yamamoto. 2004. 'Renal transport of organic compounds mediated by mouse organic anion transporter 3 (mOat3): further substrate specificity of mOat3', *Drug Metab Dispos*, 32: 479-83.

Kodidela, S., P. Dorababu, D. N. Thakkar, B. Dubashi, R. Sundaram, N. Muralidharan, R. P. Nidanapu, A. Aribandi, S. C. Pradhan, and C. R. S. Uppugunduri. 2020. 'Association of NUDT15*3 and FPGS 2572C>T Variants with the Risk of Early Hematologic Toxicity During 6-MP and Low-Dose Methotrexate-Based Maintenance Therapy in Indian Patients with Acute Lymphoblastic Leukemia', *Genes (Basel)*, 11.

Komada, F., M. Nishikawa, Y. Uemura, K. Morita, H. Hidaka, and S. Shirakawa. 1991. 'Expression of three major protein kinase C isozymes in various types of human leukemic cells', *Cancer Res*, 51: 4271-8.

Kraupp, M., and R. Marz. 1995. 'Membrane transport of nucleobases: interaction with inhibitors', *Gen Pharmacol*, 26: 1185-90.

Kraupp, M., B. Paskutti, C. Schon, and R. Marz. 1994. 'Inhibition of purine nucleobase transport in human erythrocytes and cell lines by papaverine. Investigation of structure-activity relationship', *Biochem Pharmacol*, 48: 41-7.

Kucera, O., R. Endlicher, T. Rousar, H. Lotkova, T. Garnol, Z. Drahota, and Z. Cervinkova. 2014. 'The effect of tert-butyl hydroperoxide-induced oxidative stress on lean and steatotic rat hepatocytes in vitro', *Oxid Med Cell Longev*, 2014: 752506.

Kuiper, R. P., E. F. Schoenmakers, S. V. van Reijmersdal, J. Y. Hehir-Kwa, A. G. van Kessel, F. N. van Leeuwen, and P. M. Hoogerbrugge. 2007. 'High-resolution genomic profiling of childhood ALL reveals novel recurrent genetic lesions affecting pathways involved in lymphocyte differentiation and cell cycle progression', *Leukemia*, 21: 1258-66.

Kumar, P., A. Nagarajan, and P. D. Uchil. 2018. 'Analysis of Cell Viability by the Lactate Dehydrogenase Assay', *Cold Spring Harb Protoc*, 2018.

Kurosawa, T., Y. Tega, D. Sako, T. Mochizuki, T. Yamaguchi, K. Kawabata, K. Inoue, N. Ito, H. Kusuhara, and Y. Deguchi. 2021. 'Transport Characteristics of 6-Mercaptopurine in Brain Microvascular Endothelial Cells Derived From Human Induced Pluripotent Stem Cells', *J Pharm Sci*, 110: 3484-90.

Lakey, P. S., T. Berkemeier, H. Tong, A. M. Arangio, K. Lucas, U. Poschl, and M. Shiraiwa. 2016. 'Chemical exposure-response relationship between air pollutants and reactive oxygen species in the human respiratory tract', *Sci Rep*, 6: 32916.

Landrum, M. J., J. M. Lee, G. R. Riley, W. Jang, W. S. Rubinstein, D. M. Church, and D. R. Maglott. 2014. 'ClinVar: public archive of relationships among sequence variation and human phenotype', *Nucleic Acids Res*, 42: D980-5.

Lane, A. N., and T. W. Fan. 2015. 'Regulation of mammalian nucleotide metabolism and biosynthesis', *Nucleic Acids Res*, 43: 2466-85.

Larionova, I., and L. Tashireva. 2023. 'Immune gene signatures as prognostic criteria for cancer patients', *Ther Adv Med Oncol*, 15: 17588359231189436.

Larsen, E. C., M. Devidas, S. Chen, W. L. Salzer, E. A. Raetz, M. L. Loh, L. A. Mattano, Jr., C. Cole, A. Eicher, M. Haugan, M. Sorenson, N. A. Heerema, A. A. Carroll, J. M. Gastier-Foster, M. J. Borowitz, B. L. Wood, C. L. Willman, N. J. Winick, S. P. Hunger, and W. L. Carroll. 2016. 'Dexamethasone and High-Dose Methotrexate Improve Outcome for Children and Young Adults With High-Risk B-Acute Lymphoblastic Leukemia: A Report From Children's Oncology Group Study AALL0232', *J Clin Oncol*, 34: 2380-8.

Larsen, R. H., L. L. Hjalgrim, K. Grell, K. Kristensen, L. G. Pedersen, E. D. Brunner, B. Als-Nielsen, K. Schmiegelow, and J. Nersting. 2020. 'Pharmacokinetics of tablet and liquid

formulations of oral 6-mercaptopurine in children with acute lymphoblastic leukemia', *Cancer Chemother Pharmacol*, 86: 25-32.

Lennard, L. 1992. 'The clinical pharmacology of 6-mercaptopurine', *Eur J Clin Pharmacol*, 43: 329-39.

Lennard, L., C. S. Cartwright, R. Wade, and A. Vora. 2015. 'Thiopurine dose intensity and treatment outcome in childhood lymphoblastic leukaemia: the influence of thiopurine methyltransferase pharmacogenetics', *Br J Haematol*, 169: 228-40.

Lewandowski, M., and K. Gwozdzinski. 2017. 'Nitroxides as Antioxidants and Anticancer Drugs', *Int J Mol Sci*, 18.

Li, B., H. Li, Y. Bai, R. Kirschner-Schwabe, J. J. Yang, Y. Chen, G. Lu, G. Tzoneva, X. Ma, T. Wu, W. Li, H. Lu, L. Ding, H. Liang, X. Huang, M. Yang, L. Jin, H. Kang, S. Chen, A. Du, S. Shen, J. Ding, H. Chen, J. Chen, A. von Stackelberg, L. Gu, J. Zhang, A. Ferrando, J. Tang, S. Wang, and B. B. Zhou. 2015. 'Negative feedback-defective PRPS1 mutants drive thiopurine resistance in relapsed childhood ALL', *Nat Med*, 21: 563-71.

Li, F., B. L. Fridley, A. Matimba, K. R. Kalari, L. Pelleymounter, I. Moon, Y. Ji, G. D. Jenkins, A. Batzler, L. Wang, and R. M. Weinshilboum. 2010. 'Ecto-5'-nucleotidase and thiopurine cellular circulation: association with cytotoxicity', *Drug Metab Dispos*, 38: 2329-38.

Li, J., Z. Cai, L. P. Vaites, N. Shen, D. C. Mitchell, E. L. Huttlin, J. A. Paulo, B. L. Harry, and S. P. Gygi. 2021. 'Proteome-wide mapping of short-lived proteins in human cells', *Mol Cell*, 81: 4722-35 e5.

Lin, J. H. 2007. 'Transporter-mediated drug interactions: clinical implications and in vitro assessment', *Expert Opin Drug Metab Toxicol*, 3: 81-92.

Liu, C., L. J. Janke, J. J. Yang, W. E. Evans, J. D. Schuetz, and M. V. Relling. 2017. 'Differential effects of thiopurine methyltransferase (TPMT) and multidrug resistance-associated protein gene 4 (MRP4) on mercaptopurine toxicity', *Cancer Chemother Pharmacol*, 80: 287-93.

Liu, X. 2019. 'Overview: Role of Drug Transporters in Drug Disposition and Its Clinical Significance', *Adv Exp Med Biol*, 1141: 1-12.

Liu, X., J. M. Yang, S. S. Zhang, X. Y. Liu, and D. X. Liu. 2010. 'Induction of cell cycle arrest at G1 and S phases and cAMP-dependent differentiation in C6 glioma by low concentration of cycloheximide', *BMC Cancer*, 10: 684.

Lockhead, S., A. Moskaleva, J. Kamenz, Y. Chen, M. Kang, A. R. Reddy, S. D. M. Santos, and J. E. Ferrell, Jr. 2020. 'The Apparent Requirement for Protein Synthesis during G2 Phase Is due to Checkpoint Activation', *Cell Rep*, 32: 107901.

Loi, T. H., P. Dai, S. Carlin, J. V. Melo, and D. D. F. Ma. 2016. 'Pro-survival role of protein kinase C epsilon in Philadelphia chromosome positive acute leukemia', *Leuk Lymphoma*, 57: 411-18.

Lombardo, L. J., F. Y. Lee, P. Chen, D. Norris, J. C. Barrish, K. Behnia, S. Castaneda, L. A. Cornelius, J. Das, A. M. Doweyko, C. Fairchild, J. T. Hunt, I. Inigo, K. Johnston, A. Kamath, D. Kan, H. Klei, P. Marathe, S. Pang, R. Peterson, S. Pitt, G. L. Schieven, R. J. Schmidt, J. Tokarski, M. L. Wen, J. Wityak, and R. M. Borzilleri. 2004. 'Discovery of N-(2-chloro-6-methyl- phenyl)-2-(6-(4-(2-hydroxyethyl)- piperazin-1-yl)-2-methylpyrimidin-4- ylamino)thiazole-5-carboxamide (BMS-354825), a dual Src/Abl kinase inhibitor with potent antitumor activity in preclinical assays', *J Med Chem*, 47: 6658-61.

Lonnerholm, G., A. Kreuger, B. Lindstrom, J. Ludvigsson, and U. Myrdal. 1986. 'Plasma and erythrocyte concentrations of mercaptopurine after oral administration in children', *Pediatr Hematol Oncol*, 3: 27-35.

Loor, G., J. Kondapalli, J. M. Schriewer, N. S. Chandel, T. L. Vanden Hoek, and P. T. Schumacker. 2010. 'Menadione triggers cell death through ROS-dependent mechanisms involving PARP activation without requiring apoptosis', *Free Radic Biol Med*, 49: 1925-36.

Lutzny, G., T. Kocher, M. Schmidt-Supprian, M. Rudelius, L. Klein-Hitpass, A. J. Finch, J. Durig, M. Wagner, C. Haferlach, A. Kohlmann, S. Schnittger, M. Seifert, S. Wanninger, N. Zaborsky, R. Oostendorp, J. Ruland, M. Leitges, T. Kuhnt, Y. Schafer, B. Lampl, C. Peschel, A. Egle, and I. Ringshausen. 2013. 'Protein kinase c-beta-dependent activation of NF-kappaB in stromal cells is indispensable for the survival of chronic lymphocytic leukemia B cells in vivo', *Cancer Cell*, 23: 77-92.

Lynch, T. J., D. W. Bell, R. Sordella, S. Gurubhagavatula, R. A. Okimoto, B. W. Brannigan, P. L. Harris, S. M. Haserlat, J. G. Supko, F. G. Haluska, D. N. Louis, D. C. Christiani, J. Settleman, and D. A. Haber. 2004. 'Activating mutations in the epidermal growth factor receptor underlying responsiveness of non-small-cell lung cancer to gefitinib', *N Engl J Med*, 350: 2129-39.

Ma, D., Q. Fang, P. Wang, R. Gao, W. Wu, T. Lu, L. Cao, X. Hu, and J. Wang. 2015. 'Induction of heme oxygenase-1 by Na+-H+ exchanger 1 protein plays a crucial role in imatinib-resistant chronic myeloid leukemia cells', *J Biol Chem*, 290: 12558-71.

Maemondo, M., A. Inoue, K. Kobayashi, S. Sugawara, S. Oizumi, H. Isobe, A. Gemma, M. Harada, H. Yoshizawa, I. Kinoshita, Y. Fujita, S. Okinaga, H. Hirano, K. Yoshimori, T. Harada, T. Ogura, M. Ando, H. Miyazawa, T. Tanaka, Y. Saijo, K. Hagiwara, S. Morita, T. Nukiwa, and Group North-East Japan Study. 2010. 'Gefitinib or chemotherapy for non-small-cell lung cancer with mutated EGFR', *N Engl J Med*, 362: 2380-8.

Maloney, K. W., M. Devidas, C. Wang, L. A. Mattano, A. M. Friedmann, P. Buckley, M. J. Borowitz, A. J. Carroll, J. M. Gastier-Foster, N. A. Heerema, N. Kadan-Lottick, M. L. Loh, Y. H. Matloub, D. T. Marshall, L. C. Stork, E. A. Raetz, B. Wood, S. P. Hunger, W.

L. Carroll, and N. J. Winick. 2020. 'Outcome in Children With Standard-Risk B-Cell Acute Lymphoblastic Leukemia: Results of Children's Oncology Group Trial AALL0331', *J Clin Oncol*, 38: 602-12.

Manning, G., D. B. Whyte, R. Martinez, T. Hunter, and S. Sudarsanam. 2002. 'The protein kinase complement of the human genome', *Science*, 298: 1912-34.

Marinkovic, G., J. Kroon, M. Hoogenboezem, K. A. Hoeben, M. S. Ruiter, K. Kurakula, I. Otermin Rubio, M. Vos, C. J. de Vries, J. D. van Buul, and V. de Waard. 2014. 'Inhibition of GTPase Rac1 in endothelium by 6-mercaptopurine results in immunosuppression in nonimmune cells: new target for an old drug', *J Immunol*, 192: 4370-8.

Martinez-Hernandez, A., H. Gutierrez-Malacatt, K. Carrillo-Sanchez, Y. Saldana-Alvarez, A. Rojas-Ochoa, E. Crespo-Solis, A. Aguayo-Gonzalez, A. Rosas-Lopez, J. M. Ayala-Sanchez, X. Aquino-Ortega, L. Orozco, and E. J. Cordova. 2014. 'Small MAF genes variants and chronic myeloid leukemia', *Eur J Haematol*, 92: 35-41.

Martiny-Baron, G., M. G. Kazanietz, H. Mischak, P. M. Blumberg, G. Kochs, H. Hug, D. Marme, and C. Schachtele. 1993. 'Selective inhibition of protein kinase C isozymes by the indolocarbazole Go 6976', *J Biol Chem*, 268: 9194-7.

Mathieson, T., H. Franken, J. Kosinski, N. Kurzawa, N. Zinn, G. Sweetman, D. Poeckel, V. S. Ratnu, M. Schramm, I. Becher, M. Steidel, K. M. Noh, G. Bergamini, M. Beck, M. Bantscheff, and M. M. Savitski. 2018. 'Systematic analysis of protein turnover in primary cells', *Nat Commun*, 9: 689.

Maude, S. L., N. Frey, P. A. Shaw, R. Aplenc, D. M. Barrett, N. J. Bunin, A. Chew, V. E. Gonzalez, Z. Zheng, S. F. Lacey, Y. D. Mahnke, J. J. Melenhorst, S. R. Rheingold, A. Shen, D. T. Teachey, B. L. Levine, C. H. June, D. L. Porter, and S. A. Grupp. 2014. 'Chimeric antigen receptor T cells for sustained remissions in leukemia', *N Engl J Med*, 371: 1507-17.

Maung, Z. T., L. Hogarth, M. M. Reid, S. J. Proctor, P. J. Hamilton, and A. G. Hall. 1994. 'Raised intracellular glutathione levels correlate with in vitro resistance to cytotoxic drugs in leukaemic cells from patients with acute lymphoblastic leukemia', *Leukemia*, 8: 1487-91.

McCord, J. M., and I. Fridovich. 1969. 'Superoxide dismutase. An enzymic function for erythrocuprein (hemocuprein)', *J Biol Chem*, 244: 6049-55.

Medeiros, M. S., A. Schumacher-Schuh, A. M. Cardoso, G. V. Bochi, J. Baldissarelli, A. Kegler, D. Santana, C. M. Chaves, M. R. Schetinger, R. N. Moresco, C. R. Rieder, and M. R. Fighera. 2016. 'Iron and Oxidative Stress in Parkinson's Disease: An Observational Study of Injury Biomarkers', *PLoS One*, 11: e0146129.

Mender, I., K. Batten, M. Peyton, A. Vemula, C. Cornelius, L. Girard, B. Gao, J. D. Minna, and J. W. Shay. 2020. 'SLC43A3 Is a Biomarker of Sensitivity to the Telomeric DNA Damage Mediator 6-Thio-2'-Deoxyguanosine', *Cancer Res*, 80: 929-36.

Milani, G., P. Rebora, B. Accordi, L. Galla, S. Bresolin, G. Cazzaniga, B. Buldini, R. Mura, S. Ladogana, E. Giraldi, V. Conter, G. Te Kronnie, M. G. Valsecchi, and G. Basso. 2014. 'Low PKCalpha expression within the MRD-HR stratum defines a new subgroup of childhood T-ALL with very poor outcome', *Oncotarget*, 5: 5234-45.

Millar, T. M., J. M. Kanczler, T. Bodamyali, D. R. Blake, and C. R. Stevens. 2002. 'Xanthine oxidase is a peroxynitrite synthase: newly identified roles for a very old enzyme', *Redox Rep*, 7: 65-70.

Mishra, M., S. Tiwari, and A. V. Gomes. 2017. 'Protein purification and analysis: next generation Western blotting techniques', *Expert Rev Proteomics*, 14: 1037-53.

Mlejnek, P., and P. Dolezel. 2014. 'N-acetylcysteine prevents the geldanamycin cytotoxicity by forming geldanamycin-N-acetylcysteine adduct', *Chem Biol Interact*, 220: 248-54.

Moi, P., K. Chan, I. Asunis, A. Cao, and Y. W. Kan. 1994. 'Isolation of NF-E2-related factor 2 (Nrf2), a NF-E2-like basic leucine zipper transcriptional activator that binds to the tandem NF-E2/AP1 repeat of the beta-globin locus control region', *Proc Natl Acad Sci U S A*, 91: 9926-30.

Monteiro, J. P., A. F. Martins, C. Nunes, C. M. Morais, M. Lucio, S. Reis, T. J. Pinheiro, C. F. Geraldes, P. J. Oliveira, and A. S. Jurado. 2013. 'A biophysical approach to menadione membrane interactions: relevance for menadione-induced mitochondria dysfunction and related deleterious/therapeutic effects', *Biochim Biophys Acta*, 1828: 1899-908.

Montero, J. C., S. Seoane, S. Garcia-Alonso, and A. Pandiella. 2016. 'Multisite phosphorylation of P-Rex1 by protein kinase C', *Oncotarget*, 7: 77937-49.

Moon, S. Y., J. H. Lim, E. H. Kim, Y. Nam, K. S. Yu, K. T. Hong, J. Y. Choi, C. R. Hong, H. Kim, H. J. Kang, H. Y. Shin, K. Lee, J. Song, S. Y. Lee, and S. H. Song. 2019. 'Quantification of Thiopurine Nucleotides in Erythrocytes and Clinical Application to Pediatric Acute Lymphoblastic Leukemia', *Ther Drug Monit*, 41: 75-85.

Mori, S., S. Ohtsuki, H. Takanaga, T. Kikkawa, Y. S. Kang, and T. Terasaki. 2004. 'Organic anion transporter 3 is involved in the brain-to-blood efflux transport of thiopurine nucleobase analogs', *J Neurochem*, 90: 931-41.

Moricke, A., M. Zimmermann, M. G. Valsecchi, M. Stanulla, A. Biondi, G. Mann, F. Locatelli, G. Cazzaniga, F. Niggli, M. Arico, C. R. Bartram, A. Attarbaschi, D. Silvestri, R. Beier, G. Basso, R. Ratei, A. E. Kulozik, L. Lo Nigro, B. Kremens, J. Greiner, R. Parasole, J. Harbott, R. Caruso, A. von Stackelberg, E. Barisone, C. Rossig, V. Conter, and M. Schrappe. 2016. 'Dexamethasone vs prednisone in induction treatment of pediatric ALL: results of the randomized trial AIEOP-BFM ALL 2000', *Blood*, 127: 2101-12.

Moriya, H. 2015. 'Quantitative nature of overexpression experiments', *Mol Biol Cell*, 26: 3932-9.

Moriyama, T., R. Nishii, V. Perez-Andreu, W. Yang, F. A. Klussmann, X. Zhao, T. N. Lin, K. Hoshitsuki, J. Nersting, K. Kihira, U. Hofmann, Y. Komada, M. Kato, R. McCorkle, L. Li, K. Koh, C. R. Najera, S. K. Kham, T. Isobe, Z. Chen, E. K. Chiew, D. Bhojwani, C. Jeffries, Y. Lu, M. Schwab, H. Inaba, C. H. Pui, M. V. Relling, A. Manabe, H. Hori, K. Schmiegelow, A. E. Yeoh, W. E. Evans, and J. J. Yang. 2016. 'NUDT15 polymorphisms alter thiopurine metabolism and hematopoietic toxicity', *Nat Genet*, 48: 367-73.

Motohashi, H., F. Katsuoka, J. D. Engel, and M. Yamamoto. 2004. 'Small Maf proteins serve as transcriptional cofactors for keratinocyte differentiation in the Keap1-Nrf2 regulatory pathway', *Proc Natl Acad Sci U S A*, 101: 6379-84.

Muraleedharan, A., N. Rotem-Dai, I. Strominger, N. P. Anto, N. Isakov, A. Monsonego, and E. Livneh. 2021. 'Protein kinase C eta is activated in reactive astrocytes of an Alzheimer's disease mouse model: Evidence for its immunoregulatory function in primary astrocytes', *Glia*, 69: 697-714.

Nagai, K., K. Nagasawa, Y. Kihara, H. Okuda, and S. Fujimoto. 2007. 'Anticancer nucleobase analogues 6-mercaptopurine and 6-thioguanine are novel substrates for equilibrative nucleoside transporter 2', *Int J Pharm*, 333: 56-61.

Nakanishi, T. 2007. 'Drug transporters as targets for cancer chemotherapy', *Cancer Genomics Proteomics*, 4: 241-54.

Nakashima, S. 2002. 'Protein kinase C alpha (PKC alpha): regulation and biological function', *J Biochem*, 132: 669-75.

Nelson, J. A., J. W. Carpenter, L. M. Rose, and D. J. Adamson. 1975. 'Mechanisms of action of 6-thioguanine, 6-mercaptopurine, and 8-azaguanine', *Cancer Res*, 35: 2872-8.

Neumeier, J., and G. Meister. 2020. 'siRNA Specificity: RNAi Mechanisms and Strategies to Reduce Off-Target Effects', *Front Plant Sci*, 11: 526455.

Newton, A. C. 2018. 'Protein kinase C: perfectly balanced', *Crit Rev Biochem Mol Biol*, 53: 208-30.

Nivillac, N. M., J. Bacani, and I. R. Coe. 2011. 'The life cycle of human equilibrative nucleoside transporter 1: from ER export to degradation', *Exp Cell Res*, 317: 1567-79.

Nygaard, U., N. Toft, and K. Schmiegelow. 2004. 'Methylated metabolites of 6-mercaptopurine are associated with hepatotoxicity', *Clin Pharmacol Ther*, 75: 274-81.

Ogu, C. C., and J. L. Maxa. 2000. 'Drug interactions due to cytochrome P450', *Proc (Bayl Univ Med Cent)*, 13: 421-3.

Ohtsuki, S., H. Asaba, H. Takanaga, T. Deguchi, K. Hosoya, M. Otagiri, and T. Terasaki. 2002. 'Role of blood-brain barrier organic anion transporter 3 (OAT3) in the efflux of indoxyl

sulfate, a uremic toxin: its involvement in neurotransmitter metabolite clearance from the brain', *J Neurochem*, 83: 57-66.

Oltra, A. M., F. Carbonell, C. Tormos, A. Iradi, and G. T. Saez. 2001. 'Antioxidant enzyme activities and the production of MDA and 8-oxo-dG in chronic lymphocytic leukemia', *Free Radic Biol Med*, 30: 1286-92.

Omasits, U., C. H. Ahrens, S. Muller, and B. Wollscheid. 2014. 'Protter: interactive protein feature visualization and integration with experimental proteomic data', *Bioinformatics*, 30: 884-6.

Ottmann, O. G. 2012. 'Management of Philadelphia chromosome-positive acute lymphoblastic leukemia', *Leuk Suppl*, 1: S7-9.

Pandey, A. V., and P. Sproll. 2014. 'Pharmacogenomics of human P450 oxidoreductase', *Front Pharmacol*, 5: 103.

Park, J. H., I. Riviere, M. Gonen, X. Wang, B. Senechal, K. J. Curran, C. Sauter, Y. Wang, B. Santomasso, E. Mead, M. Roshal, P. Maslak, M. Davila, R. J. Brentjens, and M. Sadelain. 2018. 'Long-Term Follow-up of CD19 CAR Therapy in Acute Lymphoblastic Leukemia', *N Engl J Med*, 378: 449-59.

Park, W. H. 2021. 'Tempol differently affects cellular redox changes and antioxidant enzymes in various lung-related cells', *Sci Rep*, 11: 14869.

Patel, J. N., and A. Papachristos. 2015. 'Personalizing chemotherapy dosing using pharmacological methods', *Cancer Chemother Pharmacol*, 76: 879-96.

Peng, X. X., Z. Shi, V. L. Damaraju, X. C. Huang, G. D. Kruh, H. C. Wu, Y. Zhou, A. Tiwari, L. Fu, C. E. Cass, and Z. S. Chen. 2008. 'Up-regulation of MRP4 and down-regulation of influx transporters in human leukemic cells with acquired resistance to 6-mercaptopurine', *Leuk Res*, 32: 799-809.

Pierre, F., P. C. Chua, S. E. O'Brien, A. Siddiqui-Jain, P. Bourbon, M. Haddach, J. Michaux, J. Nagasawa, M. K. Schwaebe, E. Stefan, A. Vialettes, J. P. Whitten, T. K. Chen, L. Darjania, R. Stansfield, K. Anderes, J. Bliesath, D. Drygin, C. Ho, M. Omori, C. Proffitt, N. Streiner, K. Trent, W. G. Rice, and D. M. Ryckman. 2011. 'Discovery and SAR of 5-(3-chlorophenylamino)benzo[c][2,6]naphthyridine-8-carboxylic acid (CX-4945), the first clinical stage inhibitor of protein kinase CK2 for the treatment of cancer', *J Med Chem*, 54: 635-54.

Pieters, R., H. de Groot-Kruseman, V. Van der Velden, M. Fiocco, H. van den Berg, E. de Bont, R. M. Egeler, P. Hoogerbrugge, G. Kaspers, E. Van der Schoot, V. De Haas, and J. Van Dongen. 2016. 'Successful Therapy Reduction and Intensification for Childhood Acute Lymphoblastic Leukemia Based on Minimal Residual Disease Monitoring: Study ALL10 From the Dutch Childhood Oncology Group', *J Clin Oncol*, 34: 2591-601.

Pieters, R., D. R. Huismans, A. H. Loonen, G. J. Peters, K. Hahlen, A. van der Does-van den Berg, E. R. van Wering, and A. J. Veerman. 1992. 'Relation of 5'-nucleotidase and phosphatase activities with immunophenotype, drug resistance and clinical prognosis in childhood leukemia', *Leuk Res*, 16: 873-80.

Pizzino, G., N. Irrera, M. Cucinotta, G. Pallio, F. Mannino, V. Arcoraci, F. Squadrito, D. Altavilla, and A. Bitto. 2017. 'Oxidative Stress: Harms and Benefits for Human Health', *Oxid Med Cell Longev*, 2017: 8416763.

Place, A. E., K. E. Stevenson, L. M. Vrooman, M. H. Harris, S. K. Hunt, J. E. O'Brien, J. G. Supko, B. L. Asselin, U. H. Athale, L. A. Clavell, P. D. Cole, K. M. Kelly, C. Laverdiere, J. M. Leclerc, B. Michon, M. A. Schorin, J. J. Welch, S. E. Lipshultz, J. L. Kutok, T. M. Blonquist, D. S. Neuberg, S. E. Sallan, and L. B. Silverman. 2015. 'Intravenous pegylated asparaginase versus intramuscular native Escherichia coli L-asparaginase in newly diagnosed childhood acute lymphoblastic leukaemia (DFCI 05-001): a randomised, open-label phase 3 trial', *Lancet Oncol*, 16: 1677-90.

Porter, D. L., W. T. Hwang, N. V. Frey, S. F. Lacey, P. A. Shaw, A. W. Loren, A. Bagg, K. T. Marcucci, A. Shen, V. Gonzalez, D. Ambrose, S. A. Grupp, A. Chew, Z. Zheng, M. C. Milone, B. L. Levine, J. J. Melenhorst, and C. H. June. 2015. 'Chimeric antigen receptor T cells persist and induce sustained remissions in relapsed refractory chronic lymphocytic leukemia', *Sci Transl Med*, 7: 303ra139.

Pozarowski, P., and Z. Darzynkiewicz. 2004. 'Analysis of cell cycle by flow cytometry', *Methods Mol Biol*, 281: 301-11.

Pui, C. H., J. J. Yang, S. P. Hunger, R. Pieters, M. Schrappe, A. Biondi, A. Vora, A. Baruchel, L. B. Silverman, K. Schmiegelow, G. Escherich, K. Horibe, Y. C. Benoit, S. Izraeli, A. E. Yeoh, D. C. Liang, J. R. Downing, W. E. Evans, M. V. Relling, and C. G. Mullighan. 2015. 'Childhood Acute Lymphoblastic Leukemia: Progress Through Collaboration', *J Clin Oncol*, 33: 2938-48.

Rahman, I., A. Kode, and S. K. Biswas. 2006. 'Assay for quantitative determination of glutathione and glutathione disulfide levels using enzymatic recycling method', *Nat Protoc*, 1: 3159-65.

Reid, G., P. Wielinga, N. Zelcer, M. De Haas, L. Van Deemter, J. Wijnholds, J. Balzarini, and P. Borst. 2003. 'Characterization of the transport of nucleoside analog drugs by the human multidrug resistance proteins MRP4 and MRP5', *Mol Pharmacol*, 63: 1094-103.

'Release notice - Canadian Cancer Statistics 2023'. 2024. *Health Promot Chronic Dis Prev Can*, 44: 34.

Relling, M. V., M. Schwab, M. Whirl-Carrillo, G. Suarez-Kurtz, C. H. Pui, C. M. Stein, A. M. Moyer, W. E. Evans, T. E. Klein, F. G. Antillon-Klussmann, K. E. Caudle, M. Kato, A. E. J. Yeoh, K. Schmiegelow, and J. J. Yang. 2019. 'Clinical Pharmacogenetics Implementation Consortium Guideline for Thiopurine Dosing Based on TPMT and NUDT15 Genotypes: 2018 Update', *Clin Pharmacol Ther*, 105: 1095-105.

Riss, T. L., R. A. Moravec, A. L. Niles, S. Duellman, H. A. Benink, T. J. Worzella, and L. Minor. 2004. 'Cell Viability Assays.' in S. Markossian, A. Grossman, M. Arkin, D. Auld, C. Austin, J. Baell, K. Brimacombe, T. D. Y. Chung, N. P. Coussens, J. L. Dahlin, V. Devanarayan, T. L. Foley, M. Glicksman, K. Gorshkov, J. V. Haas, M. D. Hall, S. Hoare, J. Inglese, P. W. Iversen, M. Lal-Nag, Z. Li, J. R. Manro, J. McGee, O. McManus, M. Pearson, T. Riss, P. Saradjian, G. S. Sittampalam, M. Tarselli, O. J. Trask, Jr., J. R. Weidner, M. J. Wildey, K. Wilson, M. Xia and X. Xu (eds.), *Assay Guidance Manual* (Bethesda (MD)).

Rooney, J. P., B. Chorley, S. Hiemstra, S. Wink, X. Wang, D. A. Bell, B. van de Water, and J. C. Corton. 2020. 'Mining a human transcriptome database for chemical modulators of NRF2', *PLoS One*, 15: e0239367.

Ruel, N. M., K. H. Nguyen, C. S. Kim, L. P. S. Andrade, and J. R. Hammond. 2022. 'Impact of SLC43A3/ENBT1 Expression and Function on 6-Mercaptopurine Transport and Cytotoxicity in Human Acute Lymphoblastic Leukemia Cells', *J Pharmacol Exp Ther*, 382: 335-45.

Ruel, N. M., K. H. Nguyen, G. Vilas, and J. R. Hammond. 2019. 'Characterization of 6-Mercaptopurine Transport by the SLC43A3-Encoded Nucleobase Transporter', *Mol Pharmacol*, 95: 584-96.

Ruiz-Aparicio, P. F., G. I. Uribe, A. Linares-Ballesteros, and J. P. Vernot. 2021. 'Sensitization to Drug Treatment in Precursor B-Cell Acute Lymphoblastic Leukemia Is Not Achieved by Stromal NF-kappaB Inhibition of Cell Adhesion but by Stromal PKC-Dependent Inhibition of ABC Transporters Activity', *Molecules*, 26.

Ruiz-Aparicio, P. F., N. P. Vanegas, G. I. Uribe, P. Ortiz-Montero, C. Cadavid-Cortes, J. Lagos, J. Flechas-Afanador, A. Linares-Ballesteros, and J. P. Vernot. 2020. 'Dual Targeting of Stromal Cell Support and Leukemic Cell Growth by a Peptidic PKC Inhibitor Shows Effectiveness against B-ALL', *Int J Mol Sci*, 21.

Rybin, V. O., J. Guo, A. Sabri, H. Elouardighi, E. Schaefer, and S. F. Steinberg. 2004. 'Stimulus-specific differences in protein kinase C delta localization and activation mechanisms in cardiomyocytes', *J Biol Chem*, 279: 19350-61.

Saba, N. S., and L. S. Levy. 2011. 'Apoptotic induction in B-cell acute lymphoblastic leukemia cell lines treated with a protein kinase Cbeta inhibitor', *Leuk Lymphoma*, 52: 877-86.

Saiz-Rodriguez, M., D. Ochoa, C. Belmonte, M. Roman, C. Martinez-Ingelmo, L. Ortega-Ruiz, C. Sarmiento-Iglesias, C. Herrador, and F. Abad-Santos. 2019. 'Influence of thiopurine S-methyltransferase polymorphisms in mercaptopurine pharmacokinetics in healthy volunteers', *Basic Clin Pharmacol Toxicol*, 124: 449-55.

Sakurada, K., K. Abe, M. Kobayashi, M. Tanaka, and T. Miyazaki. 1989. 'Effect of an inhibitory factor for protein kinase C on cell growth of leukemic cells', *Jpn J Med*, 28: 141-7.

Sallmyr, A., J. Fan, and F. V. Rassool. 2008. 'Genomic instability in myeloid malignancies: increased reactive oxygen species (ROS), DNA double strand breaks (DSBs) and error-prone repair', *Cancer Lett*, 270: 1-9.

Salser, J. S., and M. E. Balis. 1965. 'The Mechanism of Action of 6-Mercaptopurine. I. Biochemical Effects', *Cancer Res*, 25: 539-43.

Sampath, J., M. Adachi, S. Hatse, L. Naesens, J. Balzarini, R. M. Flatley, L. H. Matherly, and J. D. Schuetz. 2002. 'Role of MRP4 and MRP5 in biology and chemotherapy', *AAPS PharmSci*, 4: E14.

Saponara, E., M. Visentin, F. Baschieri, G. Seleznik, P. Martinelli, I. Esposito, J. Buschmann, R. Chen, R. Parrotta, N. Borgeaud, M. Bombardo, E. Malagola, A. Caflisch, H. Farhan, R. Graf, and S. Sonda. 2018. 'Serotonin uptake is required for Rac1 activation in Kras-induced acinar-to-ductal metaplasia in the pancreas', *J Pathol*, 246: 352-65.

Sauve, S., J. Williamson, A. Polasa, and M. Moradi. 2023. 'Ins and Outs of Rocker Switch Mechanism in Major Facilitator Superfamily of Transporters', *Membranes (Basel)*, 13.

Sawyers, C. L., C. T. Denny, and O. N. Witte. 1991. 'Leukemia and the disruption of normal hematopoiesis', *Cell*, 64: 337-50.

Schmiegelow, K., E. Forestier, J. Kristinsson, S. Soderhall, K. Vettenranta, R. Weinshilboum, F. Wesenberg, Haematology Nordic Society of Paediatric, and Oncology. 2009. 'Thiopurine methyltransferase activity is related to the risk of relapse of childhood acute lymphoblastic leukemia: results from the NOPHO ALL-92 study', *Leukemia*, 23: 557-64.

Schmiegelow, K., S. N. Nielsen, T. L. Frandsen, and J. Nersting. 2014. 'Mercaptopurine/Methotrexate maintenance therapy of childhood acute lymphoblastic leukemia: clinical facts and fiction', *J Pediatr Hematol Oncol*, 36: 503-17.

Schuetz, J. D., M. C. Connelly, D. Sun, S. G. Paibir, P. M. Flynn, R. V. Srinivas, A. Kumar, and A. Fridland. 1999. 'MRP4: A previously unidentified factor in resistance to nucleoside-based antiviral drugs', *Nat Med*, 5: 1048-51.

Senyavina, N. V., and S. A. Tonevitskaya. 2015. 'Effect of Hypoxanthine on Functional Activity of Nucleoside Transporters ENT1 and ENT2 in Caco-2 Polar Epithelial Intestinal Cells', *Bull Exp Biol Med*, 160: 160-4.

Shah, N. P., C. Tran, F. Y. Lee, P. Chen, D. Norris, and C. L. Sawyers. 2004. 'Overriding imatinib resistance with a novel ABL kinase inhibitor', *Science*, 305: 399-401.

Shaye, O. A., M. Yadegari, M. T. Abreu, F. Poordad, K. Simon, P. Martin, K. A. Papadakis, A. Ippoliti, E. Vasiliauskas, and T. T. Tran. 2007. 'Hepatotoxicity of 6-mercaptopurine (6-MP) and Azathioprine (AZA) in adult IBD patients', *Am J Gastroenterol*, 102: 2488-94.

Shen, J., M. Rasmussen, Q. R. Dong, M. Tepel, and A. Scholze. 2017. 'Expression of the NRF2 Target Gene NQO1 Is Enhanced in Mononuclear Cells in Human Chronic Kidney Disease', *Oxid Med Cell Longev*, 2017: 9091879.

Shepherd, F. A., J. Rodrigues Pereira, T. Ciuleanu, E. H. Tan, V. Hirsh, S. Thongprasert, D. Campos, S. Maoleekoonpiroj, M. Smylie, R. Martins, M. van Kooten, M. Dediu, B. Findlay, D. Tu, D. Johnston, A. Bezjak, G. Clark, P. Santabarbara, L. Seymour, and Group National Cancer Institute of Canada Clinical Trials. 2005. 'Erlotinib in previously treated non-small-cell lung cancer', *N Engl J Med*, 353: 123-32.

Shimozono, N., M. Jinnin, M. Masuzawa, M. Masuzawa, Z. Wang, A. Hirano, Y. Tomizawa, T. Etoh-Kira, I. Kajihara, M. Harada, S. Fukushima, and H. Ihn. 2015. 'NUP160-SLC43A3 is a novel recurrent fusion oncogene in angiosarcoma', *Cancer Res*, 75: 4458-65.

Slauch, J. M. 2011. 'How does the oxidative burst of macrophages kill bacteria? Still an open question', *Mol Microbiol*, 80: 580-3.

Smale, S. T. 2010. 'Luciferase assay', *Cold Spring Harb Protoc*, 2010: pdb prot5421.

Snodgrass, R., L. T. Nguyen, M. Guo, M. Vaska, C. Naugler, and F. Rashid-Kolvear. 2018. 'Incidence of acute lymphocytic leukemia in Calgary, Alberta, Canada: a retrospective cohort study', *BMC Res Notes*, 11: 104.

Sosa, V., T. Moline, R. Somoza, R. Paciucci, H. Kondoh, and L. Leonart ME. 2013. 'Oxidative stress and cancer: an overview', *Ageing Res Rev*, 12: 376-90.

Stadtman, E. R., and R. L. Levine. 2003. 'Free radical-mediated oxidation of free amino acids and amino acid residues in proteins', *Amino Acids*, 25: 207-18.

Steinberg, S. F. 2008. 'Structural basis of protein kinase C isoform function', *Physiol Rev*, 88: 1341-78.

Stet, E. H., R. A. De Abreu, Y. P. Janssen, J. P. Bokkerink, and J. M. Trijbels. 1991. '6-Mercaptopurine metabolism in two leukemic cell lines', *Adv Exp Med Biol*, 309A: 83-6.

Steyn, S. J., and M. V. S. Varma. 2020. 'Cytochrome-P450-Mediated Drug-Drug Interactions of Substrate Drugs: Assessing Clinical Risk Based on Molecular Properties and an Extended Clearance Classification System', *Mol Pharm*, 17: 3024-32.

Stocco, G., W. Yang, K. R. Crews, W. E. Thierfelder, G. Decorti, M. Londero, R. Franca, M. Rabusin, M. G. Valsecchi, D. Pei, C. Cheng, S. W. Paugh, L. B. Ramsey, B. Diouf, J. R. McCorkle, T. S. Jones, C. H. Pui, M. V. Relling, and W. E. Evans. 2012. 'PACSIN2 polymorphism influences TPMT activity and mercaptopurine-related gastrointestinal toxicity', *Hum Mol Genet*, 21: 4793-804.

Stork, L. C., Y. Matloub, E. Broxson, M. La, R. Yanofsky, H. Sather, R. Hutchinson, N. A. Heerema, A. D. Sorrell, M. Masterson, A. Bleyer, and P. S. Gaynon. 2010. 'Oral 6-mercaptopurine versus oral 6-thioguanine and veno-occlusive disease in children with

standard-risk acute lymphoblastic leukemia: report of the Children's Oncology Group CCG-1952 clinical trial', *Blood*, 115: 2740-8.

Storz, P. 2005. 'Reactive oxygen species in tumor progression', *Front Biosci*, 10: 1881-96.

Sun, C., L. Chang, and X. Zhu. 2017. 'Pathogenesis of ETV6/RUNX1-positive childhood acute lymphoblastic leukemia and mechanisms underlying its relapse', *Oncotarget*, 8: 35445-59.

Suski, J. M., M. Braun, V. Strmiska, and P. Sicinski. 2021. 'Targeting cell-cycle machinery in cancer', *Cancer Cell*, 39: 759-78.

Sutherland, D. R., M. J. Fackler, W. S. May, K. E. Matthews, and M. A. Baker. 1992. 'Activated protein kinase C directly phosphorylates the CD34 antigen in acute lymphoblastic leukemia cells', *Leuk Lymphoma*, 8: 337-44.

Suvorova, E. S., O. Lucas, C. M. Weisend, M. F. Rollins, G. F. Merrill, M. R. Capecchi, and E. E. Schmidt. 2009. 'Cytoprotective Nrf2 pathway is induced in chronically txnrd 1-deficient hepatocytes', *PLoS One*, 4: e6158.

Suzuki, D., T. Miyata, N. Saotome, K. Horie, R. Inagi, Y. Yasuda, K. Uchida, Y. Izuhara, M. Yagame, H. Sakai, and K. Kurokawa. 1999. 'Immunohistochemical evidence for an increased oxidative stress and carbonyl modification of proteins in diabetic glomerular lesions', *J Am Soc Nephrol*, 10: 822-32.

Szatrowski, T. P., and C. F. Nathan. 1991. 'Production of large amounts of hydrogen peroxide by human tumor cells', *Cancer Res*, 51: 794-8.

Talpaz, M., N. P. Shah, H. Kantarjian, N. Donato, J. Nicoll, R. Paquette, J. Cortes, S. O'Brien, C. Nicaise, E. Bleickardt, M. A. Blackwood-Chirchir, V. Iyer, T. T. Chen, F. Huang, A. P. Decillis, and C. L. Sawyers. 2006. 'Dasatinib in imatinib-resistant Philadelphia chromosome-positive leukemias', *N Engl J Med*, 354: 2531-41.

Tanaka, Y. 2017. 'Susceptibility to 6-mercaptopurine toxicity related with NUDT15 and ABCC4 variants in Japanese childhood acute lymphoblastic leukemia', *Rinsho Ketsueki*, 58: 950-56.

Tanaka, Y., A. Manabe, H. Fukushima, R. Suzuki, H. Nakadate, K. Kondoh, K. Nakamura, K. Koh, T. Fukushima, M. Tsuchida, K. Koike, N. Kiyokawa, E. Noguchi, R. Sumazaki, and T. Komiyama. 2015. 'Multidrug resistance protein 4 (MRP4) polymorphisms impact the 6-mercaptopurine dose tolerance during maintenance therapy in Japanese childhood acute lymphoblastic leukemia', *Pharmacogenomics J*, 15: 380-4.

Tandio, D., G. Vilas, and J. R. Hammond. 2019. 'Bidirectional transport of 2-chloroadenosine by equilibrative nucleoside transporter 4 (hENT4): Evidence for allosteric kinetics at acidic pH', *Sci Rep*, 9: 13555.

Tay, B. S., R. M. Lilley, A. W. Murray, and M. R. Atkinson. 1969. 'Inhibition of phosphoribosyl pyrophosphate amidotransferase from Ehrlich ascites-tumour cells by thiopurine nucleotides', *Biochem Pharmacol*, 18: 936-8.

Thul, P. J., L. Akesson, M. Wiking, D. Mahdessian, A. Geladaki, H. Ait Blal, T. Alm, A. Asplund, L. Bjork, L. M. Breckels, A. Backstrom, F. Danielsson, L. Fagerberg, J. Fall, L. Gatto, C. Gnann, S. Hober, M. Hjelmare, F. Johansson, S. Lee, C. Lindskog, J. Mulder, C. M. Mulvey, P. Nilsson, P. Oksvold, J. Rockberg, R. Schutten, J. M. Schwenk, A. Sivertsson, E. Sjostedt, M. Skogs, C. Stadler, D. P. Sullivan, H. Tegel, C. Winsnes, C. Zhang, M. Zwahlen, A. Mardinoglu, F. Ponten, K. von Feilitzen, K. S. Lilley, M. Uhlen, and E. Lundberg. 2017. 'A subcellular map of the human proteome', *Science*, 356.

Toft, N., H. Birgens, J. Abrahamsson, L. Griskevicius, H. Hallbook, M. Heyman, T. W. Klausen, O. G. Jonsson, K. Palk, K. Pruunsild, P. Quist-Paulsen, G. Vaitkeviciene, K. Vettenranta, A. Asberg, T. L. Frandsen, H. V. Marquart, H. O. Madsen, U. Noren-Nystrom, and K. Schmiegelow. 2018. 'Results of NOPHO ALL2008 treatment for patients aged 1-45 years with acute lymphoblastic leukemia', *Leukemia*, 32: 606-15.

Toksvang, L. N., B. Als-Nielsen, C. Bacon, R. Bertasiute, X. Duarte, G. Escherich, E. A. Helgadottir, I. R. Johannsdottir, O. G. Jonsson, P. Kozlowski, C. Langenskjold, K. Lepik, R. Niinimaki, U. M. Overgaard, M. Punab, R. Raty, H. Segers, I. van der Sluis, O. P. Smith, M. Strullu, G. Vaitkeviciene, H. S. Wik, M. Heyman, and K. Schmiegelow. 2022. 'Thiopurine Enhanced ALL Maintenance (TEAM): study protocol for a randomized study to evaluate the improvement in disease-free survival by adding very low dose 6-thioguanine to 6-mercaptopurine/methotrexate-based maintenance therapy in pediatric and adult patients (0-45 years) with newly diagnosed B-cell precursor or T-cell acute lymphoblastic leukemia treated according to the intermediate risk-high group of the ALLTogether1 protocol', *BMC Cancer*, 22: 483.

Topp, M. S., N. Gockbuget, and A. S. Stein. 2015. 'Correction to Lancet Oncol 2015; 16: 60, 61. Safety and activity of blinatumomab for adult patients with relapsed or refractory B-precursor acute lymphoblastic leukaemia: a multi-centre, single-arm, phase 2 study', *Lancet Oncol*, 16: e158.

Topp, M. S., N. Gokbuget, G. Zugmaier, P. Klappers, M. Stelljes, S. Neumann, A. Viardot, R. Marks, H. Diedrich, C. Faul, A. Reichle, H. A. Horst, M. Bruggemann, D. Wessiepe, C. Holland, S. Alekar, N. Mergen, H. Einsele, D. Hoelzer, and R. C. Bargou. 2014. 'Phase II trial of the anti-CD19 bispecific T cell-engager blinatumomab shows hematologic and molecular remissions in patients with relapsed or refractory B-precursor acute lymphoblastic leukemia', *J Clin Oncol*, 32: 4134-40.

Topp, M. S., P. Kufer, N. Gokbuget, M. Goebeler, M. Klinger, S. Neumann, H. A. Horst, T. Raff, A. Viardot, M. Schmid, M. Stelljes, M. Schaich, E. Degenhard, R. Kohne-Volland, M. Bruggemann, O. Ottmann, H. Pfeifer, T. Burmeister, D. Nagorsen, M. Schmidt, R. Lutterbuese, C. Reinhardt, P. A. Baeuerle, M. Kneba, H. Einsele, G. Riethmuller, D. Hoelzer, G. Zugmaier, and R. C. Bargou. 2011. 'Targeted therapy with the T-cell-engaging antibody blinatumomab of chemotherapy-refractory minimal residual disease in

B-lineage acute lymphoblastic leukemia patients results in high response rate and prolonged leukemia-free survival', *J Clin Oncol*, 29: 2493-8.

Trachootham, D., J. Alexandre, and P. Huang. 2009. 'Targeting cancer cells by ROS-mediated mechanisms: a radical therapeutic approach?', *Nat Rev Drug Discov*, 8: 579-91.

Troeger, Anja, Pascal-David Johann, Mumine Senturk, Michael D. Milsom, and David A. Williams. 2010. 'Intact Rac Signaling Is Important for Leukemia Cell Survival', *Blood*, 116: 2885.

Tu, M., A. Zhang, L. Hu, and F. Wang. 2022. 'A Retrospective Cohort Study of the Efficacy, Safety, and Clinical Value of 6-TG versus 6-MP Maintenance Therapy in Children with Acute Lymphoblastic Leukemia', *Biomed Res Int*, 2022: 7580642.

Tzoneva, G., A. Perez-Garcia, Z. Carpenter, H. Khiabanian, V. Tosello, M. Allegretta, E. Paietta, J. Racevskis, J. M. Rowe, M. S. Tallman, M. Paganin, G. Basso, J. Hof, R. Kirschner-Schwabe, T. Palomero, R. Rabadan, and A. Ferrando. 2013. 'Activating mutations in the NT5C2 nucleotidase gene drive chemotherapy resistance in relapsed ALL', *Nat Med*, 19: 368-71.

Udensi, U. K., and P. B. Tchounwou. 2014. 'Dual effect of oxidative stress on leukemia cancer induction and treatment', *J Exp Clin Cancer Res*, 33: 106.

Uhlen, M., L. Fagerberg, B. M. Hallstrom, C. Lindskog, P. Oksvold, A. Mardinoglu, A. Sivertsson, C. Kampf, E. Sjostedt, A. Asplund, I. Olsson, K. Edlund, E. Lundberg, S. Navani, C. A. Szigyarto, J. Odeberg, D. Djureinovic, J. O. Takanen, S. Hober, T. Alm, P. H. Edqvist, H. Berling, H. Tegel, J. Mulder, J. Rockberg, P. Nilsson, J. M. Schwenk, M. Hamsten, K. von Feilitzen, M. Forsberg, L. Persson, F. Johansson, M. Zwahlen, G. von Heijne, J. Nielsen, and F. Ponten. 2015. 'Proteomics. Tissue-based map of the human proteome', *Science*, 347: 1260419.

Uhlen, M., C. Zhang, S. Lee, E. Sjostedt, L. Fagerberg, G. Bidkhori, R. Benfeitas, M. Arif, Z. Liu, F. Edfors, K. Sanli, K. von Feilitzen, P. Oksvold, E. Lundberg, S. Hober, P. Nilsson, J. Mattsson, J. M. Schwenk, H. Brunnstrom, B. Glimelius, T. Sjoblom, P. H. Edqvist, D. Djureinovic, P. Micke, C. Lindskog, A. Mardinoglu, and F. Ponten. 2017. 'A pathology atlas of the human cancer transcriptome', *Science*, 357.

Valko, M., D. Leibfritz, J. Moncol, M. T. Cronin, M. Mazur, and J. Telser. 2007. 'Free radicals and antioxidants in normal physiological functions and human disease', *Int J Biochem Cell Biol*, 39: 44-84.

van Asseldonk, D. P., M. L. Seinen, N. K. de Boer, A. A. van Bodegraven, and C. J. Mulder. 2012. 'Hepatotoxicity associated with 6-methyl mercaptopurine formation during azathioprine and 6-mercaptopurine therapy does not occur on the short-term during 6-thioguanine therapy in IBD treatment', *J Crohns Colitis*, 6: 95-101.

van der Sluis, I. M., P. de Lorenzo, R. S. Kotecha, A. Attarbaschi, G. Escherich, K. Nysom, J. Stary, A. Ferster, B. Brethon, F. Locatelli, M. Schrappe, P. E. Scholte-van Houtem, M. G.

Valsecchi, and R. Pieters. 2023. 'Blinatumomab Added to Chemotherapy in Infant Lymphoblastic Leukemia', *N Engl J Med*, 388: 1572-81.

Veraitch, F. S., and M. Al-Rubeai. 2005. 'Enhanced growth in NS0 cells expressing aminoglycoside phosphotransferase is associated with changes in metabolism, productivity, and apoptosis', *Biotechnol Bioeng*, 92: 589-99.

Villa-Morales, M., L. Perez-Gomez, E. Perez-Gomez, P. Lopez-Nieva, P. Fernandez-Navarro, and J. Santos. 2023. 'Identification of NRF2 Activation as a Prognostic Biomarker in T-Cell Acute Lymphoblastic Leukaemia', *Int J Mol Sci*, 24.

Vo, T. T., J. S. Lee, D. Nguyen, B. Lui, W. Pandori, A. Khaw, S. Mallya, M. Lu, M. Muschen, M. Konopleva, and D. A. Fruman. 2017. 'mTORC1 Inhibition Induces Resistance to Methotrexate and 6-Mercaptopurine in Ph(+) and Ph-like B-ALL', *Mol Cancer Ther*, 16: 1942-53.

Volm, M., A. Sauerbrey, and F. Zintl. 1994. 'Prognostic-significance of protein-kinase-C in newly-diagnosed childhood acute lymphoblastic-leukemia', *Int J Oncol*, 4: 363-8.

Volm, M., A. Sauerbrey, F. Zintl, R. Koomagi, and T. Efferth. 2002. 'Protein expression profile of newly diagnosed acute lymphoblastic leukemia in children developing relapses', *Oncol Rep*, 9: 965-9.

Volm, M., F. Zintl, L. Edler, and A. Sauerbrey. 1997. 'Prognostic value of protein kinase C, proto-oncogene products and resistance-related proteins in newly diagnosed childhood acute lymphoblastic leukemia', *Med Pediatr Oncol*, 28: 117-26.

Vora, A., N. Goulden, C. Mitchell, J. Hancock, R. Hough, C. Rowntree, A. V. Moorman, and R. Wade. 2014. 'Augmented post-remission therapy for a minimal residual disease-defined high-risk subgroup of children and young people with clinical standard-risk and intermediate-risk acute lymphoblastic leukaemia (UKALL 2003): a randomised controlled trial', *Lancet Oncol*, 15: 809-18.

Vora, A., C. D. Mitchell, L. Lennard, T. O. Eden, S. E. Kinsey, J. Lilleyman, S. M. Richards, Council Medical Research, and Party National Cancer Research Network Childhood Leukaemia Working. 2006. 'Toxicity and efficacy of 6-thioguanine versus 6-mercaptopurine in childhood lymphoblastic leukaemia: a randomised trial', *Lancet*, 368: 1339-48.

Wadhwa, A., Y. Chen, L. Hageman, A. Hoppmann, A. Angiolillo, D. S. Dickens, J. P. Neglia, Y. Ravindranath, A. K. Ritchey, A. Termuhlen, F. L. Wong, W. Landier, and S. Bhatia. 2023. 'Poverty and relapse risk in children with acute lymphoblastic leukemia: a Children's Oncology Group study AALL03N1 report', *Blood*, 142: 221-29.

Wang, L., X. Liu, Q. Kang, C. Pan, T. Zhang, C. Feng, L. Chen, S. Wei, and J. Wang. 2022. 'Nrf2 Overexpression Decreases Vincristine Chemotherapy Sensitivity Through the PI3K-AKT Pathway in Adult B-Cell Acute Lymphoblastic Leukemia', *Front Oncol*, 12: 876556.

Wang, X., Y. Li, W. Chen, Y. Wang, L. Hui, J. Liu, N. Li, L. Zhang, Y. Zou, and F. Wang. 2017. 'Nrf-2/Gst-alpha mediated imatinib resistance through rapid 4-HNE clearance', *Exp Cell Res*, 353: 72-78.

Wang, X. Y., X. H. Zhang, L. Peng, Z. Liu, Y. X. Yang, Z. X. He, H. W. Dang, and S. F. Zhou. 2017. 'Bardoxolone methyl (CDDO-Me or RTA402) induces cell cycle arrest, apoptosis and autophagy via PI3K/Akt/mTOR and p38 MAPK/Erk1/2 signaling pathways in K562 cells', *Am J Transl Res*, 9: 4652-72.

Ward, J. L., A. Sherali, Z. P. Mo, and C. M. Tse. 2000. 'Kinetic and pharmacological properties of cloned human equilibrative nucleoside transporters, ENT1 and ENT2, stably expressed in nucleoside transporter-deficient PK15 cells. Ent2 exhibits a low affinity for guanosine and cytidine but a high affinity for inosine', *J Biol Chem*, 275: 8375-81.

Weisberg, E., P. W. Manley, S. W. Cowan-Jacob, A. Hochhaus, and J. D. Griffin. 2007. 'Second generation inhibitors of BCR-ABL for the treatment of imatinib-resistant chronic myeloid leukaemia', *Nat Rev Cancer*, 7: 345-56.

Weisenthal, L. M., Y. Z. Su, T. E. Duarte, P. L. Dill, and R. A. Nagourney. 1987. 'Perturbation of in vitro drug resistance in human lymphatic neoplasms by combinations of putative inhibitors of protein kinase C', *Cancer Treat Rep*, 71: 1239-43.

Wielinga, P. R., G. Reid, E. E. Challa, I. van der Heijden, L. van Deemter, M. de Haas, C. Mol, A. J. Kuil, E. Groeneveld, J. D. Schuetz, C. Brouwer, R. A. De Abreu, J. Wijnholds, J. H. Beijnen, and P. Borst. 2002. 'Thiopurine metabolism and identification of the thiopurine metabolites transported by MRP4 and MRP5 overexpressed in human embryonic kidney cells', *Mol Pharmacol*, 62: 1321-31.

Wijnholds, J., C. A. Mol, L. van Deemter, M. de Haas, G. L. Scheffer, F. Baas, J. H. Beijnen, R. J. Scheper, S. Hatse, E. De Clercq, J. Balzarini, and P. Borst. 2000. 'Multidrug-resistance protein 5 is a multispecific organic anion transporter able to transport nucleotide analogs', *Proc Natl Acad Sci U S A*, 97: 7476-81.

Wilkinson, S. E., P. J. Parker, and J. S. Nixon. 1993. 'Isoenzyme specificity of bisindolylmaleimides, selective inhibitors of protein kinase C', *Biochem J*, 294 (Pt 2): 335-7.

Winter, S. S., K. P. Dunsmore, M. Devidas, B. L. Wood, N. Esiashvili, Z. Chen, N. Eisenberg, N. Briegel, R. J. Hayashi, J. M. Gastier-Foster, A. J. Carroll, N. A. Heerema, B. L. Asselin, P. S. Gaynon, M. J. Borowitz, M. L. Loh, K. R. Rabin, E. A. Raetz, P. A. Zweidler-Mckay, N. J. Winick, W. L. Carroll, and S. P. Hunger. 2018. 'Improved Survival for Children and Young Adults With T-Lineage Acute Lymphoblastic Leukemia: Results From the Children's Oncology Group AALL0434 Methotrexate Randomization', *J Clin Oncol*, 36: 2926-34.

Wu, C., and W. Li. 2018. 'Genomics and pharmacogenomics of pediatric acute lymphoblastic leukemia', *Crit Rev Oncol Hematol*, 126: 100-11.

Wu, Y. P., D. D. Stenehjem, L. A. Linder, B. Yu, B. G. Parsons, R. Mooney, and M. N. Fluchel. 2018. 'Adherence to Oral Medications During Maintenance Therapy Among Children and Adolescents With Acute Lymphoblastic Leukemia: A Medication Refill Analysis', *J Pediatr Oncol Nurs*, 35: 86-93.

Xu, L., Y. Zhao, F. Pan, M. Zhu, L. Yao, Y. Liu, J. Feng, J. Xiong, X. Chen, F. Ren, Y. Tan, and H. Wang. 2019. 'Inhibition of the Nrf2-TrxR Axis Sensitizes the Drug-Resistant Chronic Myelogenous Leukemia Cell Line K562/G01 to Imatinib Treatments', *Biomed Res Int*, 2019: 6502793.

Yallop, C. A., and I. Svendsen. 2001. 'The effects of G418 on the growth and metabolism of recombinant mammalian cell lines', *Cytotechnology*, 35: 101-14.

Yamamoto, S., K. Inoue, T. Murata, S. Kamigaso, T. Yasujima, J. Y. Maeda, Y. Yoshida, K. Y. Ohta, and H. Yuasa. 2010. 'Identification and functional characterization of the first nucleobase transporter in mammals: implication in the species difference in the intestinal absorption mechanism of nucleobases and their analogs between higher primates and other mammals', *J Biol Chem*, 285: 6522-31.

Yamanaka, N., K. Nishida, and K. Ota. 1979. 'Increase of superoxide dismutase activity in various human leukemia cells', *Physiol Chem Phys*, 11: 253-6.

Yan, N. 2013. 'Structural advances for the major facilitator superfamily (MFS) transporters', *Trends Biochem Sci*, 38: 151-9.

Yang, S. K., M. Hong, J. Baek, H. Choi, W. Zhao, Y. Jung, T. Haritunians, B. D. Ye, K. J. Kim, S. H. Park, S. K. Park, D. H. Yang, M. Dubinsky, I. Lee, D. P. McGovern, J. Liu, and K. Song. 2014. 'A common missense variant in NUDT15 confers susceptibility to thiopurine-induced leukopenia', *Nat Genet*, 46: 1017-20.

Yao, S. Y., A. M. Ng, C. E. Cass, S. A. Baldwin, and J. D. Young. 2011. 'Nucleobase transport by human equilibrative nucleoside transporter 1 (hENT1)', *J Biol Chem*, 286: 32552-62.

Young, J. D., S. Y. Yao, J. M. Baldwin, C. E. Cass, and S. A. Baldwin. 2013. 'The human concentrative and equilibrative nucleoside transporter families, SLC28 and SLC29', *Mol Aspects Med*, 34: 529-47.

Young, L. H., B. J. Balin, and M. T. Weis. 2005. 'Go 6983: a fast acting protein kinase C inhibitor that attenuates myocardial ischemia/reperfusion injury', *Cardiovasc Drug Rev*, 23: 255-72.

Young, S., P. J. Parker, A. Ullrich, and S. Stabel. 1987. 'Down-regulation of protein kinase C is due to an increased rate of degradation', *Biochem J*, 244: 775-9.

Zecha, J., C. Meng, D. P. Zolg, P. Samaras, M. Wilhelm, and B. Kuster. 2018. 'Peptide Level Turnover Measurements Enable the Study of Proteoform Dynamics', *Mol Cell Proteomics*, 17: 974-92.

Zgheib, N. K., R. Akika, R. Mahfouz, C. A. Aridi, K. M. Ghanem, R. Saab, M. R. Abboud, N. Tarek, H. El Solh, and S. A. Muwakkit. 2017. 'NUDT15 and TPMT genetic polymorphisms are related to 6-mercaptopurine intolerance in children treated for acute lymphoblastic leukemia at the Children's Cancer Center of Lebanon', *Pediatr Blood Cancer*, 64: 146-50.

Zhang, W., R. Dang, H. Liu, L. Dai, H. Liu, A. A. Adegboro, Y. Zhang, W. Li, K. Peng, J. Hong, and X. Li. 2024. 'Machine learning-based investigation of regulated cell death for predicting prognosis and immunotherapy response in glioma patients', *Sci Rep*, 14: 4173.

Zhao, X., Y. Guo, W. Yue, L. Zhang, M. Gu, and Y. Wang. 2014. 'ABCC4 is required for cell proliferation and tumorigenesis in non-small cell lung cancer', *Onco Targets Ther*, 7: 343-51.

Zhao, Y., L. Zhang, and L. D. Longo. 2005. 'PKC-induced ERK1/2 interactions and downstream effectors in ovine cerebral arteries', *Am J Physiol Regul Integr Comp Physiol*, 289: R164-71.

Zhou, M., H. Duan, K. Engel, L. Xia, and J. Wang. 2010. 'Adenosine transport by plasma membrane monoamine transporter: reinvestigation and comparison with organic cations', *Drug Metab Dispos*, 38: 1798-805.

Zhou, M., L. Xia, K. Engel, and J. Wang. 2007. 'Molecular determinants of substrate selectivity of a novel organic cation transporter (PMAT) in the SLC29 family', *J Biol Chem*, 282: 3188-95.

Zhou, S. F., L. L. Wang, Y. M. Di, C. C. Xue, W. Duan, C. G. Li, and Y. Li. 2008. 'Substrates and inhibitors of human multidrug resistance associated proteins and the implications in drug development', *Curr Med Chem*, 15: 1981-2039.

Zhu, D. M., W. H. Fang, R. K. Narla, and F. M. Uckun. 1999. 'A requirement for protein kinase C inhibition for calcium-triggered apoptosis in acute lymphoblastic leukemia cells', *Clin Cancer Res*, 5: 355-60.

Zhu, D. M., R. K. Narla, W. H. Fang, N. C. Chia, and F. M. Uckun. 1998. 'Calphostin C triggers calcium-dependent apoptosis in human acute lymphoblastic leukemia cells', *Clin Cancer Res*, 4: 2967-76.

APPENDIX

SLC43A3 expression in ALL patient samples

Introduction

The *SLC43A3* is a relatively new discovery, and thus, not many functional clinical associations have been made to date. Primary literature has shown that *SLC43A3* has been implicated in two diseases, angiosarcoma (as a fusion gene) and glioblastoma (Shimozono et al. 2015; Zhang et al. 2024). In the public database, ClinVar, several single nucleotide variants have been noted, but none contain any clinically confirmed pathogenesis (Gene ID: 29015) (Landrum et al. 2014). In the Human Protein Atlas (proteinatlas.org), high *SLC43A3* expression is associated with an unfavourable prognosis in renal cancer (Uhlen et al. 2017). Aside from that and the lack of information surrounding *SLC43A3*, it is difficult to ascertain whether *SLC43A3* expression levels or polymorphisms are pathogenic in any other disease. In leukemia, no clinical associations have been made on *SLC43A3* expression or if it impacts therapy, namely 6-MP. Therefore, *SLC43A3* expression was assessed using primary samples from ALL patients. Samples were obtained from two locations, the University of Alberta Hospital (Edmonton, Alberta, Canada) and the BC Children's Hospital (Vancouver, British Columbia, Canada). The University of Alberta Hospital provided RNA samples that were reverse transcribed to cDNA prior to qPCR. The BC Children's Hospital provided primary frozen bone marrow aspirates that were thawed quickly, and RNA was extracted via TRIzol as per the manufacturer’s protocol, reverse transcribed to cDNA, and then semiquantitative RT-qPCR was done.

Results

cDNAs were used to conduct qPCR on several genes of interest related to 6-MP transport (*SLC43A3, SLC29A1, SLC29A2, SLC29A4, ABCB1, ABCC4,* and *ABCC5*) **(Figure 41)** and 6-MP metabolism (*HPRT1, TPMT, XDH/XO, NUDT15, IMPDH1*) **(Figure 42)**. As expected, all genes displayed large variation in expression between samples. Interestingly, the majority of genes appear to have roughly a similar distribution of variability between the BC Children's Hospital and University of Alberta Hospitals samples. *SLC43A3* expression varies by 19-fold and 48-fold between the highest and lowest expression in the BC Children's Hospital and University of Alberta Hospitals samples, respectively. None of the samples were found to express *SLC29A4, ABCB1*, and *XDH/XO*. Of note, one sample in the BC Children's Hospital samples had significantly higher expression of *SLC29A2* (54-fold)*, TPMT* (21-fold)*, IMPDH1* (31-fold), and *NUDT15* (42-fold). At first, it was thought there might be a problem with the reference genes being different from the rest of the samples, but that was not the case. It is unclear why these genes are higher in this patient while others are near the average and would require further investigation.

For the BC Children's Hospital dataset, clinical data on white blood cell counts, neutrophil counts, lymphocyte counts, % lymphoblasts, time of relapse, 6-MP starting dose, and 6-MP final dose were provided. Correlations were done to determine if any of the genes were correlated to the clinical data. No correlations were found to exist between the datasets.

Figure 41: qPCR analysis of 6-MP transporters in primary ALL patient samples

Gene expression of 6-MP transporters was assessed by semi-quantitative RT-PCR and is shown as a fold difference from the average from each individual gene separated between the BC Children's Hospital and the University of Alberta Hospital samples. Each column is calculated individually within each site, and gene expression is normalized to 3 separate reference genes (*GAPDH, RNA18SN5,* and *ACTB*) and quantified using the ΔΔCt method. **(A-G)** Relative expression of *SLC43A3, SLC29A1, SLC29A2, SLC29A4, ABCC4, ABCC5,* and *ABCB1* as compared to the average within each gene. The dotted line at 1 is equal to the average expression within each gene. N-values are 12 and 28 done in triplicate for the BC Children's Hospital and the University of Alberta Hospital, respectively.

Figure 41

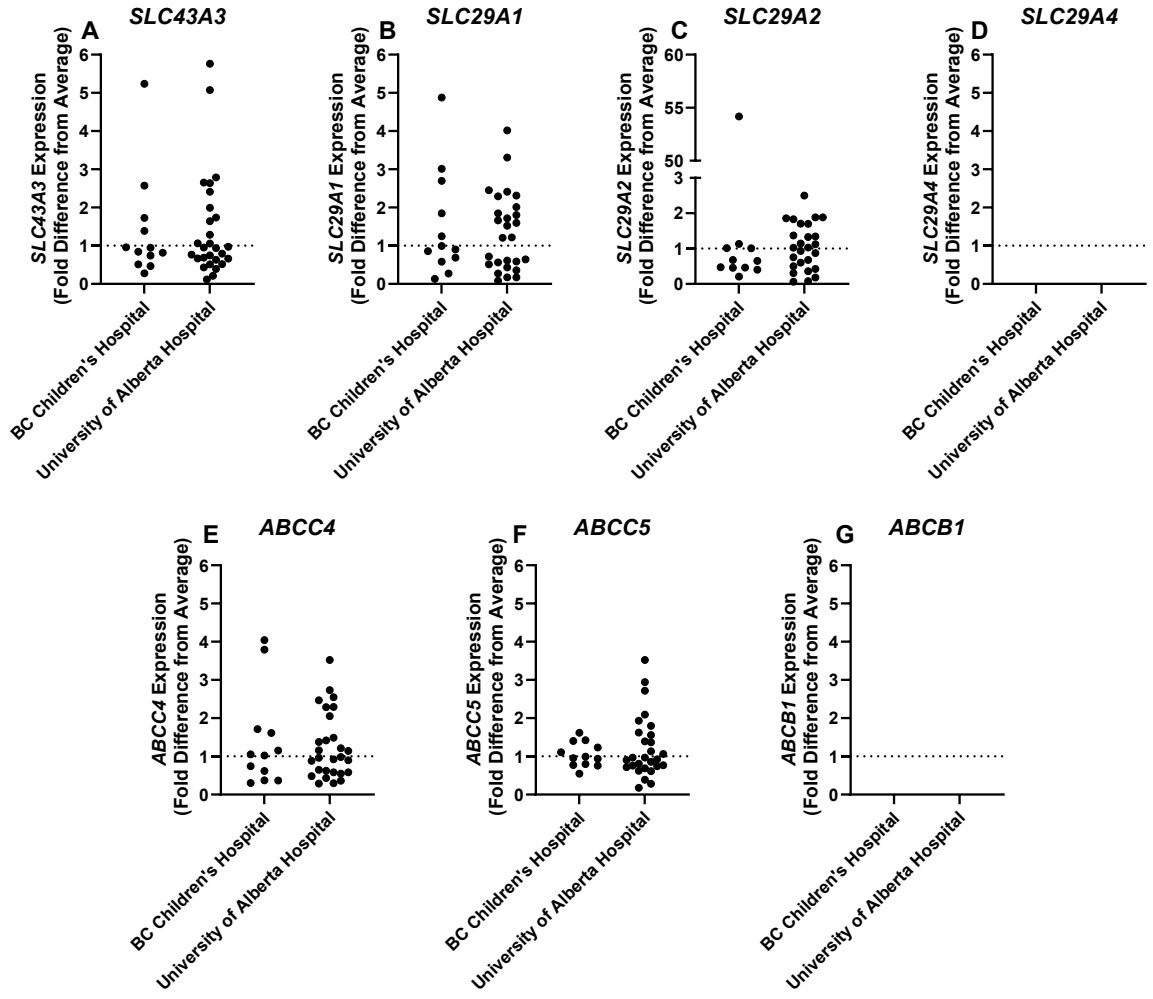
A
SLC43A3
SLC43A3 Expression (Fold Difference from Average)
B
SLC29A1
SLC29A1 Expression (Fold Difference from Average)
C
SLC29A2
SLC29A2 Expression (Fold Difference from Average)
D
SLC29A4
SLC29A4 Expression (Fold Difference from Average)
E
ABCC4
ABCC4 Expression (Fold Difference from Average)
F
ABCC5
ABCC5 Expression (Fold Difference from Average)
G
ABCB1
ABCB1 Expression (Fold Difference from Average)
BC Children's Hospital
University of Alberta Hospital

Figure 42: qPCR analysis of 6-MP metabolic enzymes in primary ALL patient samples

Gene expression of 6-MP metabolic enzymes was assessed by semi-quantitative RT-PCR and is shown as a fold difference from the average from each individual gene separated between the BC Children's Hospital and the University of Alberta Hospital samples. Each column is calculated individually within each site, and gene expression is normalized to 3 separate reference genes (*GAPDH, RNA18SN5,* and *ACTB*) and quantified using the ΔΔCt method. **(A-F)** Relative expression of *HPRT1, TPMT, XDH/XO, IMPDH1, GMPS* and *NUDT15* as compared to the average within each gene. The dotted line at 1 is equal to the average expression within each gene. N-values are 12 and 28 done in triplicate for the BC Children's Hospital and the University of Alberta Hospital, respectively.

Figure 42

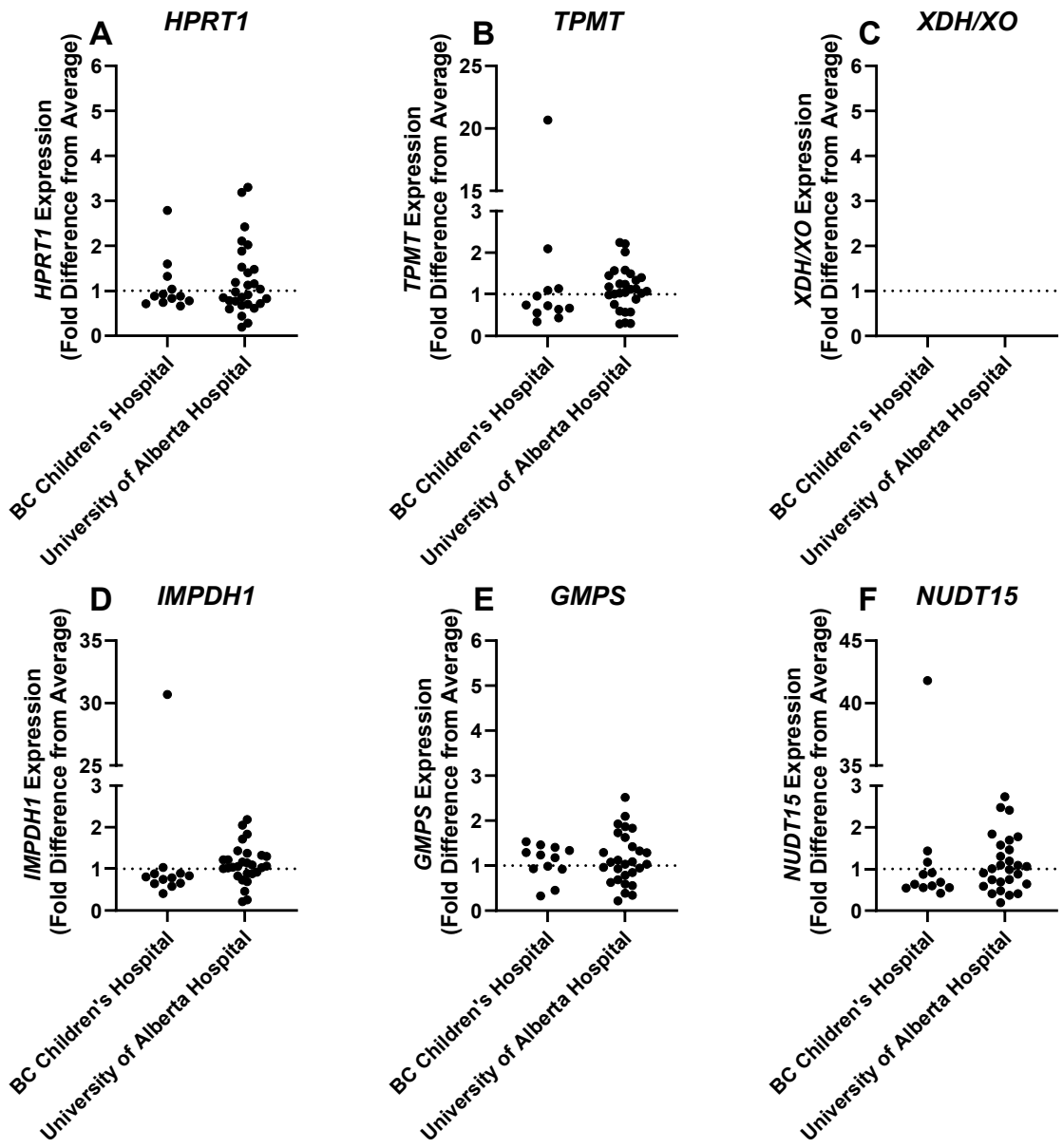
A
HPRT1
HPRT1 Expression (Fold Difference from Average)
B
TPMT
TPMT Expression (Fold Difference from Average)
C
XDH/XO
XDH/XO Expression (Fold Difference from Average)
D
IMPDH1
IMPDH1 Expression (Fold Difference from Average)
E
GMPS
GMPS Expression (Fold Difference from Average)
F
NUDT15
NUDT15 Expression (Fold Difference from Average)
BC Children's Hospital
University of Alberta Hospital

Limitations

The data only determined the relative gene expression of various transporters and enzymes in multiple patient samples. It is well known that gene expression does not always correlate to protein levels (Guo et al. 2008). Furthermore, some of the clinical data used to correlate to the gene expression data, particularly the starting 6-MP dose and the final dosage, is not particularly relevant. This is because the changes in dosing of 6-MP are based on the side effects of 6-MP therapy, which would be more sensitive to overall changes in plasma concentrations of other 6-MP metabolites, specifically 6-MeMP and 6-TGNs, and their biodistribution throughout the whole body. The qPCR data above only measures the expression of the bone marrow cells taken from the patients and would not be able to consider the overall biodistribution of 6-MP and its metabolites. Doing therapeutic drug monitoring would have been preferred so that there could be a more continuous dataset for this correlation. Interestingly, the Hammond lab has shown that a *slc43a3*-KO mouse model has a decreased absorption of 6-MP when given by oral gavage (Aaron Sayler, personal communication, April 11, 2024). These data suggest that *SLC43A3*/ENBT1 is likely more critical for the biodistribution and absorption of 6-MP in patients, which could impact their therapeutic response to 6-MP.

Conclusion

SLC43A3 expression varies widely in patient samples taken from two separate sites. The expression does not correlate with any clinical parameters. It is likely that *SLC43A3*/ENBT1 is more important in the absorption and biodistribution of 6-MP in patients. Further investigation will be undertaken to investigate this impact for potential use in predicting patient response prior to therapy initiation.